Customisable peptide hydrogels as user-defined biomimetic models of specific tissue microenvironments

Johnathan Curd

Thesis submitted to the University of Nottingham for
the degree of Doctor of Philosophy

March 2022

Acknowledgements

First and foremost, I would like to thank my supervisor, Prof Cathy Merry. I cannot begin to express my gratitude for all your patience, support, and guidance throughout this whole process. Special thanks also to all the members of the SCG group, past and present, for their help and support.

I would also like to acknowledge all the talented chemists who helped expand the scope of the project. I will never forget the chance encounter I had with Prof Neil Thomas at a bus stop, and the conversation we had whilst waiting for the bus that led to the to the idea for using "click" chemistry to modify the gels. I often wonder what direction my project would have taken without this, but I'm sure it would not have been as interesting. Thank you for all your support and guidance through the world of chemistry. I would also like to thank Chris Merrett for the hard work he did that turned this idea from a possibility into a reality. Thank you also to James Kapp for all the sortase he generously provided, without which another major aspect of my project may never have been realised.

Thank you also to Dr David Turner for hosting me for a week at the University of Liverpool and the training he provided that allowed me to explore the interesting world of gastruloids.

In addition to all the talented scientists I collaborated with, I would also like to thank one more talented scientist who has helped me throughout this journey. I never could have achieved any of this without the unconditional support and kindness from my girlfriend, Katie. I only hope that I can be as helpful to you during the rest of your PhD journey.

I would also like to thank my wonderful family for their support. Thank you to my Mum, for encouraging me to return to university and continue my studies. Thank you also to my brother, Matthew, and our sibling rivalry that always encouraged me to persevere, so that you wouldn't be the only one with a PhD!

Finally, I would like to acknowledge someone who isn't here anymore. Wherever you are now, I hope I made you proud, Dad.

Table of Contents

List of figures

List of tables

List of reaction schemes

Abbreviations

2D	two dimensional
3D	three dimensional
a.a.	after aggregation
Aha	L-azidohomoalanine
ASC	adult stem cell
AVE	anterior visceral endoderm
bFGF	basic fibroblast growth factor
BMP	bone morphogenetic protein
BSA	bovine serum albumin
CMP	collagen mimetic peptide
CS	chondroitin sulphate
CuAAC	copper-catalysed azide-alkyne cycloaddition
DBCO	dibenzocyclooctyne
DPBS	Dulbecco's Phosphate Buffered Saline
ECM	extracellular matrix
EGF	epidermal growth factor
eGFP	enhanced green fluorescent protein
EHS	Engelbreth-Holm-Swarm
ESC	embryonic stem cell
EXT1/2	exostosin-1/2
FAK	focal adhesion kinase
FBS	fetal bovine serum
FEFEFKFK	Phe-Glu-Phe-Glu-Phe-Lys-Phe-Lys

FGF	fibroblast growth factor
FGFR	fibroblast growth factor receptor
FITC	fluorescein isothiocyanate
FITC-Dextran	fluorescein isothiocyanate dextran
FN	fibronectin
GAG	glycosaminoglycan
GF	growth factor
GFAP	green acidic fibrillary protein
GFP	green fluorescent protein
GlcNAc	N-acetyl glucosamine
GPI	glycosylphosphatidylinositol
HA	hyaluronic acid/hyaluronan
HEPES	4-(2-hydroxyethyl)-1-piperazineethanesulfonic acid
HME	hereditary multiple exostoses
HMF	human mammary fibroblast
hNSC	human neural stem cell
HPLC	high-performance liquid chromatography
HRMS	high resolution mass spectrometry
HS	heparan sulphate
HSIII	heparan sulphate III
HSPG	heparan sulphate proteoglycan
IHC	immunohistochemistry
IKVAV	Ile-Lys-Val-Ala-Val
IL-8	interleukin-8

iPSC	induced pluripotent stem cell
KAT	potassium acyltrifluoroborate
LDHV	lactate dehydrogenase-elevating virus
LIF	leukaemia inhibitory factor
LOX	lysyl oxidase
LPETG	Leu-Pro-Glu-Thr-Gly
LPMTG	Leu-Pro-Met-Thr-Gly
LPRTG	Leu-Pro-Arg-Thr-Gly
mESC	mouse embryonic stem cell
MMP	matrix metalloproteinase
MS	mass spectrometry
NaOH	sodium hydroxide
NDST	N-deacetylase/N-sulfotransferase
NHS	N-hydroxysuccinimide
NMR	nuclear magnetic resonance
NPC	neural progenitor cells
PA	peptide amphiphile
PCL	poly(ε-caprolactone)
PEG	polyethylene glycol
PLA	polylactic acid
PLGA	poly(lactic-co-glycolic acid)
PU	polyurethanes
RDGLPETG	Arg-Gly-Asp-Leu-Pro-Glu-Thr-Gly
RGD	Arg-Gly-Asp

RPIP-HPLC	reverse-phase ion-pair high performance liquid chromatography
SAPH	self-assembling peptide hydrogel
Scx	scleraxis
SEM	scanning electron microscopy
SLRP	small leucine-rich proteoglycan
SPAAC	"strain promoted" azide-alkyne cycloaddition
SrtA	sortase A
TFA	trifluoroacetic acid
TGFβ	transforming growth factor beta
UV	ultraviolet
WT	wild-type

Abstract

The extracellular matrix (ECM) is comprised of a complex variety of biochemically distinct molecules including proteins, glycoproteins, proteoglycans, and polysaccharides. These provide not only the physical support for resident cells but also play a vital role in tissue homeostasis, by providing key biophysical and biochemical cues which regulate cell growth, survival, motility, and differentiation. However, current *in vitro* models typically fail the recapitulate the complexities of the native ECM, leading to a poor extrapolation of *in vitro* findings to *in vivo* relevance. This is a major contributing factor to the high attrition rate of novel drug candidates moving from the lab to the clinic. This has driven the recent interest in the development of more sophisticated 3D *in vitro* models which allow customisation of stiffness and composition to better reflect *in vivo* tissues.

However, currently there is not a single model platform which contains all the necessary features for a truly representative model. Naturally-derived biomaterials such as Matrigel® contain irrelevant animal-derived material, suffer from high batch-to-batch variability, and are poorly defined. All these features lead to difficulties in generating reproducible data and call into question whether these models truly reflect human tissues when they are composed of material of animal origin. Synthetic scaffolds and hydrogels have the advantages of being well defined, having limited batch variability, and containing no animal-derived material, but often lack complexity in terms of biochemistry. Whilst there are several methods available that allow for user-defined stiffness and porosity of these materials to better reflect the native architecture of target tissues, options for customisation with selected biomolecules to drive relevant cell behaviours are currently lacking.

The FEFEFKFK peptide hydrogel is a promising new candidate model platform that aims to address all the shortcomings of current *in vitro* models. Its stiffness can be controlled independent of its composition, allowing end users the ability to investigate the biological impact of matrix additions independently from tissue mechanics. Soluble matrix components selected to drive specific cell behaviours can also be encapsulated within the gel, allowing for a more faithful recreation of specific tissue microenvironments. However, at the beginning of this project, there existed only this single method for customisation of matrix composition. Potential loss of soluble material during cell culture, and the requirement for specific biomolecules to be covalently immobilised within the gel so that their correct *in vivo* behaviour is captured, necessitated the development of additional methods for customisation.

Therefore, it was the primary aim of this project to identify, optimise, and validate new methods for functionalising the peptide hydrogel with relevant biomolecules. Specifically, two methods for covalent immobilisation of matrix material were investigated: sortase-mediated and "click" chemistry-mediated functionalisation. Provided in this report is an initial proof of concept for these two methods and how immobilised material impacts the behaviour of encapsulated cells.

This work will allow for the creation of more complex and representative models of specific tissue microenvironments, without the need for animal-derived material. These models present researchers with the opportunity to study the underlying mechanisms of development and disease, or to better stratify novel drug candidates during preclinical screening, in an environment which produces more human-relevant and reproducible data. Compared to existing methods, the potential impact of this work will be to help reduce the high attrition rate of novel drug candidates moving from the lab to the clinic.

Declaration of collaborative work

Some aspects of this thesis were conducted in collaboration with other research groups. All collaborations were conceived and discussed with the author, and their contributions have been noted within the text. The work of Chris Merrett (PhD student co-supervised by Prof Thomas and Prof. Merry) was part of an interdisciplinary collaboration, planned and discussed in joint project meetings with input from the author as well as Prof. Cathy Merry, Prof. Neil Thomas and Chris Merrett. However, for clarity, details of results obtained in collaborations have been listed below:

- Section 3.4 – The wild-type Sortase A enzyme, the N7M sortase A enzyme, and the sort-tagged eGFP used in these experiments were generously provided by James Kapp, University of Nottingham, UK. Design of methods and practical work was carried out by the author.

- Section 3.4.5 – The H7M sortase A enzyme used in these experiments was generously provided by Stephanie Dougan, Harvard Medical School, Boston, Massachusetts. Design of methods and practical work was carried out by the author.

- Sections 3.7.2 and 3.8.4 – The wild-type sortase A enzyme used in these experiments was also provided by James Kapp, University of Nottingham, UK.

- Section 3.6.1 – Generation of the DBCO-cyclo(RGDfK) material was carried out by Chris Merrett, University of Nottingham, UK. The material was then provided for use in this project where the subsequent "click" reaction to immobilise this within the gels was done by the author.

- Section 3.6.2 – Generation of the FEFEFKFK-DBCO-Heparin material was also carried out by Chris Merrett, University of Nottingham, UK. This material was then provided for use in this project where it was incorporated into the gel fabrication procedure by the author.

- Section 3.9.0 – Practical techniques for generation of gastruloids were demonstrated by Dr David Turner, University of Liverpool, UK whilst visiting his lab in Liverpool. Generation of gastruloids for this project was then performed by the author in Nottingham.

COVID19 Impact Statement

The COVID19 pandemic, unfortunately, had a severe impact on this project. At the beginning of my third year, my group moved into the new Biodiscovery Institute (BDI), with approximately four months of total "down time" away from functional labs. We had only just been able to resume our work when the first national lockdown was implemented. During this time, I was unable to conduct any lab work. However, due to rising concerns over COVID19, we were instructed not to begin and long-term experiments in the lead-up to the lockdown, so that its impact was also felt before this.

Upon returning after lockdown, I was met with a variety of ongoing issues caused by the pandemic which continued to impact my work. Initially, access to the building where I primarily worked (BDI-3) was restricted to specific hours and only during weekdays. This made it impossible to begin any cell-based experiments requiring the use of stem cells, as these require daily media changes. Due to the nature of my work, substituting for a different type of cell was not possible. Also, due to the new capacity limit and safety measures that were implemented in the building, it was incredibly difficult to organise any training that would have allowed me to conduct the cell-free experiments I also needed to do at this time.

When my full access to BDI-3 was restored, I was still not allowed access to the other buildings within the BDI (BDI-1/2) or elsewhere at the University. This made the collaborative side of my project also incredibly difficult, as the generation of material needed for the sortase and "click" chemistry experiments had to be conducted within BDI-1/2. Had this not been the case, I would have enjoyed gaining some hands-on experience and a more in-depth understanding of the protocols used. Additionally, the availability of essential reagents and plasticware continued to be an issue during this time, due to the global supply chain issues caused by the pandemic.

Due to the nature of the project, many planned experiments had long lead times with limited/no alternatives. Where there was a potential alternative, this was often made unavailable due to the ongoing issues that arose during the period after lockdown. This had a severe impact on my ability to adapt my project during this time. Including the time lost during the move to the new building, the lead-up to the lockdown, the lockdown itself, and the period afterwards, I was functionally unable to conduct any lab work as originally planned for at least 12 months.

Also, as part of the DTP program, I was expected to complete a 3-month professional internship placement (PIP). However, as another consequence of the pandemic, potential placement hosts were generally unwilling to accommodate internships during this time. The placement I had originally organised with Sygnature Discovery Ltd. was, unfortunately, cancelled by the host and I was unable to secure another. I believe I missed out on the opportunity to gain new skills and expertise during this placement that I could have put to use during my PhD and beyond. However, I have now secured a 6-month project placement starting in April 2022 which will investigate the potential to commercialise the peptide hydrogels. This promises to deliver some of the experience that I have so far missed out on.

Despite all the setbacks, I tried to minimise the impact of the pandemic wherever possible. During the lockdown, I enrolled in online courses on "Python Programming" and "Data Science", as I believe these kinds of skills will become increasingly relevant and sought after in the industry in the future. I also made use of these new skills during the production of this report, with all the data analyses and generation of plots presented having been done using Python programming.

After returning from lockdown, I also did my best to minimise the impact the pandemic had on my work. When I was unable to begin any cell-based experiments or access any training, I used this time to produce a library of peptide hydrogels for use in future experiments. This helped to save time when weekend access and training became available again. When lack of essential reagents and plasticware became an issue, I adapted my protocols to be as economical and efficient as possible, using whatever we did have available.

However, ultimately, the COVID19 pandemic caused many setbacks and delays which resulted in a lot of unavoidable disruption to my work. I believe that this lasting impact has prevented me from achieving many of the original aims and objectives that I set out to achieve at the start of the programme. In my discussion, I have presented several suggestions for further refinement and improvement on the new methods I developed as part of the project. I believe that, had it not been for the 12+ months of disruption I encountered, I could have completed all these experiments during the course of the programme. I also believe that it is likely I could have achieved the additional aim of validating the new model platform as a preclinical screening tool. This would have involved using the new methods for matrix customisation that I developed to create a 3D tissue model of a specific disease and then testing its effectiveness at predicting the clinical outcome of past drug candidates.

Nevertheless, despite these missed opportunities, I believe I have presented here a body of work that fulfils the requirement for attaining a PhD.

1.0.0 Introduction

1.1.0 Project overview

For decades, cell-based assays used in drug discovery and investigative research have typically relied on simplistic monolayer cultures, where a single layer of cells is adhered to a polystyrene plate [1]. These types of models suffer from low cell densities, high stiffnesses, and lack the complex cell-cell and cell-matrix interactions that are present *in vivo*. These factors lead to *in vitro* artifacts in cell behaviour including cell phenotype, signalling, and drug sensitivity [2]. This limits their usefulness in extrapolating data to predict patient outcomes, and is a major contributor to the high attrition rate of novel drug candidates failing when moving from the lab to the clinic, particularly for new anti-cancer therapies [3, 4].

Therefore, there is a need for the development of new 3D *in vitro* models that can bridge the gap between *in vitro* findings and *in vivo* relevance. Recent advances in cell biology, microfabrication techniques and tissue engineering have led to the development of several such models. Each strikes a delicate balance between usability, cost, and resemblance to *in vivo* circumstances. In many research areas, but particularly in cancer research and disease modelling, there is an increasing interest in the development of new biomaterials which allow cells to be grown in 3D [5, 6].

Biomaterials for 3D cell culture provide a scaffold upon which cells can attach and self-organise into 3D structures and can be broadly separated into two categories: biologics and synthetics. Biological scaffolds typically use extracellular matrix (ECM) components, such as collagen gels and the commercially available Matrigel®, which is derived from Engelbreth-Holm-Swarm (EHS) mouse sarcoma [7]. Whilst these have proved useful in a variety of past studies, ranging from cell migration and invasion assays to regenerative medicine [8-10], their biological origin also results in high batch-to-batch variability and uncertainty whether the use of animal-derived material can ever accurately recapitulate human systems. Matrigel® is particularly problematic due to its origin and is also probably unsuitable for modelling healthy tissue, due to the presence of tumour-derived proteins including TGFs, FGFs, and MMPs [11, 12]. It is also prone to xenographic contaminants, such as with lactate dehydrogenase-elevating virus (LDHV) [13, 14], which has been shown interfere with a variety of biological processes including immune activity, drug response, and tumour behaviour [15]. These and other issues, which are discussed in more detail in a later section, have driven a recent shift towards more highly-defined synthetic alternatives [16, 17].

Synthetic scaffolds provide the physical support for the attachment and reorganisation of cells into 3D structures. Often comprised of a single ingredient, they do not suffer from the high batch-to-batch variability of their biologic counterparts, which leads to more reproducible results. They also do not rely on animal-derived material, improving the reliability of extrapolating *in vitro* results to human conditions. Instead, synthetic scaffolds are often comprised of a variety of polymeric materials including polyethylene glycol (PEG), poly(lactic-co-glycolic acid) (PLGA), polylactic acid (PLA), poly(ε-caprolactone) (PCL), and polyurethanes (PU) [18-23]. PEG in particular is a popular choice of material for the design of 3D *in vitro* models, due to it being hydrophilic, bioinert, and highly amenable to chemical modification [24]. However, 3D *in* vitro models which utilise PEG often suffer from an architecture that does not always accurately recapitulate the native collagen hydrogel of the ECM [25]. Scaffolds designed using PLGA, PLA, PCL, and/or PU allow better recapitulation of this architecture, but as yet do not offer the same variety of available methods for chemical modification [23].

The ability to chemically modify these materials with relevant bioligands is critical in model design, so that the viability and correct physiological behaviour of encapsulated cells may be supported. This also allows investigation into the minimal essential conditions necessary for cell viability and specific types of cell behaviour in a way which is impossible with biological scaffolds. However, there have yet been few synthetic models designed specifically to allow customisation of matrix composition. A few notable exceptions to this exist, including the PEG-based hydrogels developed by Lutolf et al. [26, 27]. Utilising a biocompatible *Michael*-type addition reaction previously developed [28-30], this group was able to produce a well-defined hydrogel matrix functionalised with RGD (Arg-Gly-Asp) and laminin-111, which was able to support the expansion and maturation of intestinal stem cells and organoids. This is notable as there had been, and still is, considerable interest in developing synthetic alternatives to Matrigel® for this purpose [16, 31]. However, as previously mentioned, these types of models based on PEG ignore the issue of their architecture not being physiologically relevant, which therefore may also be driving cell behaviour in a physiologically irrelevant way.

Self-assembling peptide hydrogels (SAPHs) are another type of synthetic scaffold which generally better recapitulate the native architecture of the ECM [32]. In a recent study [33], a SAPH model based on the octapeptide gelator FEFEFKFK has also been presented as a potential candidate which also allows for matrix customisation. In the study, soluble matrix additions were shown to have a direct, predictable, and measurable impact on encapsulated

cell behaviour. Soluble collagen, for example, was found to enhance human mammary fibroblast (HMF) elongation and contraction. Collagen and hyaluronic acid (HA) additions were also found to support the growth of the breast cancer cell line MCF10A.

However, this model currently only offers a single method for matrix customisation, which is achieved by encapsulating soluble additions within the peptide hydrogel. This presents several potential problems. Firstly, soluble matrix additions may diffuse out of the gel and into the surrounding cell culture medium. These additions would then be lost during media changes unless the same concentration of these additions is also supplemented in the medium. Another potential issue is that the activity of soluble matrix additions may not accurately recapitulate their biological relevance *in vivo* [34].

The main objective of this project was, therefore, to address these issues by developing new methods of customising the model that allow matrix additions to be covalently immobilised within the gel network.

1.2.0 The extracellular matrix

To better understand the need for the development of new 3D *in vitro* models, and particularly those which accurately recapitulate the tissue microenvironment, an overview of the ECM and its importance in human biology in presented here.

The ECM is the non-cellular component present within all tissues and organs, providing not only the essential physical scaffolding for the organisation of cells but also playing a vital role in tissue homeostasis. It is comprised of a complex variety of biochemically distinct molecules including proteins, glycoproteins, proteoglycans, and polysaccharides [35]. Together, these components are organised into the remarkable structural and biochemical diversity of the ECM and provide key biophysical and biochemical cues which regulate cell growth, survival, motility, and differentiation [36].

The ECM can be further subdivided into the interstitial matrix, which is produced by stromal cells, and the basement membrane, which is jointly produced by epithelial, endothelial, and stromal cells [37]. The interstitial matrix is a highly charged, hydrated, and porous structure rich in fibrillar collagens, proteoglycans, and various glycoproteins such as tenascin and fibronectin. By contrast, the basement membrane, which is located between epithelial tissues and the underlying connective tissue, is a more compact and less porous structure comprised of type IV collagen, laminins, fibronectin, and linker proteins [38].

Each tissue type has an ECM with its own unique composition and topography that is generated during tissue development through dynamic and reciprocal, biochemical and biophysical signalling events between the various cellular components. Cell adhesion to the ECM is mediated by ECM receptors, such as integrins, discoidin domain receptors, and syndecans [39-42]. Moreover, the ECM is also a highly dynamic structure. Its biophysical and biochemical properties are constantly remodelled to provide the key biological cues to the supported cells at the correct times during development and tissue homeostasis. These dynamics can be the result compositional or non-compositional changes [37]. In compositional changes, the absolute amounts of ECM components are altered. In non-compositional changes, the volume remains unchanged but existing components are instead reorganised by altering their spatial patterning and cross-linking. This remodelling is tightly regulated during development and tissue homeostasis by controlled expression and activation of ECM remodelling enzymes, including matrix metalloproteinases (MMPs), and by controlling the deposition of the ECM components themselves [43].

Provided below is a more in-depth introduction to each of the key features of the ECM and a discussion of why these are important to consider when designing a model which faithfully represents the *in vivo* circumstances.

1.2.1 Chemical composition

The ECM is primarily composed of two main classes of macromolecules: fibrous proteins and glycosaminoglycans (GAGs) [44, 45]. The main fibrous ECM proteins are collagens, elastins, fibronectins, and laminins [46]. Together these provide structural support as well as cell attachment sites. Glycosaminoglycans, on the other hand, primarily serve as signalling co-receptors but can have a wide variety of functions that reflect their unique buffering, binding, and force-resisting properties. The ECM also contains a multitude of smaller growth factors, chemokines, and matrix remodelling enzymes. Together these confer upon the ECM its highly complex and dynamic nature.

Fibrous proteins

Collagens are the most abundant protein within the interstitial ECM and constitutes up to 30% of the protein mass of a multi-cellular organism. Whilst there is no agreed upon definition, collagens are generally regarded as triple helical proteins that have functions in tissue assembly or maintenance [47]. Collagen I is the archetypal fibrous collagen in that it is triple helical, with no imperfections, and has a predominantly structural role. It contains

three polypeptide (α) chains, each of which has a repeating Gly-X-Y sequence, where the X and Y positions are frequently occupied by proline and 4-hydroxyproline, respectively [47]. Interchain hydrogen bonding between the Gly residues produces the characteristic triple helical structure. In other collagens, imperfections in this triple helix mean that they do not always assemble into fibrils. Collagen IV, for example, contains numerous imperfections and is the prototypical network collagen. It forms an interlaced network in the basement membrane and has an important function as a molecular filtration system [48]. Collagen II contains an even greater number of imperfections which severely disrupt the triple helix and typically acts as a transmembrane protein with cell adhesive properties [47].
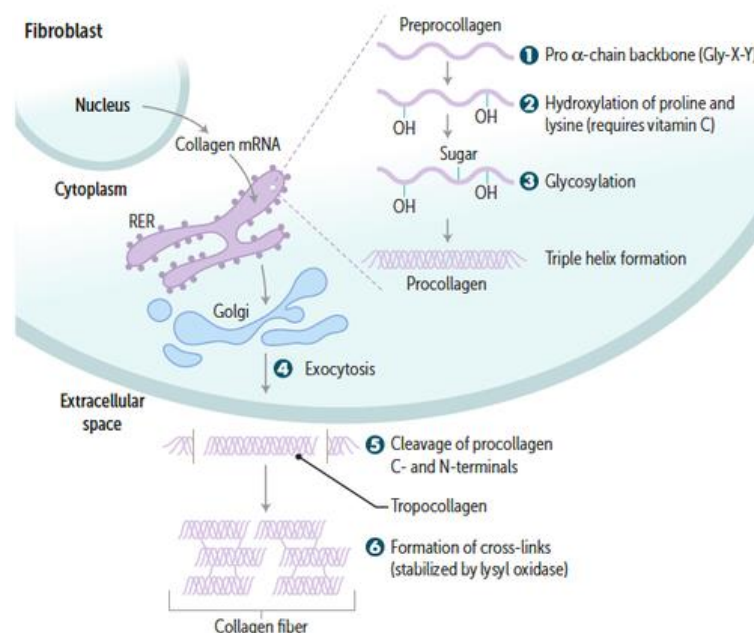
Morris, S., "Collagen synthesis and structure", *Quizlet*, https://quizlet.com/302149800/collagen-synthesis-and-structure-flash-cards/.

Figure 1 – Schematic overview of the synthesis of collagen and its formation into fibres. After translation of collagen mRNA in the rough endoplasmic reticulum (RER), it is subject to a number of post-translations modifications, including hydroxylation of proline and lysine residues, and then glycosylation of lysine residues. This allows the characteristic triple helix structure to form. It is them secreted into the extracellular space, where the N- and C-terminal propeptides are cleaved, giving tropocollagen. Formation of cross-links by lysyl oxidase then facilitate its formation into collagen fibres.

The majority of interstitial collagen is secreted in precursor form (procollagen) by fibroblasts which reside in the stroma or are recruited from neighbouring tissues [49]. Synthesis of collagen involves a number of post-translational modifications, including the hydroxylation

of proline and lysine residues, glycosylation of lysine residues, and cleavage of the N- and C-terminal propeptides [47, 48]. Collagen fibrils are then reinforced by the covalent cross-linking between lysine residues by lysyl oxidases [50] (Figure 1) .

Elastins are another major ECM fibre which provide the ECM with elasticity, allowing it to stretch when needed and then return to its original state [51]. As a result, elastin is abundant in tissues where elasticity if of major importance, such as blood vessels, ligaments, in the lung, and in skin. It primarily exists as randomly coiled, rope-like structures which interact with a variety of molecules including fibrillins, latent TGFβ-binding proteins, proteoglycans, and lysyl oxidases (LOX) [52]. Importantly, it also associates with collagen fibrils, which are responsible for the tight regulation of elastin stetch [51]. Elastin is also secreted in a precursor form (tropoelastin) by fibroblasts and is assembled into fibrils by the cross-linking of lysine residues by members of the LOX enzyme family [53]. Interactions between tropoelastin and proteoglycans such as heparan sulphate also play a pivotal role in fibre formation and stability [54].

A third fibrous protein, fibronectin, facilitates the organisation of the interstitial ECM whilst also playing a crucial role in mediating cell attachment and function. Fibronectin can be stretched several times over its resting state by cellular traction forces, thereby revealing cryptic binding sites for integrins [55]. This leads to characteristic changes in cell behaviour which implicate fibronectin as an important extracellular mechano-regulator during cell development and migration. It also contains two major heparin-binding domains that interact with heparan sulphate proteoglycans [56]. These interactions are important in directing cell behaviour and differentiation.

Glycosaminoglycans (GAGs)

Virtually all GAGs, with the exception of hyaluronic acid (HA) and Mast cell secreted heparin, exist as proteoglycans bound to the core protein at specific serine residues [45, 57]. These are produced by virtually all mammalian cells and can be found attached to the cell surface, within the ECM, or stored in secretory granules [58]. They have been classified according to their core protein, localisation, and GAG composition. The three main families are: small leucine-rich proteoglycans (SLRPs), modular proteoglycans, and surface proteoglycans [45]. The GAG chains attached to the protein core consist of long, unbranched polysaccharide chains of repeating disaccharide units which can be further subdivided into sulphated and non-sulphated GAGs [45].

Heparan sulphate proteoglycans (HSPGs) are perhaps the best studied family of proteoglycans and can be grouped into three distinct classes: syndecans, which have a single transmembrane domain; glypicans, which are attached to the cell surface via a glycosylphosphatidylinositol (GPI) anchor; and a varied group of secreted proteoglycans, such as perlecan, agrin, and collagen XVIII [59]. Interestingly, syndecan and glypican HSPGs can also be shed from the cell surface and released into the ECM, where they perform different functions [60].

All HSPGs contain one or more HS chains, containing repeating alternating N-acetyl glucosamine (GlcNAc) and glucuronic or iduronic resides, attached at specific serine residues on the core protein through a tetrasaccharide linkage region. Following chain attachment, chains are elongated by the HS-polymerase complex, consisting of the EXT1 and EXT2 enzymes. The chains can then be further modified by the action of N-deacetylase/N-sulfotransferase (NDST), epimerase, specific sulfotransferase enzymes, and sulfatases in the pericellular space. NDST enzymes convert the N-acetyl group on specific GlcNAc residues to N-sulphate, whilst epimerases modify nearby glucuronic acid residues to iduronic acid and specific sulfotransferases introduce additional sulphate groups [61-63]. However, these reactions are not carried out to completion, giving rise to the enormous structural diversity found in the sulphation patterning of mature HS chains. This diversity allows HSPGs to bind a wide variety of proteins with specificity, allowing them to influence a wide range of biological processes in a controlled and regulated manner [58, 64-66].

The classic view of HSPGs is that they primarily serve as signalling co-receptors [59]. The high degree of heterogeneity in their HS chains allows them to bind a wide variety of ligands and promote interactions with cognate receptors, thereby facilitating specific signalling events between the cell and its environment. The variable distribution and degree of sulphation of each of these HS chains during biosynthesis confers upon them incredible specificity for a particular interaction [58]. Different patterns of sulphation are therefore present in different tissue types, during development, and in different stages of disease progression. These changes can be reproduced in a variety of animal and cell-based models, providing a way to study the contribution of changes in sulphation patterning to these processes [67, 68].

One of the better studied interactions facilitated by HSPGs is the one between HS, basic fibroblast growth factor (bFGF), and its receptor (FGFR) [69-71]. In one experiment, it was found that a consequence of reducing the sulphation of HS, through treatment with 10 mM of chlorate, 3T3 fibroblasts are unable to undergo differentiation due to the abolishment of

the bFGF binding site on HSPGs, and therefore also their ability to act as co-receptors [72]. In another experiment, generation of a mutant CHO cell line deficient in HSPG binding was achieved by introducing a truncated form of FGF-2, using a retroviral delivery system [73]. In FGF-2 signalling, the formation of ternary complex between FGF-2, FGFR and cell surface HS is known to be critical for the activation of FGFR and subsequent downstream signalling [74]. Due to deficiencies in HSPG binding, these mutant CHO cells were similarly unable to undergo differentiation. Similarly, HS-deficient CHO cells which were transfected to express a low affinity FGFR, were also unable to undergo differentiation. However, in this case, it was demonstrated that exogenous HS or heparin could be provided to the culture environment to rescue the low affinity receptor, and reconstitute high affinity binding to FGF-2, restoring the ability of cells to differentiate [75]. More recently, it was also demonstrated that HS-deficient mouse embryonic stem cells (mESCs), created by knocking out the *EXT1* gene, are also unable to undergo differentiation due to a lack of HSPG facilitated FGF-2 signalling [76]. This ability could similarly be restored by exogenous HS or heparin. This general model for the requirement of HSPGs to regulate these critical factors has also been found in many other pathways, including Hedgehog, BMP, and Wnt signalling, which all require proper EXT1 function [77-79].

Additionally, HSPGs may display several other GAG chains besides HS. For example, the HPSG perlecan can also display chondroitin sulphate (CS) and its function in the growth plate can depend on this. When CS is present, perlecan acts to sequester FGF-2. When it is lost, FGF-2 is released to its receptors (FGFR-1 through 4) thereby helping to regulate chondrocyte proliferation and bone growth [80]. This dual function of perlecan, which depends on whether CS is attached or has been lost, is important to consider in the design of any *in vitro* model. Whilst it may be enough to include certain molecules as a soluble fraction, others may depend on covalent immobilisation to retain their relevant *in vivo* activity.

1.2.2 Mechanical properties

The mechanical properties of the ECM include its stiffness, porosity, insolubility, spatial arrangement, and topography. Together these determine its role in providing support to cells and its function as a barrier to physically separate distinct tissue structures. These functions are intimately linked to its chemical composition, where specific receptors and co-receptors allow signals originating from other cells or the matrix itself to be carried down signal

transduction cascades to the nucleus, resulting in changes in gene expression or other changes in cell behaviour [37].

The process whereby cells can sense and respond to changes in the mechanical properties of the ECM is called mechanotransduction [81]. The elasticity or compliance of the ECM helps determine how cells respond to external forces and thus impacts how they respond to environmental cues that direct cell behaviour. This is facilitated by the focal adhesion complex, which consists of integrins and a multitude of adaptor proteins and signalling molecules. Acting as a mechanosensory unit, it links the external ECM with the internal cytoskeleton. Many of these components undergo conformational changes in response to an applied force, thereby translating biomechanical forces into chemical ones [82, 83].

Mechanotransduction influences homeostasis in virtually every tissue type [84, 85]. Following injury, vascular damage and the formation of a fibrin clot stimulates monocyte infiltration to the damaged ECM. Cytokines and ECM-degradation products then bind to the infiltrating monocytes, causing their rapid differentiation to macrophages [86]. These activated macrophages then secrete multiple growth factors (GFs), MMPs, and cytokines which promote angiogenesis and stimulate fibroblast migration and proliferation [87]. Thereafter, recruited fibroblasts begin to synthesize and deposit new ECM products, including collagens, fibronectin, and hyaluronic acid. Under normal conditions, strict feedback mechanisms ensure restoration of normal tissue homeostasis once the wound is repopulated. In the case of severe or repeated injury, where the organisation of the ECM is completely disintegrated, these feedback mechanisms are disrupted and continuous ECM synthesis and deposition remain, leading to tissue fibrosis. A specific example of this is the case where severe tendon injury leads to the massive release of TGFβ from the ECM. This, in turn, activates the expression of the transcription factor *Scleraxis (Scx)*, via TGFβ-Smad2/3-mediated signalling. Excessive expression of *Scx* causes continuous synthesis and deposition of the pro-alpha1 chain component of type 1 collagen. These aberrant conditions promote chromic remodelling and cross-linking of the ECM, producing the altered mechanical stability and reduced elasticity that is typical of scarred tissue [88].

Disruption of normal tissue homeostasis is also characteristic of many solid tumours. In breast cancer, for example, malignant transformation is linked to an increase in stiffness, which is driven by aberrant ECM deposition and remodelling [89]. Responding to tumour associated inflammation, infiltrating macrophages begin to secrete growth factors, MMPs, and TGFβ. Secretion of growth factors supports the ability of the transformed cells to sustain

proliferative signalling through autocrine responses [90]. MMPs cause the release of sequestered growth factors and activate precursor forms of chemokines, such as interleukin-8 [91], leading to further recruitment and activation of immune cells. An overabundance of growth factors and TGFβ drives stromal fibroblast activation and their transdifferentiation to myofibroblasts. Myofibroblasts deposit copious amounts of ECM proteins, secrete further increased levels of GFs, and exert contractile forces on the ECM [49, 92]. This positive feedback loop further exacerbates the problem, leading to a continued increase in stiffness.

1.2.3 Considerations when building a model

To create a truly faithful model of the ECM, all the elements discussed above will need to be accurately represented. Firstly, it will require an underlying scaffold to allow for the reorganisation of cells into 3D structures. Then, it should be expanded to include the correct combinations of chemical components which support the viability and behaviour of cells for a particular tissue microenvironment. Whether each of these components are provided as a soluble fraction, or covalently attached to the underlying scaffold, will also need to be carefully considered to ensure that the desired *in vivo* activity is captured. The mechanical features will also need to be accurately represented, as they are intrinsically linked to its chemical composition through the multitude of signalling pathways which translate mechanical forces into chemical ones. Ideally the model should also allow for dynamic alterations to its composition and stiffness, rather than these being defined at a single point. This would allow better modelling of the dynamic nature of the ECM, which is a crucial function for tissue homeostasis, cell development, and disease progression.

1.3.0 Current *in vitro* models of development and disease

Drug discovery and investigative research has traditionally been conducted using simplistic monolayer cultures where a single monolayer of cells is adhered to a polystyrene plate [1]. These usually employ long-established continuous cell-lines that have the advantage of being easy to expand and relatively uniform. This allows for the generation of highly reproducible results, but these types of models also suffer from low cell-densities, high stiffnesses, lack oxygen and nutrient gradients, and do not accurately recapitulate the complex cell-cell and cell-matrix interactions seen in vivo. There is now a growing awareness that this a major contributing factor to the high attrition rate of novel drug candidates moving from the lab to the clinic [4]. The most compelling evidence for this is in clinical trial data, where the greatest

source of failure in phase 2 is a lack of efficacy [93-95]. This is despite the fact that efficacy would have, presumably, been robustly demonstrated in previous preclinical studies. Novel anti-cancer therapies are particularly prone to this disconnect, with the attrition rate being as high as 95% [2]. Clearly improvements to preclinical screening models, in particular for those used in cancer research, are desperately needed.

It is now generally accepted that cells grown in 3D better represent the physiological conditions that affect cell morphology, phenotype, and cell-matrix interactions [96, 97] and there are now several techniques which allow for the culture of cells in 3D. These include, for example, aggregating cells at the bottom of a drop ("hanging drop") [98], use of low-adherent plates [99-101], and using a bioreactor to drive cells to self-aggregate [102]. One of the biggest impacts of culturing cells in 3D is that it alters their sensitivity to cytotoxic compounds such as 5-fluorouracil, cisplatin, and doxorubicin [103-107]. There are several proposed mechanisms that may jointly contribute to this change in sensitivity. The first is that there may be insufficient penetration of the drugs through the cell cluster, mimicking the lack of penetration of these drugs through tumours *in vivo* which often have a poorly formed vasculature system with variable rates of blood flow [108]. The formation of a hypoxic core, and therefore the development of non-proliferative and hypoxic cells, may also contribute because these cells are often resistance to the drugs' mechanism of action [109]. The increase in E-cadherin-mediated cell-cell interactions, and associated increase in production of resistance markers such as ABCC1 multi-drug resistant efflux pumps, may also play a role [106]. This is supported by the use of antiadhesive antibodies targeting E-cadherin having been shown to sensitise tumour spheroids to chemotherapeutics *in vitro* [110]. Additionally, other physiochemical features, including temperature, pH, and oxygen have also been shown to influence drug response [111-114].

Therefore, whilst traditional monolayer culture as a model for development and disease may have been useful in the past, the growing awareness that cells grown in 2D do not accurately represent the physiological characteristics of *in vivo* tissues can no longer be ignored. This have driven the considerable research effort towards the development and optimisation of techniques which can be used to generate more physiologically relevant 3D *in vitro* models.

These 3D models are often described as being a half-way point between 2D and animal models. However, whilst animal models have been valuable tools to study human disease in the past, they nevertheless have several flaws which has driven the interest in using 3D *in vitro* models to actually replace animal models entirely. This is supported by the 3Rs

initiative, first defined in 1959 by Russel and Birch, which aims for the replacement, reduction, and refinement of the use of animals in research [115].

The primary goal of the 3Rs initiative is to completely replace the use of animals in research. Not only for ethical reasons, but also because results obtained from animal models do not always accurately predict human responses, particularly in toxicity tests for novel pharmaceuticals [116]. These results are also less reproducible compared to results obtained *in vitro* [117], due to a variety of uncontrollable variables in animal organisms [118]. There are also economic considerations, due to the high cost of conducting animal studies, which may drive the adoption of alternative 3D *in vitro* models [119]. In addition, animal studies are also time-consuming and require specific training and licensing to carry out [120]. Despite these reasons, animal studies continue to be an essential part of the drug discovery process that is required by regulatory authorities worldwide [121]. Changing this in the future will require of body of evidence to convince policymakers that 3D *in vitro* models can outperform animal models in preclinical studies. Therefore, in the short- and medium-term, reducing and refining the use of animals in research should be the current goal, until technology can securely surpass animal models in predictive power. This may be achieved, in part, by the development of innovative 3D *in vitro* models that are better able to stratify novel drug compounds prior to animal studies, allowing unsuitable drugs to "fail fast and fail cheap".

1.3.1 Sources of cells

The development of *in vitro* models for human development and disease hinges on the availability of tissue- and organ-specific cell types that accurately represent their *in vivo* phenotypes. To date, this has relied on established cells lines or primary cells derived from patients. Although primary cells are more representative of the tissues from which they are derived, they are difficult to obtain, have limited lifespans, and are poorly characterised. Established cell lines, on the other hand, are relatively easy to obtain, can be expanded easily, cultured indefinitely, and are relatively uniform.

Induced pluripotent stem cells (iPSCs) are a type of established cell line which offers enormous potential for studying human development and disease *in vitro*. Human iPSCs can be generated from somatic cells by overexpression a few key transcription factors [122, 123]. They can be generated from patients with or without specific disease conditions and the resulting cells can self-renew indefinitely. Under the appropriate conditions, these cells can then be directed to differentiate into virtually any other cell, offering a potentially unlimited

supply of cells for use in tissue engineering and modelling applications. However, these specialised cells invariably retain some aspects of their immature phenotype [124]. Whilst these cells may be relevant for studying the early stages of development or early-onset disease processes, it is less clear whether results can be accurately extrapolated to diseases in fully developed, adult tissue. Therefore, a more robust approach is needed to not only direct iPSCs to differentiate but also to facilitate their maturation into more adult-like cells. This will require a careful examination of the exact biochemical and biophysical cues that are necessary to drive this maturation, and to capture those cues using more advanced culture techniques. This could include the use of biomimetic scaffolds, bioreactors, organ-on-a-chip systems, or other techniques which allow cells to be grown in 3D and be presented with the necessary biochemical and biophysical cues.

Embryonic stem cells (ESCs) represent another class of established cell lines which also have the advantages of pluripotency and indefinite self-renewal [125]. The first ESCs to be established were derived from mouse preimplantation embryos in 1981 [126, 127], which was followed by the establishment of a human line derived from blastocysts in 1998 [128]. As the use of human embryonic stem cells is a tightly regulated area, animal derived embryonic stem cells are often used in their place. As mammalian genomes are highly evolutionary conserved, animal models such as mice, rats, and non-human primates have proved invaluable tools to study human development and disease. An example of this is provided by the Ext1$^{-/-}$ mESC line. In humans, loss of function mutations in *exostosin-1* (*EXT1*) and *exostosin-2* (*EXT2*) are the underlying cause of hereditary multiple exostoses (HME), which is characterised by the presence of multiple exostoses (osteochondromas) [129]. Their role in the synthesis of HS was first identified in two independent studies in 1998 [130, 131], with mutations in *EXT1* or *EXT2* causing a reduction of HS in cell-surface and matrix proteoglycans. This impacts a number of critical signalling events involved in proper skeletal development such as FGF, BMP, and WNT distribution [132]. Mouse models with mutations in homologues for the human *EXT1* gene, such as Ext1$^{-/-}$ mESCs, offers a convenient tool to study not just this disease but also other HS-dependant signalling events.

There also exists a huge variety of established human cancer-derived cell lines. The first cultured cancer cell line (HeLa) was derived from cervical cancer cells taken from Henrietta Lacks in 1952 [133]. Since then, hundreds more have been established and propagated, typically as monolayer cultures. Whilst they have proved useful as a fundamental tool to the study of cancer cell biology and as preclinical screening models for novel anticancer agents, they have drawn criticism for not accurately representing cancer *in vivo* [134], which is

perhaps why so many initially promising drug candidates fail when moving from preclinical trials to the clinic.

Another important consideration to make when selecting the right source of cells during the design of a 3D *in vitro* model, is that *in vivo* tissues are comprised of a varied mixed of cell types. This is of particular importance in the design of *in vitro* cancer models, where ability of the tumour stroma to influence drug sensitivity through paracrine interactions is well established [135-140]. To address this issue, investigators may combine different cell types in the preparation of 3D models, such as by mixing suspensions of tumour cells, fibroblasts, and immune cells prior to the generation of 3D tumour spheroids. The resulting multi-cellular/co-culture spheroids are better able to recapitulate the heterotypic cross-talk that occurs between tumour cells and stromal cells *in vivo*. This has been shown to lead to the formation of a more compact 3D cell cluster which, as previously discussed, influences drug sensitivity due to changes in drug penetration [108, 141]. This cross-talk has also been shown to influence gene expression changes in the tumour cells that lead to changes in their rate of proliferation and migration [136, 139, 142]. Therefore, wherever possible, investigators should attempt to include all the resident cell types of the tissue type being studied, to create a more representative *in vitro* model.

1.3.2 Spheroids

There are several approaches that have been used successfully to establish spheroid culture, including using low-adhesion plates, using the hanging-drop method [143], using a bioreactor to drive cells to self-aggregate [144], and using micro- or nano-patterned surfaces as scaffolds to support cell aggregation in defined geometries [145] (Figure 2). Regardless of the approach used, the resulting spheroids which form compensate for many of the shortfalls of monolayer culture, allowing closer recapitulation of the *in vivo* tissue microenvironment. Spheroids grow as three-dimensional clusters of cells which exhibit oxygen and nutrient gradients, creating heterogeneous cell populations (e.g., hypoxic vs normoxic, quiescent vs. replicating). Because of this, spheroid models exhibit similar drug resistance patterning to their *in vivo* counterparts, exemplified by the resistance of MCF7 breast cancer cells cultured as 3D spheroids to the chemotherapeutic doxorubicin [146]. They also have well-defined geometries and can synthesize their own ECM which enables recapitulation of native cell-cell and cell-ECM interactions [97]. Finally, the gene expression profiles of tumour spheroids have been reported to be resemble their parent tumours more closely than monolayer

cultures. This was demonstrated by comparing chromosomal copy number variations in primary cell and spheroid culture and then relating them to their parental tumour [147]. However, there are several practical challenges associated with spheroid culture. Difficulties arise when trying to maintain spheroids of uniform size, when trying to form spheroids from a small seed number, or when attempting to precisely control the ratio of cell types in co-culture models [1]. This limits their potential for development into high-throughput compatible assays.

A.

B.

C.

D.
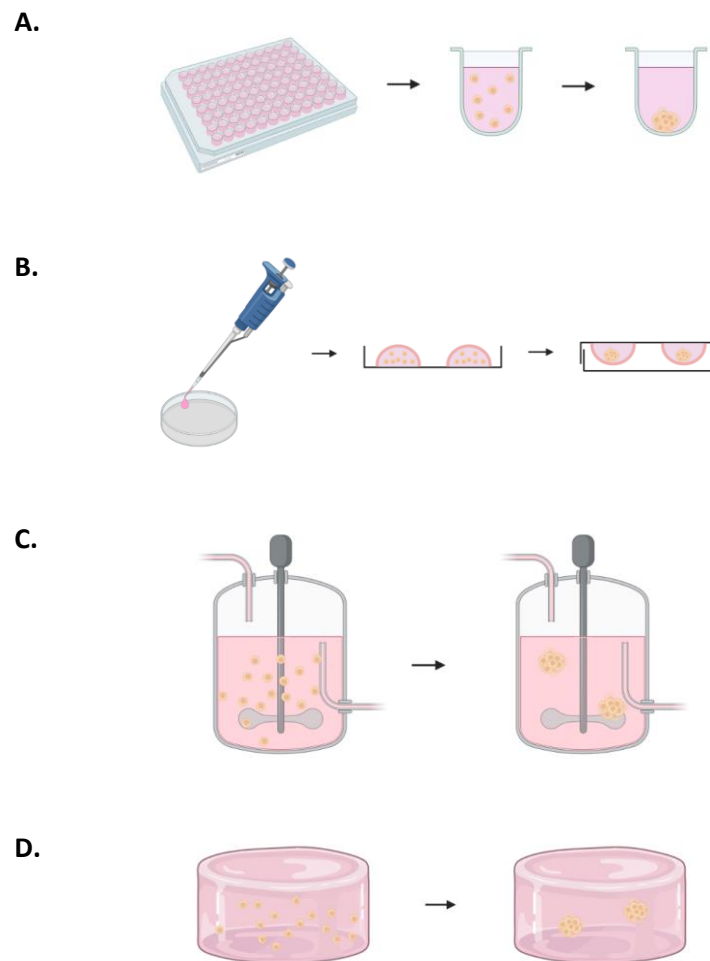
Figure 2 - Summary of methods for generating multicellular spheroids. (A) Use of low-adherent plates. A small number of cells are seeded into each well of a non-tissue culture treated well plate where they fall to the bottom form aggregates. (B) The hanging drop method. Cells are suspended in droplets that are added to the lid of a petri dish (or similar) and then carefully inverted. Spheroids fall to the bottom of each droplet where they form aggregates. (C) Spinner suspension culture. Suspended cells are continually agitated in a bioreactor until they spontaneously form cell aggregates. (D) Use of micro- or nano-patterned scaffolds. Cells are embedded in biomaterials where they grow into 3D structures.

1.3.3 Organoids

Organoids are three-dimensional, organ-specific tissue structures derived from adult stem cells (ASCs), embryonic stem cells (ESCs), or induced pluripotent stem cells (iPSCs). Such structures self-organize through cell sorting and spatially restricted lineage commitment in a manner similar to that observed *in vivo* [148]. There are several approaches available to achieve this. The first is to culture cells as a monolayer on a bed of feeder cells or on plates coated with ECM components so that the cells form organoids after they differentiate. The second is to seed them into a matrix that mimics the essential aspects of the niche in which the cells normally reside and then coax their differentiation and organisation by providing appropriate signalling conditions that target key regulatory conditions [149]. The third is to use low-adhesion plates or the hanging drop method in a similar manner to spheroid culture (Figure 2a-b).

Regardless of the method used, the resulting organoids can mimic some, but not all, of the physiological characteristics or their respective organs. They typically lack vasculature, which makes it difficult to correctly model the nutrient and oxygen gradients which exist within organs *in vivo*. However, recent advances have allowed the generation of some vascularization in kidney organoids by growing them in the presence of shear stress from the application of fluid flow [150]. They also suffer from considerable variability in organoid formation efficiency, have limited lifespans, and often contain a heterogenous mix of cell types that is not representative of the *in vivo* organ state. All these issues limit their usefulness in disease modelling, drug screening, and regenerative medicine.

1.3.4 Gastruloids

Gastruloids (also sometimes called "stembryos" [151]) are 3D aggregates of embryonic stem cells that recapitulate the axial organisation of post-implantation embryos [152]. The first protocol for the generation of gastruloids demonstrated that mESCs could be coaxed into forming elongating aggregates, containing derivatives of all three germ layers, which exhibit clearly defined anterior-posterior, left-right, and dorsal-ventral body axes [153, 154]. In the years that followed, improvements to the protocol have allowed generation of more complex models that are able to generate brain [155], somite [156, 157], neural tube [157], gut tube [157, 158], and beating "heart-like" structures [159] (Figure 3a). Recent advances

have also allowed the generation of human gastruloids, using human embryonic stem cell-based elongating mesodermal embryoid bodies [160] (Figure 3b).

The original mouse protocol involves seeding low numbers mESCs into low adherent plates with N2B27 neural differentiation medium. Cells sink to the bottom and form aggregates during the first 48 h. Upon treatment with the Wnt-agonist Chiron, they then break their symmetry and elongate at 4-5 days post-aggregation (Figure 3a). This process is thought to be reminiscent of the process of gastrulation that occurs during embryogenesis. This offers a way for researchers to study a process which is often difficult to observe *in vivo*. Moreover, it also allows investigation into the effects of knocking-out certain critical genes (such as *EXT1*) which are usually embryonic lethal [161].

However, the observation that these aggregates can form axially organised embryo-like structures in the absence of extraembryonic tissues challenges the long-standing paradigm that the prerequisite symmetry breaking relies on the gradient of signalling molecules they provide [162]. There are two possible explanations for this: either the role of the extraembryonic tissues is not to induce symmetry breaking but to ensure that it happens in the correct spatial position relative to the implantation site [153], or that gastruloids are able to break their symmetry through a mechanism that is not representative of *in vivo* circumstances.

To discern which explanation is most likely, future experiments where gastruloids are cultured in the presence of extraembryonic tissues, or an analogue of this tissue, with a localised source of Wnt antagonists, may help further elucidate the underlying mechanisms at play. Two independent studies conducted recently discovered that the formation of somite [156, 157] and neural tube-like [157] structures can be induced by embedding mouse gastruloids in low (5-10%) percentage Matrigel® at the 96 h timepoint. However, it is unclear whether the observed somitogenesis is due to the effect of a chemical component of the gel or whether the gastruloids are responding to the mechanical forces that are being exerted on them.
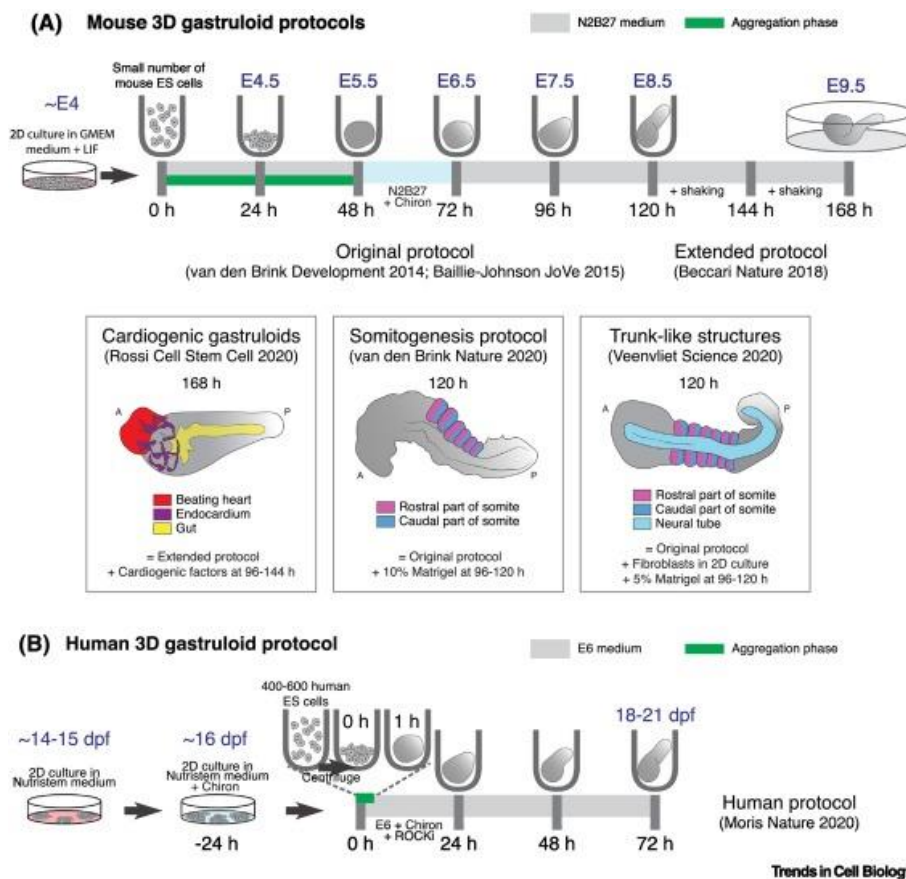
Figure 3 - Overview of currently available mouse and human 3D gastruloid protocols. (A) Mouse gastruloids are generated by seeding low numbers (150-160 per well) of mouse embryonic stem cells (mESCs) into a non-tissue culture treated U-bottomed 96-well plates in N2B27 neural differentiation medium. Cells sink to the bottom and form aggregates during the first 48 h. Upon treatment with the Wnt-agonist Chrion (StemCell, CHIR99021) the aggregates break their symmetry and elongate at 4-5 days post-aggregation. Mouse gastruloid culture can be extended by transferring to a shaker at 120 h. Formation of a morphologically correct beating "heart-like" structure can be induced by addition of cardiogenic factors (bFGF, ascorbic acid, VEGF165) and develops in close proximity to a gut-like structure from which it is separated by an endocardium-like layer. (B) Human gastruloids are generated by aggregating human embryonic stem cells (hESCs), pre-treated in 2D with Chiron for 24 h, and then cultured in the presence of Chrion and ROCKi. (Abbreviations: A, anterior; dpf, days post fertilization; E, embryonic day; h, hours after aggregation; LIF, leukaemia inhibitory factor; P, posterior).

1.3.5 Organs-on-Chips

An organ-on-a-chip refers to an artificial, miniature model of a human organ on a microfluidic cell culture chip. These chips consist of a series of intricate, well-defined structures, patterns, or scaffolds that are precisely created using microfabrication techniques such as soft lithography, photolithography, and contact printing [163]. This allows a high degree of

control over the position, shape, and the chemical/physical microenvironment of cells in culture. Microchannels in the chip also allow the precise control of concentrations of additional molecules of interest via microfluidics [164]. All these features combined allow researchers to reconstitute the structural and functional complexity of organs in miniature, with a wide range of organs-on-chips having been reported including heart [165], lung [166], skin [167], and intestine [168]. However, organs-on-chips are practically challenging to design, difficult to maintain, and are not currently amenable to high throughput. However, as technology improves, allowing for faster and more advanced microfabrication techniques, organs-on-chips may prove a promising new tool for high throughput drug screening assays in the future.

1.3.6 Scaffolds & Hydrogels

Scaffolds and hydrogels refer to a large variety of biocompatible materials with different porosities, permeability, surface chemistries, and mechanical properties designed to mimic the microenvironment of specific tissues. These can be broadly separated into two categories: biologics and synthetics. Biological scaffolds are comprised of naturally derived ECM components extracted from cells or tissues, whilst synthetics are typically comprised of lab-created materials. There is also an emerging class of products that sits somewhere between these two definitions, which is that of the non-animal derived biological materials. Here, recombinant technology is used to express mammalian proteins or glycans in bacteria, yeasts, or insect cells. This method hopes to achieve a "best of both worlds" solution, where relevant mammalian levels of bioactivity are represented, whist offering the ability to produce these materials at scale. Each of these classes of biomaterial have their own set of advantages and disadvantages, which are discussed in more detail below.

Biological scaffolds

Biological scaffolds range in complexity, from multicomponent matrices derived from cells or tissues (e.g., Matrigel®) to matrices composed of individually extracted and purified ECM components or recombinant fragments (such as those produced by BioLamina®). Each aims to recapitulate the native ECM in a more physiologically relevant way, by providing cells with material of natural origin.

Perhaps the most famous example of a biological scaffold is the commercially available Matrigel®, which is derived from EHS mouse sarcoma and contains several components of the basement membrane enriched with laminin. These components include soluble growth

factors, hormones, and other molecules which a large variety of cells are likely to interact with *in vivo* [169]. However, Matrigel® is limited in its application to investigative research and drug discovery, due to its highly complex, poorly defined, and variable composition [6, 7, 170].

Inconsistencies in the biochemical properties between and within batches of Matrigel® have led to uncertainty in interpreting results obtained in cell-based experiments. Numerous proteomic studies have now been conducted which reveal consideration variability, with each new study discovering proteins which had previously not been identified [12, 171-173]. Additionally, the biomechanical properties are also prone to batch-to-batch variability. Whilst some of this can be attributed to differences in handling [174-176], there has also been inherent differences in the mechanical properties of Matrigel® even within a single batch [177, 178]. These variations in both its biochemical and biophysical properties impact the reproducibility of any results obtained in cell-based experiments.

Additionally, the fact that Matrigel® is derived from mouse sarcoma presents another problem. Whilst it contains many of the factors that cells are likely to encounter *in vivo*, it also contains a variety tumour-derived proteins including TGFs, FGFs, and MMPs [11, 12]. The presence of these factors possibly makes Matrigel® unsuitable as an ECM mimic for modelling healthy tissue.

Its animal-derived origin also raises further issues when it is being used to study human conditions. The introduction of xerographic contaminants from animal-derived ECM can limit the potential to use cells cultured in Matrigel® for therapeutic purposes. For example, it is now understood that animal-derived ECM products, including Matrigel®, are prone to contamination with viruses such as lactate dehydrogenase-elevating virus (LDHV) [13, 14]. LDHV is a murine virus which is known to infect macrophages and interfere with a variety of biological processes including immune activity, drug response, and tumour behaviour [15].

There is also the question whether any animal-derived product could ever truly replicate the specific ECM of a human tissue in a faithful way. Whilst mammalian genomes are highly conversed, with humans and mice sharing approximately 80% of the coding regions of genes [179], there are a few key differences which may cause issues. For example, one such difference is that there is no mouse ortholog for human interleukin-8 (IL-8) [180]. IL-8 is a chemokine that is secreted by various cells of the immune system and one of the major contributors to the inflammatory response [181]. As this is not represented in mice, we must

ask whether it is appropriate to study the inflammatory response of human cells encapsulated within a mouse-derived ECM product.

Other natural gels include those composed of collagen, hyaluronic acid, fibrin, alginate, or silk fibres. Gels comprised of a single ingredient are better defined and make it easier for researchers to query the biological roles of specific molecules. For example, hydrogels based on collagen can be combined with purified laminin or fibronectin to better recapitulate some of the aspects of normal and diseased ECM [182, 183]. By varying the amount of these materials, it is possible to assess what the minimum essential conditions are which are required to drive certain observed behaviours. In a study of this kind, collagen-based gels enriched with different laminins (laminin-1, -5, and -10/11) were used to pinpoint the minimal conditions required to impart the correct polarity to encapsulated luminal epithelial cells. This process had previously been demonstrated to be reliant on the co-culture of laminin-producing myoepithelial cells, but this study revealed that laminin-1 alone could support this behaviour [183]. Moreover, collagen can be chemically or enzymatically cross-linked, producing gels which can model a range of tissue stiffnesses. This is particularly useful in modelling diseases like fibrosis and cancer, where increasing ECM stiffness is associated with disease progression. However, collagen gels are quite heterogeneous, and cross-linking as a strategy to alter gel stiffness may mimic the aberrant cross-linking of collagen seen in other diseases not being studied [50]. Cross-linking also causes changes in porosity and ligand concentration, further complicating interpretation of data gathered using these and similar gels.

Synthetic scaffolds

The limitations of biological scaffolds, and in particular Matrigel®, has driven the search for synthetic alternatives which can be customised for tissue-specific investigations. These artificial matrices use synthetic hydrogels or other biocompatible scaffolds to generate the physical supports for the attachment and reorganisation of cells into 3D structures. These types of scaffolds promise to deliver more clearly defined and tuneable compositions, organisation, mechanics, and ECM remodelling capabilities.

Polyethylene glycol (PEG) is one the best studied and widely used materials in the construction of synthetic scaffolds that support the adhesion, viability, and growth of cells in 3D [18-20]. This material has the advantage of being hydrophilic, bioinert, and highly amenable to chemical modification [24]. It can therefore be modified with a variety of functional groups and formed into hydrogels using various polymerization techniques

including photopolymerization [184], *Michael*-addition reactions [185], or enzymatic reactions [28]. However, the resulting architecture of these gels does not always accurately recapitulate that of the ECM *in vivo*. To address this issue, collagen mimetic peptides (CMPs) can be conjugated to PEG which increases its retention of cell-secreted collagens and allows it to form physical cross-links which more accurately represent that of the collagen hydrogel present in the native ECM [25].

PEG-based matrices also allow for covalent modification with ECM ligands and growth factors, via a biocompatible *Michael*-addition reaction [28-30]. For example, Licht et al. [30] recently demonstrated an enzymatically cross-linked PEG-based gel could be functionalised with a recombinant fibronectin (FN) fragment to provide cell adhesive and growth factor binding domains. This modification was also shown to support neurite outgrowth from the dorsal root ganglion structure of encapsulated nerve cells. These types of gel can also be combined with hyaluronic acid (HA) by transglutaminase-mediated covalent linking of HA moieties to the PEG macromer, resulting in a hybrid HA-PEG hydrogel [186]. These types of gels bridge the gap between biologics and synthetics, and have been shown to modulate the phenotype of human mammary cancer epithelial cells and mouse myofibroblasts [186].

Other commonly used synthetic scaffolds include those comprised of poly(lactic-co-glycolic acid) (PLGA), polylactic acid (PLA), poly(ε-caprolactone) (PCL), and polyurethanes (PU) [21-23]. However, in contrast to PEG-based hydrogels, scaffolds comprised of these materials are biodegradable, making them generally more suitable as implantable medical devices rather than for *in vitro* modelling. PLGA-based scaffolds have nontoxic degradation products (i.e., lactic acid and glycolic acid) [187, 188], which has made PLGA a popular source of material for medical devices such as biodegradable sutures and tissue engineering scaffolds [189]. Porous PLGA scaffolds have also been shown to promote host vascularization and cell infiltration upon their *in vivo* implantation [190, 191]. PCL-based scaffolds are also biodegradable *in vivo* but at a much slower rate, typically on the order of months to years depending on the specific configuration [187, 188, 192, 193]. This material is therefore more useful in instances where an implantable device must remain in the body over a longer period of time, such as for long-term drug delivery. PU-based scaffolds, which are formed by the linking of isocyanate and hydroxyl group containing compounds via urethane bonds, may also incorporate numerous other potential chemical moieties, such as polyesters, carbonate, urea, and ether functional groups. Such modifications can be used to control *in vivo* degradation rate, mechanics (including stiffness and porosity), and hydrophobicity [194]. PU-based scaffolds are, therefore, particularly useful in skeletal muscle tissue engineering,

where tight mechanical and structural control is necessary to promote the correct phenotype and behaviour of myoblasts and myocytes [195].

Self-assembling peptide hydrogels (SAPHs) are another class of synthetic scaffolds comprised of peptides with alternating hydrophobic and hydrophilic amino acid residues. Under the right conditions, this allows them to self-assemble into distinct nanostructures [196, 197]. The first SAPH was discovered in yeast [198] and its peptide sequence (AEAEAKAK) has since inspired the design of other peptides capable of self-assembly and gelation [199-202]. One such SAPH is RADA16, which boasts comparable results in supporting cell viability to naturally-derived hydrogels such as Matrigel® [203], and its commercialisation to PuraMatrix™ has made it one of the most widely used SAPH in investigative research today. It is comprised of 16 amino acids in a repeating R (positively charged arginine), A (hydrophobic alanine), and D (negatively charged aspartic acid) sequence. The presence of hydrophobic amino acids and positively charged sequences along the peptide allows spontaneous self-assembly into stable β-sheet nanofibers in aqueous acidic environments [204-206], and the resulting 3D structure of the hydrogel closely resembles the 3D architecture of the native ECM [32]. However, it is also difficult and costly to synthesise [207] and recent studies have cast doubt over the stability of its structure in response to temperature and pH changes [208].

To create a better 3D *in vitro* model, the more physiologically relevant 3D architecture of peptide-based hydrogels should be combined with the customisation options available to PEG-based gels. In a recent study [33], a self-assembling peptide hydrogel model, based on the octapeptide gelator FEFEFKFK (Phe-Glu-Phe-Glu-Phe-Lys-Phe-Lys), has been presented as a potential candidate which contains this architecture and allows for customisation of matrix composition. This study laid the foundation for the research carried out as part this project and, as such, is discussed in more detail below.

1.4.0 FEFEFKFK

The SAPH FEFEFKFK offers a competitive advantage over longer SAPHs as it is cheaper to synthesise, thus providing a more cost-effective approach to building biomimetic models for research. Its success in 3D culture has also already been established and a wide variety of cell types have been shown to be viable when encapsulated within gels of this type [33, 209-212]. This model also currently offers the ability to customise biophysical and biochemical

properties of the gel to suit specific research needs. Below is an overview of the peptide hydrogel preparation process and current avenues for customisation.

1.4.1 Controlled gelation produces a fully-defined environment

The peptide hydrogel preparation process is primarily a two-step process, but offers multiple points at which customisation of the final model can be achieved, as illustrated in Figure 4a. The first stage involves dissolution of peptide powder, which also offers the first opportunity for customisation. By varying the mass of peptide used, and thereby the final peptide concentration, the stiffness (G') of the final gel can be fine-tuned by the user and currently offers a range of between 0.4 and 2.4 kPa. Gelation of this initially acidic peptide solution is then triggered by an increase in pH and temperature until the solution becomes optically clear and self-supporting. This process involves the self-assembly of the gelator peptide molecules into β-sheet nanofibers which then entangle above a critical gelation concentration (Figure 4b) [204-206].

The second stage in the process is neutralisation of this precursor gel by addition of cell culture media. It is at this stage that the model currently offers the second opportunity for customisation, by incorporating soluble matrix components and cells of interest within this medium. This suspension of soluble matrix components and cells is encapsulated within the gel by the combined action of mixing and gentle reverse-pipetting. Because the precursor gels are colourless and optically transparent, whilst most culture medium is red/pink in colour due to the presence of phenol red, this mixing is performed until the gels are homogeneously pink in colour, thereby also ensuring a homogenous distribution of soluble matrix components and cells throughout the gel. The peptide hydrogel can then be plated out, where it is washed several times in media to achieve total neutralisation. The cells encapsulated within these gels are then able to self-organise into 3D structures and exhibit behaviours which more faithfully recapitulate the *in vivo* circumstances, in an environment where the biophysical and biochemical properties of the model are fully-defined.

: β-sheet forming peptide
CGC : Critical gelation concentration
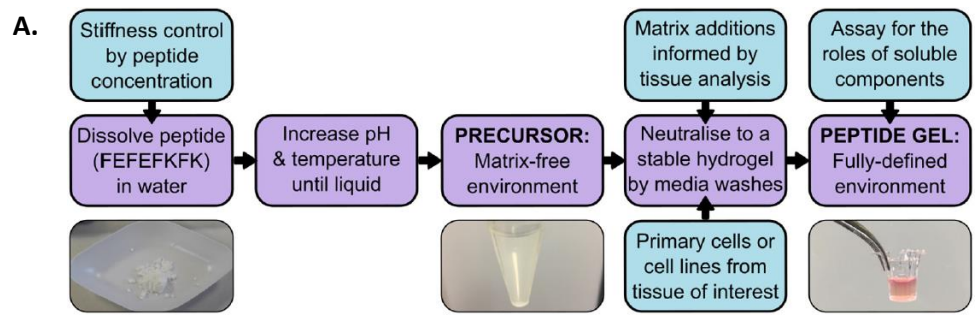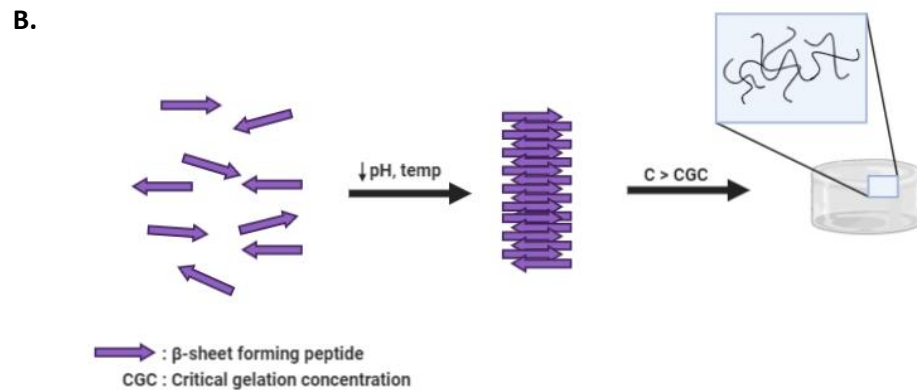
Figure 4 - Schematic illustration of the peptide hydrogel design and gelation process. (A) Initial formation of cell-and matrix-free precursor gel is achieved by dissolution of FEFEFKFK peptide powder in water and subsequent pH- and temperature-controlled gelation. Final gel formation is then accomplished by neutralisation with cell culture media. Functionalisation is currently achieved by inclusion of soluble matrix components during neutralisation. (B) Control of pH and temperature causes dissolved peptides to self-assemble into β-sheet nanofibers which then entangle above a critical gelation concentration to form precursor gels.

1.4.2 Independent control of matrix stiffness

As previously mentioned, a significant advantage to the peptide hydrogels is that their mechanical properties may be altered with no change in matrix composition, simply by controlling the amount of peptide added to the precursor gel. This approach can be used to create gels with a range of stiffnesses, with average elastic modulus (G') values spanning from approx. 0.4 to 2.4 kPa (Figure 5a). This allows a variety of host tissue stiffnesses to be modelled and is also representative of the increase in stiffness seen in the disease progression of breast cancer [89]. This gives it a clear advantage over other types of hydrogel products which either do not offer ways to alter their stiffness (e.g., Matrigel®, which has a G' value of approx. 450 Pa) or where altering its stiffness also requires changes to the composition or architecture of the gel network (e.g., cross-linking of collagen-based gels [213]).

To demonstrate the utility of this feature, a study was conducted to determine whether the viability of different breast cancer cell lines, representing different stages of malignancy, was related to matrix stiffness by encapsulated them within peptide hydrogels of varying stiffnesses [33]. Three different cell lines were chosen: MCF10A (non-tumorigenic, normal breast), MCF10DCIS (ductal carcinoma *in situ*, pre-invasive), and MCF7 (invasive breast cancer). These cells were encapsulated within gels of varying stiffnesses, cultured for seven days, and subjected to a cell viability assay. The results demonstrated that the more malignant the cell type, the greater its viability in the gels, with only the most invasive strain (MCF7) being viable across all conditions (Figure 5b).

Image taken from: Ashworth, J.C. et al., 2020
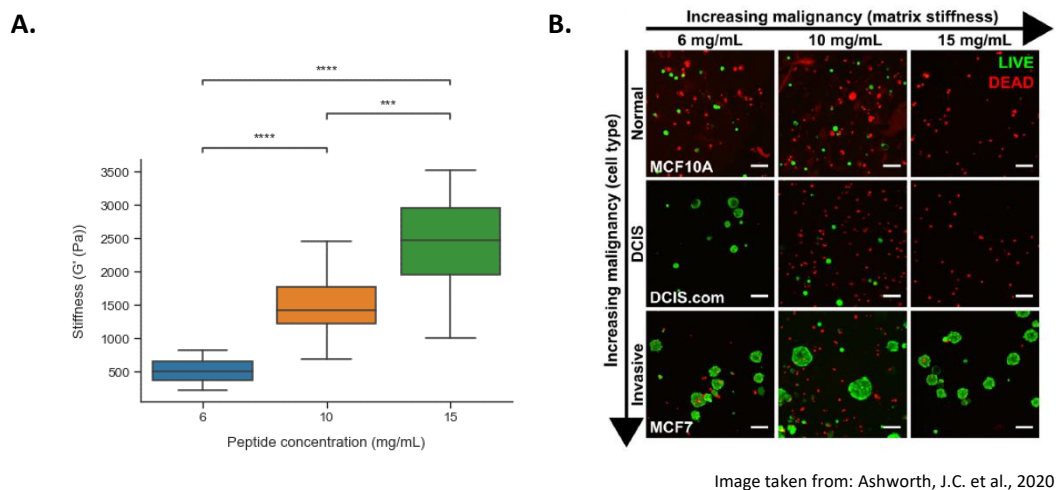
Figure 5 - Increasing peptide hydrogel concentration leads to corresponding increase in stiffness. (A) Box plots showing G' results of increasing peptide concentration of gels measured via bulk oscillatory rheology (compared via independent t-test; n ≥ 17; ***: p < 0.001, ****: p < 0.0001). (B) LIVE/DEAD staining of breast cell lines MCF10A, MCF10DCIS, and MCF7 in peptide hydrogels of increasing stiffness. Scale = 100 µm.

At the start of this project, the peptide hydrogel model offered only a single point at which the tuning of gel stiffness could be achieved. One of the aims of this project was to evaluate and trial methods to dynamically alter gel stiffness on demand, to better model the increasing stiffness associated with diseases such as cancer within a single experiment. Such methods have demonstrated in the past and is exemplified by the sortase-mediated dynamically tuneable gels recently developed by Arkenberg et al. [214]. They used an enzymatic approach to reversibly cross-link a functionalised PEG-based hydrogel, providing

a way to dynamically stiffen and soften the gels on-demand during a single experiment. It remained to be seen, however, whether this approach could be adapted to the peptide hydrogels.

1.4.3 Control of matrix composition

Whilst the matrix-free environment of unfunctionalised "blank" peptide hydrogels allows users to investigate the effect of matrix stiffness in the absence of any chemical signals coming from the scaffold itself, it is sometimes necessary or beneficial to include certain matrix components. These components may be required by specific cell types for their viability within the gels or to promote specific behaviours which may be the subject of study.

For example, in a previous study, specific matrix additions were found to be essential to support the growth of the breast cell line MCF10A within the peptide hydrogels. Matrigel®, collagen I, hyaluronic acid (HA), and a combination of both collagen I and HA were all tested. In contrast to unfunctionalised gels, MCF10A growth was supported in all the modified conditions. However, it was also found that the formation of the classic polarised single-cell layer acini, previously observed using 100% Matrigel® [215, 216], only occurred in gels functionalised with 10% Matrigel and not in other conditions. As the stiffness of 100% Matrigel® and gels functionalised with 10% Matrigel® was found to be similar, this indicates that there is an additional chemical component beyond just collagen I and HA that is required to promote this effect.

In the same study, it was also discovered that when human mammary fibroblasts (HMFs) were encapsulated in unfunctionalised gels they did not exhibit their characteristic contracted phenotype, as evaluated by measuring their macroscopic morphology and staining for activated focal adhesion kinase. Focal adhesion kinase (FAK) is a non-receptor tyrosine kinase that acts as a central node in signalling networks which arise from focal adhesions. Focal adhesions are multi-protein complexes which mediate cell contact with the matrix and relay information between the cell and its environment [217]. By contrast, when gels were functionalised with collagen, cells began to adopt a more typical contracted phenotype in a dose-dependent manner.

1.4.4 Issues and limitations

In the previous work by Ashworth et al. [33], functionalisation of the gel was achieved by simply stirring in the desired matrix additions. This may present a number of potential issues

in future applications. The first is that smaller soluble matrix additions may diffuse out of the gel and into the surrounding cell culture medium, where they would then be lost during media changes. Therefore, to maintain the correct concentration of matrix additions within the gel, those same additions would also need to be included in the culture media. However, this is wasteful and doesn't solve the second issue with soluble additions.

The second issue is that the biological activity of soluble matrix additions may not accurately recapitulate their proper biological relevance. For example, proteins containing the Arg-Gly-Asp (RGD) motif, such as fibronectin and collagen, together with the integrins that serve as receptors for them, constitute a major recognition system for cell adhesion and signalling [34]. These interactions can be reproduced by short synthetic peptides containing this sequence. RGD functionalised materials have, therefore, been the subject of numerous past academic studies and medical applications [218]. However, recent studies have revealed that the activity of these synthetic peptides can depend on how they are presented to cells. In one such study, it was shown that the presence of an RGD-containing peptide could support the differentiation of mESCs to neural progenitor cells (NPCs) but only when it was covalently attached to a nanofiber substrate and not when it was provided in solution [219].

These issues highlight the need for the development of new methods for functionalisation which would allow matrix additions to be covalently immobilised within the gel network. This would not only solve the issue of those additions potentially being lost during media changes but also allow users to select the most appropriate method for functionalisation which would preserve their correct *in vivo* biological activity. Several potential methods for this were the focus of this project and are discussed in more detail in the following sections.

Another apparent issue with the gels that was encountered during this project was that the effectiveness of DAPI to stain for DNA within the gels could be inconsistent. Following fixation and staining of cells within gels, several images obtained using a scanning laser confocal microscope showed weak staining for DNA when DAPI was used. The use of Hoechst was later shown to be more effective for staining DNA in the gels and is now the preferred method. The reason for this difference remains unclear, but it has been hypothesized that the enhanced cell membrane permeability of Hoechst allows it to penetrate further into the tight cell clusters that arise when culturing cells in 3D within these gels.

1.5.0 Sortase-mediated functionalisation

Sortases are transpeptidase enzymes that are found in the cell envelope of many Gram-positive bacteria, where they are responsible for anchoring surface proteins to the bacterial cell wall [220]. The most widely studied is sortase A (SrtA), which was first identified in *Staphylococcus aureus (S. aureus).* SrtA exists as a membrane-bound extracellular enzyme and is responsible for the covalent attachment of surface proteins with the recognition sequence LPXTG (X = any amino acid, except proline) onto oligoglycine functionalities in the peptidoglycan cross bridges of the bacterial cell wall, via a two-step transpeptidation [221, 222]. First, the cysteine residue in the active site of SrtA nucleophilically attacks and cleaves the peptide bond between threonine and glycine in the LPXTG motif, forming a thioacyl bond within the LPXT-SrtA complex, while the glycine is cleaved. This intermediate is then resolved by a further nucleophilic attack of an N-terminal oligoglycine, forming a peptide bond between the carboxylic acid of the threonine in LPXT and the amino group of the oligoglycine. This reaction scheme is presented in Scheme 1.
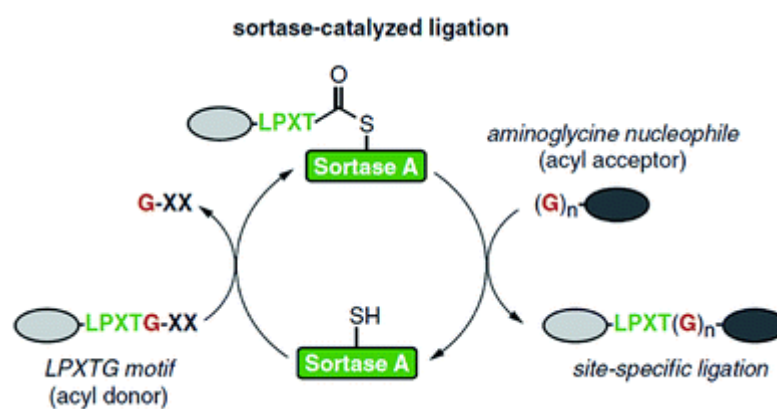
Image taken from: Xiaolin, D. et al., 2019

Scheme 1 - Catalytic cycle of sortase-mediated ligation, involving the formation of the thioacyl intermediate and subsequent nucleophilic attack by oligoglycine.

There has been a growing interest in utilising SrtA for site-specific covalent attachment of proteins to solid supports and surfaces, with multiple papers published which use this enzyme to attach proteins to different biomaterials, including hydrogels [223-225]. The high selectivity towards specific recognition sequences, the commercial accessibility of all required compounds (including several commercially available SrtA variants), and the

simplicity of performing the reaction have all contributed to its current interest. Furthermore, the recognition sequences are extremely rare within proteins of eukaryotic origin, which allows the reaction to be carried out in the presence of these cells *in vitro*, or *in vivo*, without concern for off-target effects [226].

However, there are a few notable disadvantages to using SrtA as a conjugation tool. The first problem is that the sortase reaction is reversible. The formation of the LPXTGGG sequence in the final product again represents a substrate for the enzyme. Therefore, a quantitative conversion of substrate is nearly impossible. To overcome this, an excess of one substrate can be used to shift the equilibrium of the reaction. It is also possible to induce the formation of β-hairpins, by the addition of the amino acids WTWTW at both peptide motifs, which then cannot be recognised by the SrtA, thus removing the reverse reaction [227]. Despite efforts of some to overcome the problem with the reversible nature of the reaction, others have viewed it as an opportunity. In a study using polyethylene glycol (PEG) based hydrogels containing PEG-peptide conjugates engineered to express both sortase recognition motifs (i.e., PEG-GGGG and PEG-LPRTG), the authors were able to take advantage of the reversible nature of the reaction to achieve dynamic control of hydrogel stiffness via sortase-mediated cross-linking [214]. Hypothetically, the same approach could also be utilised to dynamically alter the chemical components of biomaterials, where sortase-tagged biomolecules are immobilised at one timepoint and then later removed by introducing an excess of another.

The second problem is its low catalytic activity, requiring comparably high concentrations of SrtA for the reaction to produce a good yield. This shortcoming has been partially resolved by recent advances in engineering mutant variants of the SrtA enzyme with up to 140-fold increase in activity [228]. The wild-type variant of SrtA also requires calcium (Ca^{2+}) as a co-factor for a satisfactory yield. In *S. aureus*, calcium binds near the active site of SrtA, inducing a conformational change of a surface loop that recognises newly translocated proteins [229]. This presents a significant problem when the reaction needs to be carried out in the presence of cells, as Ca^{2+} is an important intracellular messenger involved in a diverse range of cellular processes, such as gene transcription, muscle contraction, and proliferation [230]. The potential for unanticipated side-effects on cells caused by additional Ca^{2+} in the culture environment is, therefore, considerable. The generation of calcium-independent variants of SrtA have recently been achieved to help mitigate this risk [231].

The final potential issue with using sortase is that, in nature, the enzyme only acts to join proteins with other proteins. However, several strategies have been developed to broaden

the scope of SrtA mediated ligation to include other biomolecules. As a major constituent of the ECM, GAGs represent an attractive target for sortase-mediated immobilisation and would allow a more faithful recapitulation of the *in vivo* circumstances in models that have been functionalised in this way. It has been proposed that specific sugar amino groups mimic the glycine nucleophiles that act as the substrate for the sortase reaction [232]. Indeed, is has been demonstrated that sortase mediated conjugation can occur between peptides containing an LPETG sequence and the -CH_2-NH_2 moieties of 6-aminohexoses [232]. This presents the possibility that glycans could be appended with a 6-aminohexose moiety to allow them to be conjugated to proteins engineered to express the complementary LPXTG recognition sequence.

Given that most of the major drawbacks of using SrtA as a bioconjugation tool have been addressed, this enzyme presents an exciting potential avenue for functionalising peptide-based hydrogels. For example, by extending the FEFEFKFK gelator peptide to include either an oligoglycine or LPXTG motif, and engineering a molecule of interest to express the other, it should be possible to utilise SrtA to covalently immobilise matrix material within the gel network. This hypothesis is supported by a previous study which also aimed to utilise SrtA as a bioconjugation tool to immobilise the DNA-binding protein Tus to a peptide hydrogel similar in composition to the one used in this project. The authors were also able to demonstrate that Tus was still accessible within the gel network by incubating gels with fluorescein labelled *Ter* DNA (which binds Tus) and Cy5 labelled non-specific DNA [224]. In a separate study, SrtA was used to immobilise epidermal growth factor (EGF) to a PEG-based hydrogel and its activity was demonstrated through stimulation of DNA synthesis in primary human hepatocytes and endometrial epithelial cells [223]. The potential for adapting these protocols to work with the FEFEFKFK peptide hydrogel and developing SrtA into a functionalisation tool was, therefore, worthy of investigation in this project.

1.6.0 "Click" chemistry-mediated functionalisation

"Click" chemistry is a term first introduced by K. B. Sharpless in 2001 [233] and describes reactions which are high yielding, wide in scope, simple to perform, are stereospecific, and can be performed in easily removable or benign solvent systems whilst producing by-products which can also be easily removed without chromatography. Development of this concept was driven by the needs of the pharmaceutical, materials, and other industries

which would benefit from new methodologies that would allow more rapid generation of novel compound libraries for screening in discovery research.

Several types of reactions have been identified which fulfil the above criteria. For example, an examination of the azide-alkyne cycloaddition reaction shows that it fulfils many of the prerequisites. Many of the starting monosubstituted alkynes and organic azides are commercially available, or can be easily synthesized, with a wide range of functional groups, and their cycloaddition reaction selectively produces 1,2,3-triazoles. However, these reactions are not always stereospecific, and instead produce a mixture of regioisomers. For example, the classic Huisgen 1,3-dipolar cycloaddition produces an approximately 1:1 mixture of both the 1,4-substitued and 1,5-substitued regioisomers (Figure 6a). Furthermore, this reaction has a high activation barrier which leads to a low rate of reaction, even at elevated temperatures. Therefore, this particular reaction does not fulfil all of the criteria to be a true "click" reaction.

Several variants on the classic Huisgen 1,3-dipolar cycloaddition have been developed to address its shortcomings. The copper-catalysed azide-alkyne cycloaddition (CuAAC) benefits from a huge increase in reaction efficiency, often featuring an increase in the rate of reaction of between 10^7 to 10^8 [234] compared to the classic 1,3-dipolar cycloaddition. This allows it to succeed over a broad range of temperatures and pH, can be carried out in aqueous conditions producing, and produces a single 1,4-distributed regioisomer product (Figure 6b). However, whilst this reaction now fulfils all the requirements to be considered a true "click" reaction, the presence of copper prevents its use in biological systems due to its highly cytotoxic nature. A search for alternative catalysts revealed that the reaction could also be catalysed by a series of ruthenium-containing complexes, including Cp*RuCl(PPh$_3$)$_2$, Cp*RuCl(COD), and Cp*RuCl(NBD) [235]. This ruthenium-catalysed azide-alkyne cycloaddition (RuAAC) also benefits from increased rate acceleration and selectively produces a single 1,5-distributed regioisomer (Figure 6c). However, whilst not as toxic as copper, ruthenium complexes do display some toxicity to cells, which is currently being exploited to develop novel anticancer drug candidates [236, 237].

An alternative strategy for a more biorthogonal, catalyst-free cycloaddition has recently been identified which takes advantage of "ring strain". This phenomenon was first described in 1961, where it was noted that the reaction between cyclooctyne, the smallest of the stable cycloalkynes, and phenyl azide would proceed at an extremely high rate of reaction, under physiological conditions, without the need for additional catalysts, and produced a single

product [238]. This was accounted for by the massive bond deformation of the acetylene to 163° [239], which produces approximately 18 kcal/mol of ring strain [240]. The destabilization of the ground state versus the transition state of the reaction provides a dramatic rate acceleration, compared to unstrained alkynes [241]. Taking advantage of this effect, so-called "strain promoted" azide-alkyne cycloaddition (SPAAC) has emerged as a promising new tool, based on a nearly forgotten reaction discovered more than 60 years ago.

This reaction between a highly-strained cyclooctyne and an organic azide allows for covalent modification of biomolecules in living systems, and is an ideal candidate for use in functionalising biomaterials used as cell culture scaffolds. Whilst this reaction has been exploited previously to control the cross-linking of PEG-based [242] and HA-PEG hybrid gels [243], its potential to be used to introduce bioactive molecules remains to be fully explored. However, in a promising first step, a recent study was able to demonstrate SPAAC could be used to immobilise fluorescent dyes within engineered elastin-like protein hydrogels, even post-cell encapsulation [244]. Therefore, it should be possible to extend the FEFEFKFK gelator peptide to include a non-natural azide-containing amino acid (i.e., FEFEFKFK(Aha)) which can then be joined to a molecule of interest through a cyclooctyne linker (such as dibenzocyclooctyne (DBCO)), via SPAAC (Figure 6d). This method of functionalisation would also provide a way to immobilise a greater variety of biomolecules more easily, compared to the sortase-mediated method outlined above which is generally only amenable to immobilising peptides.
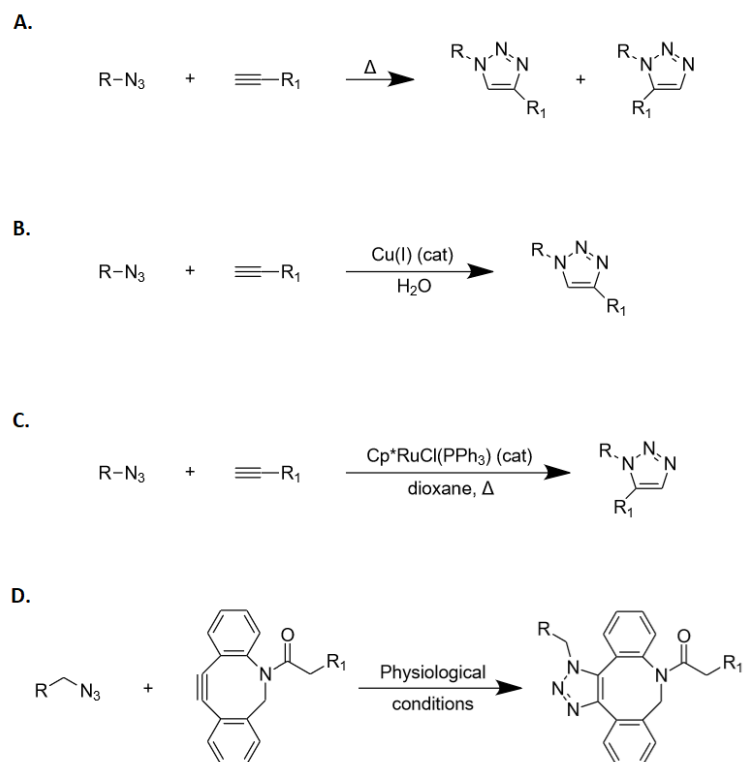
Figure 6 - Reaction schemes for common "click" reactions. (A) Classic Huisgen 1,3-dipolar cycloaddition. (B) Copper-catalysed azide-alkyne cycloaddition (CuAAC). (C) Ruthenium-catalysed azide-alkyne cycloaddition (RuAAC). (D) Strain-promoted azide-alkyne cycloaddition, (SPAAC), utilising a dibenzocyclooctyne (DBCO) linker.

1.7.0 Project hypothesis

Taking together the current landscape of *in vitro* models of development and disease, the previous work done by Ashworth et al. [33], the current issues and limitations of their peptide hydrogel technology, and the new methods for customisation that have been identified from the literature, the overarching hypothesis for this project can be stated as:

> "Development of new techniques for covalently immobilising relevant biomolecules within the peptide hydrogels, using sortase-mediated and "click" chemistry-mediated functionalisation, will lead to the creation of a more complex gel environment which will also drive more complex and physiologically relevant behaviour for encapsulated cells."

1.8.0 Project aims

The primary focus of this project was to explore the above potential methods for covalently functionalising the FEFEFKFK peptide hydrogel. Validation of each new method would require that they meet certain specific criteria, including that they produce a relevant, predictable, and measurable biological impact on encapsulated cells. Therefore, as a prerequisite to this work, it was necessary to first create a series of "test environments", where the biological impact of soluble matrix components on the cell behaviour could be evaluated. The results from these tests would then act as a control, which would then be compared against the results of immobilising those same components using one of the new methods.

It is also worth pursuing multiple methods for functionalising the peptide hydrogels to provide future end users a greater degree of choice in how they approach functionalisation. There are several reasons why this may be useful to future end users. The first is that one method may be more effective than the other at immobilising specific molecules of interest. Another benefit of providing multiple methods for functionalisation is that each could be used simultaneously to immobilise a separate molecule at the same time. This would be useful for modelling complex biological processes where the activity of one molecule is altered by the presence of another.

An example of this is provided by the role of HSPGs in Wg signalling in *Drosophila.* Wg is the prototypical Wnt gene found in *Drosophila* and is required in a variety of developmental signalling events [245]. Baeg et al. [246] were able to demonstrate that the activity of Wg is modulated by HSPGs during wing development, through generation of mutant cells lines deficient in GAG synthesis. Without the critical ability of HSPGs to sequester Wg, they showed that the reduced accumulation of Wg at the cell surface led to multiple wing margin nicks in adult flies. Complex processes such as this, where the activity of one molecule depends on another, gives justification for developing multiple methods for functionalisation, allowing for better modelling of critical signalling events in development and disease.

Multiple functionalisations would also allow end users to create morphogen gradients of multiple biomolecules. The combined effect of different morphogen gradients is critical for a variety of processes, including intestinal stem cell differentiation. In the intestinal crypt, resident stem cells respond to the antagonistic gradient of both Wnt and BMP. A higher concentration of Wnt at the bottom of the crypt promotes stemness, whilst the higher

concentration of BMP at the top promotes differentiation [247]. Generation of a peptide hydrogel model for this process would also require an antagonistic gradient of these molecules, achieved through multiple functionalisations.

As a secondary aim, the batch-to-batch variability of the peptide hydrogels was also evaluated. A significant advantage of the peptide hydrogel platform is that it should have limited batch-to-batch variability, due to its synthetic origin. Whilst the exact specifications of the methods used by the supplier of the FEFEFKFK gelator peptide are not publicly available, it is understood that they use solid-phase peptide synthesis (SPPS). SPPS involves the successive addition of protected amino acid derivatives to a growing peptide chain, which is immobilised at one end onto a solid phase scaffold [248]. Its immobilisation means the peptide chain remains insoluble, allowing for rapid filtration and washing after each synthetic reaction. Once complete, the chain is detached from the scaffold and then purified, using suitable procedures, to remove any remaining contaminants from the synthetic steps or from the scaffold itself.

Nevertheless, it had often proved difficult in the past to obtain reliable materials for the purpose of creating peptide-based hydrogels and at the beginning of this project the lab had recently switched to a different supplier of the FEFEFKFK peptide powder, due to rising concerns with the batch variability from the previous supplier. It appeared that even when working with companies that produce synthetic peptides, their method for quality control testing were insufficient for the group's needs. These quality control tests typically involve using mass spectrometry (MS), and sometimes also high-performance liquid chromatography (HPLC), to confirm the presence of the desired product and to check for any contaminating fragments. However, these techniques are often not sufficient to detect the presence of other contaminants, such as trifluoroacetic acid (TFA). In other applications, this does not matter to the end user as the peptide is often used in highly diluted concentrations. In contrast, when the peptide is to be used in the design of a pH-sensitive cell culture model this is of the utmost concern. Therefore, to confirm this new supplier could provide more reliable material, and to ensure that any problems with batch variability could be quickly identified in the future, a novel batch testing protocol was designed that examined several critical features of the peptide and its use in model design.

Another aim for this project, overlapping with the previous aim for developing new methods for covalent functionalisation, was to investigate the effective pore size of the peptide hydrogels. This was important to allow future end users the ability to identify which

molecules were likely able to escape the gel and potentially be lost during media changes, therefore requiring them either to be covalently immobilised or supplemented in the media. This involved the design of a novel assay using fluorescently labelled molecules of varying sizes, so that the diffusion of these molecules through the gel could be used to infer the effective pore size of peptide hydrogels at various peptide concentrations.

1.8.1 Summary of aims

The aims of this project can be summarised as:

- To create a series of "test environments", so that novel techniques for covalently functionalising the gels can be evaluated later. This will involve measuring the biological impact of soluble matrix additions on cells encapsulated within the peptide hydrogels.
- To evaluate current methods in the literature for covalently functionalising biomaterials and identify those which also have the potential to be adapted to functionalise the peptide hydrogels.
- To adapt and optimise those methods so that they can be used to covalently immobilise specific biomolecules (both proteins and GAGs) within the peptide hydrogels.
- To validate those new methods by measuring the biological impact of covalently immobilised material on encapsulated cells. As part of this, a comparison will be made to the impact of functionalising with soluble material (i.e., comparison to previously developed "test environments").
- To investigate the effective pore size of the peptide hydrogels, to allow end users to select which biomolecules would benefit the most from covalent immobilisation based on size.
- Finally, to develop a robust batch testing protocol which can identify any variability between batches of peptide power, or between the peptide hydrogels themselves, to ensure reproducibility of any data gathered in the future.

2.0.0 Materials and methods

2.1.0 Cell culture

2.1.1 Culture media constituents

A summary of all culture media constituents used throughout the project are presented in Table 1.

Table 1 - Summary of cell culture media constituents.

Media	Composition
mESC culture media	500 mL Knockout DMEM (Gibco, 10829-018)
	10 % (v/v) Hyclone FBS (Perbio, CH30160.03)
	5 mL L-glutamine (Gibco, 25030-024)
	5 mL MEM-NEAA (Gibco, 11140-122)
	500 μL 2-Mercaptoethanol (Gibco, 31250-010)
	1000 U/mL LIF (Milipore, ESG1107)
N2B27	250 mL DMEM F12 with L-glutamine (Sigma, D8062-500ML)
	250 mL Neurobasal medium (Gibco, 21103-049)
	1.25 mL L-glutamine (Gibco, 25030-024)
	5 mL B27 supplement (Gibco, 17504-044)
	2.5 mL N2 supplement (Gibco, 17502-048)
	12.5 mL BSA Fraction V (Gibco, 15260-037)
2i-LIF media	40 mL N2B27
	1 μM MEK inhibitor (StemCell Technologies, 72184)
	3 μM GSK3 inhibitor (Tocris Bioscience, 4424)

2.1.2 Cell line maintenance

The mouse embryonic stem cell (mESC) line E14TG2a (E14) was a kind gift from Prof. Austin Smith, (University of Cambridge, UK) and was originally derived by Martin L. Hooper et al. [249]. The HS-deficient mESC line Ext1$^{-/-}$ was generously provided by Prof. Dan Wells (University of Houston, Texas) and was originally generated and characterised by Lin et al. [250, 251].

These cell lines were selected as they had several critical features that made them ideally suited for this project. The first is that they are viable and grow well in the unfunctionalised

"blank" peptide hydrogels and. The second is that a previous study had demonstrated Ext1$^-$/$^-$ mESCs, which lack the enzyme required to produce heparan sulphate (HS), were unable to undergo neural specification but also that this potential could be restored by the addition of heparan sulphate III (HSIII) or heparin to the culture environment [68]. This provided a convenient baseline for evaluating new methods for immobilising HS or heparin within the gels. Finally, based on the literature, the cells were also likely to respond to the presence of immobilised RGD, which would also be evaluated later [219].

All cell lines were maintained in tissue culture flasks coated with 0.1 % gelatin (Gibco, G1890), in mESC culture medium (see Table 1) and incubated at 37 °C and 5 % CO_2 in a humidified atmosphere. Cells were passaged when reaching 60-70 % confluency or when cell colonies reached a diameter of more than 250 µm. Passaging was achieved by aspirating culture media, washing cells with 1X Dulbecco's Phosphate Buffered Saline (DPBS; Gibco, 12037-539), and then incubating with Trypsin-EDTA 0.25 % (Gibco, 25200-056) at 37 °C for 2 min. Detached cells were removed from the plastic and residual trypsin neutralised with culture media and cells re-seeded as single cells (typically using a 1:10-12 split ratio). Cells were observed daily and passaged every 48 h. Cells were also routinely tested for mycoplasma and consistently tested negative.

2.1.3 Cell line characterisation

Whilst genotyping would have been the preferred method to characterise these cells, this was unfortunately unavailable due to budgetary constraints. Instead, a variety of different methods were used in a weight-of-evidence based approach. Firstly, the approximate proliferative rate during cell culture was assessed and compared to the expected result from the available literature. Secondly, the morphology of cells during culture was also compared. Finally, the ability of cells to produce heparan sulphate (HS) was also evaluated via immunofluorescence staining and imaging.

2.2.0 Peptide hydrogel preparation

The protocol for peptide hydrogel preparation was adapted from published reports from our group [33, 252]. A schematic overview of this process is presented in Figure 7. Several different batches of peptide powder were used throughout the project, and a summary of

each   of   these   is   also   presented   in

Table 2.
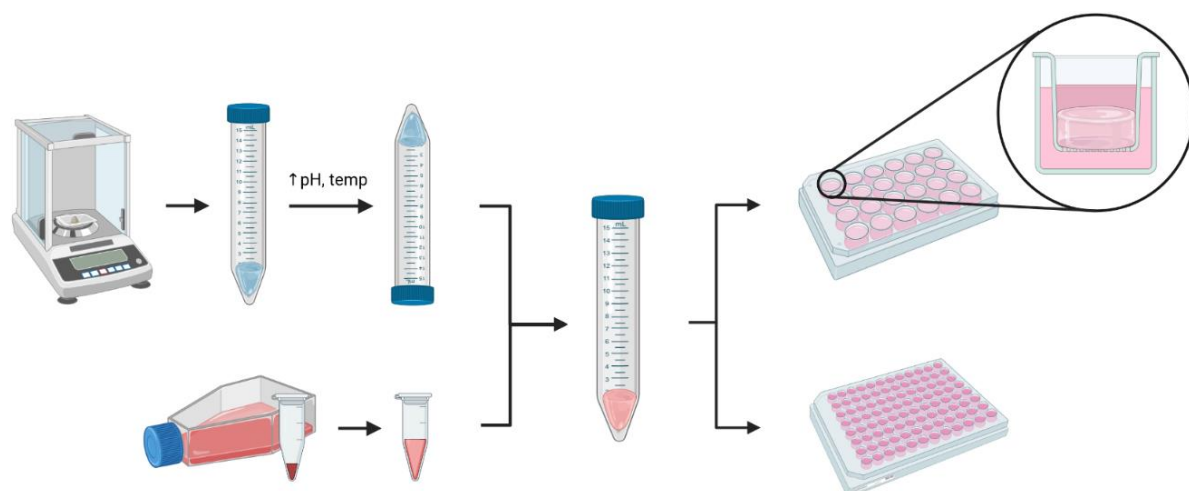
Figure 7 – Schematic overview of the peptide hydrogel preparation process. FEFEFKFK peptide powder (Pepceuticals) is first weighed out using a fine balance and then dissolved in 800 µL sterile water (Sigma, W3500), using a 3 min vortex step followed by centrifugation (3 min at 300 x g) and incubation at 80 °C for 2 h. The resulting peptide solution is then buffered by addition of 100 µL 10X Dulbecco's Phosphate Buffered Saline (DPBS; Gibco, 70011) and gelation triggered through incremental addition of 0.5M NaOH (Sigma, S2770), until the gels are optically clear and self-supporting. These precursor gels are then incubated overnight at 80 °C. Gels are then cooled to 37 °C and final peptide hydrogel formation achieved by encapsulating 250 µL cell culture medium or cell suspension (with or without desired soluble matrix additions) into the gels, by gentle reverse-pipetting and mixing. The final cell-gel mix can then be plated out at 200 µL per well into a hanging insert within a 24-well plate (Millipore, MCRP24H48), or 100 µL per well in a 96-well plate, and then covered in cell culture medium.

Table 2 - Summary of peptide powder batches.

Batch No.	Source	Composition	Description
CMUN281019	Pepceuticals, UK	FEFEFKFK	Unfunctionalised "blank" peptide powder
CMUN120121	Pepceuticals, UK	FEFEFKFK	Unfunctionalised "blank" peptide powder
CMUN130521*	Pepceuticals, UK	FEFEFKFK	Unfunctionalised "blank" peptide powder
CMUN130521R*	Pepceuticals, UK	FEFEFKFK	Unfunctionalised "blank" peptide powder
CMUN180621	Pepceuticals, UK	FEFEFKFK	Unfunctionalised "blank" peptide powder
CMUN100220	Pepceuticals, UK	GGGG-FEFEFKFK	Sortase-tagged peptide powder
CMUN171218.2	Pepceuticals, UK	FEFEFKFK-LPETG	Sortase-tagged peptide powder
CMUN100619	Pepceuticals, UK	FEFEFKFK(Aha)	"Clickable" peptide powder

2.2.1 Precursor formation

Unfunctionalised "blank" peptide hydrogels

To form each precursor, a total mass of between 7.5 and 18.75 mg of peptide powder was dissolved in 800 µl sterile water (Sigma, W3500), using a 3 min vortex step followed by centrifugation (3 min at 300 x g) and a 2 h incubation at 80 °C. After incubation, gels were buffered by addition of 100 µL 10X Dulbecco's Phosphate Buffered Saline (DPBS; Gibco, 70011). Gelation was triggered by incremental addition of 0.5M NaOH (Sigma, S2770), followed by a short vortex and centrifugation step, until gels were optically clear and self-supporting. Utmost care was taken at this step to prevent gels from transitioning back to liquid phase, through addition of excess NaOH, from which gels cannot be recovered. The resulting precursors were then incubated at 80 °C overnight. The following day, the precursors could then be used immediately or stored at 4 °C until required. Table 3 shows the relationship between initial mass of peptide and approximate volume of 0.5M NaOH required to trigger gelation, as well as final peptide concentration of prepared gel.

Sortase-primed peptide hydrogels

The protocol to form sortase-primed precursor gels is largely the same as for unfunctionalised "blank" peptide hydrogels (see above). To form each precursor, a total mass of between 7.5 and 18.75 mg of peptide powder, comprised of 50% unfunctionalised peptide and 50% sortase-tagged peptide, was dissolved in 800 µL sterile water (Sigma, W3500), using a 3 min vortex step followed by centrifugation (3 min at 300 x g) and a 2 h incubation at 80 °C. The remainder of the protocol is the same as for unfunctionalised "blank" peptide hydrogels. Table 4 shows the relationship between mass of peptides used and approximate volume of 0.5M NaOH required to trigger gelation, as well as final peptide concentration of the prepared gel.

Dynamically tuneable precursor gels

The protocol to form dynamically tuneable peptide hydrogels is largely the same as for unfunctionalised "blank" peptide hydrogels (see above). To form each precursor, a total mass of 12.5mg peptide powder, comprised of varying quantities of unfunctionalised "blank" peptide (CMUN120121) and sortase-tagged peptide (CMUN100220 & CMUN171218.2) (see Table 5), was dissolved in 800 µL of sterile water (Sigma, W3500), using a 3 min vortex step followed by centrifugation (3 min at 300 x g) and a 2 h incubation at 80 °C. The remainder of

the protocol is the same as for unfunctionalised "blank" peptide hydrogels. Table shows the relationship between mass of peptides used and approximate volume of 0.5M NaOH required to trigger gelation, as well as final peptide concentration of prepared gel.

"Clicked-in" RGD functionalised precursor gels

The protocol to form "clicked-in" RGD-functionalised peptide hydrogels is largely the same as for unfunctionalised "blank" peptide hydrogels (see above). To form each precursor, a total mass of 7.5 mg peptide powder, comprised of 50% unfunctionalised "blank" peptide (CMUN120121) and 50% "clickable" peptide (CMUN100619), was used. This was dissolved in solution containing approximately 667.5 µg/mL of "clickable" RGD (DBCO-cyclo(RGDfK); generated by Chris Merrett, University of Nottingham, UK) in 800 µL sterile water (Gibco, W3500), using a 3 min vortex step followed by centrifugation (3 min at 300 x g) and a 2 h incubation at 80 °C. Confirmation of the "click" reaction was carried out at this stage via high resolution mass spectrometry (HMRS). Gelation was then triggered by incremental addition of 0.5M NaOH (Sigma, S2770), followed by a short vortex and centrifugation step, until gels were optically clear and self-supporting. A total volume of approximately 35 µL was necessary to trigger gelation.

"Clicked-in" heparin functionalised precursor gels

The protocol to form "clicked-in" heparin-functionalised peptide hydrogels is largely the same as for unfunctionalised "blank" peptide hydrogels (see above). Due to limited supply of material, this protocol was performed only three times. To form each precursor, a total mass of 12.5 mg of unfunctionalised "blank" peptide powder was dissolved in a solution containing approximately 0.05 mg/mL of "clicked-in" heparin (FEFEFKFK(Aha)-DBCO-Heparin; generated by Chris Merrett, University of Nottingham, UK) in 800 µL of sterile water (Gibco, W3500), using a 3 min vortex step followed by centrifugation (3 min at 300 x g) and a 2 h incubation at 80 °C. Gelation was then triggered by incremental addition of 0.5M NaOH (Sigma, S2770), followed by a short vortex and centrifugation step, until gels were optically clear and self-supporting. A total volume of approximately 70 µL was necessary to trigger gelation.

Table 3 - Summary of blank peptide hydrogel preparation.

Gel type	Final concentration (mg/mL)	Batch No.	Mass of peptide (mg)	Volume of 0.5M NaOH (µL)
Unfunctionalised "blank" peptide hydrogel	6	CMUN281019	7.5	45 (±7)
	10		12.5	71 (±6)
	15		18.75	112 (±6)
	6	CMUN120121	7.5	44 (±5)
	10		12.5	74 (±3)
	15		18.75	112 (±3)
	6	CMUN180621	7.5	43 (±3)
	10		12.5	74 (±3)
	15		18.75	116 (±3)

Table 4 - Summary of sortase-functionalised peptide hydrogel preparation.

Gel type	Final concentration (mg/mL)	Batch No.	Mass of peptide (mg)	Volume of 0.5M NaOH (µL)
Sortase-functionalised peptide hydrogel	6	CMUN120121	3.75	40 (±7)
		CMUN100221	3.75	
	10	CMUN120121	6.25	65 (±10)
		CMUN100220	6.25	
	15	CMUN120121	9.37	109 (±6)
		CMUN100220	9.38	

Table 5 - Summary of dynamically tuneable peptide hydrogel preparation.

Gel type	Final concentration (mg/mL)	Batch No.	Mass of peptide (mg)	Peptide ratio	Volume of 0.5M NaOH (µL)
Dynamically tuneable peptide hydrogel	10	CMUN100220	3.13	25:50:25	68 (±8)
		CMUN120121	6.25		
		CMUN171218.2	3.12		
	10	CMUN100220	6.25	50:50	75 (±10)
		CMUN171218.2	6.25		

2.2.2 Final peptide hydrogel formation

Final peptide hydrogel formation was achieved similarly for all precursor types. Prior to final peptide hydrogel formation, precursor gels were heated to 80 °C until liquid to ensure homogeneity before transferring to a 37 °C water bath. Final gel formation was then induced by pH neutralisation with addition of 250 µL of culture media, producing gels with a final approximate volume of 1.25 mL. Medium was thoroughly mixed by gentle reverse-pipetting and stirring, before being plated at 100 µL per well into a 96-well plate, or at 200 µL per well into a hanging insert within a 24-well plate (Millipore, MCRP24H48). Wells were then flooded with culture medium and incubated at 37 °C and 5% CO_2 in a humidified atmosphere.

2.2.3 Final peptide hydrogel formation with soluble matrix modifications

Peptide hydrogels with soluble matrix modifications were created by using the method above, by incorporating soluble matrix additions into the 250 µL culture medium added to the precursor.

Soluble heparan sulphate and heparin additions

For soluble heparan sulphate additions, 1 mg of heparan sulphate fraction III (HSIII; Iduron, GAG-HSIII, approx. mol. Wt. 9 kDa) was dissolved in 1 mL sterile water (Gibco, W3500), according to manufacturer's instructions, to a final concentration of 1 mg/mL. For soluble heparin additions, 2 mg heparin saccharide (Iduron, HO30, average mol. wt. >9000) was dissolved in 1 mL sterile water (Gibco, W3500), according to manufacturer's instructions, to a final concentration of 2 mg/mL. Modified peptide hydrogels were then created by incorporating 20 µL of heparin or HSIII solution within the 250 µL of culture medium mixed into the gel.

Soluble fibronectin additions

For soluble fibronectin additions, 1 mg fibronectin from Bovine plasma (StemCell Technologies, 07159) was dissolved in 1 mL sterile water (Gibco, W3500), according to manufacturer's instructions, to a final concentration of 1 mg/mL. Modified peptide hydrogels were then created by incorporating 20 µL of fibronectin solution within the 250 µL of culture medium mixed into the gel.

Soluble RGD additions

For soluble RGD additions, 10 mg of RGDLPETG peptide powder (Pepceuticals, CMUN170320) was dissolved in 10 mL sterile water (Gibco, W35000), to a final concentration

of 1 mg/mL. Modified peptide hydrogels were then created by incorporating 20 µL RGDLPETG solution within the 250 µL of culture medium mixed into the gel.

2.3.0 Probing effective pore size of peptide hydrogels

To probe the effective pore size of peptide hydrogels, a specific assay was designed utilising fluorescein isothiocyanate-dextrans (FITC-Dextrans) of varying lengths. A summary of the FITC-Dextrans used in this project can be found in Table 6. A stock solution of each of these was created by dissolving in sterile water (Gibco, W3500) to a concentration of 25 mg/mL, as per the manufacturer's instructions.

Table 6 - Summary of fluorescein isothiocyanate dextrans (FITC-Dextrans) used throughout the project.

Product No.	Source	Average mol. wt. (Da)
FD40S	Sigma	40,000
FD70S	Sigma	60,000 – 76,000
FD250S	Sigma	250,000
FD500S	Sigma	500,000
FD2000S	Sigma	2,000,000

2.3.1 Initial validation and optimisation

Initial validation and optimisation of the protocol was carried out using unfunctionalised "blank" peptide hydrogels and FD40S. Peptide hydrogels were prepared as described above, using mESC culture medium, and plated at 100 µL per well into a 96-well plate. Solutions of FD40S were prepared at varying concentrations by diluting the stock solution in culture medium. The concentrations tested were 10 µM, 20 µM, and 30 µM. Gels were then covered in 100 µL of FD40S solution and incubated for 24 h at 37 °C and 5% CO_2 in a humidified atmosphere. The following day, the FD40S solution was aspirated, and gels were washed twice with Dulbecco's Phosphate Buffered Saline (DPBS; Gibco, 12037-539). Fluorescence signal was then detected using a Fluostar Omega Plate Reader (BMG LabTech) to determine which concentration(s) of FITC-Dextran were appropriate for the remainder of the project.

2.3.2 Final protocol

Following initial validation and optimisation of the protocol (see above), a concentration of 20 μM was chosen for the remainder of the project. The final protocol expanded on the initial validation protocol to also assess how well FITC-Dextrans were retained in the peptide hydrogels over a course of several days, more closely simulating future experiments.

Peptide hydrogels were prepared as described above, using mESC culture medium, and plated at 100 μL per well into a 96-well plate. Solutions of various sized FITC-Dextrans were prepared by diluting in culture medium. Gels were then covered in 100 μL of FITC-Dextran solution and incubated for 24 h at 37 °C and 5% CO_2 in a humidified atmosphere. The following day, the solutions were aspirated, and gels were washed twice with Dulbecco's Phosphate Buffered Saline (DPBS; Gibco, 12037-539). Fluorescence signal was detected using a Fluostar Omega Plate Reader (BMG LabTech). Gels were then covered in 100 μL culture medium and returned to the incubator. This process was repeated over a period of seven days, to determine how well each gel retained each sized FITC-Dextran.

2.4.0 Generation of "clickable" and "clicked-in" material

The work in this section was carried out by Chris Merrett, under the supervision of Prof. Neil Thomas (University of Nottingham, UK). The details are included here as they are necessary to understand the inclusion of these modifications in the hydrogels.

2.4.1 DBCO-cyclo(RGDfK)

Generation of the DBCO-cyclo(RGDfK) was performed by Chris Merrett (University of Nottingham, UK). To facilitate amide bond formation, a DBCO-NHS ester was synthesized via carbodiimide-activation of the carboxylic acid residue with 1-ethyl-3-(3-dimethylaminopropyl)carbodiimide and hydrochloride (EDC·HCl) and N-hydroxysuccinimide (NHS). Amide coupling with cyclo(RGDfK) (Karebay Biochem Inc.) was then achieved, without the need for a coupling reagent and the reaction was confirmed with high resolution mass spectrometry (HRMS). The product was then purified by high-performance liquid chromatography (HPLC).

2.4.2 FEFEFKFK(Aha)-DBCO-Heparin

Generation of the DBCO-Heparin was performed by Chris Merrett (University of Nottingham, UK). DBCO-NH$_2$ was synthesised using a protocol adapted from methods outlined in [253]. Conjugation of DBCO-NH$_2$ to heparin (Iduron, HO30, average mol. wt. >9000) was then achieved via reductive amination by incubating at 65 °C, in the presence of acetic acid, with periodic shaking to ensure thorough mixing. Following neutralisation of the acetic acid with sodium hydrogen carbonate, a pre-packed PD-10 desalting column was used to desalt the product. This allowed size-exclusion purification of the product from salt, free labels, and impurities. UV/Visible absorption spectroscopy was employed to identify the fraction containing the desired product. Conjugation with FEFEFKFK(Aha) was then caried out using strain promoted azide-alkyne cycloaddition (SPAAC). The final product was then freeze-dried, producing FEFEFKFK(Aha)-DBCO-Heparin powder.

2.5.0 Sortase-mediated functionalisation of peptide hydrogels

The protocol for sortase-mediated functionalisation of peptide hydrogels was adapted from [224, 254]. A significant degree of optimisation was required, however, to produce a protocol that worked in the peptide hydrogel system described in this project.

2.5.1 Sortase-mediated control of matrix composition

Initial validation

Initial validation of the sortase protocol was carried out using 10 mg/mL sortase-primed peptide hydrogels, prepared as described above, using mESC culture medium, and plated at 100 μL per well into a 96-well plate. A tethering solution was created comprising 15 μM wild-type sortase A enzyme (provided by James Kapp, University of Nottingham, UK) and 20 μM sortase-tagged eGFP-LPETG (also provided by James Kapp) dissolved in a calcium buffer (150 mM NaCl, 50 mM CaCl$_2$, and 50 mM HEPES [Sigma, H3374] dissolved in sterile water [Gibco W3500]). Gels were then covered with 100 μL of tethering solution and incubated for 2 h at room temperature. Following incubation, the tethering solution was aspirated away, and gels were washed five times with Dulbecco's Phosphate Buffered Saline (DPBS; Gibco 120237-539), to remove any unbound eGFP. Fluorescence signal was then detected using a Fluostar Omega Plate Reader (BMG LabTech).

Optimisation of incubation protocol

To optimise the incubation protocol and align the protocol with future experiments, which would likely need to be carried out at 37 °C, several new incubation protocols were tested. Sortase-primed peptide hydrogels of 10 mg/mL concentration were prepared, as described above, using mESC culture medium, and plated at 100 µL per well into a 96-well plate. A tethering solution was created, as described above, comprising 15 µM wild type sortase A and 20 µM eGFP, in calcium buffer. Gels there then covered in 100 µL tethering solution and incubated using several different test protocols (2 h at 37 °C, 2 h at 37 °C followed by an overnight incubation at 4 °C, or 24 h at 37 °C). Following incubation, the tethering solution was aspirated away, and gels washed five times with DPBS, to remove unbound eGFP. Fluorescence signal was then detected using a Fluostar Omega Plate Reader (BMG LabTech).

Optimisation of recognition motif

To investigate which sortase motif is most efficient in the molecule of interest for this protocol, two different eGFP molecules were tested (eGFP-LPETG and eGFP-LPMTG; both provided by James Kapp, University of Nottingham, UK). Sortase-primed peptide hydrogels of 10 mg/mL concentration were prepared, as described above, using mESC culture medium, and plated at 100 µL per well into a 96-well plate. Two different tethering solutions were prepared, as described above, using either 20 µM eGFP-LPETG or 20 µM eGFP-LPMTG, and 15 µM wild-type sortase A, in calcium buffer. Gels were then covered in 100 µL tethering solution and incubated for 24 h at 37 °C. Following incubation, the tethering solution was aspirated away, and gels were washed five times with DPBS, to remove unbound eGFP. Fluorescence signal was then detected using a Fluostar Omega Plate Reader (BMG LabTech).

Optimisation of tethering solution

The requirement for additional calcium in the tethering solution, compared to relying on the calcium already present in culture medium, was then investigated. Sortase-primed peptide hydrogels of 10 mg/mL concentration were prepared, as described above, using mESC culture medium, and plated at 100 µL per well into a 96-well plate. Two different tethering solutions were then created, as described above, comprising 15 µM wild-type sortase A and 20 µM eGFP-LPETG, dissolved in either calcium buffer or mESC culture medium. Gels were then covered in 100 µL tethering solution and incubated for 24 h at 37 °C. Following incubation, the tethering solutions were aspirated away, and gels washed five times with DPBS, to remove unbound eGFP. Fluorescence signal was then detected using a Fluostar Omega Plate Reader (BMG LabTech).

Investigating use of calcium-independent 7M sortase A

The use of a calcium-independent variant of sortase A was then investigated, to determine whether this would lead to higher efficiency when using mESC culture medium in the tethering solution. Two different calcium-independent variants were tested: the calcium-independent 7M sortase A originally described in [231] (H7M sortase A; samples generously provided by Stephanie Dougan, Harvard Medical School, Boston, Massachusetts) and a calcium independent 7M sortase A generated at the University of Nottingham (N7M sortase A; provided by James Kapp, University of Nottingham, UK). Sortase-primed peptide hydrogels of 10 mg/mL concentration were prepared, as described above, using mESC culture medium, and plated at 100 µL per well into a 96-well plate. Two different tethering solutions were then created, as described above, comprising either 15 µM H7M sortase A or 15 µM N7M sortase A, and 20 µM eGFP-LPETG, dissolved in either calcium buffer or mESC culture medium. Gels were then covered in 100 µL tethering solution and incubated for 24 h at 37 °C. Following incubation, the tethering solution was aspirated away, and gels washed seven times with DPBS, to remove unbound eGFP. Fluorescence signal was then detected using a Fluostar Omega Plate Reader (BMG LabTech).

Final protocol validation

Following the investigations and optimisations above, the final protocol for sortase-mediated functionalisation of peptide hydrogels, used throughout the remainder of the project, was selected. The final validation test was also expanded to also assess how well eGFP is retained in the peptide hydrogels over a course of several days, more closely resembling future experiments.

In the final protocol, sortase-primed peptide hydrogels were prepared, as described above, using mESC culture medium, and plated at 100 µL per well into a 96-well plate. A tethering solution was then created, comprising 15 µM wild-type sortase A and 20 µM eGFP-LPETG in mESC culture medium. Gels were then covered in 200 µL tethering solution and incubated for 2 h at 37 °C. Fluorescence was then detected using a Fluostar Omega Plate Reader (BMG LabTech). Gels were then returned to the incubator and the following day the tethering solution was aspirated away, and gels washed once with DPBS. Fluorescence signal was then detected using a Fluostar Omega Plate Reader (BMG LabTech). Gels were then covered in 200 µL culture medium and returned to the incubator. This process was repeated over a period of seven days, to determine how well each gel retained the eGFP-LPETG.

2.5.2 Sortase-mediated control of matrix stiffness

To investigate whether sortase could also be used to modify the stiffness of peptide hydrogels, dynamically tuneable peptide hydrogels of various peptide concentrations were prepared, as described above, using mESC culture medium, and plated at 200 µL per well into a hanging insert within a 24-well plate (Millipore, MCRP24H48). A tuning solution was then created, comprising 15 µM wild-type sortase A dissolved in either calcium buffer or mESC culture medium. Gels were then covered in 200 µL tuning solution, wells flooded with mESC culture medium, before being incubated for 24 h at 37 °C. Following incubation, gels stiffness was assessed via bulk-oscillatory rheometry (described below).

2.6.0 Bulk oscillatory rheology

2.6.1 Sample preparation

Peptide hydrogels were prepared for bulk oscillatory rheology, as described above, and plated at 200 µL per well into a hanging insert within a 24-well plate (Millipore, MCRP24H48). Gels were then covered with 200 µL mESC culture medium (or tuning solution – see above) and wells also flooded with culture medium, before being incubated for 24 h at 37 °C.

2.6.2 Loading the sample

Culture medium was first carefully aspirated away from the top of the gels and then inserts removed from the 24-well plate. Samples were then removed using a scalpel to carefully remove the membrane from the bottom of the inserts, before mounting on the Peltier plate of a Physica MCR 301 rheometer (Anton Paar). An 8 mm diameter PP08 probe was selected for use in each test, as this had approximately the same diameter of the gels prepared in this way. The spacing between the probe and the plate was then set at 3-4 mm, depending on the height of each individual gel. Any overtrim, where the gel overhung the diameter of the probe, was removed using a plastic pipette tip. The Peltier plate was also set at 37 °C, to help maintain the correct physiological temperature of the gels throughout the test.

2.6.3 Performing the tests

To determine the linear viscoelastic region for each set of samples, an amplitude sweep from 0.1 to 100% strain at 1 rad/s was first carried out. This region indicates the range in which

the test can be carried out without destroying the structure of the sample. Similarly, a frequency sweep from 0.1 to 100 rad/s was also performed. This was the same method used by Ashworth et al. [33] and confirmed that a constant strain of 0.5% at 1 rad/s was most appropriate setting for all sample types in this study. Therefore, in objective tests, a frequency sweep with a constant strain of 0.5% and constant frequency of 1 rad/s, with 10 measurements in 5 min, was used to determine approximate stiffness of each sample. Stiffness for each sample is expressed as the ratio of tensile stress (σ) to tensile strain (ϵ), or its Young's modulus (G'), which is a measure of the material's ability to withstand changes in its length when under lengthwise tension or compression.

2.7.0 Mouse embryonic stem cell differentiation in peptide hydrogels

The protocol for encapsulating cells within the peptide hydrogels was adapted from previous work published by our group [33, 252]. The protocol for stem cell differentiation and directing stem cell fate was adapted from a protocol originally performed in 2D, found in previously published work by Merry et al. [76].

2.7.1 Directing mouse embryonic stem cell fate in unfunctionalised "blank" peptide hydrogels

Unfunctionalised "blank" precursor gels were prepared, as described above, and heated to 80 °C until liquid, before being transferred to a 37 °C water bath. For cell encapsulation, the 250 µL volume of culture medium was prepared as a cell suspension. Trypsin-EDTA (0.25%) was used to detach E14 or Ext1$^{-/-}$ mouse embryonic stem cells (mESCs) from 2D culture at sub-confluence Cells were then resuspended in 250 µL mESC culture medium at a density of 2.5 x 10^5 cells/mL. The cell suspension was then thoroughly mixed into the gel by gentle reverse-pipetting and stirring, giving a final seeding density of 5 x 10^4, before being plated at 100 µL per well into a 96-well plate. Wells were then flooded with N2B27 media and incubated at 37 °C and 5% CO_2 in a humidified atmosphere. Media was refreshed every day.

2.7.2 Directing mouse embryonic stem cell fate in peptide hydrogels functionalised with soluble matrix modifications

Peptide hydrogels with soluble matrix modifications were created using the method above, by incorporating matrix additions into the 250 µL cell suspension that is stirred into gel precursor.

Soluble heparan sulphate and heparin additions

For soluble heparan sulphate additions, 1 mg of heparan sulphate fraction III (HSIII; Iduron, GAG-HSIII, approx. mol. wt. 9 kDa) was dissolved in 1 mL sterile water (Gibco, W3500), according to manufacturer's instructions, to a final concentration of 1 mg/mL. For soluble heparin additions, 2 mg heparin saccharide (Iduron, HO30, average mol. wt. >9000) was dissolved in 1 mL sterile water (Gibco, W3500), according to manufacturer's instructions, to a final concentration of 2 mg/mL. Modified peptide hydrogels were then created by incorporating 20 µL of HSIII or heparin solution within the 250 µL of cell suspension mixed into the gel and plated at 100 µL per well into a 96-well plate. Wells were then flooded with N2B27 media and incubated at 37 °C and 5% CO_2 in a humidified atmosphere. Media was refreshed every day.

Soluble fibronectin additions

For soluble fibronectin additions, 1 mg fibronectin from Bovine plasma (StemCell Technologies, 07159) was dissolved in 1 mL sterile water (Gibco, W3500), according to manufacturer's instructions, to a final concentration of 1 mg/mL. Modified peptide hydrogels were then created by incorporating 20 µL of fibronectin solution within the 250 µL of cell suspension mixed into the gel and plated at 100 µL per well into a 96-well plate. Wells were then flooded with N2B27 media and incubated at 37 °C and 5% CO_2 in a humidified atmosphere. Media was refreshed every day.

Soluble RGD additions

For soluble RGD additions, 10 mg of RGDLPETG peptide powder (Pepceuticals, CMUN170320) was dissolved in 10 mL sterile water (Gibco, W35000), to a final concentration of 1 mg/mL. Modified peptide hydrogels were then created by incorporating 20 µL RGDLPETG solution within the 250 µL of cell suspension mixed into the gel and plated at 100 µL per well into a 96-well plate. Wells were then flooded with N2B27 media and incubated at 37 °C and 5% CO_2 in a humidified atmosphere. Media was refreshed every day.

2.7.3 Directing mouse embryonic stem cell fate with sortase-immobilised RGD

Sortase-primed precursor gels were prepared, as described above, and heated to 80 °C until liquid, before being transferred to a 37 °C water bath. For cell encapsulation, the 250 µL volume of culture medium was prepared as a cell suspension. Trypsin-EDTA (0.25%) was used to detach E14 or Ext1$^-$/$^-$ mouse embryonic stem cells (mESCs) from 2D culture at sub-confluence. Cells were then resuspended in 250 µL mESC culture medium at a density of 2.5 x 10^5 cells/mL. The cell suspension was then thoroughly mixed into the gel by gentle reverse-pipetting and stirring, giving final seeding density of 5 x 10^4, before being plated at 100 µL per well into a 96-well plate. Gels were then covered in a tethering solution containing 15 µM wild-type sortase A and 20 µM RGDLPETG in N2B27 media and incubated at 37 °C and 5% CO_2 in a humidified atmosphere. The following day, the tethering solution was replaced with N2B27 media. Media was refreshed every day.

2.7.4 Directing mouse embryonic stem cell fate in "clicked-in" heparin

"Clicked-in" heparin functionalised peptide hydrogels were prepared, as described above. For cell encapsulation, the 250 µL volume of culture medium was prepared as a cell suspension. Trypsin-EDTA (0.25%) was used to detach E14 or Ext1$^{-/-}$ mouse embryonic stem cells (mESCs) from 2D culture at sub-confluence. Cells were then resuspended in 250 µL mESC culture medium at a density of 2.5 x 10^5 cells/mL. The cell suspension was then thoroughly mixed into the gel by gentle reverse-pipetting and stirring, giving final seeding density of 5 x 10^4, before being plated at 100 µL per well into a 96-well plate. Wells were then flooded with N2B27 media and incubated at 37 °C and 5% CO_2 in a humidified atmosphere. Media was refreshed every day.

2.8.0 Gastruloid formation and embedding in peptide hydrogels

2.8.1 Gastruloid formation

The protocol for gastruloid formation was adapted from previously published work by Turner et al. supported by in-person training in Dr David Turner's lab at The University of Liverpool [255]. E14 or Ext1$^{-/-}$mouse embryonic stem cells (mESCs) were maintained in mESC culture medium, as described above. A "2i pulse" was performed for the 24 h immediately preceding gastruloid formation, by replacing the standard mESC culture medium was 2i+LIF medium. Cells were then harvested using trypsin-EDTA (0.25%) to detach cells and resuspended in

mESC media, to inactive the trypsin. Cells were counted using a BioRad automated cell counter, centrifuged for 3 min at 300 x g, and then resuspended in NDiff® 227 (Takara, Y40002) at a density of 8750 cells/mL. This cell suspension was then transferred to a reservoir. Using a multichannel micropipette, 40 µL of cell suspension was transferred from the reservoir into each well of U-bottomed, non-tissue culture-treated 96-well plate, pipetting the droplet into the centre of each well. Cells were then incubated at 37 °C and 5% CO_2 in a humidified atmosphere. After 48 h, and using a multichannel micropipette, 150 µL of NDiff® 227 containing 3 µM chiron (Tocris, CHIR99021) was added to each well by pipetting carefully down the side of each well. After 72 h, 150 µL media was exchanged with fresh NDiff® 227. Further media changes were carried out at 96 and 120 h.

2.8.2 Gastruloid embedding

To embed gastruloids within peptide hydrogels, gastruloids were first cultured for at least 72 h. Unfunctionalised "blank" precursor gels were prepared, as described above, and heated to 80 °C until liquid, before being transferred to a 37 °C water bath. Gastruloids were then harvested by using a multichannel micropipette equipped with wide bore tips (or tips with end cut back 0.5 mm using sterile scissors) and gently pipetting up and down in each well 2-3 times to dislodge gastruloids from the bottom of the plate, before removing the resulting gastruloid suspensions and transferring them to a reservoir. The gastruloid suspension was then transferred from the reservoir to a 15 mL centrifuge tube and placed in a 37 °C water bath and gastruloids allowed to settle to the bottom over 5-10 min. Following this, excess culture media was carefully aspirated away and remaining gastruloids were carefully resuspended in 250 µL, using a pipette equipped with a wide bore tip. This 250 µL gastruloid suspension was then carefully mixed into the peptide hydrogels, by gentle reverse pipetting and stirring, before being plated at 100 µL per well into a 96-well plate. Wells were then flooded with N2B27 medium and incubated at 37 °C and 5% CO_2 in a humidified atmosphere. Media was refreshed every day during culture.

2.9.0 Live cell imaging and detection

For detection of live cells, peptide hydrogels containing encapsulated cells were washed with Dulbecco's Phosphate Buffered Saline (DPBS; Gibco 120237-539) and then incubated for 15 min at room temperature in a solution of 40 µM ethidium homodimer and 20 µM calcein AM (Fisher, L3224) in DPBS. Gels were then washed twice with DPBS and fluorescence images

were then obtained using a Leica TCS SPE laser scanning confocal microscope. This approach was used to measure cell viability as it can be easily performed and produces data which is easy to interpret. It also uses reagents and equipment that future end users are likely to have access to already. This increases the likelihood that this research may have a wider reaching impact. Other commonly used viability assays which could have also been used include the RealTime-Glo™ MT Cell Viability Assay (Promega; G9711), which has the advantages of allowing measurements of cell viability in real-time over the course of several days and allowing simple kinetic monitoring to determine dose response. The CellTiter-Glo® 3D Cell Viability Assay (Promega; G9681) could have also been used, which was specifically designed to assess the viability of cells grown in 3D, by using a reagent which also lyses the cells, in order to achieve better penetration of 3D cell clusters.

Each test was performed a minimum of three times (three biological repeats). Within each test, three wells were plated per test condition (three technical repeats). Cells in gels were typically cultured for 5-7 days, as this was the length of time required to observe any difference in viability of encapsulated cells. Following this, and for each test condition, at least three representative images were taken, focusing on a single cell cluster but often with others visible. Each final image consisted of a series of images taken in a z-stack, spanning the entire cell cluster. Image processing was performed in Fiji 1.52d, where 3D projections were generated for each image using the z-stack.

2.10.0 Immunofluorescence staining and imaging

2.10.1 Staining and imaging cells in 2D

For immunofluorescence staining and imaging cells cultured in 2D, cells were first cultured to 60-70% confluency in 24-well plates. Cells were then washed with Dulbecco's Phosphate Buffered Saline (DPBS, Gibco 120237-539) and then incubated for 15 min at room temperature in paraformaldehyde (Thermo Fisher, 28906) diluted to 4% (v/v) in DPBS. Cells were then washed again in DPBS and then incubated for 1 h at room temperature in blocking buffer, consisting of 0.1% Triton-X (Sigma, 9036-19-5), 0.5% Bovine serum albumin (Sigma, A9418), and 5% goat serum (Sigma, G9023). Blocking buffer was then removed and cells incubated in a solution of primary antibody in blocking buffer (see Table 7 for summary of antibodies used) overnight at 4 °C. The next day, primary antibody solution was removed, and cells washed in DPBS. Cells were then incubated in a solution of secondary antibody, with co-stains rhodamine phalloidin and DAPI, in blocking buffer overnight at 4 °C. Following

this, secondary antibody solution was removed, cells washed in DPBS, and then fluorescence images obtained using a Leica TCS SPE laser scanning confocal microscope.

Staining and imaging of cells in 2D was performed to demonstrate that the E14 and Ext1$^{-/-}$ cell lines that were provided for use throughout this project were HS-competent and HS-deficient, respectively. In this test, cells were plated out in a 24-well plate and grown to 60-70% confluency (approx. 48 h after seeding) before fixing, staining, and imaging. For each cell type, three test wells were seeded, alongside one control well where no primary antibody was used (to evaluate any non-specific binding of secondary antibodies). After visually verifying uniform distribution (or lack thereof) of HS within each sample, a single image was taken for each well at 10X magnification.

2.10.2 Staining and imaging cells in 3D

For immunofluorescence staining and imaging, peptide hydrogels containing encapsulated cells or embedded gastruloids were washed with Dulbecco's Phosphate Buffered Saline (DPBS, Gibco 120237-539) and then incubated for 1 h at room temperature in paraformaldehyde (Thermo Fisher, 28906) diluted to 4% (v/v) in DPBS. Gels were then washed again in DPBS and then incubated for 1 h at room temperature in blocking buffer, consisting of 0.1% Triton-X (Sigma, 9036-19-5), 0.5% Bovine serum albumin (Sigma, A9418), and 5% goat serum (Sigma, G9023). Blocking buffer was then removed and gels incubated in a solution of primary antibody in blocking buffer (see Table 7 for summary of antibodies used) overnight at 4 °C. The next day, primary antibody solution was removed, and gels washed in DPBS. Gels were then incubated in a solution of secondary antibody, with co-stains rhodamine phalloidin and DAPI, in blocking buffer overnight at 4 °C. Following this, secondary antibody solution was removed, gels washed in DPBS, and then fluorescence images obtained using a Leica TCS SPE laser scanning confocal microscope.

Unless stated otherwise, each test was performed a minimum of three times (three biological repeats). Within each test, three wells were plated out per test condition (three technical repeats), alongside one control well where no primary antibody was used (to evaluate any non-specific binding of secondary antibody). Cells in gels were typically cultured for 7-10 days, as this was the length of time required to observe differentiation of encapsulated cells. Following this, and for each test condition, at least three representative images were taken, focusing on a single cell cluster but often with others visible. Each final image consisted of a series of images taken in a z-stack, spanning the entire cell cluster. Image processing was

performed in Fiji 1.52d, where 3D projections were generated for each image using the z-stack.

Table 7 - Summary of primary antibodies used.

1° antibody	Raised in	Clonality	Type	Source	Code	Ratio used	2° used
10E4	Mouse	Monoclonal	IgM	Amsbio	370255-1	1:200	AF-488 goat anti-mouse
β-III-tubulin	Rabbit	Polyclonal	IgG	Abcam	AB18207	1:200	AF-488 goat anti-rabbit
GFAP	Rabbit	Polyclonal	IgG	Abcam	AB7260	1:200	AF-488 goat anti-rabbit
Oct4	Rabbit	Polyclonal	IgG	Abcam	AB19857	1:200	AF-488 goat anti-rabbit
Sox-2	Rabbit	Polyclonal	IgG	Abcam	AB97959	1:200	AF-488 goat anti-rabbit IgG
Nestin	Mouse	Monoclonal	IgG1	Abcam	AB6320	1:200	AF-488 goat anti-mouse IgG

Table 8 - Summary of secondary antibodies and co-stains used.

2° antibody	Source	Code	Ratio used
AF-488 goat anti-mouse IgG	Invitrogen	A11029	1:500
AF-488 goat anti-rabbit IgG	Invitrogen	A11034	1:500
DAPI	Invitrogen	D1306	1:500
Rhodamine phalloidin	Invitrogen	R415	1:500

2.11.0 Statistics

All statistical analyses and generation of plots were performed using Python 3.9, within a Jupyter Notebook environment, and using the following libraries: pandas, matplotlib, seaborn, SciPy, and statannotations. Normality of data was evaluated using the Shapiro test for normality. Data were then subsequently assessed via an independent student's t-test or the Mann-Whitney U test for normal and non-normal data, respectively. Statistical significance for all tests was declared at $p < 0.05$. Each test, unless otherwise stated, was conducted a minimum of three times (three biologically repeats). Within each test, unless otherwise stated, three technical repeats were also conducted. All raw data and analyses are available on request via GitHub.

3.0.0 Results

3.1.0 Batch testing

Three-dimensional (3D) *in vitro* models are excellent tools for studying the complexities of biological systems in a manner which is vastly superior to 2D culture. These models better recapitulate the influence of the tissue microenvironment on cells, providing cell-cell and cell-matrix interactions that more closely resemble the *in vivo* circumstances. However, many of the models which are currently available, such as those based on Matrigel®, suffer from high batch-to-batch variability, often owing to their natural origin.

A significant advantage of the peptide hydrogel platform is that it should have limited batch-to-batch variability, due to its synthetic origin. Nevertheless, it can be hard to obtain reliable materials for the purpose of creating peptide-based hydrogels, even when working with companies that produce synthetic peptides and perform their own quality control testing. Therefore, to test the variability of different peptide batches in the context of our specific application, and to further characterise the peptide hydrogels, a more specialised batch testing protocol was designed. This involved a multi-step process where both the mechanical and biological properties of peptide hydrogels prepared using each batch were assessed.

Provided below are representative results from testing five different batches of peptide powder, which are summarised in Table 9. Included in these batches are the three batches that were selected for use in experiments throughout the remainder of the project (CMUN281019, CMUN120121, CMUN180621). Also included is a batch that failed the batch test (CMUN130521). This is included to highlight the importance of batch testing and the utility of the protocol. Once this batch was identified as being unsuitable, it was returned to the supplier where it was re-processed before being sent back. This re-processed material (CMUN130521R) was then tested again to confirm that the issues with it had resolved.

Table 9 - Summary of peptide batches which were evaluated through batch testing and deemed fit for use in future experiments.

Batch No.	Source	Composition	Outcome
CMUN281019	Pepceuticals, UK	FEFEFKFK	Passed
CMUN120121	Pepceuticals, UK	FEFEFKFK	Passed
CMUN180621	Pepceuticals, UK	FEFEFKFK	Passed
CMUN130521	Pepceuticals, UK	FEFEFKFK	Failed – returned to supplier
CMUN130521R	Pepceuticals, UK	FEFEFKFK	Passed

3.1.1 Peptide hydrogel preparation

The first step in the batch testing process was to assess how each peptide powder preparation responded during the peptide hydrogel preparation process. Precursor gels of three frequently used peptide concentrations were created, by weighting specific amounts of peptide powder (7.5 mg, 12.5 mg, and 18.75 mg). At this stage, a moment was taken to compare the appearance of each batch, taking note of any obvious differences in colour, texture, and density. It was at this stage that a potential problem with batch CMUN130521 was first identified. In comparison to the other batches, this batch had a more yellow colour, a more flocculant texture, and required a greater volume of powder per mg weighed. In contrast, no obvious differences in colour, texture, or density were observed among the other batches.

Each sample was then dissolved in 800 µL sterile water using a 3 min vortex step followed by centrifugation (3 min at 300 x g). Any differences in the solubility and resulting appearance of the peptide solutions were documented. Despite the initial differences observed in the appearance of the peptide powders, all batches readily dissolved and formed clear peptide solutions. Gels were then incubated for 2 h at 80 °C and gelation of the peptide solutions was triggered by incremental addition of 0.5M NaOH, followed by a short vortex and centrifugation step, until gels were optically clear and self-supporting. Great care had to be taken here as an excess of NaOH would cause the gels to transition back to liquid phase, with no way of recovering them. This step is also the most informative in the preparation process, as any major differences in the volume of 0.5M NaOH was usually the first indication that a batch was not suitable for use in future experiments. The total volume of 0.5M NaOH required to trigger proper gelation was recorded, compared, and is presented in Figure 8.
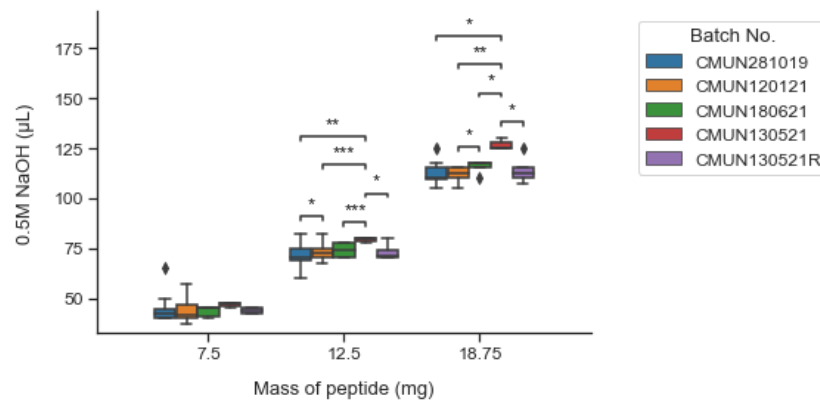
Figure 8 - Volume of 0.5M NaOH required to trigger gelation in precursor gels. Samples from each batch were used to prepare precursor gels, following the standard peptide hydrogel preparation process, and the volume of 0.5M NaOH required to trigger gelation was recorded. Results indicate a significant and meaningful difference in the volume of 0.5M NaOH required to trigger gelation in precursor gels made with batch CMUN130521, for gels prepared using 12.5 mg or 18.75 mg of peptide powder. Results also indicate a small, but statistically significant, difference between several other gels. However, these smaller differences were not predicted to have any future impact on cell viability (Mann-Whitney U test; n≥8 for CMUN281019, n≥16 for CMUN120121, n≥6 for CMUN180621, n≥3 for CMUN130521, n≥6 for CMUN130521R; ♦: outliers, defined as such if a datapoint is less than Q1 − 1.5 * IQR or greater than Q3 + 1.5 * IQR; *: p < 0.05; **: p < 0.01; ***: p < 0.001).

This was the second stage at which a potential problem with CMUN130521 was identified. Compared to the other batches, there was both a significant and meaningful increase in the volume of 0.5M NaOH required to trigger gelation in precursor gels made with batch CMUN130521 for gels prepared using 12.5 or 18.75 mg peptide powder. This increase in 0.5M NaOH predicts future problems with this batch because this often correlated with poorer cell viability of encapsulated cells. This reason for this is that it is hypothesized that this required increase in NaOH is caused by an increase in a specific impurity in the peptide powder preparation, trifluoroacetic acid (TFA). TFA is toxic to cells and neutralisation of TFA by NaOH also yields a toxic product (sodium trifluoroacetate). In the re-processed material, no significant differences were detected across all peptide concentrations. Where there was a significant difference detected in other batches, the difference itself was much smaller and therefore not predicted to have any future impact on cell viability.

The final step in the peptide hydrogel preparation process was neutralisation with culture medium. For this step, mouse embryonic stem cell (mESC) culture medium was chosen. This type of media was chosen because it was the one used most frequently during remainder of the project, so any observable differences would be more readily apparent. Final gel

formation was induced with addition of 250 μL of culture media, which was thoroughly mixed by gentle reverse-pipetting and stirring. How each precursor responded was recorded, paying particular attention to how the viscosity changed. No meaningful differences between any of the batches tested were observed at this stage.

3.1.2 Bulk oscillatory rheology

A major advantage of the peptide hydrogel platform is that the end stiffness of the peptide hydrogel can be tuned by adjusting the mass of peptide powder used in the preparation process [33, 252]. This is a critical feature, as the ability to model a range of stiffnesses is essential to accurately recapitulate the range of stiffnesses that exist within different tissue types. Therefore, verifying that each batch of peptide powder can be used to prepare peptide hydrogels with a predictable range of stiffnesses based on mass of peptide used is essential.

Peptide hydrogels representing a range of frequently used peptide concentrations were prepared, as described above, and evaluated via bulk oscillatory rheology. As shown in Figure 9, a positive relationship between peptide concentration and average stiffness (G') was observed across all batches, ranging from approx. 0.4 to 2.4 kPa. This range is relevant to human tissues and is also characteristic of the change of stiffness associated with the increasing stiffness during tumorigenesis in breast cancer [89]. There were also no significant differences in stiffness detected, given the same peptide concentrations, across all batches. This was surprising, as it was expected that the increased volume of 0.5M NaOH required to trigger gelation for batch CMUN130521 would have had an impact on stiffness, owing to the fact that the gels are pH sensitive. This highlights the importance of the batch testing protocol being a multi-step process, so that end users are not mislead in believing a batch is acceptable based on a single result.
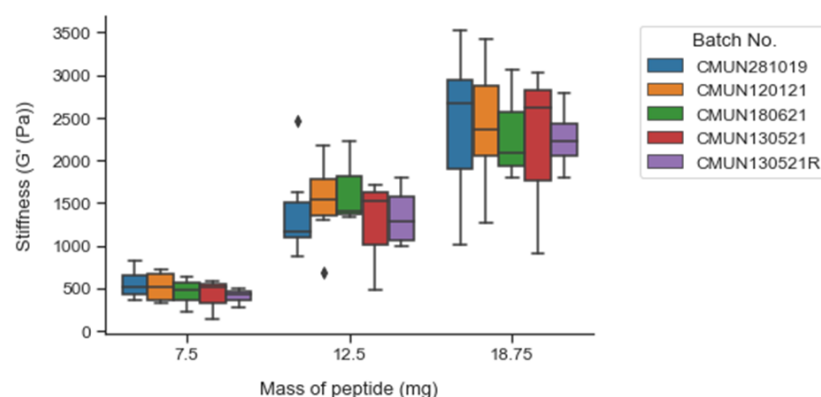
Figure 9 – Stiffness (G') of peptide hydrogels prepared during batch testing. Samples from each batch were used to prepare peptide hydrogels, following the standard peptide hydrogel preparation process, and then assessed via bulk oscillatory rheology. Results indicate no significant difference between all batches tested, given the same peptide concentration These results also demonstrate a positive relationship between peptide concentration and final stiffness of gel, indicating these batches produce gels of a predictable, tuneable stiffness (Mann-Whitney U test; n≥6 for CMUN281019, n≥8 for CMUN120121, n≥3 for CMUN180621, n≥3 for CMUN130521, n≥4 for CMUN130521R; ♦: outliers, defined as such if a datapoint is less than Q1 − 1.5 * IQR or greater than Q3 + 1.5 * IQR).

3.1.3 Cell viability

The final step was to assess the viability of cells encapsulated within the peptide hydrogels. E14 mESCs were chosen for this step as this cell type was the one used most often throughout the project, so any observable differences in cell viability or phenotype would be more readily apparent. It is suggested that end users wanting to employ this protocol consider carefully what cell type to use at this stage. It should be one that the user has good experience with, to allow them to quickly identify any issues with their batch of peptide. Peptide hydrogels of 10 mg/mL concentration were also chosen for this test for the same reason, as they were used more often than any other type throughout the project, and the expected viability and behaviour of E14 mESCs within gels of this type had previously been studied.

Precursor gels were prepared, as described above, and neutralised with a 250 μL cell suspension containing 2.5×10^5 cells/mL. Gels were then plated at 100 μL per well into a 96-well plate and cultured for seven days, following the standard procedure, and brightfield images taken periodically. On day seven, cells were then subject to a live/dead cell assay, by staining with a solution of ethidium homodimer and calcein AM before being visualised under a scanning laser confocal microscope. This test was repeated three times (three

biological repeats), and with three wells plated per test condition (three technical repeats). At least three images were then taken per test condition, with figures shown in Figure 10 being representative. This allowed for an empirical approach, where any differences between batches could be compared and contrasted with one another.

The images obtained show that gels prepared using batch CMUN130521 were visibly cloudy when viewed under a brightfield microscope and cells appeared to have reduced viability, compared to other batches. Whilst there didn't appear to be an increase in dead cells within gels prepared using CMUN130521, the fluorescence signal detected was much weaker. This is likely due to the gels having a cloudy appearance, as seen in the previous brightfield images. An important feature of the peptide hydrogels is that they should be optically clear. When this is not the case, it leads to poorer quality of images obtained in an end-point experiment. In the gels prepared using the re-processed material, these issues appeared to have been resolved.

This approach was used to measure cell viability as it can be easily performed and produces data which is easy to interpret. It also uses reagents and equipment that future end users are likely to have access to already. This increases the likelihood that this research may have a wider reaching impact. Other commonly used viability assays which could have also been used include the RealTime-Glo™ MT Cell Viability Assay (Promega; G9711), which has the advantages of allowing measurements of cell viability in real-time over the course of several days and allowing simple kinetic monitoring to determine dose response. The CellTiter-Glo® 3D Cell Viability Assay (Promega; G9681) could have also been used, which was specifically designed to assess the viability of cells grown in 3D, by using a reagent which also lyses the cells, in order to achieve better penetration of 3D cell clusters.

Figure 10 - Cell viability of E14 mouse embryonic stem cells (mESCs) in 10 mg/mL peptide hydrogels, prepared using different batches of peptide. E14 mESCs were encapsulated within 10 mg/mL peptide hydrogels at a density of 2.5 x 10^5 cells/mL and cultured for seven days. Brightfield images were taken every day during culture. On day 7, a live/dead cell assay was performed, and fluorescence images obtained using a laser scanning confocal microscope. Images shown are representative over three biological repeats (n=3). Results indicate that, for the majority of batches, cells had a similar viability and cell clusters adopted a similar morphology. However, there was a reduced viability of cells grown in gels prepared with batch CMUN130521. These gels also adopted a cloudy appearance which was apparent in the brightfield images and produced fluorescent images of reduced quality. These issues appear to have been resolved in the re-processed batch (CMUN130521R). Scale = 100 μm.

3.1.4 Conclusion

Given that no meaningful differences between batches CMUN180621, CMUN120121, and CMUN180621 were detected, these batches were deemed fit for use in future experiments throughout the project. It was also assumed, based on the evidence of the above tests, that peptide hydrogels produced using any one of these batches were functionally identical and, therefore, could be used within the same experiment. Any changes observed in cell

behaviour in future cell-based assays would be due to the effect of a controlled variable and not on any innate differences between gels themselves.

In contrast, and given the observations made during the peptide hydrogel preparation process and in particular the cell viability test, the CMUN130521 batch was deemed unsuitable for use in future experiments. As previously mentioned, it is hypothesized that the underlying issue that caused all the problems with this batch was the presence of excess TFA, left behind by the manufacturing process. When this batch was returned and re-processed, this excess TFA was likely removed which enabled batch CMUN130521R to then pass through the testing protocol successfully.

3.2.0 Probing effective pore size

Cells encapsulated within the peptide hydrogels require continuous access to nutrients [256], relying on the transport of solutes and dissolved oxygen from the culture medium outside the gel and within the gel network itself. Solutes can move into and through the network due to the concentration gradients which exist within the model. As encapsulated cells consume nutrients within the gel, nutrients from outside the gel move inwards and waste products move outwards. The constant supply of new nutrients and removal of waste products is achieved by regular media changes and this process is reliant on the gels being permeable to those products moving in and out of the gel.

However, when encapsulating soluble biomolecules within the gel as a method for functionalisation, there is a potential risk that these molecules could also escape the gel and be lost during media changes. This risk may be dependant of the size of the molecule, where smaller molecules readily diffuse out of the gel whilst larger molecules may become hydrodynamically trapped upon encapsulation. The aim of this experiment was therefore to probe the effective pore size of the gels, to ascertain which molecules would likely be lost and which would remain during media changes. Those molecules small enough to be lost would then either need to be provided in the culture media (to nullify the concentration gradient that exists between the media and the gel) or be somehow covalently immobilised within the gel. To achieve this aim, a novel assay was designed utilising fluorescein isothiocyanate-dextrans (FITC-Dextrans) of varying lengths.

3.2.1 Initial validation and optimisation

To determine the optimum concentration of FITC-Dextrans for use in this assay, initial validation and optimisation was carried out using unfunctionalised "blank" peptide hydrogels and a FITC-Dextran approximately 40 kDa in size (FD40S). Peptide hydrogels of varying peptide concentrations were prepared, as described above, and plated at 100 µL per well into a 96-well plate. Solutions of FD40S were prepared at varying concentrations by diluting a stock solution in mESC culture medium. FD40S was chosen for optimising the protocol as it was reasonable to expect that molecules of this would be able to diffuse into the gel because it was already apparent that molecules of a similar size present in the culture medium were able to, otherwise encapsulated cells would not be viable within the gels. The concentrations tested were 10 µM, 20 µM, and 30 µM. For each concentration of FD40S tested, three gels of each concentration were also plated out (giving three technical repeats per test condition). Gels were incubated in 100 µL of the FITC-Dextran solution for 24 h at 37 °C before being washed with Dulbecco's Phosphate Buffered Saline (DPBS) and signal detected via a plate reader. Results from this experiment are presented in Figure 11. All concentrations of FITC-Dextran tested produced a measurable signal in each gel tested. In future experiments, a concentration of 20 µM would be used, as not only did this produce a measurable signal, but was also the concentration used for soluble matrix additions in later experiments so would offer better consistency throughout the project.
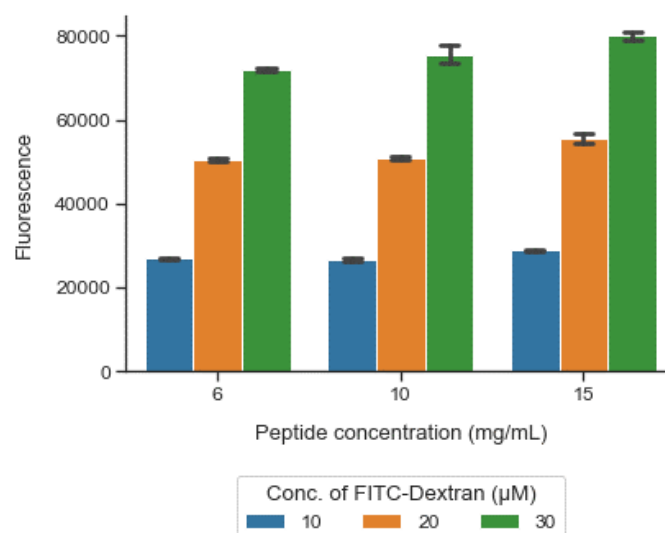
Figure 11 - Initial validation and optimisation of fluorescein isothiocyanate dextran (FITC-Dextran) gel permeability assay. Unfunctionalised "blank" peptide hydrogels of varying peptide concentrations were incubated with FITC-Dextran solutions, containing molecules of size 40 kDa, for 24 h at 37 °C, washed with Dulbecco's Phosphate Buffered Saline (DPBS), and fluorescence detected using a plate reader (n=1). These results demonstrate that a detected signal could be obtained in future tests using any of the concentrations of FITC-Dextran evaluated here.

Table 10 - Summary of fluorescein isothiocyanate-dextrans (FITC-Dextrans) used throughout the project.

Product No.	Source	Average mol. wt. (Da)
FD40S	Sigma	40,000
FD70S	Sigma	60,000 – 76,000
FD250S	Sigma	250,000
FD500S	Sigma	500,000
FD2000S	Sigma	2,000,000

3.2.2 Final evaluation

Informed by the previous validation and optimisation test, the permeability of unfunctionalised "blank" peptide hydrogels and were further evaluated. This protocol was also extended over seven days, to better evaluate how molecules of a certain size are lost over time and to be more informative of future cell culture assays. Peptide hydrogels were prepared, as described above, and plated at 100 µL per well into a 96-well plate. Solutions of FITC-Dextran of varying lengths (summarised in Table 10) were prepared by diluting a stock solution in mESC culture medium to a concentration of 20 µM. For each type and

concentration of FITC-Dextran tested, two gels of each concentration were plated out per test (giving two technical repeats per test – using as much gel material as was available per test). A total of three tests were conducted (giving three biological repeats). Gels were covered in 100 μL of FITC-Dextran solution and incubated for 24 h at 37 °C. The following day, gels were washed with DPBS and fluorescence signal detected via a plate reader before being covered in culture medium and returned to the incubator. This was repeating for seven days. In this way, the loss of soluble material of different sizes was evaluated over a length of time typical in future experiments. Results are presented in Figure 12. These results indicate that FITC-Dextrans up to 2000 kDa in size are able to diffuse into the gel within the first 24 h of incubation. Following this, the loss of FITC-Dextrans largely depends on their size, with the smaller molecules appearing to have greater ability to escape the gel and subsequently be lost during media changes. There also appears to be a marginal increase of retention in gels of a higher peptide concentration.

These results demonstrate that when encapsulating soluble biomolecules as a strategy to functionalise the peptide hydrogels, smaller molecules would also need be present in the culture medium, to maintain the desired concentration within the gels. However, this is wasteful and the development of alternative solutions to this problem was a focus in this project. It is also worth noting that the activity of certain biomolecules changes depending on whether they are attached to a scaffold or provided in solution [219]. This means that larger, hydrodynamically trapped molecules may also require covalent immobilisation when evaluating specific activities. There is, therefore, a need for developing new methods for control of matrix composition within the gel, not only to overcome the potential loss of material during cell culture but also to allow their function to be correctly regulated.
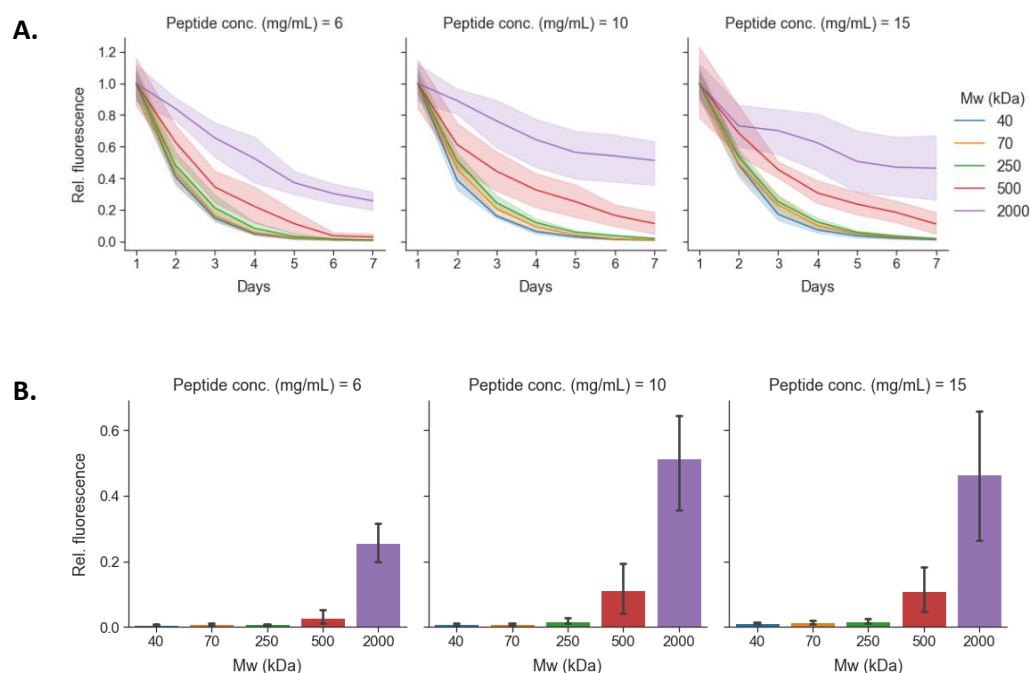
Figure 12 – Permeability and retention of fluorescein isothiocyanate dextrans (FITC-Dextrans) of various sizes in unfunctionalised "blank" peptide hydrogels. (A) Unfunctionalised "blank" peptide hydrogels were prepared and plated out at 100 µL per well of a 96-well plate. Gels were then covered with FITC-Dextran solutions containing molecules of various sizes (40-2000 kDa) and incubated for 24 h at 37 °C. The following day, gels were washed with Dulbecco's Phosphate Buffered Saline (DPBS) and fluorescence signal was detected using a plate reader. Gels were then covered with mouse embryonic stem cell (mESC) medium and returned to the incubator. This was repeated every day for seven days. Fluorescence signal was normalised to the reading taken on day 1. Shaded areas represent the standard deviation (n=3). (B) Results obtained on day seven. Error bars represent the standard deviation (n=3).

3.3.0 Developing "test environments" to evaluate future methods for functionalisation

Before launching into any investigation which aimed to develop new methods for functionalising the peptide hydrogels, it was necessary to create a series of "test environments". Each of these would provide a set of conditions that would act as a control, against which the effects of covalently immobilising matrix material could be tested.

3.1.1 Characterisation of cell lines

Characterisation of cell lines used in any study is critical, due to the emerging evidence that cell lines are frequently misidentified or contaminated by other cell types [257]. This can create problems for the study, where conclusions drawn from data gathered using the wrong cell type may not be appropriate for the intended cell type. Particularly in the field of cancer

research, where drugs may be tested on the wrong cell type, this can lead to unreliable results which delay the discovery of novel treatments [258].

Two different mouse embryonic cell (mESC) lines were provided for use throughout the project. These cell lines were selected as they had several critical features that made them ideally suited for the project. The first is that they are viable and grow well in the unfunctionalised "blank" peptide hydrogels. The second is that a previous study had demonstrated $Ext1^{-/-}$ mESCs, which lack the enzyme required to produce heparan sulphate (HS), were unable to undergo neural specification but that this potential could be restored by the addition of exogenous heparan sulphate III (HSIII) or heparin to the culture environment [68]. This provided a convenient baseline for evaluating new methods for immobilising HS or heparin within the gels. Finally, based on the literature, these cells were also likely to respond to the presence of immobilised RGD, which would also be evaluated later [219].

Whilst genotyping would have been the preferred method to characterise these cells, this was unfortunately unavailable due to budgetary constraints. Instead, a variety of different methods were used in a weight-of-evidence based approach. Firstly, the approximate proliferative rate of the cells during continuous culture was compared to the expected standards. This appeared consistent with the literature, with passages typically being required every 48 h, when seeded at a ratio of 1:10-12 [259, 260]. Secondly, the morphology of cells during culture was also compared to example images provided in the literature and was also found to be consistent. However, perhaps the most critical characterisation that was performed was to assess the ability of these cells to produce heparan sulphate (HS). This was assessed by using an existing protocol within the group which utilises the anti-HS antibody 10E4, which selective binds to the 10E4 epitope of HS but does not react with hyaluronan, chondroitin sulphate, dermatan sulphate, keratan sulphate or DNA. Cells were first seeded at a density of $1x10^5$ cell per well into a 24-well plate and cultured to 60-70% confluency (typically 48 h post-seeding), then fixed, stained, and imaged using a scanning laser confocal microscope. The images obtained demonstrated the presence of HS in E14 mESCs and the absence of HS in $Ext1^{-/-}$ mESCs, as expected (Figure 13). Therefore, we can conclude with a reasonable degree of certainty that the identities of the two cell lines are correct.
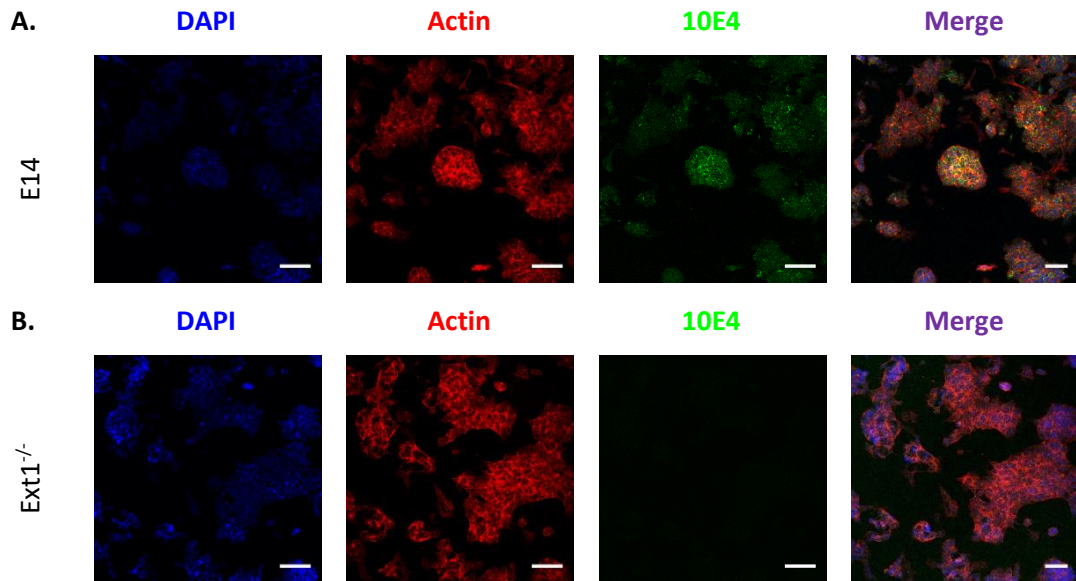
Figure 13 - Characterisation of mouse embryonic stem cells (mESCs) with 10E4 staining. E14 and Ext1⁻/⁻ mESCs were seeded at a density of 5x10⁵ per well into a 24-well plate. Cells were cultured until 60-70% confluency (typically 48 h post-seeding) before being fixed, stained, and imaged using a scanning laser confocal microscope. (A) E14 mESCs with positive staining for 10E4, indicating the presence of endogenous heparan sulphate, as expected for this cell type (n=3). Scale = 100 µm. (B) Ext1⁻/⁻ mESCs with negative staining for 10E4, indicated the absence of endogenous heparan sulphate, as expected for this cell type (n=3). Scale = 100 µm. These results, combined with other observations of proliferative rate and morphology during continuous culture, provide evidence that the stated identity of these cells is correct.

3.3.2 Directing mouse embryonic stem cell (mESC) fate with soluble glycans

Development of this test environment began as an attempt to replicate a previous study performed in 2D [68]. In this study, it was discovered that Ext1⁻/⁻ mESCs, which lack the enzyme required to produce heparan sulphate (HS), were unable to undergo neural specification but this potential could be restored by the addition of heparan sulphate III (HSIII) or heparin to the culture environment. To investigate whether the same effect would be observed in 3D, these cells were encapsulated in peptide hydrogels modified with soluble HSIII or heparin and cultured in N2B27 differentiation media. E14 mESCs were used as a control. After seven days, gels were stained for the neural specific marker β-III-tubulin and visualised under a scanning laser confocal microscope. Images are presented in Figure 14 and Figure 15.

Both E14 and Ext1⁻/⁻ mESCs were viable within unfunctionalised "blank" peptide hydrogels and those that had been functionalised with soluble HSIII or heparin. E14 cells were able to undergo neural specification with or without the presence of exogenous HSIII or heparin, whilst Ext1⁻/⁻ cells were only able to do so when these were provided. It also appeared that Ext1⁻/⁻ cells were able to progress further in the presence of heparin, compared to other

conditions or E14 cells. This is evidenced by the enhanced staining for β-III-tubulin and the higher degree of organisation of both β-III-tubulin and actin into extracellular filaments extending away from the cell cluster. These filaments can also be seen by day 5 in the brightfield images.

The reason for this enhanced response to heparin from Ext1$^{-/-}$ cells in unclear. However, when this experiment was previous performed in 2D, it was discovered that the effect of heparin is dose-dependent, peaking at 6 μg/mL before starting to decline [76]. Therefore, it is possible that there was an overabundance supplied to the E14 cells here, leading to inhibition, rather the activation, of FGFR signalling.

It is worth mentioning here, also, that the lack of DAPI staining in some conditions is a known issue with the gels. The use of Hoechst was later shown to be more effective for staining DNA in the gels and is now the preferred method. However, to remain consistent within the project, DAPI was used in all experiments.

Nevertheless, these results demonstrate that E14 and Ext1$^{-/-}$ stem cell fate can be modulated by the addition of specific soluble glycans within the gels, mirroring previous observations made in 2D. It also provides a testable hypothesis for evaluating future methods of covalently functionalising the gels: in gels covalently functionalised with HSIII or heparin, Ext1$^{-/-}$ cells should be able to undergo neural specification, providing the immobilised heparin is still accessible to cells and has retained its biological activity.
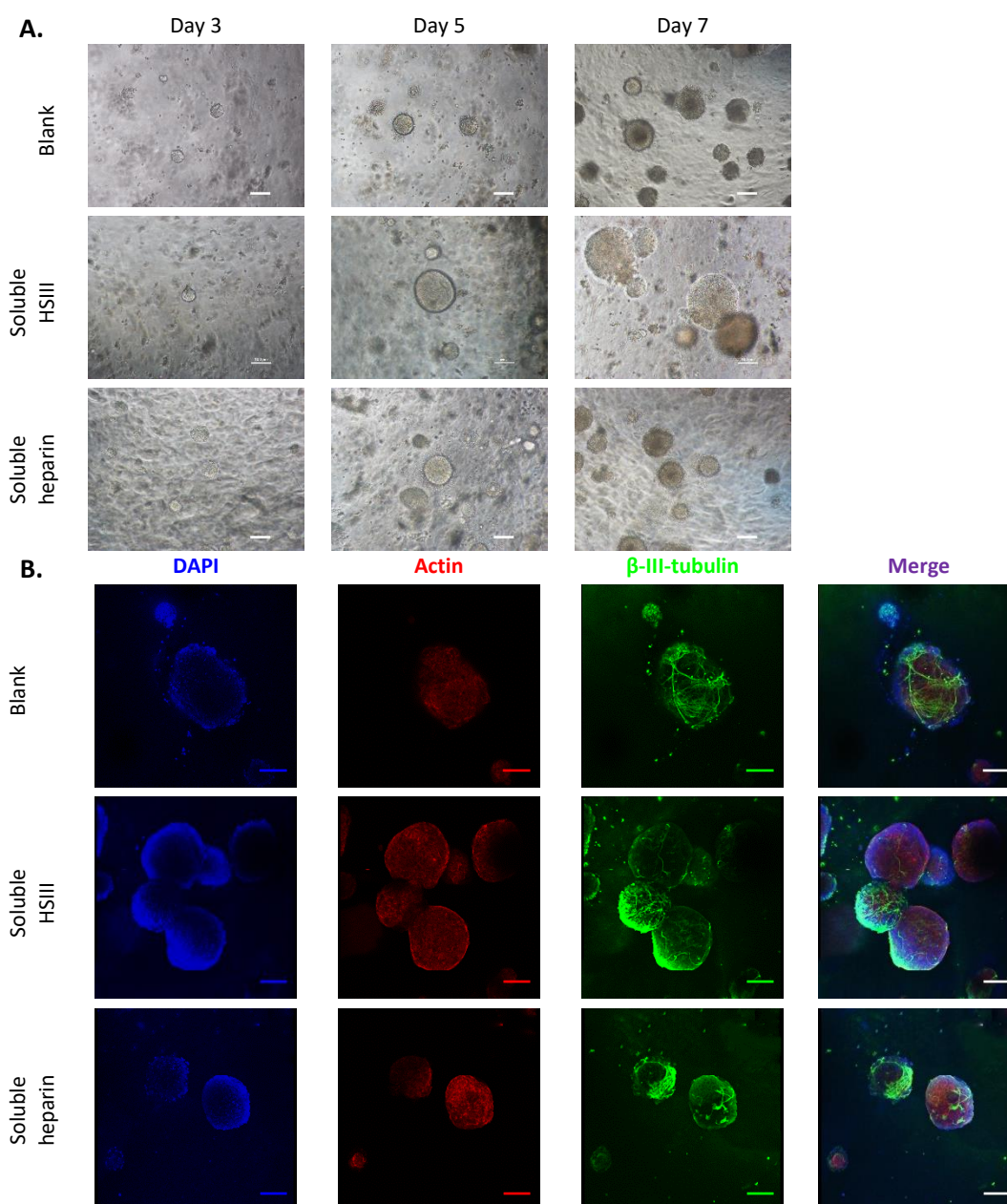
Figure 14 - E14 mouse embryonic stem cell (mESC) differentiation in peptide hydrogels functionalised with soluble heparan sulphate III (HSIII) or heparin. E14 mESCs were encapsulated in 10 mg/mL unfunctionalised "blank" peptide hydrogels, or gels functionalised with 0.05 mg/mL soluble HSIII or heparin, and then cultured in N2B27 differentiation medium for a period of seven days. (A) Representative brightfield images taken during culture (n=3). Scale = 100 μM. (B) Representative fluorescence images obtained on day 7, after cells were fixed and stained for DAPI, actin, and the neural specific marker β-III-tubulin (n=3). Scale = 100 μM. These results indicate that E14 mESCs are able to undergo neural specification both in the absence and presence of additional HSIII or heparin.
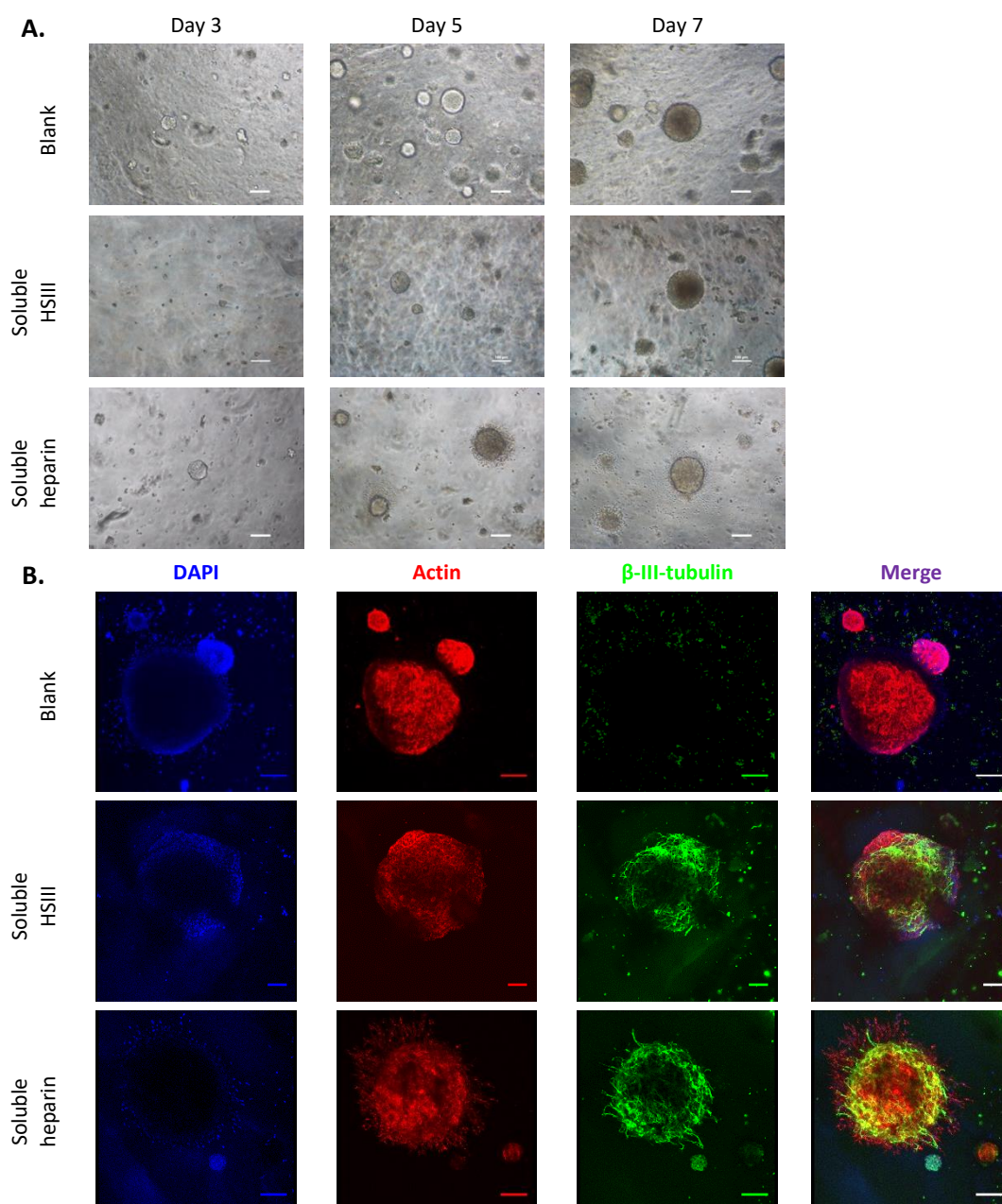
Figure 15 – Ext1⁻/⁻ mouse embryonic stem cell (mESC) differentiation in peptide hydrogels functionalised with soluble heparan sulphate III (HSIII) or heparin. Ext1⁻/⁻ mESCs were encapsulated in 10 mg/mL unfunctionalised "blank" peptide hydrogels, or gels functionalised with either 0.05 mg/mL HSIII or soluble heparin, and then cultured in N2B27 differentiation medium for a period of seven days. (A) Representative brightfield images taken during culture (n=3). Scale = 100 µM. (B) Representative fluorescence images obtained on day 7, after cells were fixed and stained for DAPI, actin, and the neural specific marker β-III-tubulin (n=3). Scale = 100 µM. These results indicate that Ext1⁻/⁻ mESCs are only able to undergo neural specification both in the presence of additional HSIII or heparin.

3.2.3 Directing embryonic mouse stem cell (mESC) fate with soluble peptides

Proteins that contain the Arg-Gly-Asp (RGD) attachment site, such as fibronectin and collagen, together with the integrins that serve as receptors to them, constitute a major recognition system for cell adhesion [34]. These interactions can also be reproduced by short synthetic peptides containing the RGD sequence. Development of a test environment to evaluate new methods for covalently immobilising RGD within the peptide hydrogels would, therefore, first need to evaluate the effect of soluble RGD within the gels.

E14 and Ext1$^{-/-}$ mESCs were again chosen for the development of this test environment. Cells were encapsulated within peptide hydrogels functionalised with either full length soluble fibronectin or a short, synthetic RGD-containing peptide. Cells were then cultured for seven days in N2B27 differentiation media before staining with the neural specific marker β-III-tubulin and visualised using a scanning laser confocal microscope. Images are presented in Figure 16 and Figure 17.

In contrast to the previous experiment using HSIII and heparin, the differentiation potential of E14 cells appeared to be inhibited by the presence of soluble fibronectin or RGD. In gels functionalised with fibronectin, most cell clusters stained positive for β-III-tubulin, but others did not. In gels functionalised with soluble RGD, this inhibitory effect appeared even greater. The results for Ext1$^{-/-}$ cells were more surprising. These cells were unable to undergo neural specification in the presence of soluble fibronectin or RGD, as expected. They did, however, begin to exhibit a change in phenotype in the presence of soluble RGD. Cell clusters within RGD functionalised gels appeared to adopt an altered, "lemon-shaped" morphology.

In a recent study investigating the effect of immobilising RGD on synthetic nanofibers found that the presence of RGD leads to downregulation of β-III-tubulin and an increase in early expression of green acidic fibrillary protein (GFAP) in mESCs [219]. This pushed the cells towards a non-neuronal, glial linage and may be what is being observed here in the peptide hydrogels. To test if cells were being directed to a glial lineage, the RGD functionalised gels were also stained for GFAP. However, no detectable GFAP expression was observed.

It is possible that, because of the peptide's small size, much of it was being lost during media changes and that by the end of the experiment there was not enough RGD to continue to support the differentiation towards a glial lineage. Therefore, this produces a testable hypothesis for evaluating methods for covalently immobilising RGD within the peptide hydrogels: in these modified gels, the concentration of RGD remains high enough throughout

culture to support differentiation of E14 and Ext1$^-$/$^-$ cells towards a detectable β-III-tubulin$^-$, GFAP$^+$ glial lineage.
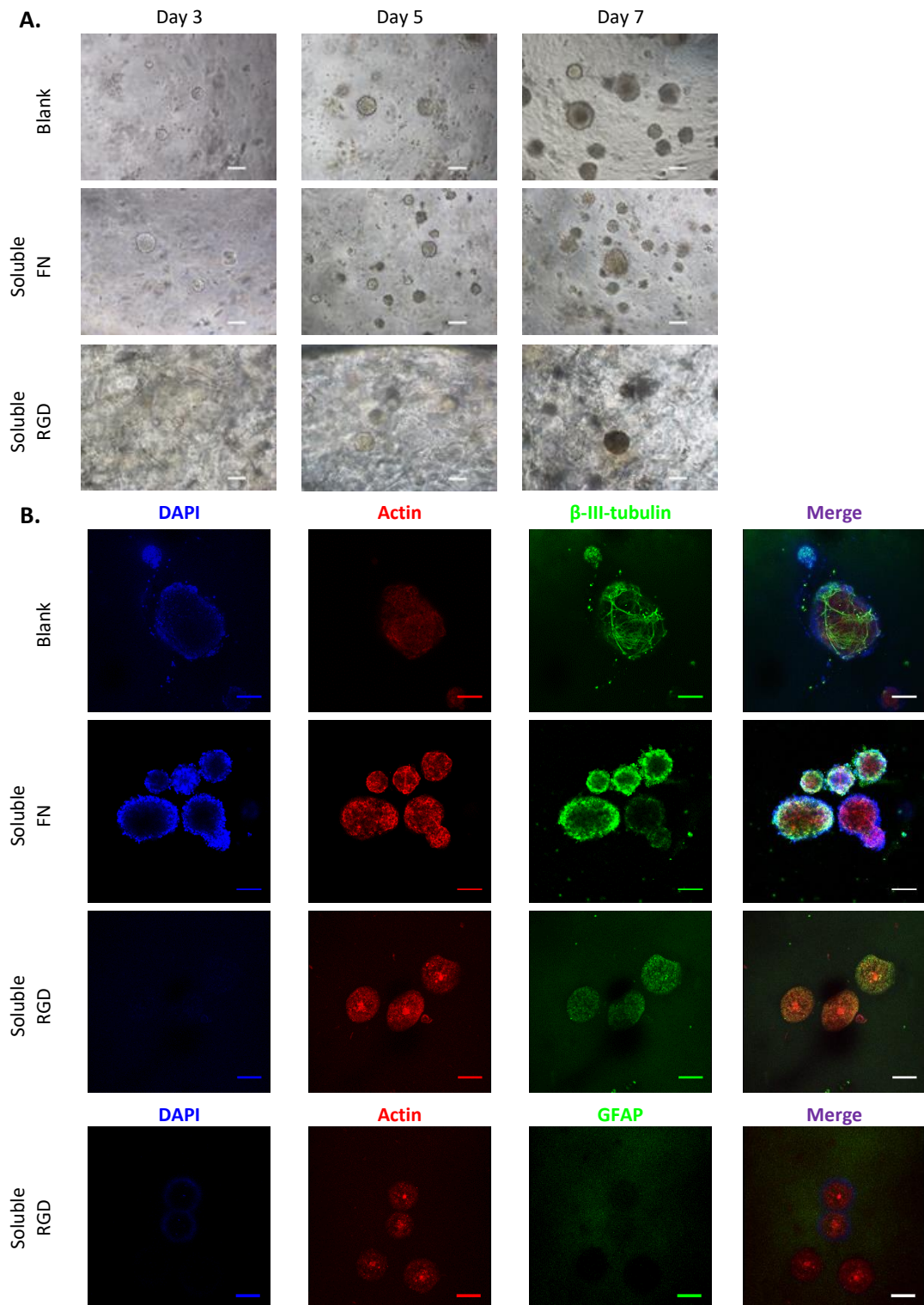
Figure 16 – E14 mouse embryonic stem cell (mESC) differentiation in peptide hydrogels functionalised with soluble fibronectin (FN) or RGD. E14 mESCs were encapsulated in 10 mg/mL unfunctionalised "blank" peptide hydrogels, or gels functionalised with either 20 µM FN or RGD, and then cultured in N2B27 differentiation medium for a period of seven days. (A) Representative brightfield images taken during culture (n=3). Scale = 100 µM. (B) Representative fluorescence images obtained on day 7, after cells were fixed and stained for DAPI, actin, and either the neural specific marker ϐ-III-tubulin or the glial specific marker GFAP (n=3). Scale = 100 µM.
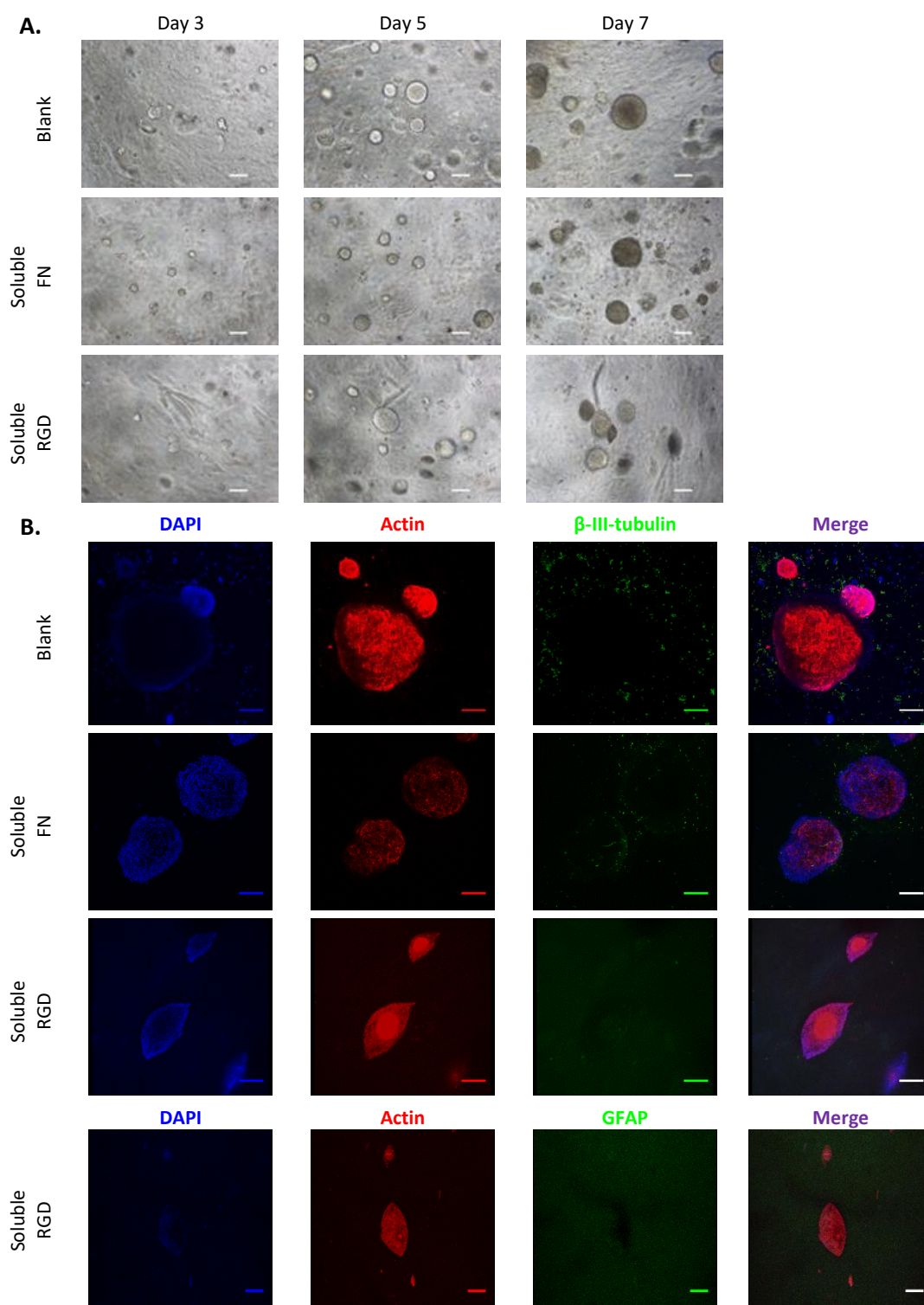
Figure 17 – Ext1$^{-/-}$ mouse embryonic stem cell (mESC) differentiation in peptide hydrogels functionalised with soluble fibronectin (FN) or RGD. Ext1$^{-/-}$ mESCs were encapsulated in 10 mg/mL unfunctionalised "blank" peptide hydrogels, or gels functionalised with either 20 µM FN or RGD, and then cultured in N2B27 differentiation medium for a period of seven days. (A) Representative brightfield images taken during culture (n=3). Scale = 100 µM. (B) Representative fluorescence images obtained on day 7, after cells were fixed and stained for DAPI, actin, and either the neural specific marker β-III-tubulin or the glial specific marker GFAP (n=3). Scale = 100 µM.

3.3.4 Conclusion

Now with two individual test environments for evaluating the effect of covalently immobilising specific glycans (HSIII or heparin) and peptides (FN or RGD), investigations into new methods for achieving this type of functionalisation could now be carried out. In the future, it is suggested that the same principles applied here could be applied to the development of specific test environments for each new biomolecule to be covalently immobilised.

3.4.0 Sortase-mediated control of matrix composition

Sortase-mediated functionalisation had previously been employed in several past studies to functionalise other biomaterials. In 2015, Cambria et al. used sortase to modify a polyethylene glycol (PEG)-based hydrogel containing the LPRTG sortase substrate with sort-tagged epidermal growth factor (GGG-EGF) [223]. Another group, Piluso et al. (2013), were also able to use sortase to modify a peptide-based hydrogel similar in composition to the peptide hydrogel used in this project [224]. Using the above studies as a starting point, an investigation was launched to see if the sortase approach to functionalising biomaterials could be adapted to work with the peptide hydrogels.

3.4.1 Initial validation

The first step in investigating sortase A (SrtA) as a bioconjugation tool for the peptide hydrogel model was to perform an initial validation experiment. The protocol for this experiment was adapted from [224]. This study had used SrtA to immobile Tus, a DNA-binding protein, to a hydrogel which was similar in composition to the peptide hydrogel used in this project. This provided a useful starting point for this investigation.

Sortase-primed peptide hydrogels of 10 mg/mL peptide concentration were prepared using 50% unfunctionalised peptide (FEFEFKFK) and 50% sortase-tagged peptide (GGGG-FEFEFKFK). To verify that the inclusion of the sortase-tagged peptide did not have any undesirable effects on the properties of the gels, a similar testing protocol to that used earlier (for batch testing) was employed to characterise this new type of peptide hydrogel. No meaningful differences were detected (Figure 18), so the initial validation test could proceed.
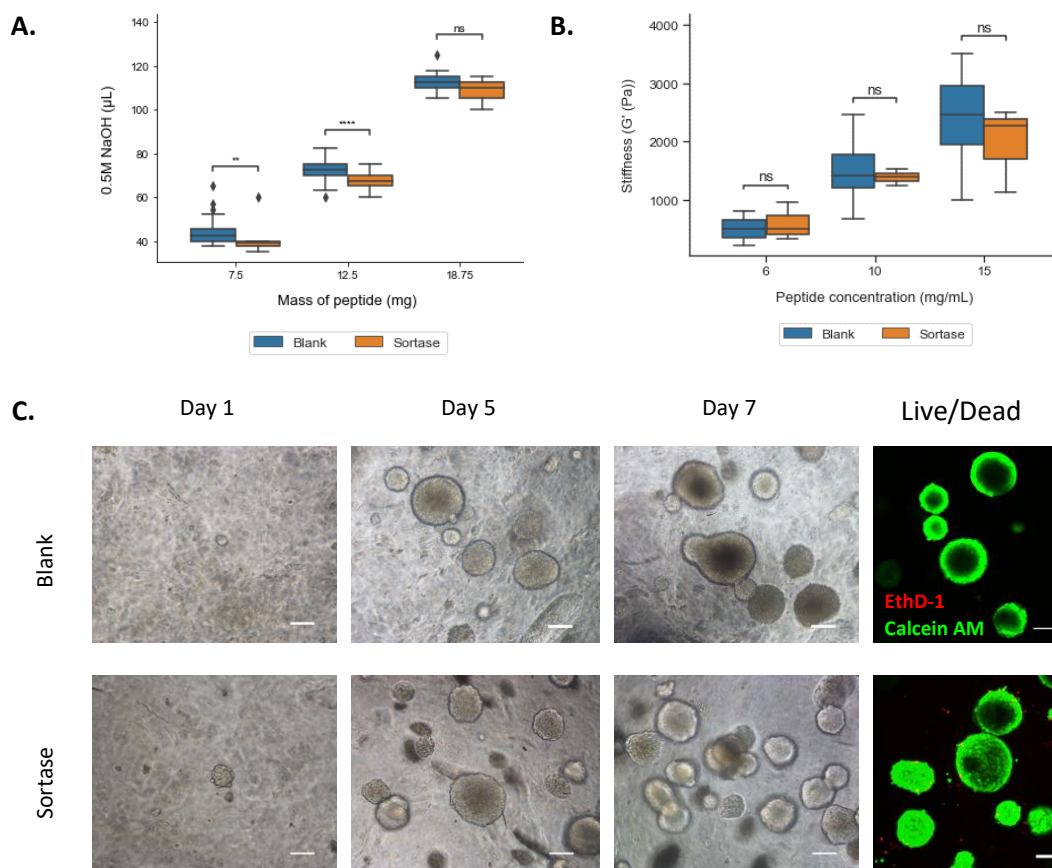
Figure 18 – Viability testing of sortase-primed peptide hydrogels. (A) Comparison of volume of 0.5M NaOH required to trigger gelation in unfunctionalised "blank" (blank) and sortase-primed precursor gels (sortase) (Mann-Whitney U test; n≥30 for blank gels, n≥7 for sortase gels; ♦: outliers, defined as such if a datapoint is less than Q1 – 1.5 * IQR or greater than Q3 + 1.5 * IQR; ns: not significant; **: p < 0.01; ****: p < 0.0001). (B) Stiffness (G') of blank and sortase gels, assessed via bulk oscillatory rheology (Mann-Whitney U test; n≥17 for blank gels, n≥3 for sortase gels; ns: not significant). (C) Cell viability of E14 mouse embryonic stem cells (mESCs) in blank and sortase gels. Cells were encapsulated and cultured for seven days. Brightfield images were taken every day. On day 7, a live/dead assay was performed, and images obtained using a scanning confocal microscope. Images shown are representative over three biological repeats (n=3). Scale = 100 µM. These results indicate that there is no meaningful difference between blank and unmodified sortase gels, and that any subsequent tests which reveal changes in cell behaviour in modified sortase gels are due to that modification.

To carry out the sortase reaction within these gels, a tethering solution was created. This solution contained 15 µM wild-type (WT) SrtA (provided by James Kapp, University of Nottingham, UK) and 20 µM sortase-tagged eGFP-LPETG (also provided by James Kapp) dissolved in a calcium buffer (150 mM NaCl, 50 mM CaCl$_2$, and 50 mM HEPES dissolved in sterile water). The concentrations for the WT SrtA and eGFP-LPETG were selected based on the concentrations used in [224]. A second, control solution was prepared, as above, but without any sortase.

The sortase-primed gels were plated at 100 µL per well into a 96-well plate and then covered with the tethering solution. Gels were incubated for 2 h at room temperature, which was the incubation protocol used in [224]. After 2 h, gels were washed five times with DPBS, to remove any unbound eGFP-LPETG. The presence of immobilised eGFP-LPETG was inferred by measuring the fluorescence signal within the gels using a plate reader. A significant apparent increase in the retention of eGFP-LPETG was detected in gels where WT SrtA was present in the tethering solution (Figure 20a). To confirm that this eGFP-LPETG was distributed uniformly throughout the gel, gels were also visualised on a scanner laser confocal microscope, with a series of images taken spanning approximately 150 µm in the z-axis (Figure 19).

These results demonstrate the potential utility of WT SrtA as a bioconjugation tool to modify the peptide hydrogels. However, there still existed several potential avenues for optimisation of the reaction that were investigated before a final specific protocol for sortase-mediated functionalisation was selected.
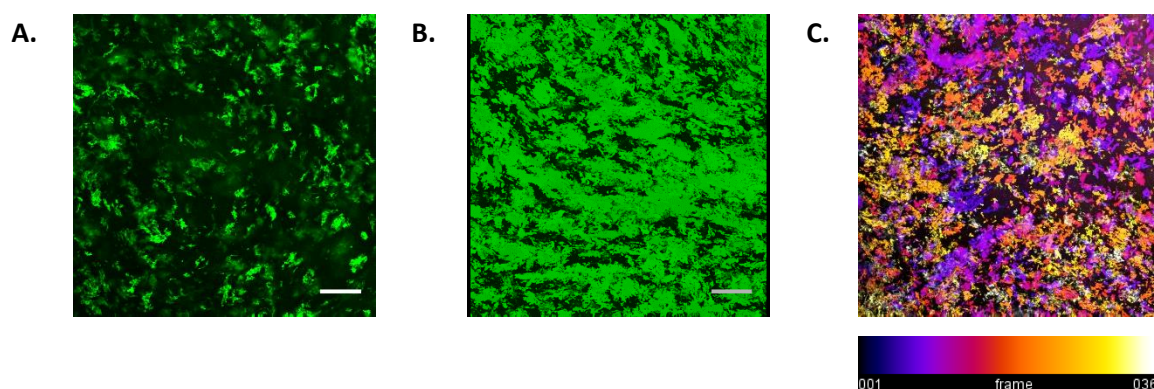
Figure 19 - Distribution of eGFP-LPETG throughout sortase-primed peptide hydrogels. Sortase-primed peptide hydrogels of 10 mg/mL concentration were plated at 100 µL per well into a 96-well plate and then covered in a tethering solution, containing 15 µM WT SrtA and 20 µM eGFP-LPETG in a calcium buffer. Gels were then incubated for 2 h at room temperature, washed five times with DPBS, and visualised using a scanning laser confocal microscope (n=3). (A) A single representative 2D frame, showing uniform distribution in the x- and y-axis. Scale = 100 µm. (B) A 3D projection of 36 frames, spanning approx. 150 µm in the z-axis, showing uniform distribution also in the z-direction. Scale = 100 µm. (C) A 3D projection of 36 frames, spanning approx. 150 µM, with each frame a different colour to show more clearly the uniform distribution in the z-direction. Scale = 100 µm. Whilst the author has done their best to display the uniform distribution of eGFP in the x-, y-, and z-directions, the use of a 2D image for this purpose obviously has its limitations. Therefore, the original image data is also available upon request, which would allow the reader to view each frame independently.

3.4.2 Optimisation of incubation protocol

Whilst many similar studies looking into using sortase as a bioconjugation tool used a 1-2 h incubation at room temperature [223-225], others have investigated a longer incubation at 37 °C [261] . This longer incubation at a more biologically relevant temperature would have the advantage of being more amenable for use in future cell-based assays. There have also been studies where a longer incubation at 4 °C had been used [262]. Given that the peptide hydrogels can be stored at 4 °C for a period of up to four weeks [33], this presents a possible avenue for preparing functionalised gels in batch and then storing them for later. Three different incubation protocols were therefore tested:

- 2 h at 37 °C
- 2 h at 37 °C, followed by an overnight incubation at 4 °C
- 24 h at 37 °C

Sortase-primed peptide hydrogels were prepared and plated out, as described above. A tethering solution containing 15 µM WT SrtA and 20 µM eGFP-LPETG in calcium buffer was created, along with a control solution containing no sortase. Gels were covered in these solutions and incubated according to one of the above incubation protocols. Finally, gels were washed five times in DPBS, and fluorescence detected using a plate reader.

The results of this optimisation test are presented in Figure 20b. Results indicate that there was a significant increase in the retention of eGFP-LPETG when using one of the longer incubation protocols, compared to the 2 h at 37 °C protocol. There was also no significant difference detected between these longer incubation protocols. These results demonstrate that the most significant increase in efficiency is obtained by an increase in incubation time and not with an increase in temperature. However, in the following tests and in future experiments, the incubation protocol chosen for further study was 24 h at 37 °C, as this would offer the greatest convenience when the sortase reaction would need to be carried out in the presence of encapsulated cells.

3.4.3 Optimisation of recognition motif

The second attempt at optimising the sortase reaction was to investigate the effect of altering the recognition motif on the protein of interest. Whilst WT SrtA should recognise any LPXTG (X = any amino acid, except proline) sequence, a search of the literature revealed that there may be as much as a three-fold increase in efficiency when using LPMTG,

compared to LPETG [261]. Two different eGFP molecules were produced to test this, one containing the LPETG sequence and one containing a LPMTG sequence (provided by James Kapp, University of Nottingham, UK).

Sortase-primed peptide hydrogels of 10 mg/mL were prepared and plated out, as described above. Two different tethering solutions were then created, one containing 20 µM eGFP-LPETG and another containing 20 µM eGFP-LPMTG, dissolved in a solution of 15 µM WT SrtA in calcium buffer. A third control solution was prepared, as above, but without any sortase. Gels were then covered in 100 µL of one of each of these solutions and incubated for 24 h at 37 °C, before being washed five times with DPBS to remove unbound eGFP, and fluorescence detected using a plate reader.

The results of this test are presenting in Figure 18c. These results indicate that there was a significant increase in the retention of both eGFP-LPETG and eGFP-LPMTG in gels where WT SrtA was present in the tethering solution. The results also demonstrate that there was a significant increase in efficiency where LPETG was the recognition motif used, compared to LPMTG. Based on the previous search of the literature, this was not the expected result and highlights the importance of testing our assumptions, as they may not always hold true when moving from one context to another. Therefore, in future experiments, LPETG was the recognition motif used for immobilising peptides within the peptide hydrogels.

3.4.4 Optimisation of tethering solution

Past studies have typically used additional calcium (usually as $CaCl_2$) [223, 225, 263] in their tethering solutions, as it is thought that this increases the efficiency of the sortase reaction. In *Staphylococcus aureus*, calcium binds near the active site of the enzyme, inducing a conformational change of a surface loop that recognises newly translocated proteins [229]. It stands to reason a similar effect would increase the efficiency of the sortase reaction *in vitro*.

However, additional calcium does not always appear to be necessary [224] and may have undesirable side-effects on the phenotype of encapsulated cells. The presence of calcium is also thought to influence peptide hydrogel stiffness (discussed in a later section) which could also indirectly influence cell phenotype. Therefore, the requirement for additional calcium in the tethering solution was investigated.

Sortase-primed peptide hydrogels of 10 mg/mL peptide concentration were prepared and plated out, as described above. Two different tethering solutions were then created containing 15 µM WT SrtA and 20 µM eGFP-LPETG either in calcium buffer or mESC culture medium (which likely contains approx. 1.8 mM calcium, but will vary by batch [264]). The choice to use mESC culture medium was made because this would also have the advantage of providing extra nutrients to encapsulated cells, providing an additional benefit to this protocol in future experiments. A third control solution was created with 20 µM eGFP-LPETG in mESC culture medium, without sortase. Gels were then covered in 100 µL of one of each of these solutions and incubated for 24 h at 37 °C, before being washed seven times with DPBS, to remove unbound eGFP, and fluorescence detected using a plate reader. The number of wash steps was increased from five to seven for this and future experiments to better simulate a typical seven-day cell culture experiment.

The results from this test are presented in Figure 20d. These results demonstrate that additional calcium is not an absolute requirement for the sortase reaction, as there was a significant increase in retention of eGFP-LPETG also in the absence of calcium. However, the results do confirm that additional calcium does increase the efficiency of the reaction. Therefore, to optimise the reaction further, an investigation was undertaken into the use of a calcium-independent mutant variant of sortase A.
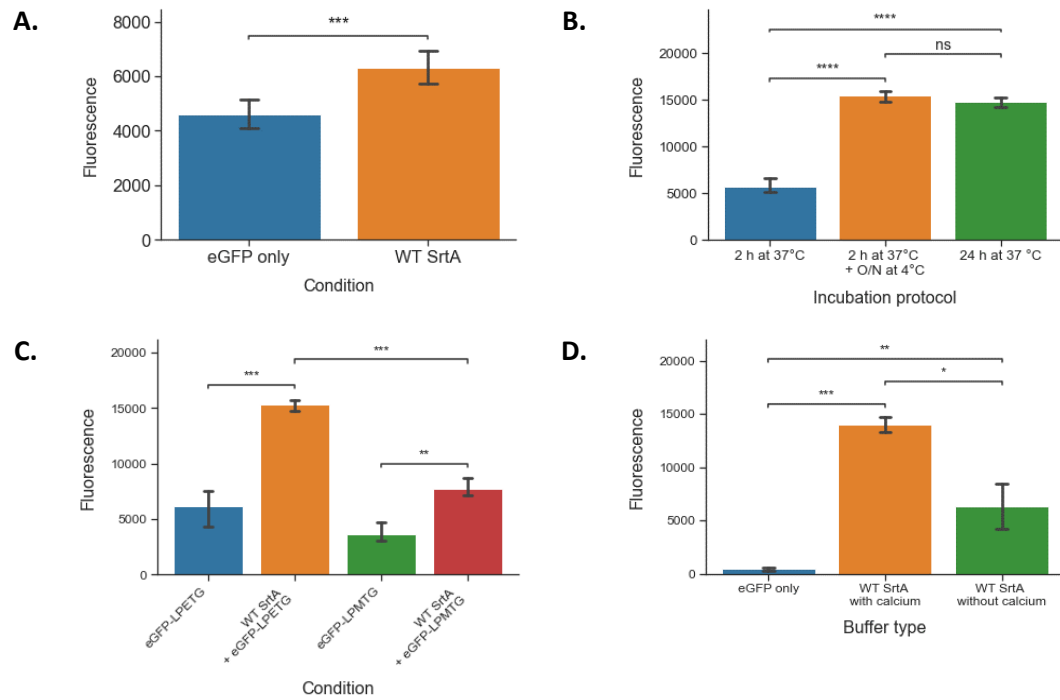
*Figure 20 – Initial validation and optimisation of the sortase protocol. (A) Initial validation of sortase-mediated functionalisation. Sortase-primed peptide hydrogels of 10 mg/mL were were plated at 100 µL per will into a 96-well plate and covered with a tethering solution containing 15 µM WT SrtA and 20 µM eGFP-LPETG, in a calcium buffer. A sortase-free solution was used as a control. Gels were then incubated for 2 h at room temperature, washed five times with DPBS, and fluorescence detcted using a plate reader (n=3). (B) Optimisation of incubation protococal. Sortase-primed peptide hydrogels were prepared, plated out, and covered in a tethering solution, as described above. Gels were then incubated according to three different protocols, washed five times in DPBS, and fluorescence detcted with a plate reader (n=3). (C) Optimisation of recognition motif. Sortase-primed peptide hydrogels were prepared and plated, as described above. Two different tethering solutions were prepared, containing 15 µM WT SrtA and either 20 µM eGFP-LPETG or eGFP-LPMTG, in a calcium buffer. Sortase-free solutions were used as controls. Gels were covered in these tethering solutions, incubated for 24 h at 37 °C, washed seven times in DPBS, and fluoresence detcted with a plate reader (n=3). (D) Optimisation of tethering solution. Sortase-primed peptide hydrogels were prepared and plated, as described above. Two different tethering solutions were prepared containing 15 µM WT SrtA and 20 µM eGFP in either a calcium buffer or mouse embryonic stem cell (mESC) culture medium. A sortase-free solution in mESC culture medium was used as a control. Gels were incubated for 24 h at 37 °C, washed seven times with DPBS, and fluorescence detected with a plate reader (n=10). (All above (A-D) were evaluated by Mann-Whitney U test; n ≥ 3; ns: not significant; *: $p < 0.05$; **: $p < 0.01$; ***: $p < 0.001$; ****: $p < 0.0001$).*

3.4.5 Investigating use of calcium-independent sortase A

To optimise the reaction further, a calcium-independent sortase enzyme would be necessary. An enzyme of this type would also be better for use in cell-based applications, where additional calcium could have undesirable side-effects, either directly on encapsulated cells or by affecting peptide hydrogel stiffness.

In a recent study [231], generation of a calcium-independent sortase A (7M SrtA) with enhanced activity for protein and cell surface labelling was achieved. The study reported that this enzyme was active at both 0 and 10 mM $CaCl_2$, in applications such as N- and C-terminal protein labelling and protein-protein conjugation, although the activity was generally slightly higher in the presence of calcium. Nevertheless, this enzyme had higher activity at low calcium concentrations than the wild type SrtA (WT SrtA) did at high concentrations. This enzyme, therefore, offered a promising next step in increasing the efficiency of the sortase reaction for use in functionalising the peptide hydrogels.

Generation of this enzyme was performed by James Kapp, University of Nottingham, UK, using the same methods described in the original paper. The authors of this paper also kindly offered to send a limited number of samples of their enzyme from Harvard Medical School, to use as a control against the enzyme generated in-house in Nottingham. Hereafter, each enzyme will be referred to as either **N**7M SrtA ("**N**ottingham" 7M SrtA) or **H**7M SrtA ("**H**arvard" 7M SrtA).

To test this new variant in the peptide hydrogel system, sortase-primed gels of 10 mg/mL peptide concentration were prepared and plated, as described above. The following tethering solutions were then prepared:

- 15 µM WT SrtA + 20 µM eGFP-LPETG, in calcium buffer
- 15 µM WT SrtA + 20 µM eGFP-LPETG, in mESC culture medium
- 15 µM N7M SrtA + 20 µM eGFP-LPETG, in calcium buffer
- 15 µM N7M SrtA + 20 µM eGFP-LPETG, in mESC culture medium
- 15 µM H7M SrtA + 20 µM eGFP-LPETG, in calcium buffer
- 15 µM H7M SrtA + 20 µM eGFP-LPETG, in mESC culture medium

Gels were covered in these tethering solutions and incubated for 24 h at 37 °C, washed seven times in DPBS, and fluorescence detected using a plate reader. Results are presented in Figure 21.

The results of this assay revealed that the most efficient tethering solution contained 15 µM WT SrtA in calcium buffer. This was surprising, as the results from the original paper had suggested that the calcium-independent variants should have had greater activity even in the absence of additional calcium. Most surprisingly was that there also appeared to be no significant difference between using WT SrtA without calcium and any of the conditions tested where a calcium-independent variant was used. The reason for this is not currently known but there appeared to be some characteristic of the peptide hydrogel system preventing a direct correlation of results from the original paper. Unfortunately, due to constraints of time and sortase material available, further investigation into this was not possible and WT SrtA was chosen as the variant for use in the final protocol.
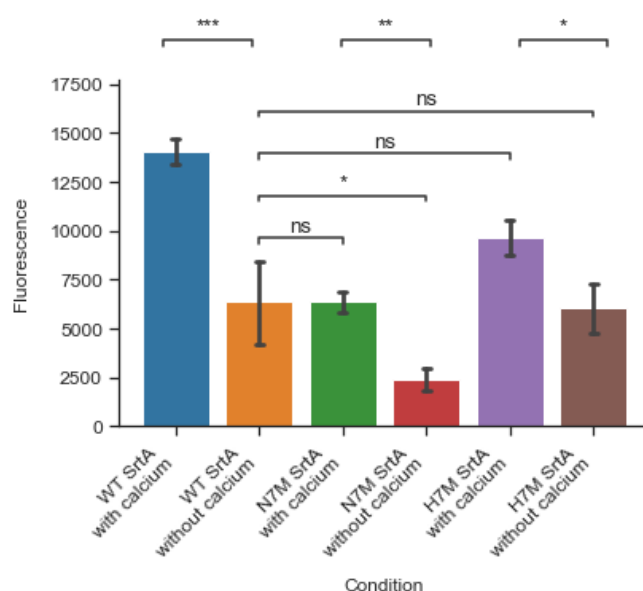
Figure 21 - Investigating use of calcium-independent sortase A. Sortase-primed peptide hydrogels of 10 mg/mL were prepared and plated at 100 µL into a 96-well plate. Several tethering solutions were prepared containing 20 µM eGFP-LPETG and 15 µM of one of several variants of sortase A, with or without additional calcium. Gels were incubated for 24 h at 37 °C, washed seven times with DPBS, and fluorescence detected with a plate reader. (Independent t-test; n=3; ns: not significant; *: p < 0.05; **: p < 0.01; ***: p < 0.001). These results revealed that there was no apparent benefit in using calcium-independent sortases, compared to wild-type, for the purpose of modifying the peptide hydrogels. In fact, for the calcium-independent sortase produced at Nottingham, there seemed to a reduction in reaction efficiency. The results also seem to reveal that the calcium-independent sortases actually do benefit from the presence of additional calcium in the reaction buffer.

3.4.6 Final protocol evaluation

The final protocol chosen to carry forward to future experiments throughout the project was decided upon consideration of several factors. Based on the previous optimisation tests, the most efficient protocol appeared to be:

- Incubation protocol: 24 h at 37 °C
- Recognition motif: LPETG
- Buffer type: calcium buffer (150 mM NaCl, 50 mM CaCl$_2$, and 50 mM HEPES, dissolved in sterile water)
- Sortase A variant: wild-type

However, in cell-based applications, a compromise must be struck between reaction efficiency and avoidance off potential undesirable side effects on encapsulated cells. Therefore, in the final test, both types of sortase buffer were evaluated (with and without additional calcium). Additionally, to better model a typical cell-based experiment, this final experiment was extended over seven days, with once wash per day, instead of performing all washes on the same day.

Sortase-primed peptide hydrogels of 10 mg/mL concentration were prepared and plated, as described above, and covered in tethering solutions containing 15 µM WT SrtA and 20 µM eGFP-LPETG in in calcium buffer or mESC culture medium. A sortase-free solution was used as a control. Gels were then incubated for 24 h at 37 °C. The following day, gels were washed with DPBS, fluorescence measured using a plate reader, and gels covered with mESC culture medium before being returned to the incubator. This process was repeated for a period of seven days and the results from this are presented in Figure 22a-b.

These results mirror previous results obtained during the permeability tests using FITC-Dextrans (Figure 12). Where sortase was not present, the majority of eGFP-LPETG was lost over the course of the first three days. Where sortase was used, the retention of eGFP-LPETG followed a trend which more closely resembled that of the larger FITC-Dextrans. The results obtained on day 7 also demonstrate that, by this timepoint, the use of WT SrtA as a bioconjugation tool leads to an increase in retention of between 37-52% (depending on the presence of additional calcium). Whilst there was a significant increase in reaction efficiency when performed in the presence of additional calcium, this increase was not considered meaningful enough to justify the potential for undesirable side-effects on encapsulated cells. Therefore, in future experiments, mESC culture medium was used as the reaction buffer.

At this point, it was also necessary to ensure that the sortase reaction could be carried out in the presence of encapsulated cells, without affecting their viability. To verify this, the final protocol was carried out on sortase-primed gels with 2.5×10^5 cell/mL encapsulated E14 mESCs. Brightfield images were taken every day and revealed no obvious effect on cell viability or phenotype (Figure 22c). On day seven, gels were stained with DAPI and rhodamine phalloidin and visualised using a laser scanning confocal microscope (Figure 22c). These images also revealed a greater retention of eGFP-LPETG in gels where WT SrtA had been present in the tethering solution. Interesting, the distribution of eGFP here appears even more homogeneous than seen previously (Figure 19). This is possibly due to the secretion of matrix material by encapsulated cells, and subsequent matrix remodelling [33].
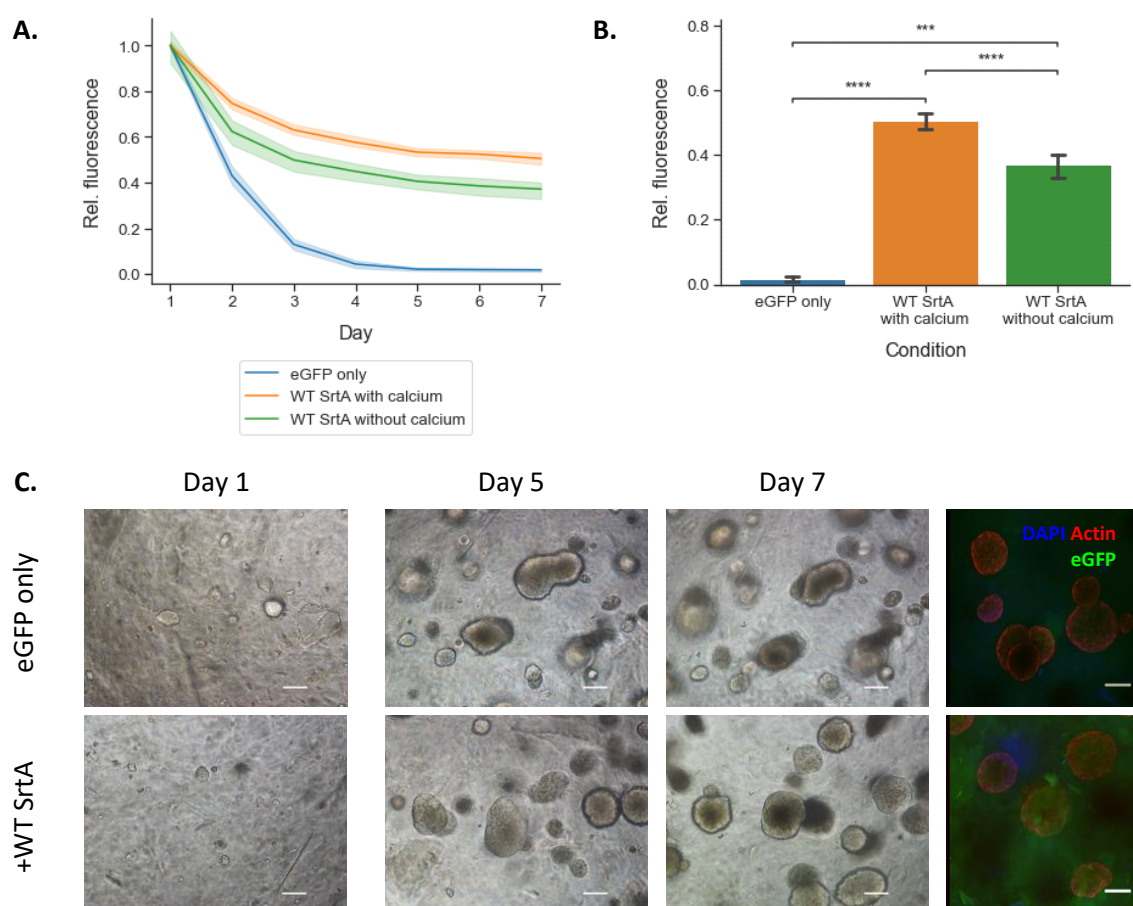
Figure 22 – Evaluation of final sortase-mediated functionalisation protocol. (A) Sortase-primed peptide hydrogels of 10 mg/mL concentration were plated at 100 µL per well into a 96-well plate and covered in tethering solution containing 15 µM WT SrtA and 20 µM eGFP-LPETG in either a calcium buffer or mESC culture medium. A sortase-free solution was used as a control. Gels were incubated for 24 h at 37 °C, washed in DPBS, and fluorescence detected using a plate reader. Gels were then covered in mESC culture medium and returned to the incubator. This was repeated over a period of seven days. Fluorescent signal was normalised to the first reading. Shaded areas represent standard deviation (n=3). (B) Final readings taken on day seven (Mann-Whitney U test; n=3; ***: p < 0.001; ****: p < 0.0001). (C) Cell viability of E14 mouse embryonic stem cells (mESCs) encapsulated in gels prepared, and functionalised, as described above. Cells were cultured in mESC culture medium for a period of seven days. Brightfield images were taken every day. On day 7, cells were fixed, stained with DAPI and rhodamine phalloidin, and visualised using a laser scanning confocal microscope. Images shown are representative over three biological repeats (n=3). Scale = 100 µM. These results demonstrate the benefit of using sortase-mediated immobilisation as a strategy to modify the peptide hydrogels, with an approximate increase of 37-52% in the retention of material over 7 days (depending on the presence of additional calcium in the reaction buffer).

3.5.0 Sortase-mediated control of matrix stiffness

As discussed earlier, a significant advantage of the peptide hydrogel platform is that a range of tissue stiffnesses can be modelled, simply by adjusting the mass of peptide used in the preparatory process [33, 252]. However, at present there exists only a single point at which this customisation can be achieved by the user. Encapsulated cells will, therefore, exist within gels of approximately the same stiffness throughout the experiment (with possibly some alteration made as a result of the secretion and degradation of the matrix by the cells themselves [33]). This does not accurately model diseases like cancer, where disease progression often correlates with a much larger increase in stiffness [89]. The ability to increase the stiffness of gels on demand, at any point during an experiment, would therefore be a valuable additional to the features of this model.

To achieve this, a protocol was designed to utilise sortase-mediated transpeptidation, adapted from [214]. In this study, the authors used a polyethylene glycol (PEG) based hydrogel containing PEG-peptide conjugates engineering to express both sortase recognition motifs (i.e., PEG-GGGG and PEG-LPRTG). Dynamical control of stiffness was then achieved by incubating the gels in the presence of sortase A to induce hydrogel crosslinking, leading to an increase in stiffness. Due to the reversible nature of the sortase reaction, the authors were also able to achieve dynamic softening of cross-linked hydrogels by incubating with sortase A and oligoglycine, leading to degradation of those cross-links.

To investigate whether the same could be achieved in the peptide hydrogel model, sortase-primed gels were prepared using various ratios of FEFEFKFK, GGGG-FEFEFKFK, and FEFEFKFK-LPETG peptide powder. A summary of the gels used in this test are presented in Table 11. These gels were prepared and plated out at 200 µL per well into a hanging insert within a 24-well plate. Gels were then covered in a tuning solution containing 15 µM WT SrtA in either a calcium buffer (150 mM NaCl, 50 mM $CaCl_2$, and 50 mM HEPES dissolved in sterile water) or mESC culture medium. Two different sortase-free solutions of only calcium buffer or mESC culture medium were used as controls. Gels were incubated for 24 h at 37 °C and then evaluated via bulk oscillatory rheology.

This preliminary test produced a number of surprising results. Firstly, there unfortunately appeared to be no meaningful stiffening of gels via sortase-mediated transpeptidation. This may be due to the recognition motifs being spatially separated and "locked" in-place within the gel network, following final neutralisation. The sortase enzyme would, therefore, not be able to cross-link the hydrogel. Secondly, the stiffness of the dynamically tuneable gels

appeared much lower than the unfunctionalised "blank" peptide hydrogels. This was not necessarily a cause for concern. If this protocol proved useful, this difference could be adjusted for in the future by increasing the mass of peptide used in the preparatory process. The most concerning conclusion drawn from these results was that there appeared to be a large increase in gel stiffness in response to the presence of additional calcium, irrespective of the presence of sortase.

Given that the presence of additional calcium appears to have such a large impact on gel stiffness, this provides further justification for the use of mESC culture medium, instead of a calcium buffer, for functionalising the gels via sortase. Also, whilst it would have been useful to be able to dynamically alter gel stiffness on demand, these results present a different opportunity. By preparing sortase-primed gels containing different ratios of both recognition motifs, two different molecules of interest could be immobilised within these gels at different concentrations, without the concern of altering gel stiffness via hydrogel cross-linking. These modifications could also be carried out at different time points, offering better temporal control of matrix composition.

Table 11 - Summary of peptide hydrogels used to test protocol for dynamic control of stiffness, via sortase-mediated transpeptidation.

Gel type	Final concentration (mg/mL)	Batch No.	Mass of peptide (mg)	Peptide ratio
Unfunctionalised "blank" peptide hydrogel	10	CMUN120121	12.5	Blank control
Dynamically tuneable peptide hydrogels	10	CMUN100220	3.13	25:50:25
		CMUN120121	6.25	
		CMUN171218.2	3.12	
	10	CMUN100220	6.25	50:50
		CMUN171218.2	6.25	
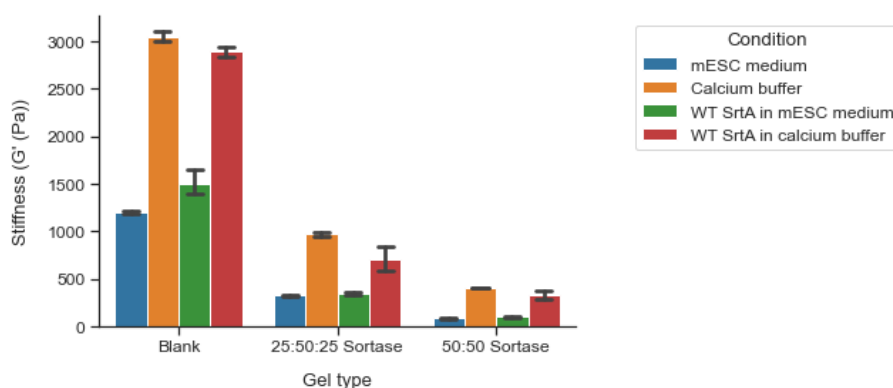
Figure 23 - Dynamic control of peptide hydrogel stiffness via sortase-mediated transpeptidation. Dynamically tuneable peptide hydrogels of 10 mg/mL concentration were plated at 200 µL per well into a hanging insert within a 24-well plate. Gels were then covered in various tuning solutions containing 15 µM WT SrtA in either a calcium buffer or mESC culture medium. Sortase-free solutions of calcium buffer or mESC culture medium were used as controls. Gels were incubated for 24 at 37 °C and then evaluated via bulk oscillatory rheology (n=3).

3.6.0 "Click" chemistry-mediated control of matrix composition

A second method for covalently immobilising matrix additions within the peptide hydrogels was also investigated, utilising "click" chemistry. "Click" chemistry, specifically the 1,3-dipolar cycloaddition between bio-orthogonally complementary azide and alkyne moieties, has previously been employed in many hydrogel systems, either to induce chemical cross-linking to generate the scaffold or as a strategy to attach bioactive molecules within the hydrogel [265-269]. Inspired by [270, 271], where functionalisation of spider silk via the incorporation of the non-natural amino acid L-azidohomoalanine (Aha) and subsequent "click" reaction with alkyne-presenting molecules, the gelator peptide was extended with an Aha residue at its C-terminus (FEFEFKFK(Aha)). Molecules of interest could then be modified to present alkyne handles, making them amenable to "click"-mediated covalent immobilisation within the gel. This method of modification also has an advantage over sortase-mediated functionalisation, as greater range of target molecules can be equipped with an alkyne handle, including both proteins and glycosaminoglycans.

To test this approach within the peptide hydrogel system, two different bioactive molecules were selected to be immobilised within the gel using this method: the glycosaminoglycan heparin and a short, synthetic RGD-containing peptide. Each of these presented their own set of challenges, which are discussed below.

3.6.1 "Click" chemistry-mediated immobilisation of RGD

The gelator peptide FEFEFKFKF has previously been extended to include the RGD motif for use as an injectable hydrogel scaffold for the delivery and retention of rat cardiac progenitor cells (CPCs) into the heart [212]. More recently, a "clickable" cyclo(RGDfK) molecule has been incorporated into spider silk cell scaffolds in an attempt to improve cellular adhesion [271]. Cyclisation of the RGD motif to cyclo(RGDfK) is found to enhance biological activity, compared to its linear counterpart. This is due to a reduction in the loss of entropy required for the change of a linear sequence from its randomly coiled to its frozen bound conformation [272]. Therefore, incorporation of a "clicked-in" cyclo(RGDfK) would potentially have an advantage over current methods for functionalising the gelator peptide with an RGD motif.

To achieve functionalisation with cyclo(RGDfK), a dibenzocyclooctyne (DBCO) linker was used to provide the alkyne handle necessary for the subsequent "click" reaction. DBCO allows for copper-free "click" chemistry to be carried out, within a physiological range of pH and temperature, and in the presence of living cells (due to the fact it does not bind the amines or hydroxyls naturally present in many biomolecules). It also provides physical space between the gelator peptide and the cyclo(RGDfK), ensuring that the presence of the cyclo(RGDfK) does not interfere with the gelation process. It may also allow for enhanced bioactivity, due to the fact that the linker will allow the cyclo(RGDfK) to "spin". This would increase the likelihood of the effector portion of the molecule falling into a favourable position that allows binding with the cell-surface integrins of encapsulated cells.

Generation of the DBCO-cyclo(RGDfK) was performed by Chris Merrett (University of Nottingham, UK). To facilitate amide bond formation, a DBCO-NHS ester was synthesized via carbodiimide-activation of the carboxylic acid residue with 1-ethyl-3-(3-dimethylaminopropyl)carbodiimide and hydrochloride (EDC·HCl) and N-hydroxysuccinimide (NHS). Amide coupling with cyclo(RGDfK) was then achieved, without the need for a coupling reagent (Scheme 2) and the reaction was confirmed with high resolution mass spectrometry (HRMS). The product was then purified by HPLC.
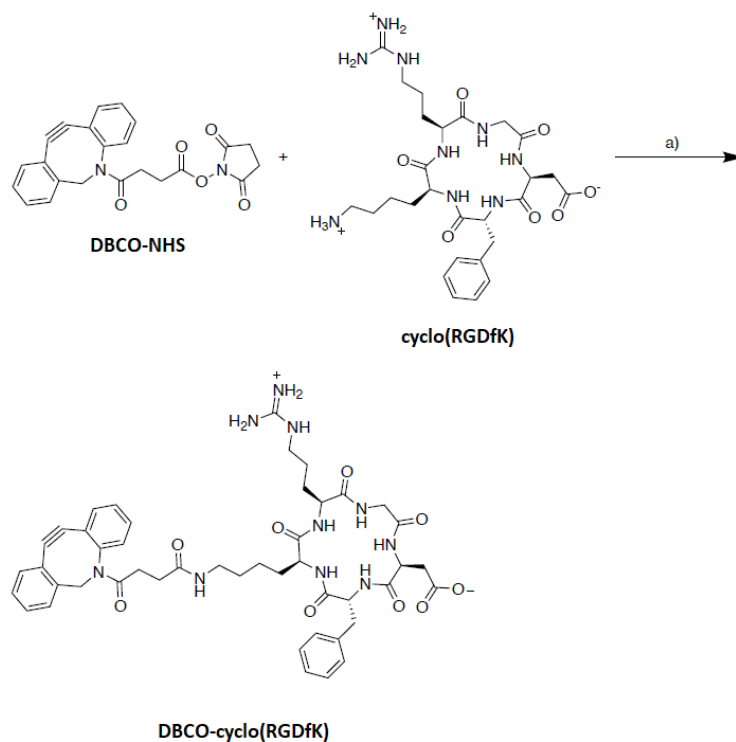
Scheme 2 – Amide coupling of DBCO-NHS ester with cyclo(RGDfK).

This material was then provided for use in this project. It was predicated that the final "click" reaction (Figure 24a) would progress through the initial vortex and centrifugation steps of the normal precursor gel formation protocol. To test this, two 6 mg/mL "clickable" gels were fabricated, with an intended degree of RGD functionalisation of 10 wt.%. A total mass of 7.5 mg of peptide powder was weighed (comprising 50% FEFEFKFK and 50% FEFEFKFK(Aha)) and dissolved in an aqueous solution of approx. 667.5 μg/mL DBCO-cyclo(RGDfK). Following a 2 h incubation step at 80 °C, gelation was then triggered by incremental addition of 0.5M NaOH, before a second overnight incubation step at 80 °C. Final precursor gels where then stored at 4 °C until needed.

The appearance and disappearance of chemical species at different time points along the procedure was observed via HRMS. Figure 24b presents data obtained from the HRMS analysis after the 2 h incubation step. This mass spectrum identifies two peaks (m/z = 713.6846 and 1070.0225) that correspond to the desired FEFEFKFK(Aha)-DBCO-cyclo(RGDfK) product, as triply and doubly charged adduct species. Also displayed are peaks for the FEFEFKFK (m/z = 561.2845 and 1121.5632) and FEFEFKFK(Aha) (m/z = 624.3129 and

1247.6187) peptides, as singly and doubly charged adduct species. A value that would represent the DBCO-cyclo(RGDfK) molecule was not present, indicating a high reaction efficiency.

It is also important to note that the adaptations made to the gel fabrication procedure did not appear to have any deleterious effect on gel formation. All products readily dissolved to form clear solutions and upon gelation formed clear, self-supporting gels. These results, therefore, provide an initial proof of concept for an *in situ* "click" protocol as a viable method for gel functionalisation. However, consideration must be taken that this protocol was only performed twice. Unfortunately, due to limited production of the DBCO-cyclo(RGDfK) material, it was impossible to repeat this a third time.
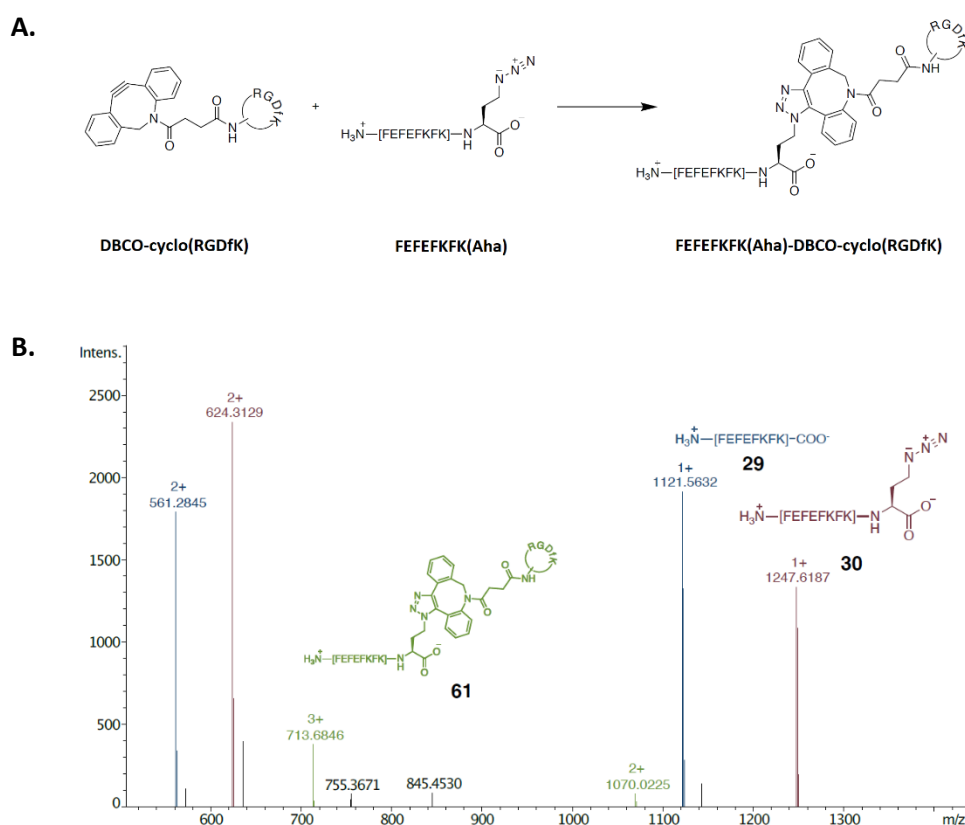
Figure 24 - Summary of "in situ" click reaction to introduction RGD functionalisation to peptide hydrogels. (A) Scheme for final, in situ, "click" reaction between DBCO-cyclo(RGDfK) and FEFEFKFK(Aha). (B) Structures and corresponding m/z of chemical species identified via HRMS, following 2 h incubation at 80 °C step of the in situ "click" gel fabrication procedure. This mass spectrum identifies two peaks (m/z = 713.6846 and 1070.0225) that correspond to the desired FEFEFKFK(Aha)-DBCO-cyclo(RGDfK) product, as triply and doubly charged adduct species. Also displayed are peaks for the FEFEFKFK (m/z = 561.2845 and 1121.5632) and FEFEFKFK(Aha) (m/z =

624.3129 and 1247.6187) peptides, as singly and doubly charged adduct species.   A value that would represent

the DBCO-cyclo(RGDfK) molecule was not present, indicating a high reaction efficiency.

3.6.2 "Click" chemistry-mediated immobilisation of heparin

A previously discussed, a potential advantage that the "click" chemistry-based approach has over the sortase method is that it can be used immobilise a greater range of biomolecules, including glycosaminoglycans (GAGs). GAGs have many protective, structural, organizational, and barrier functions. GAG constituents of extracellular matrix (ECM) molecules, such as proteoglycans, often also provide binding sites for other specific biomolecules, allowing a greater degree of organisation of the matrix.

To investigate "click" chemistry as a tool to immobilise GAGs, a heparin oligosaccharide 30 monosaccharides in length (average mol. wt. >9000) was tested, to mirror a study previously carried out with soluble heparin [68, 76]. The alkyne handle required for the subsequent "click" reaction with FEFEFKFK(Aha) was provided by a DBCO linker. Just as peptides feature an N- and C-terminus, sugars display a reducing and non-reducing end. These provide two unique sites at which the DBCO linker could be attached. It is important that the linker has only one point of attachment to a single terminus in the GAG, as the correct orientation and presentation of sulphated residues is essential to preserve the biological function of the immobilised heparin [273].

Generation of the DBCO-Heparin was performed by Chris Merrett (University of Nottingham, UK). DBCO-NH$_2$ was synthesised using a protocol adapted from methods outlined in [253]. Conjugation of DBCO-NH$_2$ to heparin was then achieved via reductive amination by incubating at 65 °C, in the presence of acetic acid, with periodic shaking to ensure thorough mixing (Scheme 3). Following neutralisation of the acetic acid with sodium hydrogen carbonate, a pre-packed PD-10 desalting column was used to desalt the product. This allowed size-exclusion purification of the product from salt, free labels, and impurities. UV/Visible absorption spectroscopy was employed to identify the fraction containing the desired product. Conjugation with FEFEFKFK(Aha) was then caried out using strain promoted azide-alkyne cycloaddition (SPAAC) (Scheme 4). The final product was then freeze-dried, producing FEFEFKFK(Aha)-DBCO-Heparin powder. Unfortunately, because of the limitations of the mass spectrometry instrument available, it was not possible to confirm this reaction via HRMS. Investigation into using HPLC as a method of confirmation is currently being

undertaken. In the meantime, the success of final "click" reaction would be assessed via a biological assay and is discussed later.
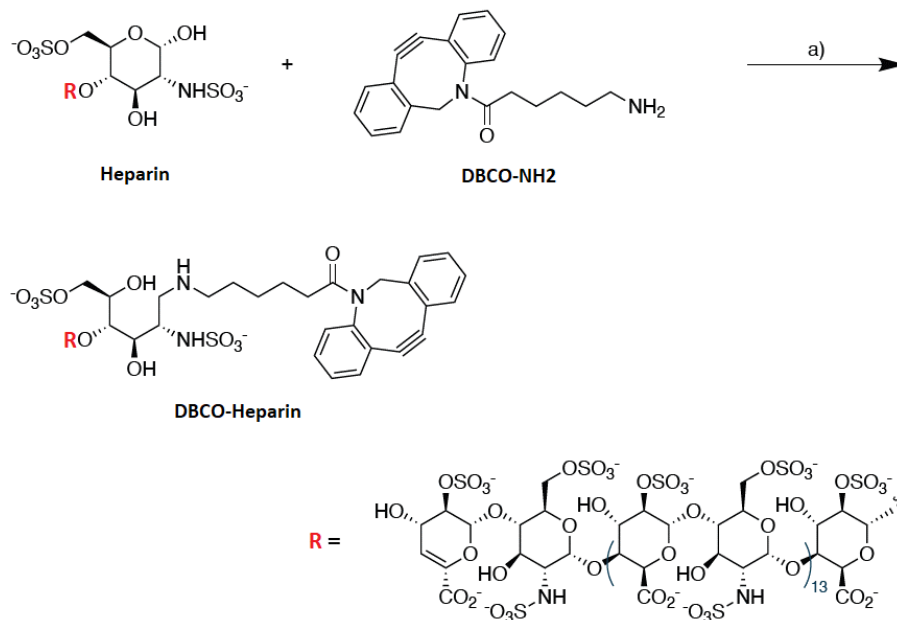
a) NaCNBH₃, AcOH, DMSO, H₂O, 65 °C, 24 h, 74%.

Scheme 3 - Reductive amination of heparin with DBCO-NH₂.
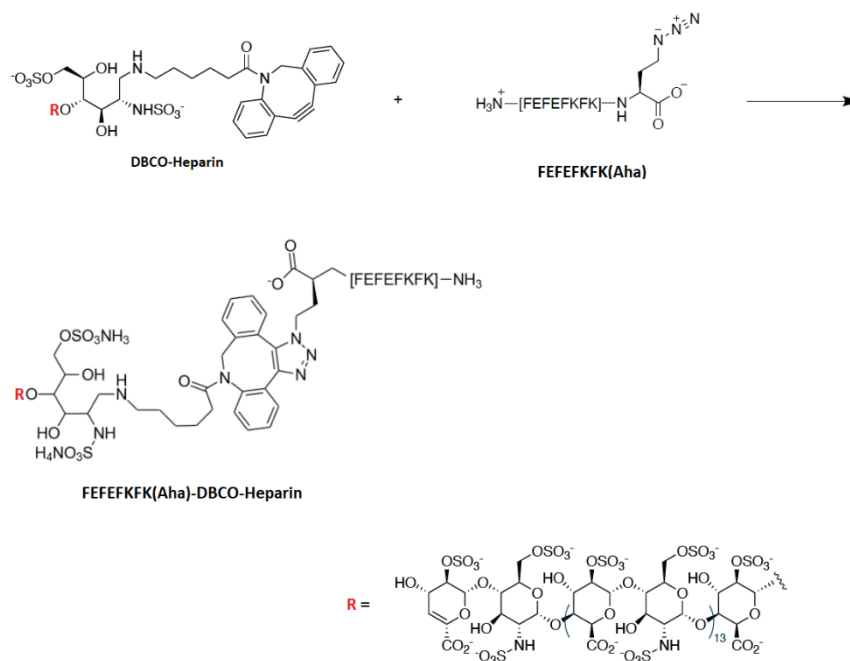
Scheme 4 - Strain promoted azide-alkyne cycloaddition (SPAAC) between DBCO-NH$_2$ and FEFEFKFK(Aha).

The assumed FEFEFKFK(Aha)-DBCO-Heparin material was then provided for use in this project. To form each "clicked-in" heparin precursor gel, a total mass of 12.5 mg peptide powder was dissolved in a solution containing approx. 0.05 mg/mL FEFEFKFK(Aha)-DBCO-Heparin, using a 3 min vortex step followed by centrifugation (3 min at 300 x *g*) and a 2 h incubation step at 80 °C. It's worth noting at this point that, unlike proteins, GAGs are stable to high temperatures without loss of activity. Gelation was then triggered by incremental addition of 0.5M NaOH. Gels were then further incubated overnight at 80 °C. The inclusion of the FEFEFKFK(Aha)-DBCO-Heparin did not appear to have any impact on gel formation during this process. The precursor gels were then stored at 4 °C until needed.

3.7.0 Probing the impact of immobilised biomolecules on matrix stiffness

To evaluate whether the effect of immobilising specific biomolecules using the newly developed methods had any undesirable impact on matrix stiffness, functionalised gels were evaluated via bulk oscillatory rheology. This was important to be able to demonstrate later that any effects observed in the future cell-based assays were the result of the biological activity of the immobilised material and not of some off-target effect on the gel's mechanical features.

3.7.1 Evaluating the impact of immobilising heparin

Unfortunately, due to a limited amount of FEFEFKFK-DBCO-Heparin material that could be generated, only three peptide hydrogels covalently functionalised with heparin could be produced. One of these was selected to be evaluated via bulk oscillatory rheology whilst the other two were used in future cell-based assays. Presented in Figure 25 are the results from this evaluation and a comparison between unfunctionalised "blank" peptide hydrogels and gels that had been functionalise with soluble heparin. Although it is not currently possible to make a statistical evaluation between the "clicked-in" gels and the others, these results nonetheless provide some initial insight into the impact of immobilising heparin within the gel. Based on these results, it appears as though the effect of immobilising heparin has little meaningful impact on gel stiffness. Therefore, what we can begin to conclude from these results is that any changes in cell behaviour observed in later cell-based assays is likely to be due to the biological impact of the immobilised heparin and not due to some off-target impact on matrix stiffness. These results also suggest that the FEFEFKFK-DBCO-Heparin peptide-glycan conjugate was able to self-assemble alongside the FEFEFKFK peptide, due to the limited effect on gel stiffness.
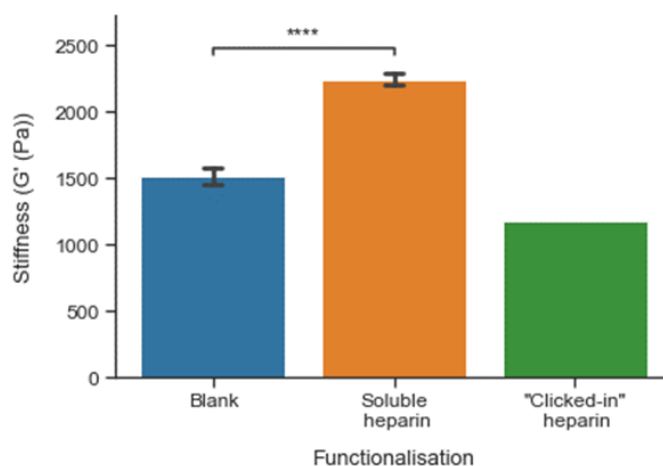
*Figure 25 – Stiffness (G') of peptide hydrogels functionalised with heparin. Gels of 10 mg/ml peptide concentration functionalised with either soluble (n=3) or "clicked-in" heparin (n=1) were compared to unfunctionalised "blank" peptide hydrogels (n=19) via bulk oscillatory rheology. Due to a limited amount of material, only one "clicked-in" gel could be produced, and as such no statistical comparison is made between this condition and the others. Results indicate a significant increase in stiffness when functionalising the gels with soluble heparin. Results also suggest a smaller impact on stiffness caused by "clicked-in" heparin, but more repeats are needed before this can be stated conclusively. (Mann-Whitney U test; n≥3; ****: p < 0.0001).*

3.7.2 Evaluating the impact of immobilising RGD

The effect of immobilising RGD within the gels via sortase-mediated functionalising and "click" chemistry mediated functionalised was also assessed. Presented in Figure 26 are the results from these evaluations. These results reveal a significant increase in stiffness when peptide hydrogels are functionalised with either soluble or sortase-immobilised RGD. However, there also appears to be no significant difference caused between these two methods. Therefore, in future cell-based assays, we can conclude that any observed differences in cell behaviour is likely caused by the biological impact of RGD and not from some off-target impact on gel stiffness.

Unfortunately, there was also a limited amount of DBCO-cyclo(RGDfK) material that could be generated and as such only two gels with "clicked-in" RGD could be produced. One of these was selected to be evaluated via bulk oscillatory rheology whilst the other was used in a future cell-based assay. Whilst it is not possible to make a statistical comparison between this gel and the others, this result does provide some insight. Based on this result, it would appear that there is no meaningful difference in stiffness between the "clicked-in" RGD gel and the unfunctionalised "blank" peptide hydrogels. If future repeats confirm this, this may indicate that "click" chemistry-mediated functionalisation of RGD may be a better approach compared to the sortase method. This would be because it would be more likely that any differences observed in cell behaviour are from the biological impact of RGD.
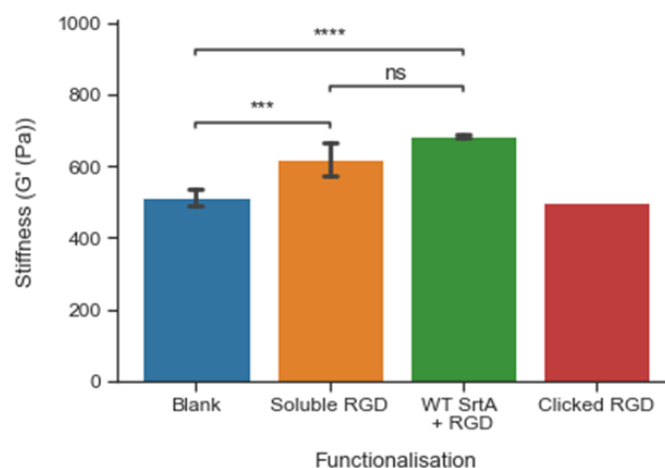
*Figure 26 - Stiffness (G') of peptide hydrogels functionalised with RGD. Gels of 6 mg/ml peptide concentration functionalised with either soluble (n=3), sortase-immobilised (n=3) or "clicked-in" RGD (n=1) were compared to unfunctionalised "blank" peptide hydrogels (n=19) via bulk oscillatory rheology. Due to a limited amount of material, only one "clicked-in" gel could be produced, and as such no statistical comparison is made between this condition and the others. Results indicate a significant increase in stiffness when functionalising the gels with soluble or sortase-immobilised RGD, with no statistical difference between these two methods. Results also suggest that the impact of functionalising the gels with "clicked-in" RGD may be smaller, but more repeats are needed before this can be stated conclusively. (Mann-Whitney U test; n≥3; ***: p < 0.001; ****: p < 0.0001).*

3.8.0 Probing the impact of immobilised biomolecules on cell behaviour

Given the previous results revealing no meaningful impact on peptide hydrogel stiffness after functionalisation via sortase- and "click" chemistry-mediated immobilisation of biomolecules, these new methods could now be assessed for their biological impact. This relied on comparisons made to the previous experiments that were done in development of individual test environments for each specific biomolecule.

3.8.1 Evaluating the impact of "clicked-in" heparin

To evaluate the biological impact of immobilising heparin within the peptide hydrogels via "click"-chemistry mediated functionalisation, its effect on encapsulated $Ext1^{-/-}$ mESCs was evaluated. These cells lack the critical Ext1 enzyme that is required for chain elongation of heparan sulphate. Without endogenous heparan sulphate, these cells had previously been shown to be unable to undergo neural specification, due to a lack of FGF-mediated cell signalling, but that this ability could be restored by the addition of exogenous heparan sulphate III (HSIII) or heparin [68]. It was also demonstrated during the course of this project

that the ability of these cells to undergo neural specification within the peptide hydrogels could be similarly restored by also encapsulating soluble HSIII or heparin. This provided a convenient baseline to compare the impact of immobilising heparin via "click" chemistry.

Ext1$^{-/-}$ mESCs were encapsulated within peptide hydrogels functionalised with "clicked-in" heparin, as previously described. These cells were then cultured for seven days in N2B27 differentiation media, before being fixed, stained for the neural specific marker β-III-tubulin, and then visualised with a scanning laser confocal microscope. Unfortunately, as there was a limited amount of FEFEFKFK-DBCO-Heparin that could be generated, this test could only be carried out a limited number of times (two biological repeats). However, within each of these tests, three wells were plated out per test condition (three technical repeats). Due to the limited number of tests that could be performed, only Ext1$^{-/-}$ mESCs were used for these tests. This was because these cells offered better opportunity to evaluate this method of functionalisation, compared to E14 mESCs, as these cells had previously given a more clearly observable response to soluble heparin in previous tests (Figure 15 and Figure 16).

The hypothesis tested here was that the "clicked-in" heparin would also restore the ability of these HS-deficient Ext1$^{-/-}$ mESCs to differentiate towards a neural lineage, if this immobilised material was accessibly to cells and had retained its biologically relevant activity. This would provide good preliminary evidence that this strategy for functionalising the gels was a valid approach.

The images obtained from these tests show positive staining for β-III-tubulin, confirming that that the Ext1$^{-/-}$ cells were able to undergo neural specification when encapsulated in gels functionalised with "clicked-in" heparin (Figure 27), reflecting results obtained for functionalisation with soluble HSIII and heparin (Figure 15). This provides good preliminary evidence that "click" chemistry-mediated immobilisation is a valid strategy for functionalising the peptide hydrogels. However, it would be necessary to repeat this experiment at least once more before this could be stated conclusively.

Figure 27 - Ext1⁻/⁻ mouse embryonic stem cell (mESC) differentiation in "click" functionalised peptide hydrogels. Ext1⁻/⁻ mESCs were encapsulated in 10 mg/mL peptide hydrogels functionalised with approx. 0.05 mg/mL heparin via "click" chemistry. Cells were then cultured in N2B27 differentiation medium for a period of seven days. (A) Representative brightfield images taken during culture (n=2). Scale = 100 μM. (B) Representative fluorescence images obtained on day 7, after cells were fixed and stained for DAPI, actin, and the neural specific marker β-III-tubulin (n=2). The presence of β-III-tubulin indicates that the ability of these cells to undergo neural specification had been restored by the "clicked-in" heparin, providing evidence that this immobilised material was still accessible to cells and had retained its biological activity. This also provides evidence that "click" chemistry-mediated immobilisation of matrix material is a valid strategy for functionalising the peptide hydrogels. Scale = 100 μM.

3.8.2 Evaluating the impact of "clicked-in" RGD

Unfortunately, due to the limited amount of DBCO-cyclo(RGDfK) material that could be generated, only two "clicked-in" RGD gels could be produced. To perform a preliminary analysis, Ext1⁻/⁻ mESCs were encapsulated within these gels and cultured for seven days in N2B27 differentiation medium. Cell viability within these gels was, however, very poor and no useful results could be obtained. Due to the limited number of repeats, it is impossible to say whether this was due to some unknown toxicity introduced into the gel when functionalising them with the DBCO-cyclo(RGDfK) material or whether this was due to the normal variability that exists between typical cell culture experiments.

3.8.3 Evaluating the impact of sortase-immobilised RGD

To evaluate the biological impact of immobilising RGD within the peptide hydrogels via sortase-mediated immobilisation, its effect on encapsulated E14 and Ext1⁻/⁻ mESCs was

evaluated. In a recent study evaluating the effect of immobilising RGD on synthetic nanofibers, it was found that the presence of RGD leads to downregulation of the neural-specific marker β-III-tubulin and an increase in early expression of the glial-specific marker green acidic fibrillary protein (GFAP) [219]. It was also demonstrated during the course of this project that the presence of soluble RGD leads to a change in phenotype for these cells, where cell clusters adopted an elongated, "lemon-shaped" morphology (Figure 16 and Figure 17). However, whilst there had been a downregulation of β-III-tubulin, the presence of GFAP could not be detected in these tests. The reason for this was thought to be because, due to its small size, much of the soluble RGD was being lost during media changes. This would then mean that the concentration of RGD decreased over the course of the experiment and crossed below the threshold required to support the differentiation of these cells towards a glial lineage.

Therefore, the hypothesis tested here was that when sortase-mediated immobilisation was used as a strategy to functionalise the gels with RGD, the concentration of RGD would be better maintained throughout the course of the experiment, keeping it above the threshold needed to support differentiation towards a glial lineage. This would result in negative staining for the neural-specific marker β-III-tubulin and positive staining for the glial-specific marker GFAP, if this immobilised material was also still accessible to cells and had retained its biological activity.

To test this, E14 and Ext1$^{-/-}$ mESCs were encapsulated within sortase-primed gels which were then covered in a tethering solution containing 15 μM WT SrtA and 20 μM RGDLPETG. The following day, the tethering solution was removed, and cells cultured for a further six days in N2B27 differentiation media. On day seven, gels were stained for the neural specific marker β-III-tubulin and the glial specific marker GFAP, and then visualised using a scanning laser confocal microscope. This test was conducted three times (three biological repeats). Within each test, three wells were also plated out per test condition (three technical repeats). At least three images were obtained per test condition and images presented in Figure 28 and Figure 29 are representative.

The images obtained from these tests show further downregulation of β-III-tubulin (negative staining in all samples, compared to weak staining in some samples for soluble RGD) and the emergence of positive staining for GFAP. This supports the hypothesis that sortase-mediated immobilisation leads to better retention of RGD within the gels throughout the course of the experiment, so that it can continue to support differentiation of these cells towards a β-III-

tubulin⁻, GFAP⁺ glial lineage. It also provides good preliminary evidence that sortase-mediated immobilisation is a valid strategy for functionalising the peptide hydrogels.

Figure 28 – E14 mouse embryonic stem cell (mESC) differentiation in sortase functionalised peptide hydrogels. E14 mESCs were encapsulated in 10 mg/mL peptide hydrogels functionalised with 20 µM RGD via sortase-mediated immobilisation. Cells were then cultured in N2B27 differentiation medium for a period of seven days. (A) Representative brightfield images taken during culture (n=3). Scale = 100 µM. (B) Representative fluorescence images obtained on day 7, after cells were fixed and stained for DAPI, actin, and either the neural specific marker β-III-tubulin or the glial specific marker GFAP (n=3). The absence of β-III-tubulin and emergence of GFAP supports the hypothesis that sortase-mediated immobilisation leads to better retention of RGD within the gels throughout the course of the experiment. This better retention of RGD maintains the concentration of RGD above the critical threshold required to support the differentiation of these cells towards a β-III-tubulin⁻, GFAP⁺ glial lineage. It also provides good preliminary evidence that sortase-mediated immobilisation is a valid strategy for functionalising the peptide hydrogels. Scale = 100 µM.

A.

Day 3 Day 5 Day 7

WT SrtA + RGD

B.

DAPI Actin β-III-tubulin Merge

WT SrtA + RGD

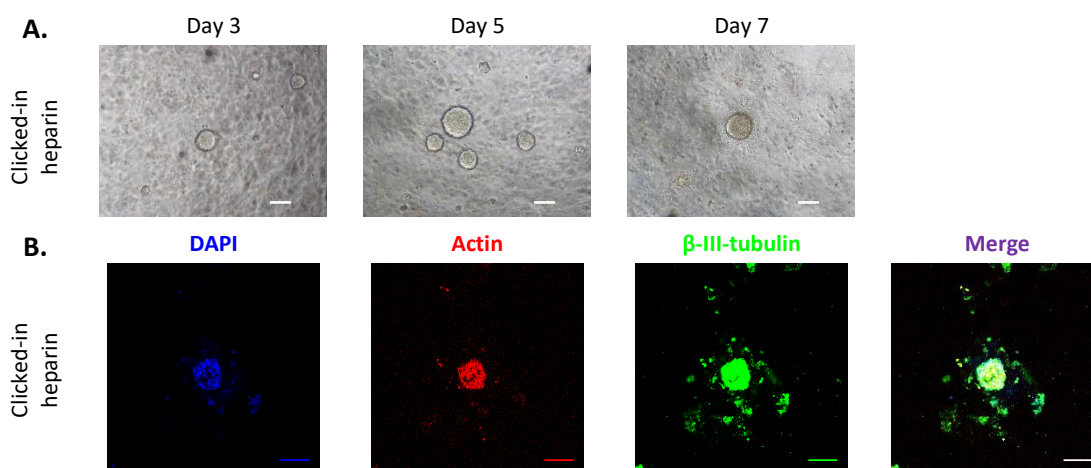DAPI Actin GFAP Merge

WT SRTA + RGD

Figure 29 – Ext1$^{-/-}$ mouse embryonic stem cell (mESC) differentiation in sortase functionalised peptide hydrogels. Ext1$^{-/-}$ mESCs were encapsulated in 10 mg/mL peptide hydrogels functionalised with 20 µM RGD via sortase-mediated immobilisation. Cells were then cultured in N2B27 differentiation medium for a period of seven days. (A) Representative brightfield images taken during culture (n=3). Scale = 100 µM. (B) Representative fluorescence images obtained on day 7, after cells were fixed and stained for DAPI, actin, and either the neural specific marker β-III-tubulin or the glial specific marker GFAP (n=3). The absence of β-III-tubulin and emergence of GFAP supports the hypothesis that sortase-mediated immobilisation leads to better retention of RGD within the gels throughout the course of the experiment. This better retention of RGD maintains the concentration of RGD above the critical threshold required to support the differentiation of these cells towards a β-III-tubulin$^-$, GFAP$^+$ glial lineage. It also provides good preliminary evidence that sortase-mediated immobilisation is a valid strategy for functionalising the peptide hydrogels. Scale = 100 µM.

3.8.4 Towards the creation of a more complex gel environment

A major advantage of offering multiple methods for functionalisation is that future end users can chose whichever method is the most suitable for their specific needs. Where these methods can be used in tandem, it also helps to enable the creation of more complex gel environments that have been selectively functionalised with a variety of different biomolecules. These more complex environments would be better able to recapitulate the complexities of the native ECM, which itself is also comprised of a wide variety of biomolecules. This ought to lead to the generation of more physiologically relevant cell behaviour and consequently also the generation or more relevant and reliable data.

However, it should be noted that this will only be the case where the choice to include specific biomolecules has been informed by proteomic and glycomic studies of specific tissues, so that only relevant biomolecules are included. Therefore, in a final experiment, the ability to perform multiple functionalisations, using different methods, was evaluated. Due to constraints of time, this experiment was performed only once (one biological repeat), with three wells plated out per test condition (three technical repeats). However, the results from this test are included here to demonstrate the intended future direction for this research.

For this experiment, the effects of both soluble heparin and sortase-immobilised RGD on Ext1$^{-/-}$ mESCs were evaluated. Due to the lack of "clicked-in" material that could be generated, this method, unfortunately, could not be included in this final test. Ext1$^{-/-}$ mESCs were chosen for this test as they had previously demonstrated a clearly observable response to both soluble heparin (Figure 15) and sortase-immobilised RGD (Figure 29). Separately, each of these had either promoted the expression of β-III-tubulin or GFAP. It was unknown what the combined impact both molecules would have. In this way, this final experiment was carried out in a more speculative sense, in contrast to previous experiments which had an established predicted outcome. Again, this was largely due to constraint of time, as where was only enough time at the end of the project to perform this experiment once.

Ext1$^{-/-}$ cells were encapsulated within sortase-primed peptide hydrogels modified with soluble heparin. Gels were then covered in a tethering solution containing 15 µM WT SrtA and 20 µM RGDLPETG in N2B27. The following day, the tethering solution was removed, and cells cultured for a further six days in N2B27 differentiation media. On day seven, gels were stained for the neural specific marker β-III-tubulin or the glial specific marker GFAP, and then visualised using a scanning laser confocal microscope (Figure 30).

The results from this experiment show that, under these conditions, Ext1$^{-/-}$ cells are directed towards a β-III-tubulin$^+$, GFAP$^+$ phenotype. This phenotype was not observed in past experiments and so provides some preliminary evidence that multiple functionalisations can be carried out in tandem on the peptide hydrogels. As previously mentioned, this ability will be important in the future for researchers trying to create more complex environments which more faithfully recapitulate the biochemical diversity of the native ECM. These results perhaps also demonstrates the importance of selecting the right biomolecules, informed by proteomic and glycomic analysis of relevant primary tissues, as β-III-tubulin and GFAP is not usually co-expressed *in vivo*, except possibly in midgestational human foetal astrocytes

[274]. However, consideration must be taken that this experiment was only performed once, and this test should be repeated to strengthen these conclusions.
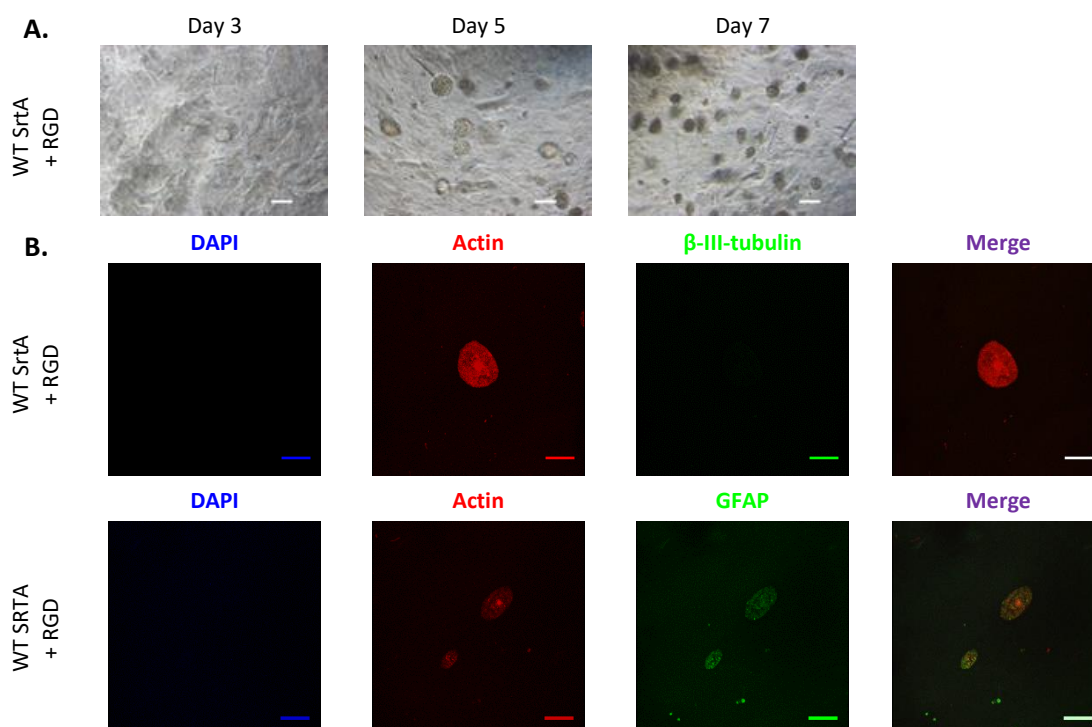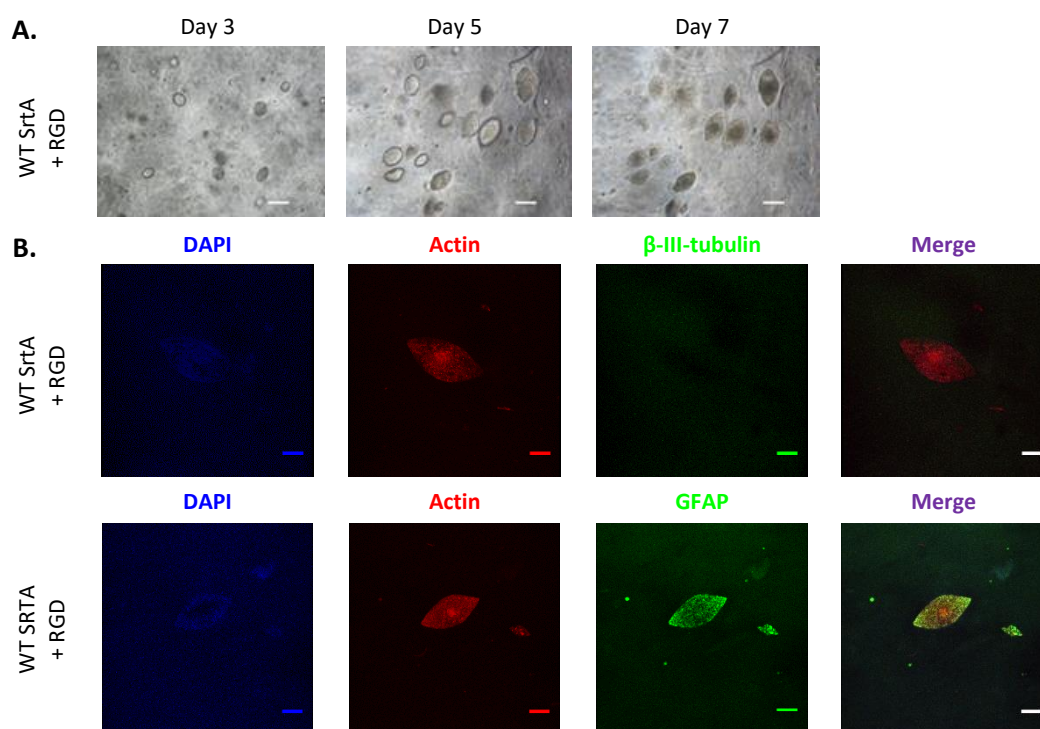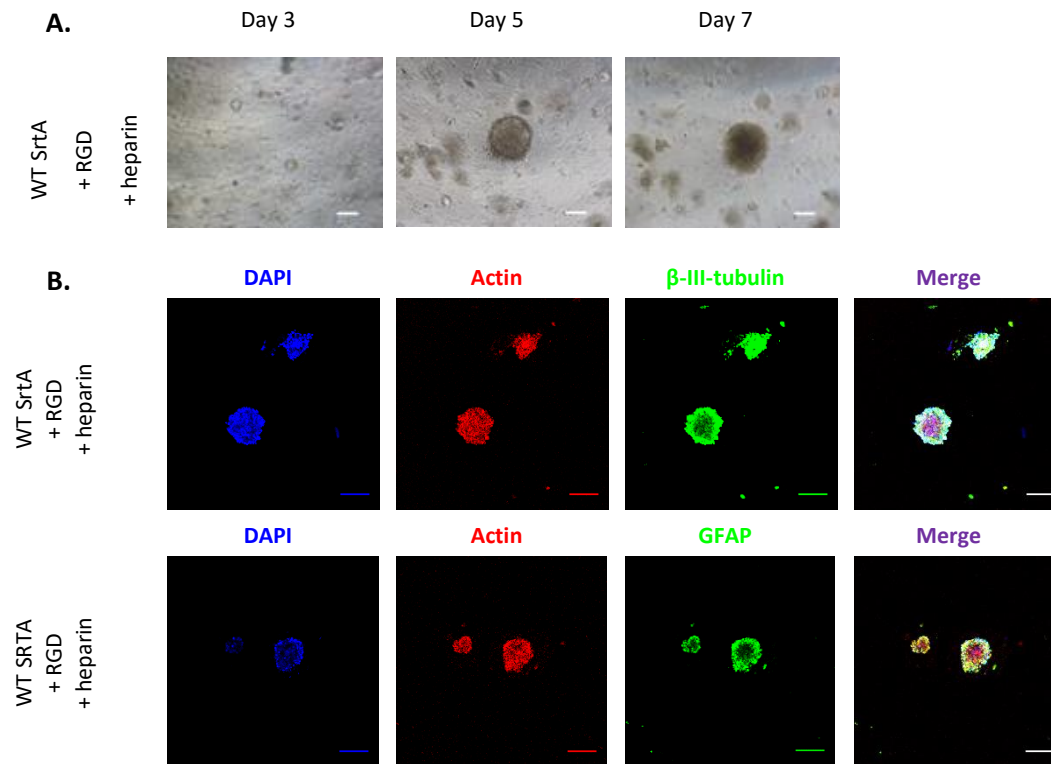

Figure 30 - Ext1$^{-/-}$ mouse embryonic stem cell (mESC) differentiation in multi-functionalised peptide hydrogels. Ext1$^{-/-}$ mESCs were encapsulated in 10 mg/mL peptide hydrogels functionalised with approx. 0.05 mg/mL soluble heparin and 20 μM RGD via sortase-mediated immobilisation. Cells were then cultured in N2B27 differentiation medium for a period of seven days. (A) Representative brightfield images taken during culture (n=1). Scale = 100 μM. (B) Representative fluorescence images obtained on day 7, after cells were fixed and stained for DAPI, actin, and either the neural specific marker β-III-tubulin or the glial specific marker GFAP (n=1). In this test, Ext1$^{-/-}$ mESCs were directed to a previously unsee β-III-tubulin$^+$, GFAP$^+$ phenotype, providing evidence that multiple functionalisations can be carried out in tandem on the peptide hydrogels. The presence of both β-III-tubulin and GFAP in these cells also demonstrates the need to make informed choices when choosing which biomolecules to include, as these are not usually co-expressed in vivo. Scale = 100 μM.

3.9.0 Embedding gastruloids within peptide hydrogels

Gastruloids are 3D aggregates of embryonic stem cells that recapitulate the axial organisation of post-implantation embryos [152]. The first protocol for the generation of gastruloids demonstrated that mESCs could be coaxed into forming elongating aggregates, containing derivatives of all three germ layers, which exhibit clearly defined anterior-posterior, left-right, and dorsal-ventral body axes [153, 154]. In the years that followed,

improvements to the protocol have allowed generation of more complex models that are able to generate brain [155], somite [156, 157], neural tube [157], gut tube [157, 158], and beating "heart-like" structures [159]. Recent advances have also allowed the generation of human gastruloids, using human embryonic stem cell-based elongating mesodermal embryoid bodies [160].

The observation that gastruloids can form axially organised embryo-like structures in the absence of extra-embryonic tissue challenges the long-standing paradigm that establishment of antero-posterior axis relies on the anterior visceral endoderm (AVE) [162]. There are two possible explanations for this: either the role of the AVE is not to induce symmetry breaking but to ensure that it happens in the correct spatial position relative to the implantation site [153], or that gastruloids are able to break their symmetry through a mechanism that is not representative of *in vivo* circumstances.

Two independent studies conducted recently discovered that the formation of somite [156, 157] and neural tube-like [157] structures can be induced by embedding mouse gastruloids in low (5-10%) percentage Matrigel® at the 96 h timepoint. However, it remains unclear whether this is due to the effect of a chemical component of the gel or whether the gastruloids are responding to the mechanical forces that are being exerted on them.

To answer this question, a protocol was devised for embedding gastruloids within the peptide hydrogels. Unlike Matrigel®, the peptide hydrogels can be prepared with no additional matrix components, providing a medium into which gastruloids can be encapsulated and presented with mechanical signals in the absence of chemical ones. The protocol for generation of gastruloids was adapted from [152]. E14 and Ext1$^{-/-}$ mESCs were seeded at a density of 350 cells per well into a non-tissue culture treated, U-bottomed 96-well plate. Cells quickly fell to the bottom of the well and formed aggregates. After 48 h, cells were treated with a "Chiron pulse" to induce symmetry breaking and subsequent elongation. At 72 h, gastruloids were harvested and embedding within peptide hydrogels and cultured for a further 3 days.

The results of this initial validation experiment are presented in Figure 31. E14 mESCs were able to form stable aggregates which remained intact during harvesting and embedding in the peptide hydrogels. They also appeared to show early signs of elongation by the 72 h timepoint and remained viable until the 120 h timepoint. To demonstrate this more conclusively, immunofluorescence staining for brachyury should reveal longitudinal polarisation, where the expression of brachyury localises to the posterior end of the

gastruloid [275]. This was attempted but due to constraints of time the staining protocol could not be sufficiently optimised to produce quality images.

It is important to note here that this protocol had never been attempted with Ext1$^{-/-}$ mESCs before. It was hypothesized that due to their lack of endogenous HS that they would likely be unable to undergo gastrulation. The images obtained from this experiment show that aggregates of these cells appear less viable when embedded in the peptide hydrogels, compared to the E14 aggregates. They also do not appear to show any clear signs of elongation. To test whether their ability to gastrulate could be rescued, the protocol was repeated with Ext1$^{-/-}$ aggregates cultured in the presence of soluble heparin and then embedded in peptide hydrogels also functionalised with soluble heparin. The results from this test are also presented in Figure 31 and show that whilst the presence of heparin appears to increase the viability of the Ext1$^{-/-}$ aggregates within the gels, it was apparently not sufficient to restore their ability to gastrulate.

There were several limiting factors which prevented this investigation from progressing any further. Firstly, there was a limited supply of "pre-made" NDiff® 227, which was generously provided by David Turner, University of Liverpool, UK. Attempts were made using the "home-made" N2B27 also used in other experiments during this project, but mESCs did not form stable aggregates when using this formulation. The other limiting factor was time. As this experiment was performed during the final months of the project, there was not sufficient time to optimise the immunofluorescence staining protocols or to investigate what set of conditions might restore the ability of Ext1$^{-/-}$ aggregates to gastrulate within the gels. Nevertheless, these results provide a promising proof of concept for a protocol for encapsulating gastruloids within the peptide hydrogels.
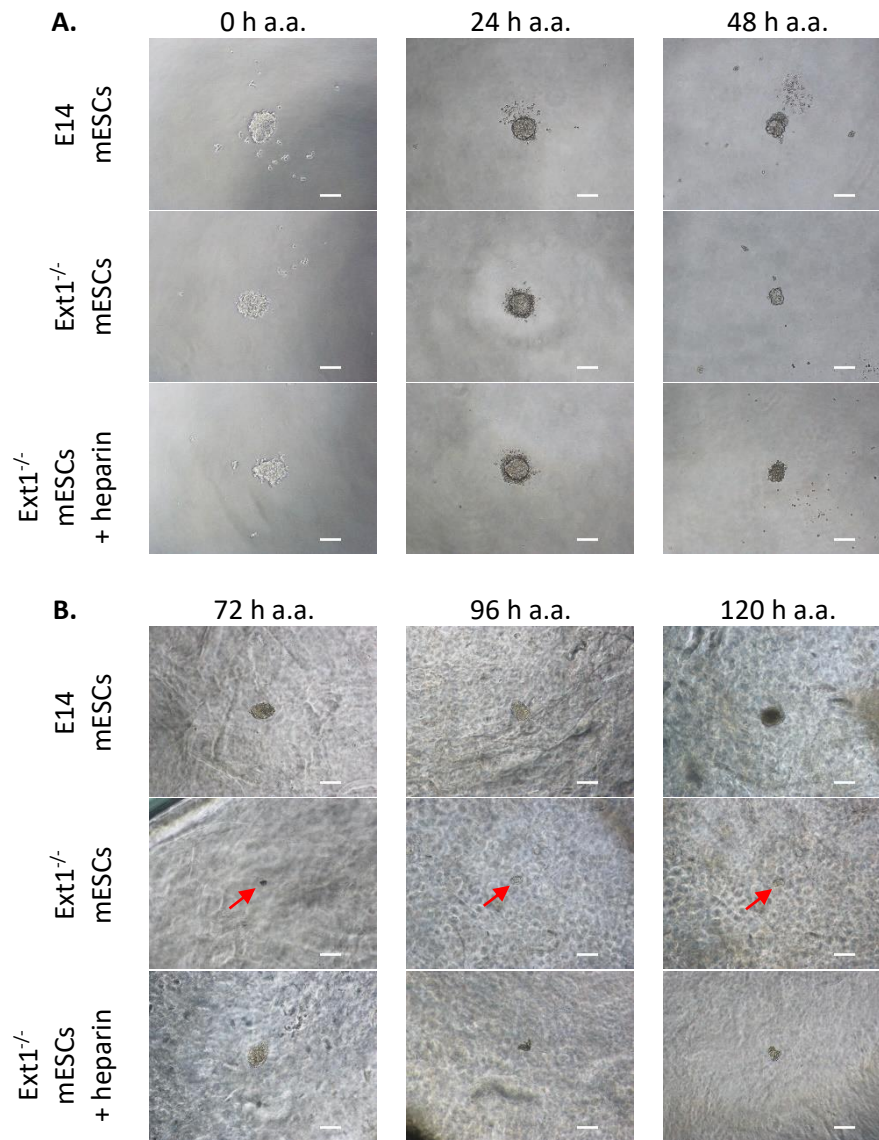
Figure 31 – Initial validation of a protocol for embedding gastruloids within the peptide hydrogels. (A) E14 mouse embryonic stem cells (mESCs) were seeded at a density of 350 cells per well into a non-tissue culture-treated, U-bottomed 96-well plate. Ext1$^{-/-}$ mESCs were similarly seeded but also provided with 0.05 mg/mL additional soluble heparin. After 48 h, cells were treated with a "Chiron pulse" to induce symmetry breaking and subsequent elongation (n=1). (B) At 72 h, aggregates were embedded in either unfunctionalised "blank" peptide hydrogels, or gels functionalised with 0.05 mg/mL soluble heparin, and cultured for a further 3 days. Results show good viability of E14 aggregates and improved viability of Ext1$^{-/-}$ when in the presence of added heparin (n=1). (Abbreviations: a.a.: after aggregation).

4.0.0 Discussion

4.1.0 Review of aims

The primary aim of this project was to identify, optimise, and validate new methods for covalently functionalising a peptide hydrogel used as a 3D cell culture model of development and disease. The need for this becomes readily apparent when we consider the methods currently available for modelling specific tissue microenvironments. Whilst recent advances in cell biology, microfabrication techniques, and tissue engineering have produced many promising new modelling techniques, challenges remain following careful examination of their capabilities and limitations.

Traditional 2D monolayer cultures suffer from low cell densities, high stiffnesses, and lack the complex cell-cell and cell-matrix interactions that are present *in vivo*, limiting their usefulness in extrapolating data to predict patient outcomes. The recent interest in developing more sophisticated 3D *in vitro* models has, so far, addressed many of these issues, but there has yet been a single model produced which has effectively addresses all of them in a single platform.

Current *in* vitro methods for growing cells in 3D allow for better recapitulation of *in vivo* circumstances, as these cell clusters will exhibit oxygen and nutrient gradients, creating heterogenous populations of cells (e.g., hypoxic vs. normoxic, quiescent vs. replicating). As a result, these cell clusters also exhibit similar drug resistance patterning when compared to cells *in vivo* [146]. However, there are a number of practical challenges associated with current methods.

Traditional approaches for generating spheroids and organoids, such as the hanging drop method, are limited in their reproducibility and the use of labour- and time-intensive techniques. These methods create difficulties when trying to maintain clusters of a uniform size or with the correct ratio of cell types, causing issues when trying to scale to high-throughput [147]. To combat this issue, newer protocols which utilise 3D printing and acoustofluidic techniques are currently being investigated, and have shown early promise in allowing for the generation of more uniform spheroids [276, 277].

Whilst current techniques for generating 3D cell clusters have produced many effective models for studying cell-cell communication and behaviour, the extracellular matrix (ECM) needs to be better represented for the study of cell-matrix interactions. This is despite the fact that these cell clusters have been shown to secrete their own ECM proteins [278, 279].

Unfortunately, this ability is insufficient in generating a fully formed matrix without a medium to encapsulate these products. It also ignores the contributions of the mechanical properties of the matrix on cell signalling, differentiation, motility, and other changes in cell behaviour.

To address this shortcoming, there has been a recent focus on the development of new biocompatible materials, which aim to provide a way to faithfully mimic both the chemical and mechanical features of the native ECM. These new materials offer a substrate into which cells or previously generated 3D clusters of cells can be encapsulated, thereby acting as an ECM surrogate for these cells. As previously discussed, such materials can be broadly separated into biologics and synthetics. Biologics offer superior biocompatibility, but their ill-defined and variable composition leads to uncertainty in cell-based experiments and a lack of reproducibility. In contrast, synthetics promise to deliver more clearly defined and tuneable compositions, organisation, mechanics, and ECM remodelling capabilities.

Self-assembling peptide hydrogel (SAPH) models, such as the FEFEFKFK model, are a class of synthetic scaffold that offers the opportunity to combine all the best features of both biologics and synthetics. They are well-defined, have limited batch-to-batch variability, and their mechanical and chemical properties can be fine-tuned by the end user. To increase the scope of the FEFEFKFK model, new techniques for covalent immobilisation of matrix material were investigated, to allow it to compete with other synthetic scaffolds used as 3D cell culture models. Additionally, these new techniques for covalent functionalisation are likely compatible with other self-assembling peptide-based models, creating an opportunity for other researchers to adapt this work for their needs.

4.2.0 Batch Testing

4.2.1 Why is it important?

One of the major advantages that synthetic scaffolds have over products of biological origin, such as Matrigel®, is that they are chemically-defined and offer reduced batch variability. This allows researchers to generate more reproducible data, as the reagents used in any experiment are also more reproducibly manufactured. A popular method for generating synthetic peptides is solid-phase peptide synthesis (SPPS), which involves the successive addition of protected amino acid derivatives to a growing peptide chain, which is immobilised at one end onto a solid phase scaffold [248]. This method also allows for rapid

filtration and washing after each synthetic step, and the product can be further purified via chromatography to remove any impurities.

However, as previously discussed, it had often proved difficult in the past to obtain reliable materials for the purpose of creating peptide-based hydrogels. This is possibly due to the fact that peptide manufacturers typically only employ mass spectrometry (MS), and sometimes also high-performance liquid chromatography (HPLC), to confirm the presence of the desired product and to check for any contaminating fragments. However, these techniques are often not sufficient to detect the presence of other contaminants, such as trifluoroacetic acid (TFA). In the design of pH-sensitive cell culture model, the presence of excess TFA can have a huge impact on peptide hydrogel preparation and encapsulated cell behaviour. In fact, at the beginning of this project, the lab had recently switched to a different supplier of the FEFEFKFK peptide powder, due to rising concerns with the batch variability from the previous supplier. Therefore, a specific batch testing protocol was needed to evaluate this new supplier and each future batch of peptide received within the context of the design of cell culture models.

4.2.2 Batch testing peptides for cell culture models

To confirm that this new supplier provided better material, a specific batch testing protocol was designed which examined several critical features of the peptide hydrogel throughout the preparatory process and then the subsequent evaluation of the gels in a rheological and cell-based assay.

Additionally, development of this protocol was important to define a standard set of tests that would allow the user to assess variability introduced due to engineered modifications (such as those that allow for sortase- and "click" chemistry-mediated functionalisation). A standardised test protocol would also be useful in the future, as the peptide hydrogel platform is designed to be used by lots of different people in different labs.

The first stage in the process was to assess how each batch of peptide powder responded during hydrogel preparation. A series of careful examinations at certain critical steps in the process quickly revealed underlying issues with isolated batches. These observations, particularly the volume of 0.5M NaOH that was required to trigger gelation, predicted future issues with the gel with a high degree of confidence. The next stage was to assess the rheological properties of the resulting gels via bulk oscillatory rheology. This was crucial, as

a major advantage to the peptide hydrogel model is that it allows for a user-defined stiffness. Therefore, it was important to confirm this ability is consistent across batches. The final stage was to assess the viability and behaviour of a well-studied cell type once encapsulated in the gels. For cell viability tests, multiple biological (n=3) and technical (n=3) repeats were necessary to allow an empirical approach, where any differences in cell behaviour could be compared among batches. With each new batch that arrived at the lab, requiring this protocol to be repeated, this produced also more historical data that could also be considered when making assessments of a new batch.

Testing of each batch of peptide powder that arrived at the lab using this protocol required approximately two weeks, including preparation of gels, rheological assessment, culture of cells within gels, and subsequent live/dead staining and imaging. However, for the protocol to be effective, a volume of data was required to allow a robust comparison between different batches, which took much longer (on the order of several months).

4.2.3 The problem with CMUN130521

It is hypothesized that the underlying issue with this batch was an excess of a specific impurity, trifluoroacetic acid (TFA). Whilst the exact specifications of the manufacturing process employed by the supplier is not publicly available, it is understood that TFA as an impurity that is introduced at some stage in the process but is subsequently removed in a final purification step.

There were several observations made during the testing of this batch that support this hypothesis. Firstly, an excess of TFA would explain the change of colour in the peptide powder, giving it a slightly yellow colour. It would also explain why a greater volume of 0.5M NaOH was required to trigger gelation, as the presence of excess TFA would decrease the pH of the peptide solution created in the initial steps of the gel fabrication procedure. It would also explain the reduction in cell viability, as neutralisation of TFA by NaOH yields a toxic product (sodium trifluoroacetate).

After this batch was returned to the supplier, they were able to "re-process" the material and then returned it. Upon testing this new "re-processed" batch (CMUN130521R), all the previous issues had disappeared. It is thought that the method used to re-process this batch was to perform the final purification step again, to remove the excess TFA left behind by the previous purification step.

4.2.3 Conclusions and future work

The batch testing protocol outlined in this project achieved its aims in demonstrating that, for the majority of batches, there is very limited batch-to-batch variability. The only outlier was a single batch (CMUN130521), which the protocol was able to quickly identify. This demonstrates the utility of the batch testing protocol for rapid identification of problem batches before they are used in more valuable experiments.

In the future, there are several improvements that could be made to the batch testing protocol, which would make it more robust. One simple improvement which could be made would be to incorporate pH measurements at certain critical timepoints, using an appropriate pH probe. Using the batch test of CMUN130521 as an example, this would reveal whether the assumptions about the changes in pH at various stages, caused by the presumptive excess of TFA, were true. The reason this was not done during the testing of CMUN130521 was because it had previously not been necessary for the gel fabrication procedure. Convenient visual cues, such as changes in the opacity and viscosity of the peptide solution prior to gelation, had allowed users of the peptide hydrogels to reliably pinpoint the volume of 0.5M NaOH needed to trigger gelation. Measurements taken after every incremental increase of 0.5M NaOH would have slowed the process. However, in the case of batch testing, this extra time would be more than justified in the future.

Another improvement would be to incorporate measurements of the effective pore size of gels into the protocol. Elsewhere in the project, a specific assay was designed and utilised to probe effective pore size. This also clearly demonstrated the need to covalently immobilise smaller molecules, below the effective pore size, which were otherwise likely to be lost during media changes. However, it could also be used to probe for any variability existing between batches. If any significant variability exists, then the decision to immobilise certain molecules may also vary between batches and is therefore valuable information to end users of the peptide hydrogels.

Conversion of image data into objective measurements would also allow a more robust, quantitative assessment of viability. This would also allow a statistical comparison among batches. Use of high-content screening systems, which combine high-throughput imaging and analysis, would allow for the best conversion of data in this context. However, access to such an instrument was not available during the course of the project. Instead, an attempt to gather objective data was made using a plate reader to measure the signal from the

calcein AM and ethidium homodimer used to label live and dead cells, respectively. However, the plate reader instrument available ((Fluostar Omega Plate Reader (BMG LabTech)) did not appear able to properly detect the ethidium homodimer signal.

The cell viability tests could also be broadened to include other kinds of viability assays, such as the RealTime-Glo™ MT Cell Viability Assay (Promega; G9711), which has the advantages of allowing measurements of cell viability in real-time over the course of several days and allowing simple kinetic monitoring to determine dose response. The CellTiter-Glo® 3D Cell Viability Assay (Promega; G9681) could have also been used, which was specifically designed to assess the viability of cells grown in 3D, by using a reagent which also lyses the cells, in order to achieve better penetration of 3D cell clusters.

Other improvements include improving the evaluation of the mechanical features of the gel with a microrheological assessment, increasing the variety of cell types used in the viability testing, and making more precise measurements of the optical density of the gels. However, it should be considered that a drawback of increasing the complexity of the batch testing protocol is that it will also increase lead times and cost. Since the current protocol already appears able to quickly identify problem batches, further refinement may not be necessary. However, future end users of the peptide hydrogels are encouraged to strike their own balance here to suit their specific research needs. It is also suggested that manufacturers of synthetic peptides may wish to employ some of these tests, if the peptides are to be used in cell-based applications, to ensure that their product meets their clients' specific needs. The combination of tests they choose would also likely differ, as a chemical company is less likely to have access to cell culture facilities compared to a biological research lab.

4.3.0 Probing effective pore size

4.3.1 Why is it important?

Based on previous studies, where a variety of cell types have been shown to be viable within the gels [33, 76, 280], it was assumed that the vital constituents of cell culture media were able to diffuse into the peptide hydrogels. In these studies, cell culture media was often supplemented with foetal bovine serum (FBS). A major component of FBS is bovine serum albumin (BSA), which is a globular protein approximately 66.5 kDa in size. We can conclude, therefore, that it is likely that any molecule that is approximately the same size and shape as BSA would be able to diffuse in and out of the gel freely. However, this also implies that any similarly sized or smaller molecule that is the target for functionalisation would also be able

to move freely within the gel, and that any negative gradient created between the gel and the surrounding media would cause these soluble additions to diffuse out be subsequently lost during media changes. Therefore, these additions need to be immobilised within the gel in some way, or be continually supplemented in the media, to maintain its target concentration in the gel network throughout an experiment.

However, it was not known what the upper limit to this effect was. It would be useful to know whether there was a certain size at which covalent immobilisation or supplementation was unnecessary because these molecules would become hydrodynamically trapped and unable to escape the gel after encapsulation. Therefore, wan to estimate this upper limit was needed, which could also further demonstrate the need to develop new methods for covalent functionalisation.

4.3.2 The FITC-Dextran protocol

To estimate the effective pore size of the peptide hydrogels, an assay using fluorescein isothiocyanate-dextrans (FITC-Dextrans) of varying lengths was developed. Development of this assay first required some initial validation and optimisation work, to determine the optimum concentration of FITC-Dextrans for future use in the assay. This involved using unfunctionalised "blank" peptide hydrogels and a FITC-Dextran approximately 40 kDa in size (FD40S). FD40S was chosen for this as it was reasonable to expect a molecule of this size would be able to diffuse into the gel, based on the reasons outlines above. The concentrations tested were 10 µM, 20 µM, and 30 µM. This initial test demonstrated that all of these concentrations would produce a measurable signal for the assay, but 20 µM was selected due to it being the same concentration used when functionalising the peptide hydrogels with soluble matrix components in other tests, thereby providing better consistency among experiments.

The result obtained from the subsequent objective tests demonstrated that FITC-Dextrans up to 2000 kDa in size were able to diffuse into the gel within the first 24 h. Following this, the loss of FITC-Dextrans depended primarily on their size. It is hypothesized that during the first 24 h the gel is more permeable, as the gel network has not yet adopted its final configuration. A previous study found that there was an approximate order of magnitude increase in viscosity between precursor gels and peptide hydrogels, following neutralisation with culture medium [33]. This increase occurred over the course of an overnight incubation at 37 °C. Therefore, it is possible that this is associated with changes in the gel network which

occur over the same period. This is supported by the observation that whilst the larger FITC-Dextrans can diffuse into the gel during the first 24 h, they are better retained during the remainder of the experiment and in gels of a higher final peptide concentration (and therefore final viscosity). The results also revealed that effective pore size was related to peptide concentration, where an increase in the peptide concentration of gels was related to greater retention of encapsulated molecules. This was not surprising, as an increase of peptide concentration was already known to be proportional to gel stiffness [33].

4.3.1 Conclusions and future work

The result obtained using the FITC-Dextran protocol effectively demonstrated the risk that smaller molecules may diffuse out of the gel and subsequently be lost during media changes, which was one of the major concerns which drove the need to develop methods for covalent immobilisation. It will also allow future end users a way to identify which molecules would benefit the most from immobilisation, based on the size of the molecule and stiffness of gel.

However, despite the results of this assay providing a good starting point in probing the effective pore size of the peptide hydrogels, the protocol also has several limitations that require consideration. The most important is that FITC-Dextrans are linear polysaccharides and are therefore not necessarily representative of similarly sized molecules that adopt different 3D structures. Therefore, a greater variety of fluorescently labelled molecules, representing a greater variety of 3D structure, should be included in the future. This would allow a more accurate approximation of the effective pore size of the gels. It is also worth considering whether these molecules or their conjugated dyes are hydrophobic or hydrophilic, and whether this may influence their ability to diffuse throughout a material which comprised almost entirely of water. Whilst both dextran and FITC is hydrophilic in nature, other dyes, such as Cy5.5, can be highly hydrophobic.

However, to properly ascertain the exact pore size of the gels, alternative techniques would likely be required. Ideally, these techniques need to preserve the native microstructure of the hydrogels. However, this has proved difficult in the past when evaluating the microstructure of other hydrogels. Scanning electron microscopy (SEM) and X-ray diffraction often cause alterations to the hydrogel microstructure due to their vacuum operating conditions, causing liquid water to evaporate from the gels [281]. Evaporation can be reduced by operating at low temperatures (i.e., cyro-SEM), but water can exist in many different crystalline structures at these temperatures, which may affect gel microstructure

due to their lower density/higher volume compared to liquid water. Use of nuclear magnetic resonance (NMR) relaxation times in hydrogels to evaluate pore size offers a method which is rapid and non-invasive, without the need for preparatory procedures which may alter gel network structure [282]. Unfortunately, this technique requires access to specific instruments and a high level of technical expertise that would limit its wide-spread adoption across different research labs.

4.4.0 Development of "test environments"

4.1.1 Why is it important?

Before launching into any investigation which aimed to develop new methods for covalently functionalising the peptide hydrogels, the question of how each of these would be evaluated needed to be addressed. For any new method to be deemed a success, it needed to meet the following criteria:

- The act of immobilising the target material does not irrevocably alter gel stiffness
- Encapsulated cells can interact with the immobilised material
- These interactions produce a relevant, predictable, and measurable biological response

For the first criterion, it would be straightforward to ensure the new method does not alter gel stiffness by evaluating the functionalised gels via bulk oscillatory rheology and making a comparison with unfunctionalised gels. In most cases where there was a significant and meaningful difference in stiffness detected, this could likely be recovered by adjusting the mass of peptide used in the gel fabrication procedure. This reinforces the advantage that the peptide hydrogel platform has over similar 3D *in vitro* models that do not offer a way to alter matrix stiffness independently of matrix composition.

The second criterion is essential to demonstrate that the functionalised material is not simply immobilised within the gel but that it can also interact with encapsulated cells it in a biologically relevant way. This was carefully considered when the new methods were initially designed. To increase the likelihood of interactions with cells, and to reduce the likelihood that the immobilised material would interfere with the self-assembly process, each method was designed to attach target material only at the ends of the gelator peptide, whilst also incorporating a linker sequence to spatially separate the material from the gelator sequence (LPETGGG and DBCO for the sortase- and "click"-chemistry mediated approaches,

respectively). This strategy, particularly use of a glycine-based spacer, has been employed previously in other SAPHs to separate the self-assembling backbones from functional motifs [283-285].

For the final criterion, it was necessary to develop individual "test environments" for each target molecule that was to be immobilised. This involved measuring the effect of functionalising the gels with specific soluble material, providing conditions that would generate a set of control data. This would allow the effect of covalently functionalising the gels with that same material to be evaluated, by comparing it against the control data.

4.4.2 Directing stem cell fate with soluble glycans in 3D

Development of the first test environment began as an attempt to replicate a similar previous study conducted in 2D [68]. Mouse embryonic stem cells (mESCs) express a low sulphated version of heparan sulphate (HS) that becomes more complex and sulphated during progression to neural progenitor cells. Sulphated epitopes facilitate recognition and binding to a wide variety of ligands, including members of the fibroblast growth factor (FGF) family. Ext1$^{-/-}$ mESCs, which lack the critical EXT1 enzyme needed for chain elongation of HS, are therefore unable to undergo neural specification due to a reduction in FGF signalling. However, this ability can be restored in 2D by providing cells with exogenous HS or heparin. In a follow-up to this study, it was also demonstrated that the effect of heparin to promote this effect is concentration and size dependant [76]. In this study, it was found that the ability of heparin to promote acquisition of Sox1 expression (an early marker of neural specification) in 46c mESCs peaked at 6 µg/mL, before starting to decline. It was also found that smaller heparin oligosaccharides would inhibit, rather than promote, this effect.

To investigate whether this effect would translate to 3D, HS-deficient Ext1$^{-/-}$ mESCs were encapsulated within peptide hydrogels functionalised with soluble HS or heparin. HS-competent E14 mESCs were used as a control. Cells were then subjected to a seven-day neural differentiation assay, before cells were fixed and stained for the neural specific marker β-III-tubulin. Positive staining for β-III-tubulin would reveal whether the ability of HS-deficient Ext1$^{-/-}$ cells to differentiate to a neural lineage had been restored. The results of this assay not only demonstrated, for the first time, that this effect translates to 3D but also presents a convenient GAG-free system for evaluating the impact of functionalising biomaterials with GAGs in the future. This had been challenging in the past, where it had been difficult to distinguish between exogenous GAG and that which is produced by cells.

This GAG-free 3D culture environment provided a convenient set of control conditions for evaluating future methods for covalently immobilising HS or heparin within the gel. However, some surprising observations were made during the development of this assay. The first was that it appeared that HS-deficient Ext1$^{-/-}$ mESCs were able to progress further in response to soluble heparin, compared to the HS-competent E14 mESCs. This was evidenced by the enhanced staining for the neural specific marker β-III-tubulin and the higher degree of organisation of both β-III-tubulin and actin into extracellular filaments extending away from the cell cluster (this enhanced effect was observed approximately 50% of the time, across multiple biological repeats (n>3)). There are a couple of different possible explanations for this.

The first is that, as previously mentioned, the response of cells grown in 2D to exogenous heparin is dose-dependent, peaking at 6 µg/mL before starting to steadily decline [76]. It is possible that this same effect also translates to 3D, where there is also a peak concentration for promoting differentiation. In the case of HS-competent E14 cells, providing exogenous heparin in the gel environment may have pushed the concentration over this threshold, leading to an inhibition, rather than activation, of FGFR signalling [286].

The second possible explanation is that the enhanced response seen in Ext1$^{-/-}$ mESCs is due to the highly sulphated nature of the heparin oligosaccharide used for this project. As previously mentioned, it is the sulphated epitopes that facilitate binding to FGFs. Specifically, the N- and 2-O-sulphate groups of heparins have been shown to be essential for binding FGF-2. Moreover, sulphate at the 2-O- and 6-O-positions are critical for binding of heparin to a lysine-rich peptide sequence in the extracellular domain of FGFR-1. Therefore, when providing HS-deficient mESCs with highly sulphated heparin, there is a higher concentration of sulphated epitopes compared to the concentration found in the native ECM surrounding HS-competent cells. The observations made when gels were functionalised with soluble HS-III, which contains fewer sulphated epitopes compared to heparin, agrees with this second hypothesis.

4.4.3 Directing stem cell fate with soluble peptides in 3D

To evaluate new methods for covalently immobilising specific peptides within the peptide hydrogels, additional test environments were developed which investigated the effects of functionalising the gels with soluble fibronectin (FN) and the RGD motif. Fibronectin is a fibrous protein and a major constituent of the interstitial matrix, where it facilitates cell

attachment and function. It achieves this through interactions with RGD-containing cryptic binding sites, which are revealed when it adopts its stretched conformation in response to cellular traction forces [55]. These interactions can also be replicated with short synthetic peptides containing the RGD sequence. RGD functionalised materials have, therefore, been the subject of numerous past academic studies and medical applications [218]. Therefore, functionalising gels with soluble FN or RGD was proposed as a control for evaluating future methods of covalently immobilising these molecules.

The same cell system was used for testing cell responses to FN and RGD, as was used for testing HS and heparin. Other studies have demonstrated that FN and/or isolated RGD motifs could also influence differentiation of mESCs. For example, one study demonstrated that effect of conditioned media from human hepatocarcinoma cells (HepG2-CM) to promotes osteogenesis of mESCs was, in part, due to the influence of FN [287]. They showed this by providing FN directly to the basal medium and found that it would reproduce, to a degree, the stimulatory effect of HepG2-CM. Another study provided evidence that the FN-mediated upregulation of α1β1 integrin and adhesion to specific ECM molecules is linked to mESC commitment to meso-endodermal differentiation. In another study, a cyclised RGD peptide was found to mimic the effect of mechanical stimulation on mESC pluripotency gene expression, downregulating many core transcription factors, Oct4, Sox2, and Nanog [288]. It was therefore thought that the effect of functionalising the gels with FN or RGD would have the effect of enhancing differentiation of mESCs.

Therefore, E14 and Ext1$^{-/-}$ mESCs were encapsulated in gels functionalised with either soluble FN or RGD, and then subjected to the same seven-day differentiation assay as before. Surprisingly, and in contrast to the previous results measuring the effects of soluble HS and heparin, the differentiation potential of E14 cells actually appeared to be inhibited by the presence of soluble FN or RGD. Whilst most cell clusters encapsulated in gels functionalised with FN stained positive for β-III-tubulin, others did not. In gels functionalised with soluble RGD, this inhibitory effect appeared even greater, as a greater number of cell clusters appeared to lack β-III-tubulin expression. For Ext1$^{-/-}$ mESCs, cell clusters appeared to respond to the presence of FN or RGD by adopting an altered, "lemon-shaped" morphology.

It was hypothesized that the reason for these changes was that the presence of RGD leads to activation of an alternative pathway, pushing the mESCs towards a different lineage. A recent study investigating the effect of immobilising RGD on synthetic nanofibers found that the presence of RGD leads to downregulation of β-III-tubulin and an increase in early

expression of green acidic fibrillary protein (GFAP) in mESCs [219]. This pushed the cells towards a non-neuronal, glial lineage. The lack of endogenous HS in Ext1$^{-/-}$ mESCs could also explain why the effect of RGD is greater than for E14 mESCs, as there is no predisposition to differentiate to a neural linage to overcome. To test if cells were being directed to a glial lineage, the RGD functionalised gels were also stained for GFAP. However, no detectable GFAP expression was observed.

The observed response of encapsulated E14 and Ext1$^{-/-}$ mESCs to soluble RGD nevertheless provided a testable hypothesis for evaluating future methods for covalently functionalising RGD within the gel: where RGD is effectively immobilised within the gel, and where it is accessible to cells and retains its relevant biological activity, the concentration of RGD remains high enough throughout culture to drive the differentiation of encapsulated Ext1$^{-/-}$ mESCs towards a β-III-tubulin$^-$, GFAP$^+$ glial phenotype.

4.4.4 Conclusions and future work

The above test environments were ultimately employed with great success to evaluate the new methods for covalent functionalisation that were developed for this project. However, there are several limitations that currently exist which need to be addressed in the future. The first is that they rely heavily on a single cell type, specifically the HS-deficient Ext1$^{-/-}$, and the associated neural differentiation assay. In the future, it may be necessary to evaluate methods for immobilising material which is not expected to have any relevant impact on this process.

To address this issue, the protocol should be expanded to include a greater variety of cell types and biological processes. However, the utility of this as a GAG-free test system should be preserved, or else it may prove difficult to query the role of GAG-functionalised materials when those same GAGs could be produced by encapsulated cells. Therefore expansion to other cell types will require either than they are similarly genetically modified to create GAG-deficient clones or GAG synthesis could be inhibited by treatment with specific inhibitors such as chlorate [289, 290].

The second issue is that is also relies too heavily on immunohistochemistry (IHC). This technique is effective at revealing morphological changes and large changes in the expression levels of certain target molecules, but it less effective when that change is small,

requiring the use of sophisticated imaging techniques that aim to convert subjective image data into more objective data amenable to statistical analysis.

To overcome this second issue, changes in expression level could also be evaluated using DNA microarrays, which are better equipped to detect smaller relative changes in gene expression levels and are highly amenable to high throughput. This technique has been used previously as a supplement to IHC-based techniques. For example, Kenny et al (2007) [291] used IHC and confocal imaging to assess the morphological differences of 25 different breast cancer cell lines grown in 3D, before then assessing gene expression profile changes of cells grown in 2D and 3D, via an Affymetrix microarray. Similarly, Fontoura et. al (2020) [292] used SEM and confocal imaging to assess morphological changes in mouse melanoma B16F10 GFP cell clusters grown on different scaffolds but then also used gene expression analysis to corroborate the similarities between 3D *in vitro* and *in vivo* conditions, compared to 2D. These examples also highlight the need to approach these kinds of evaluations from multiple angles.

However, a further issue with using IHC and DNA microarrays is that they can only be performed as an end-point experiment, requiring the encapsulated cells to be fixed/lysed first. Using fluorescently labelled marker cell lines could also allow end users to gather data throughout the entire experiment. For example, the Oct4GFP mESC line co-expresses green fluorescent protein (GFP) alongside the stemness marker Oct4, driven by the Oct4 promoter. Similarly, the 46c mESC line co-expresses GFP alongside Sox1, which is a marker for neural specification. If these cells were encapsulated in the peptide hydrogels and subjected to a neural differentiation assay, it should be possible to track the relative change in expression for each of these markers as the cells progress towards a neural lineage, by measuring the fluorescence signal associated with each marker via a plate reader. The point at which these two signals "cross-over" could be used as a baseline to evaluate different methods for functionalising the gels (see Figure 32). This protocol was, in fact, attempted during the course of this project but a fluorescence signal could not be detected using the plate reader instrument available.

Another advantage of using reporter cell lines is that it allows for live cell imaging over the course of the experiment. Generation of cell lines with multiple lineage specific reporters has also allowed for increasingly informative assays. For example, the reporter line RUES2-GLR expresses markers for the mesoderm (*BRA*), endoderm (*SOX17*), and neuroectoderm (*SOX2*)[293]. This has allowed researchers to follow the process of symmetry-breaking and

segregation of germ line progenitors in human gastruloids, via live cell imaging [160]. Similarly, BRA/SOX2 reporters have been used to track symmetry breaking in a 3D model of a human epiblast [294]. These types of multi-lineage readouts would create a more informative differentiation assay for evaluating the effect of functionalising the peptide hydrogels. Adapting this protocol to work with automated microscopes for live cell imaging (such as the Celldiscoverer platform) would also make this more amenable to high throughput.
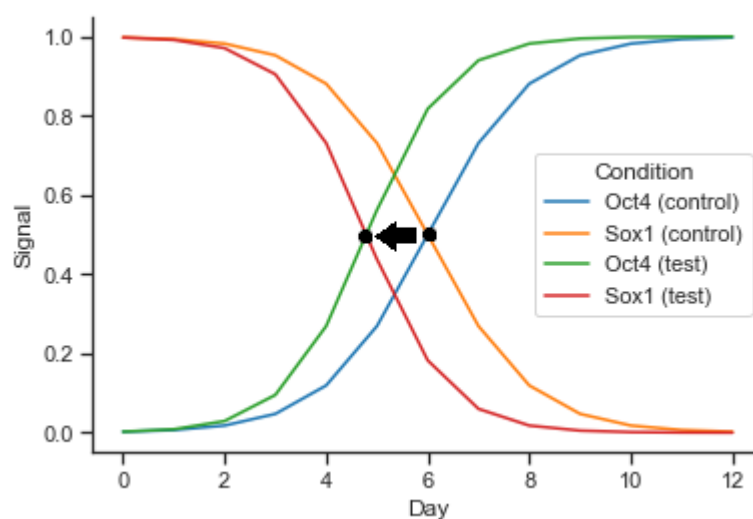
Figure 32 - Example of data obtained using fluorescently labelled marker cell lines. In this mock data, we imagine that both Oct4GFP and 46c mESCs were encapsulated separately in either unfunctionalised "blank" peptide hydrogels or gels that had been functionalised with a molecule found to enhance their differentiation to neural progenitor cells. This would have the effect of moving the "cross-over" point to the left. Similarly, if the gels had been functionalised with a molecule that inhibited their differentiation, this point would have instead moved to the right.

Despite the improvements which could still yet be made to the test environment protocol, the specific protocol that was used for this project was sufficient for an initial evaluation of the new methods. However, future end users may wish to consider incorporating some of the suggested improvements above, where they may be useful to answer their specific research question.

4.5.0 Sortase-mediated functionalisation

4.5.1 Why is it important?

Following the results of the gel permeability tests, the need to develop new methods for covalently functionalising the gels became increasingly apparent. The results demonstrated that this was of particular concern for target molecules less than 2000 kDa. This was also compounded by the fact that some molecules behave differently depending on whether they are provided to cells in solution or are attached to a substrate, as evidenced by previous studies looking at the effect of immobilising RGD-containing peptides to synthetic scaffolds [219]. To address these issues, the primary aim of this project was to identify, optimise, and validate novel methods for covalent functionalisation.

Two methods were investigated to achieve this project's primary aim: sortase-mediated functionalisation and "click" chemistry-mediated functionalisation. These were both identified as potential candidates based on a review of the literature, which revealed that these or similar techniques had already proven effective in functionalising other biomaterials [223, 224, 270, 271]. Additionally, it was worth pursuing multiple methods for functionalising the peptide hydrogels, to provide future end users a greater degree of choice in how they approach functionalisation. There are several reasons why this may would be useful to future end users, which are discussed in further detail in a later section. This section focuses on the development of the sortase method, with a later section focusing on the "click" chemistry method.

4.5.2 Development of the sortase method

Sortase-mediated functionalisation had previously been employed in several past studies to functionalise biomaterials. In 2015, Cambria et al. used sortase to modify a polyethylene glycol (PEG)-based hydrogel containing the LPRTG sortase substrate with sortase-tagged epidermal growth factor (GGG-EGF) [223]. They were also able to confirm the biological activity of the immobilised EGF through the phenotypic response of human primary epithelial cells. Based on previous studies, the effect of immobilised EGF was predicted to stimulate DNA synthesis of these cells [295, 296]. Therefore, in this test, cells were seeded on hydrogels that had been functionalised with EGF and cells actively synthesizing DNA quantified using the Click-iT EdU Alexa Fluor 488 kit (Life Technologies). The results demonstrated enhanced DNA synthesis under these conditions. Another group, Piluso et al. (2013), were also able to use sortase to modify a peptide-based hydrogel similar in composition to the peptide

hydrogel used in this project [224]. In their study, they were able to immobilise the DNA-binding protein Tus and then confirm its biological activity by treating the functionalised gels with Ter DNA (a substrate of Tus) labelled with fluorescein. Gel fluorescence was measured via a plate reader and found to be higher in gels where sortase had been used to immobilise the Tus, after performing a series of wash steps to remove unbound Tus.

Whilst each of the studies outlined above had confirmed sortase as a promising potential bioconjugation tool to functionalise specific biomaterials, each fell short of demonstrating what was needed for this project. In the Cambria et al. study, they showed that the immobilised material maintained its biological activity on cells, but their model system was based on different chemistry (i.e., PEG-based, not peptide-based) than the one used in this project. In the Piluso et al. study, their model system was based on similar chemistry, but they failed to demonstrate that their methods were amenable to cell-based applications.

Using the above studies as a starting point, sortase was investigated as a tool to functionalise the FEFEFKFK peptide hydrogels. To achieve this, an assay was designed to probe the effectiveness of sortase as a tool to immobilise sortase-tagged enhanced fluorescent protein (eGFP-LPETG) within peptide hydrogels containing the complementary GGGG sortase substrate. This assay is able to provide a rapid readout on the effectiveness of any specific sortase protocol and was subsequently used to evaluate each potential modification of the original protocol.

The results from the optimisation tests were often surprising, going against predictions based on the available literature. This also dramatically slowed down the development process, especially in the beginning, where it took approximately 6 months before the protocol began to produce consistent results that could be included in this thesis. At each subsequent stage, numerous minor tweaks and alterations were also necessary before obtaining reproducible results. Altogether, development of the final sortase protocol took approximately 12 months.

However, the results that were obtained during this process were, nevertheless, often interesting and informative. The first interesting result obtained was that the length of the incubation step was more important than the temperature. This was surprising, as it was assumed that a temperature closer to 37 °C would be the most effective, as this is the optimum growth temperature for *S. aureus*. The second surprising result was that the LPETG motif was a more effective substrate for the enzyme than LPMTG. This also contradicted what was suggested by the available literature [261].

Perhaps the most startling discovery came from the tests which aimed to optimise the composition of the reaction buffer. In previous studies, the presence of additional calcium in the reaction buffer was critical for an efficient reaction [223, 225, 263]. However, in cell-based applications, the presence of additional calcium could have undesirable side-effects on encapsulated cells. Therefore, an investigation was launched to determine whether the concentration of calcium already present in cell culture medium was sufficient to drive an efficient reaction within the peptide hydrogels. The results revealed that whilst this concentration was sufficient, providing additional calcium led to a more efficient reaction.

To close this gap, an investigation into the use of a calcium-independent sortase variant was undertaken. This variant was first described by Jeong et al. [231], and was used to demonstrate that it was effective at covalently linking a sort-tagged hemagglutinin (HA-LPETG) probe to the cell surface of C57BL/6 mice spleen cells, without the need for additional calcium in the reaction buffer. Using the methods outlined in their paper, this variant could be synthesized at the University of Nottingham and tested in our system. The authors also generously provided samples of their enzyme to use as a control. However, the results from testing these calcium-independent variants revealed that neither could produce a more efficient reaction than the wild-type variant. In a more surprising twist, the results also revealed that providing additional calcium in the reaction buffer led to a significant increase in the reaction efficiency of the so-called "calcium-independent" sortases. This effect was also observed in the original paper, but not to the same degree.

These observations highlight the requirement to test assumptions, particularly when working with biomaterials where the exact specifications may well be different and where a direct extrapolation of results from one model to another is not always possible or wise. Nevertheless, in the final version of the protocol it was demonstrated that sortase could be utilised effectively to immobilise eGFP within the peptide hydrogels, without any negative impact on gel stiffness or on the viability of encapsulated cells. This therefore allowed us to test the protocol with more biologically relevant material.

4.5.3 Sortase-mediated control of matrix composition

A previously discussed, the only true test of whether a new method for functionalising the peptide hydrogels was a valid approach was that it produces a relevant, predictable, and measurable biological impact on encapsulated cells. To validate the adapted sortase method,

an RGD peptide was immobilised within sortase-primed gels and its effect on encapsulated E14 and Ext1$^{-/-}$ mESCs was evaluated.

Based on previous experiments, investigating the effects of soluble FN and RGD peptide on these cells, the predicted outcome was that when sortase was employed to immobilise RGD within the gels, the concentration of RGD within the gel environment would be better maintained throughout culture, enabling the cells to differentiate towards a β-III-tubulin^{-}, GFAP^{+} phenotype. This hypothesis was tested, and the theory was confirmed. In E14 mESCs, immobilisation of RGD led to the complete disappearance of positive β-III-tubulin (compared to FN where some positive staining was still detectable) and the emergence of the "lemon-shaped" morphology with associated GFAP^{+} staining. In Ext1$^{-/-}$ mESCs, the emergence of positive GFAP staining was also observed.

4.5.4 Conclusions and future work

The experiments conducted which utilised sortase to immobilise RGD within the peptide hydrogels were able to effectively demonstrate that all the criteria for assessing the validity of the new methods had been met:

- ☑ Sortase-immobilised RGD did not significantly alter gel stiffness, compared to gels functionalised with soluble RGD
- ☑ Encapsulated cells were able to interact with the immobilised material
- ☑ This interaction produced a relevant, predictable, and measurable biological response

Furthermore, this was also validated over multiple biological and technical repeats (n=3, with three technical repeats per test).

However, whilst this new method was successful at immobilising eGFP and RGD within the gels, it will be necessary in the future to demonstrate that it can be used to immobilise a greater variety of target molecules. Each would first require the development of a new test environment for evaluating the protocol's effectiveness with respect to that particular target molecule. For example, in 2004 Silva et al. [297] demonstrated that peptide amphiphile (PA) gels covalently functionalised with the laminin-derived IKVAV (Ile-Lys-Val-Ala-Val) sequence enhanced the differentiation of neural progenitor cells (NPCs) to neurons, while discouraging the development of astrocytes. They also found that this effect was greater than when cells were provided with soluble IKVAV or laminin, due to the enhanced adhesion of cells to the

gels through interactions with the immobilised IKVAV. This experiment would provide a good starting point to investigate the effectiveness of immobilising IKVAV within the FEFEFKFK peptide hydrogels, where the corresponding test environment would include gels functionalised with soluble IKVAV.

Additionally, exploiting the reversible nature of the sortase reaction could be investigated. As previously discussed, the formation of the LPXTGGG sequence, following sortase-mediated conjugation, provides another substrate for the enzyme. In a recent study, this feature was used to design dynamically tuneable polyethylene glycol (PEG)-based hydrogels [214]. These hydrogels could be stiffened via sortase-mediated crosslinking and then later softened by incubating with sortase and a soluble oligoglycine substrate, degrading the cross-links. It is possible that this protocol could be adapted to also allow dynamic tuning of matrix composition. A molecule of interest containing the LPETG substrate could be immobilised within the gel at one time-point and then later removed by incubating the gels with sortase and an excess of an inert LPETG-presenting substrate. This would provide end users with the ability to investigate the effect of matrix-derived, time-dependant signalling in a variety of cell processes.

Another peculiarity of the reaction that could be exploited is the formation of β-hairpins, generated when the enzyme is presented with substrates also containing the WTWTW sequence (i.e., $(X)_n$-WTWTW-LPETG and GGGG-WTWTW-$(X)_n$). The formation of these structures nullifies the reversible nature of the reaction, as the enzyme is blocked from accessing the LPXTGGG sequence in the final product. This could be used to remove the requirement of providing an excess of a single substrate, which is currently necessary to shift the equilibrium of the reaction towards a more quantitative conversion. It could also be used to create more dynamically tuneable gels. For example, by providing an excess of WTWTW-LPETG motifs within the gel network, a more precise amount of a target molecule containing the complementary GGGG-WTWTW motif could be immobilised at one time point, consuming some of those motifs, and then another target molecule at a second time point, consuming the rest.

There are also several improvements that could be made to the core protocol itself. The first being that further investigation into the use of a calcium-independent sortase variant may still be justified. Whilst the tests performed during the course of this project revealed no clear benefit to using the calcium independent variant, this variant is just one of many that have been identified. Although the results obtained by Jeong et al. (2017) [231] suggested

that this variant was the most efficient of the ones they identified, they had only tested its performance with respect to cell-surface and protein labelling. It is possible that a different variant would have been more successful in the specific context of functionalising the peptide hydrogels.

Another improvement would be to broaden the scope of the protocol to allow immobilisation of a greater variety of molecules. As previously discussed, it has been proposed that specific sugar amino groups mimic the glycine nucleophiles that act as a substrate for the sortase reaction [232]. Given that it has already been demonstrated that a sortase reaction can occur between peptides containing an LPETG sequence and the $-CH_2-NH_2$ moieties of 6-aminohexoes [232], a future experiment could look at appending this sequence to glycans such as HS or heparin and then attempting to immobilise these within the gel network via sortase. The tests performed in this project to evaluate the impact of soluble heparin and "click" chemistry-mediated immobilised heparin could be used as a baseline to assess this new method for immobilising glycans.

With the multitude of potential avenues for further refinement and improvement that could be made to this protocol, the initial validation of the approach presented here sets the stage for an exciting new area of research. It is hoped that this will provide a useful starting point for future end users to adapt this work to suit their specific research needs.

4.6.0 Sortase-mediated control of matrix stiffness

In addition to the method outlined above for using sortase to immobilise matrix material within the peptide hydrogels, sortase was also investigated as a tool to alter the stiffness of the gels. A significant advantage of the peptide hydrogel platform, compared to other model platforms such as those based on Matrigel®, is its ability to model a range of different tissue stiffnesses, simply by adjusting the mass of peptide used during the preparatory process. Importantly, this offers a way for end users to adjust the stiffness of gels independent of matrix composition, allowing stiffness to be controlled for when investigating the biological impact of matrix additions that would have otherwise also caused an impact on the mechanical property of the gel. The ability to model a range of stiffnesses is also critically important when studying diseases such as fibrosis and cancer, where increasing stiffness often correlates with disease progression [89, 298, 299].

However, using the current protocol, control of matrix stiffness was only achievable at a single point. Several recent studies have already investigated the potential of offering end users dynamic control of matrix stiffness in similar biomaterials. Photo-crosslinkable hydrogels in particular have recently gained significant interest [300]. Their mechanical properties can be manipulated in a spatiotemporal manner through exposure to light of specific wavelength to achieve the desired functionality. These gels are basically comprised of a polymeric network containing photoreactive moieties that are usually made up of a photochromic chromophore. However, these photoreactive moieties usually require expose to light in the ultraviolet (UV) range to trigger the desired effect, which is problematic in cell-based applications where exposure to UV light can be damaging to cells. Therefore, these types of hydrogels are generally investigated more for their potential as drug delivery vehicles rather than tissue model systems.

A review of the literature revealed an alternative approach that may be more amenable to cell-based applications. In one study, the authors were able to achieve dynamic control of matrix stiffness in a polyethylene glycol (PEG)-based hydrogel using an enzymatic approach based on sortase-mediated transpeptidation [214]. By engineering PEG-peptide conjugates with both sortase substrates (i.e., PEG-GGGG and PEG-LPRTG), they were able to create a hydrogel which could by dynamically stiffened by incubating with sortase, to induce hydrogel cross-linking. Due to the reversible nature of the sortase reaction, they were also able to achieve dynamic softening by incubating with sortase and oligoglycine, which induced degradation of those cross-links.

It appeared that a direct translation of these results to the peptide hydrogel platform ought to be possible. Dynamically tuneable peptide hydrogels containing peptides with both sortase substrates (i.e., GGGG-FEFEFKFK and FEFEFKFK-LPETG) were produced, and then incubated with a variety of sortase solutions containing varying concentrations of additional calcium. The results were, again, surprising. It appeared that the presence of sortase had no effect on gel stiffness at all. This was possibly due to the configuration of the gel network keeping the substrates for the enzyme spatially separated so that no crosslinking could occur. To test for this in the future, it may be possible to immobilise different fluorescent molecules onto each recognition sequence presented by the tuneable gels and then visualise the gels under a confocal microscope. These images could reveal the localisation of the different sortase substrates in the gel.

More surprising was the apparent effect of calcium on gel stiffness. It appeared that when additional calcium was provided in the reaction buffer, there was also massive increase in gel stiffness independent of the presence of sortase. There are several potential explanations for the increase in stiffness caused by the additional calcium. The $CaCl_2$ in the calcium buffer could be reacting with the HCO_3 in the mESC culture medium used to neutralise the gels. This reaction yields HCl and $Ca(CO_3)_2$. Given that the gels are pH sensitive, this release of HCl could be affecting the stiffness. The $CaCl_2$ could also be reacting with the small amount of trifluoroacetic acid (TFA) left behind during the peptide powder manufacturing process. This would yield $Ca(CF_3CO_2)_2$, which could also be affecting gel pH. Finally, it could be that the presence of calcium is having a more direct effect on the stiffness of the hydrogel, as a similar effect has also been observed in other types of peptide hydrogel [301].

Unfortunately, there was insufficient time to allow an investigation into the basis of these results. However, it is believed that this method warrants further investigation in the future and that the development of a calcium-free protocol using a calcium independent variant of sortase would be an important first step towards developing a method for sortase-mediated control of matrix stiffness.

4.7.0 "Click" chemistry-mediated functionalisation

The second method that was investigated to allow covalent functionalisation of the peptide hydrogels aimed to take advantage of "click" chemistry. Multiple protocols for "click" chemistry-mediated functionalisation of biomaterials had been previously described in the literature which provided evidence that this could also potentially be adapted to functionalise the peptide hydrogels. In 2016, Harvey et al. had utilised "click" chemistry for the site-specific functionalisation of recombinant spider silk. In this study, they incorporated the non-natural methionine homologue L-azidohomoalanine (L-Aha) into 4RepCT, a self-assembling recombinant dragline silk protein, originally derived from the nursery-web spider *Euprosthenops australis* [302, 303]. This protein is a miniaturized version of the silk monomers (spidroins) found in nature, consisting of a repetitive domain and a non-repetitive C-terminal domain essential to fibre formation. These can self-assemble into immune tolerated fibres, demonstrating their potential to be used as a biomaterial in regenerative medicine [303-308]. However, the applications of 4RepCT were limited due to a lack of options for functionalisation. By incorporating three L-Aha residues into 4RepCT, yielding 4RepCT[3Aha], the authors were able to achieve site-specific functionalisation with both a fluorescent probe and the antibiotic levofloxacin, via copper-catalysed alkyne-azide cycloaddition (CuAAC). Importantly, they were also able to demonstrate that the fluorescent

properties of the probe and the antimicrobial properties of levofloxacin were maintained after attachment to the spider silk protein, via an immunofluorescence and bacterial inhibition assay, respectively. However, it is important to consider here that this method for functionalisation obviously did not have any requirement for cell tolerance, which would be important in our methods.

It was thought that by applying some of these same principles to the peptide hydrogel platform, a new method for site-specific covalent functionalisation could be developed. The process required extending the gelator octapeptide to include the L-Aha residue, yielding FEFEFKFK(Aha), and incorporation of the complementary alkyne handle to a molecule of interest, to allow for a subsequent "click" reaction. However, the original authors had used a copper-catalysed reaction. To conserve biocompatibility, copper was removed from the final product by washing functionalised fibres with buffers containing ethylenediaminetetraacetic acid (EDTA) and by utilizing *tris*(3-hydroxypropyltriazolylmethyl)amine (THPTA), which binds and stabilizes the Cu (I) ion in the click reaction. They then confirmed that all detectable traces of copper had been removed, via energy-dispersive X-ray spectroscopy. They note that this is effective because the potential for copper to bind the 4RepCT[3Aha] protein is low, due to the presence of only two glutamic acid residues in its non-repetitive C-terminal domain (in a protein which is at least 23 kDa [309]). In the peptide hydrogel model, the gelator peptide also only has two glutamic acid residues but these two residues represent a much larger proportion of the entire molecule. It was therefore thought that a copper-catalysed reaction would not be appropriate.

Therefore, a different approach was necessary for the "click" reaction itself. Strain-promoted azide-alkyne cycloaddition (SPAAC) was selected to provide a better approach that would address all the potential issues with a copper catalysed reaction. This would allow the reaction to take place without the need for a copper catalyst, within a physiological range of temperature and pH, and could potentially be carried out in the presence of living cells. To facilitate this, two different dibenzocyclooctyne (DBCO) linkers were created. When joined to molecule of interest, each of these would then present the prerequisite strained alkyne for the subsequent "click" reaction.

The first linker that was created was DBCO-NHS, which can be conjugated to organic molecules such as DNA and peptides, through amide bond formation between the linker and the amine functional groups that are abundant in these types of molecules. The second linker

was DBCO-NH$_2$, which allows conjugation to molecules harbouring electrophilic moieties, such as the carboxylic acid functional groups in found in glycans. By creating two different linkers, each of which allowed conjugation with a different class of molecule, future end users of the peptide hydrogel model have greater flexibility in how they approach functionalisation. It also allows the creation of more complex models containing a greater variety of biomolecules.

4.7.1 Functionalising peptide hydrogels with RGD via "click" chemistry

Proteins which contain the tripeptide motif RGD, along with the integrins which serve as receptors to them, constitute a major recognition system for cell adhesion and signalling [34]. Integrin-mediated cell attachment influences and regulates cell migration, growth, differentiation, and apoptosis, as well as playing a role in cancer progression and metastasis [310]. This was, therefore, thought to provide a good first opportunity to observe a measurable impact on encapsulated cells in later cell-based tests, thereby validating this new method for functionalisation. The choice to use the cyclised version of this motif was made because it has been shown to boast enhanced biological activity, due to a reduction in the loss of entropy required for RGD to adopt the frozen bound conformation necessary for its interaction with receptor molecules [272]. It would also hold an advantage over previous methods for functionalising the peptide hydrogel with RGD, in which the gelator peptide was simply extended to contain the linear version (i.e., FEFEFKFK-RGD) [212].

Amide coupling between the DBCO-NHS linker and cyclo(RGDfK) was performed and confirmed with high resolution mass spectrometry (HRMS), before purification by high performance liquid chromatography (HPLC). This demonstrates that the DBCO-NHS linker can be effectively conjugated to small peptides, such as cyclo(RGDfK), providing them with the strained alkyne handle for the subsequent click reaction that would immobilise them within the peptide hydrogels. In the future, it would be necessary to confirm this is also possible with larger peptides and other classes of molecule containing an amine functional group. However, this single result provided a reassuring proof of concept.

The next step was to perform the final "click" reaction that would immobilise the DBCO-cyclo(RGDfK) product within the gel. This was carried out "*in situ*" by simple mixing of a solution of DBCO-cyclo(RGDfK) into the peptide solution that is prepared as a normal part of the gel fabrication procedure. HMRS analysis confirmed that the "click" reaction had occurred with great efficiency, following the centrifugation and 2 h incubation step. The ease

of this protocol offers future end users the ability to perform "click" chemistry-mediated functionalisation without the need for additional equipment or major changes in the gel fabrication.

However, consideration must be given here to the fact that this was only attempted twice. This was due to the limited supply of DBCO-cyclo(RGDfK) material available. Considerable research effort was required, with multiple rounds of optimisation requiring approx. 6 months of work, before the protocol could produce even small amounts. Nevertheless, in the future, it will be necessary to further validate this by additional repeats and with other molecules of interest.

Despite the success of the previous steps, no useful results could be obtained to evaluate the biological impact of immobilising RGD within the gels via "click" chemistry. Again, this was due to the limited supply of material that only provided enough to make two functionalised gels. One of these gels was assessed via bulk oscillatory rheology, to evaluate if this new method of functionalisation had any effects on the mechanical features of the gels. Here we found it had no meaningful impact on gel stiffness. This is important to demonstrate that any effects observed in the following cell-based assay were the result of the biological activity of the immobilised the material and not due to the gel's mechanical features. This result also suggests that the FEFEFKFK(Aha)-DBCO-cyclo(RGDfK) molecules were able to self-assemble with the unfunctionalised FEFEFKFK peptides, as the change in stiffness was lower than that seen in gels which had simply been functionalised with soluble RGD.

The second functionalised gel was used in a cell-based assay to provide a preliminary analysis of the biological impact of this functionalisation on encapsulated cells. Ext1$^{-/-}$ mESCs were encapsulated within the gel and subjected to a neural differentiation assay, but the viability of these encapsulated cells was very poor. The most likely explanation for this result is that it is representative of the variability that exists between typical cell culture experiments, where sometimes cells cultures fail for no discernible reason. However, we must not discount the possibility that this new method of functionalising the gels had somehow created a toxic gel environment which caused the reduction in viability. In the future, this experiment would need to be repeated to first determine whether there is a real problem, and whether further investigation is required to pin-point what that this could be.

4.7.2 Functionalising peptide hydrogels with heparin via "click" chemistry

Previous experiments had already provided a convenient baseline for testing the bioactivity of heparin within the gels. In a previous study, it had been demonstrated that addition of soluble HS, or its analogue heparin, to the 2D culture of HS-deficient Ext1$^{-/-}$ mESCs restored their ability to undergo neural specification [273]. In a similar experiment conducted for this project, the same effect was observed when this experiment was translated to 3D, by encapsulating Ext1$^{-/-}$ mESCs in peptide hydrogels functionalised with soluble heparin. Therefore, by repeating this experiment using gels that had been functionalised with immobilised heparin, it would be possible to ascertain whether the immobilised heparin had retained its relevant biological activity.

Generation of the DBCO-Heparin molecule was achieved via reductive amination of the DBCO-NHS linker and a heparin oligosaccharide that was 30 monosaccharides in length. Unlike the above method for generating DBCO-cyclo(RGDfK), it was not possible at this stage to verify the DBCO-Heparin product via high resolution mass spectrometry. This is because the size and charge of the molecule made this impossible. However, as this was not available at the time, the decision was made to move forward under the assumption that this reaction had worked, and attempt verify it later with a biological assay.

The final "click" reaction between the DBCO-Heparin and FEFEFKFK(Aha) was then carried out, and the product freeze-dried. The resulting FEFEFKFK(Aha)-DBCO-Heparin powder could then be incorporated into the normal gel fabrication procedure by including this in the total mass of peptide powder. In this way, future end users would be able to vary the degree of functionalisation, by varying the ratio of functionalised to unfunctionalised peptide powder. The remaining steps of the gel fabrication procedure were carried out as normal, producing three peptide hydrogels functionalised with approximately 0.05 mg/mL heparin. Unfortunately, it was not possible to produce more, due to a limited supply of DBCO-Heparin material. Similarly to the protocol for producing the DBCO-cyclo(RGDfK) material, the protocol for generating DBCO-Heparin also required multiple rounds of optimisation before producing reliable material. Heparin being a much larger and variable molecule also made this comparatively more difficult than RGD, taking approx. 12 months to optimise the protocol.

To verify that the previous reactions were successful and that this new method for functionalising the peptide hydrogels leads to a relevant, predictable, and measurable biological impact on encapsulated cells, the experiment testing the impact of soluble heparin

on the differentiation of Ext1$^{-/-}$ mESCs was repeated using these "click" functionalised gels. As previously mentioned, only three gels were produced. One of these was assessed via bulk oscillatory rheology, to evaluate if this new method of functionalisation had any impact on the mechanical features of the gels, and it was found that to have no meaningful impact on gel stiffness. This result also suggests that the FEFEFKFK(Aha)-DBCO-Heparin molecules were able to self-assemble with the unfunctionalised FEFEFKFK peptides, as the change in stiffness was lower than that seen in gels which had been functionalised with soluble heparin.

The remaining two gels were used to provide a preliminary analysis of the biological impact of this functionalisation on encapsulated cells. Ext1$^{-/-}$ mESCs were encapsulated in these gels and subjected to a seven-day neural differentiation assay, mirroring the previous assay using soluble heparin. On day seven, gels were fixed and stained for the neural specific marker β-III-tubulin, revealing that the presence of immobilised heparin had restored the cells' ability to undergo neural specification.

4.7.3 Conclusions and future work

This result obtained after functionalisation with "clicked-in" heparin demonstrate that immobilising heparin within the gels leads to a relevant, predictable, and measurable outcome. However, consideration must be made that this was performed only twice. In the future, it would be necessary to repeat this at least a third time before it can be conclusively stated that this experiment was a success. However, these initial results provide promising preliminary data that this is the case.

In addition to the need to repeat the above experiments to provide more conclusive evidence of this new method's success, there are also several refinements or improvements that could be made. The first would be to validate this new approach with a greater variety of target biomolecules. Another important glycan species which would be an interesting target is hyaluronic acid. Hyaluronic acid (HA) is an anionic, non-sulphated glycosaminoglycan (GAG) and a major component of the ECM, widely distributed in connective, epithelial, and neuronal tissue [311]. It exists at the cell surface and interacts with a number of different cell surface receptors including CD44, RHMM, and ICAM-1 [312, 313]. These interactions play a pivotal role in tissue homeostasis, cell proliferation, and cell migration. Due to its biocompatibility and low immunogenicity, it has also garnered significant interest as a potential biomaterial for regenerative medicine and tissue modelling [314-317]. However, a major disadvantage of hydrogel models comprised of HA, or other

similar molecules of natural origin, is that it makes it impossible to query the role of HA in the system. A better hydrogel model would provide an inert scaffold upon which HA, or other important ECM components, could be added or taken away. This would better allow the evaluation of the minimal essential conditions which drive certain cell behaviours. The peptide hydrogel model presented in this project represents such a potential model. The peptide hydrogel could first be functionalised with soluble HA, and its impact on encapsulated cells evaluated, before using this as a test environment to evaluate "click" chemistry-mediated immobilisation of HA.

There is also a need to develop a technique to verify the synthesis of DBCO-Heparin product, following conjugation between DBCO-NH$_2$ and heparin, and its subsequent conjugation with FEFEFKFK(Aha). One possibility would be to use reverse-phase ion-pair high performance liquid chromatography (RPIP-HPLC), which is currently being investigated as a solution. This chromatographic technique is one which is becoming increasingly popular for the separation of charged compounds, such as HS and heparin [318]. Further refinement of the DBCO linkers to increase solubility, by including a polyethylene glycol (PEG) moiety (i.e., DBCO-(PEG)$_n$-NHS/NH$_2$) within the linker, would help facilitate this. This work would also be necessary to verify the synthesis of other large, charged molecules of interest, such as FEFEFKFK(Aha)-DBCO-HA.

The question of whether the gelator peptide can still self-assemble when it is functionalised with large molecules, such as heparin or HA, also needs to be answered. Preliminary evidence suggests that they can, as the change in stiffness of "clicked-in" heparin gels was smaller than gels that had been functionalised with soluble heparin. To test for this more conclusively, the DBCO linker could be adapted to include a fluorescent probe. Fluorescence of "click" functionalised gels could then be measured before and after a series of wash steps to reveal whether the "clicked-in" material had self-assembled within the gel network or had remained in solution and been washed away.

Despite the unavoidable setbacks, and the improvements which are still needed, the data collected for this project presents an initial proof of concept for an exciting new method for functionalising the peptide hydrogels. Combined with the validated sortase method, these offer future end users several new methods for creating user-defined biomimetic models of specific tissue microenvironments for use in drug discovery and investigative research. Care must be taken though to make informed choices on which biomolecules to include, and should be

4.6.0 Creating multi-functional peptide hydrogels

4.6.1 Why is it important?

The peptide hydrogel platform now offers three different methods for control of matrix composition: stirring in soluble components, sortase-mediated immobilisation, and "click" chemistry-mediated immobilisation. A major advantage of offering multiple methods for functionalisation is that future end users can choose which method is ideally suited for functionalising with specific matrix components. It also makes it easier to perform multiple functionalisations with a greater variety of target molecules. This enables end users to create more complex gel environments which more faithfully recapitulate the complexities of the native ECM, leading to the generation of more relevant cell behaviour and consequently also the generation of more relevant and reliable data.

Attempts at creating multi-functionalised hydrogels have been attempted previously and examples are given in the literature. In one study [319], the authors created a multi-functionalised gel environment by combining several functionalised and branched self-assembling peptides, all sharing the same (LDLK)$_3$ self-assembling backbone, selected from previously published works [320-322]. They were able to demonstrate that four different human neural stem cell (hNSC) lines were viable when encapsulated within this gel for up to six weeks. They also demonstrated enhanced differentiation to neurons, by tracking expression of β-III-tubulin, GFAP, GALC/O4, and Nestin, compared to 2D culture with Cultrex^{TM} (derived from EHS mouse sarcoma). This work establishes the potential for multi-functionalised synthetic hydrogels to compete with biologics in the future, where they are able to support relevant cell responses in a more reproducible system. However, it did not employ different functionalisation strategies (each functionalised self-assembling peptide had been functionalised by direct extension of the gelator peptide).

In another example, dual covalent functionalisation of PEG-based hydrogels was achieved using multiple different orthogonal chemical ligations [323]. Hydrogels containing two different functional groups – azide and potassium acyltrifluoroborate (KAT) *or* azide and hydroxylamine – were prepared that would allow for subsequent functionalisation via SPAAC, KAT ligation, or thiol-*Michael* addition. Different fluorescently labelled BSA proteins containing the complementary functional groups were also created (BSA-Fluo-CO, BSA-Rhod-KAT, and BSA-Rhod-HA). These were then immobilised within the appropriate gels to demonstrate that multiple functionalisations, using different ligation strategies, within the

gels could be achieved. However, this study had not demonstrated the utility of performing these multiple functionalisations within a cell-based assay. Therefore, in a final experiment, the ability to functionalise the peptide hydrogels using a different strategy for each target molecule was evaluated in a cell-based assay.

4.6.2 Functionalising peptide hydrogels with RGD and heparin

In this experiment, the effects of both soluble heparin and sortase-immobilised RGD on $Ext1^{-/-}$ mESCs were evaluated. Separately, each of these had either promoted the expression of β-III-tubulin or GFAP. It was unknown what the combined impact both molecules would have. In this way, this final experiment was carried out in a more speculative sense, in contrast to previous experiments which had an established predicted outcome. This was largely due to constraints of time, as there was only enough lab time available at the end of this project to perform this experiment once. As $Ext1^{-/-}$ mESCs had previously demonstrated a clearly observable response to both soluble heparin and sortase-immobilised RGD, this cell line was thought to provide the best chance at producing a measurable response for this test too.

$Ext1^{-/-}$ mESCs were encapsulated within these sortase-primed gels modified with soluble heparin, which were then subsequently also modified with RGD via sortase-mediated immobilisation. Cells were then subjected to a seven-day neural differentiation assay. On day seven, cells were fixed and stained for the neural specific marker β-III-tubulin or the glial specific marker GFAP. The results of this test were perhaps the most surprising of any presented here for this project. It appeared that, under these conditions, the $Ext1^{-/-}$ cells had adopted a β-III-tubulin⁺, GFAP⁺ phenotype. This is surprising as these two molecules are not usually co-expressed *in vivo*, except possibly in midgestational human foetal astrocytes [274].

4.6.1 Conclusions and future work

Consideration must be taken as this experiment was only performed once, and that the results may not be representative of future repeats, but if these results are representative then this provides preliminary evidence that multiple functionalisations can be carried out in tandem on the peptide hydrogels. The presence of both β-III-tubulin and GFAP perhaps also highlights the importance of choosing the right biomolecules for functionalisation, so that

the gel environment reflects the target tissue type being modelling in a biologically relevant way. The ECM is a complicated and dynamic structure, containing a complex variety of biochemically distinct molecules. Increasing the complexity of the gel environment, by adding a greater variety of biomolecules, will allow the model to better represent this complexity, but only if the right biomolecules are included at the right concentrations.

To understand which molecules should be included, the specific proteomes and glycomes of target tissues will need to be better characterised and understood. The Human Proteome Project has so far identified 89% of all the 19,823 predicted coding genes [324], and is likely to achieve its aim to fully characterise the entirety of the human proteome in the near future. Similarly, the Human Glycome Project currently aims to bring together a community of scientists dedicated to achieving the comparable goal of a fully characterised human glycome. In the meantime, there are several public databases which provide information on the proteins and glycans that have been identified thus far which can be used to help identify which important proteins and glycans to include.

It may also become necessary in the future to use data from patient-specific samples. This would allow generation of a model that more faithfully recapitulates the ECM of a specific patient, rather than the human species as a whole. Particularly in drug discovery research, this more personalised approach may allow better identification of suitable therapies to treat diseases such as cancer, where there is a large degree of difference in how different patients respond to chemotherapeutics [325-327].

Beyond a fully characterised human proteome and glycome, it will also become necessary to better understand how to model the correct organisation of the included matrix additions. This will be important to model specific complex biological processes, such as the differentiation of intestinal stem cells. As previously mentioned, the differentiation of these cells is driven by the antagonistic gradients of Wnt and BMP [247]. A potential method for representing this type of gradient within the peptide hydrogels would first involve creating gels that are amenable to different methods of functionalisation. These gels could then be plated out, one on top of the other, and subsequently functionalised with each molecule, creating localised areas of each functionalisation.

4.7.0 Final conclusions

4.7.1 Aims and objectives

The primary aim of this project was to identify, optimise, and validate new methods for covalently functionalising the peptide hydrogel model. Validation of these new methods required that they meet certain specific criteria, including that they could produce a relevant, predictable, and measurable biological impact on encapsulated cells. In doing this, the peptide hydrogel model could be transformed into a platform which enables future end users to create user-defined biomimetic models of specific tissue microenvironments.

The first method to be investigated was sortase-mediated functionalisation. The realisation of the final protocol for this required considerable optimisation of multiple features, driving the need to develop specific assays to measure the impact of each attempted optimisation. When the optimal protocol was finally identified, this was used with a high level of efficiency to immobilise matrix material which produced a relevant, predictable, and measurable biological impact on encapsulated cells. In this way, this method has been fully validated as a viable approach to functionalise the gels in the future. The second method that was investigated utilised "click" chemistry to immobilise matrix material. This also required significant optimisation, with further refinement currently being needed to fully validate this approach. However, preliminary data is encouraging, suggesting that this method is a viable approach for the future.

As a secondary aim of this project, the batch-to-batch variability of peptide hydrogels was evaluated. This required the design of a batch testing protocol, and this protocol was proven effective at measuring the variability in several critical features of the peptide hydrogels, including peptide solubility, gel stiffness, and the viability of encapsulated cells. Another secondary aim was to evaluate the effective pore size of the peptide hydrogels, to allow identification of which molecules would benefit the most from covalent immobilisation. This also required the development and optimisation of a novel assay and in its final version was employed successfully to achieve this aim.

The work presented here has largely met each of the above aims. Also presented are several suggestions for further refinement and improvements which could be made to the new protocols developed for functionalising the peptide hydrogels. In the future, this will enable the creation of increasingly complex gel environments, moving the model platform towards one which allows increasingly faithful recapitulation of natural tissue microenvironments. In this way, the platform aims to disrupt the landscape of drug discovery and investigative

research. Alongside other customisable 3D *in vitro* models, this platform aims to end the reliance on inferior 2D models which suffer from low cell densities, high stiffnesses, and lack the complex cell-cell and cell-matrix interactions that are present *in vivo*. Synthetic models also aim to replace the use of 3D *in vitro* models using animal-derived ECM products, which suffer from their ill-defined composition, high batch-to-batch variability, and lack of options for customisation.

4.7.2 Potential impact

It is envisioned that one of the most exciting applications of this model platform in the future will be in drug discovery research. Currently, there is a high attrition rate of novel drug candidates moving from the lab to the clinic. This is thought to be caused by the use of inferior 2D *in vitro* preclinical models used to predict the patient outcomes. More faithful, 3D *in vitro* models would be better equipped for this task, accelerating the drug development process towards a more precise and personalised standard of care. There are multiple features which make the FEFEFKFK peptide hydrogels ideally suited to this task, compared to other types of 3D model. The first is that, because it is synthetic, it can be produced at scale with low batch variability. This makes it more amenable to high throughput screening assays, compared to models using biologics such as Matrigel®. The second is that the relatively short sequence of the gelator peptide (compared to other SAPHs such as RADA16) keeps costs down as it is cheaper to synthesise.

To demonstrate the effectiveness of the peptide hydrogel as a drug screening platform, assays could be designed that replicated previous preclinical screening experiments. If the peptide hydrogel model could correctly identify past drug candidates that later failed when moved to the clinic, this would validate the model as a superior preclinical screening platform. Also, if this were the case, there may be justification to re-assess past drug candidates that failed preclinical screening experiments, as they may also have similarly been incorrectly labelled as being unsuitable.

However, the potential applications of the model platform extend beyond drug discovery research and will also provide researchers a superior approach to investigative research. Particularly when studying how cells and tissues interact with the ECM, a better 3D *in vitro* model may reveal new druggable targets for diseases like cancer, which do not appear when conducting the same study in a less faithful culture environment. For example, there are currently no good *in vitro* assays which allow researchers to evaluate the effect of reversing

the matrix stiffening that is associated with a poor prognosis. Therefore, it is difficult to design drugs which do this without using animal models, which are more costly, slow, and have important ethical concerns. Similarly, there are no good assays for the development of drugs to combat the increasing problem of lung fibrosis associated with long COVID. Currently, drug companies use simple 2D cell assays that are unsuitable for the development of this class of drug [328, 329]. A 3D *in vitro* model that offers ability to customise both its chemical and mechanical properties could help to solve these issues.

4.7.3 Potential route to commercialisation

In addition to the potential research impact of the model platform, it also has several other features which potentially make it an attractive target for commercialisation. Due to its synthetic origin, it presents a potential solution to the current global shortage of Matrigel® and similar products of animal origin. This shortage is probably due to ongoing supply chain issues caused by the COVID19 pandemic. However, others have suggested that it is also due to the recent increase in organoid research, which generally requires use of Matrigel® as a cell culture reagent [330]. The manufacture of Matrigel® requires the use of animals, which is time-consuming, costly, and requires specific training and licensing to carry out [120]. Techniques for the manufacture of synthetic peptides, such as solid-phase peptide synthesis, are more rapid, cost effective, and require no such licensing.

Its synthetic origin is also an attractive feature to researchers looking to make more ethically conscious choices in how they approach their research. With the efforts of the National Centre for the Replacement, Refinement and Reduction of Animals in Research (NC3Rs) and other similar organisations, more researchers would now rather use a synthetic alternative to an animal-derived product where possible. However, the limitations of current synthetic *in vitro* model platforms have prevented many researchers from making this change. To increase adoption, more complex synthetic models are needed which better recapitulate the native ECM and drive cell behaviours in more physiologically relevant ways. It is hoped that the research presented here may lead to the development of such models.

Other features which make it attractive for commercialisation include its long-shelf life, the ability to transport the gels at room temperature, better handling properties compared to Matrigel® (i.e., not requiring it to be kept on ice to prevent premature gelation during the set-up of an experiment), having multiple options for customisation of its stiffness and

composition, and its amenability to typical end-point experiments using only reagents and equipment that end users likely already have access to.

4.7.4 Obstacles and challenges

Several obstacles and challenges were encountered throughout the course of this project which had to be overcome. Many of these were caused by the COVID19 pandemic and its knock-on effects. The biggest challenge was how to adapt after returning from lockdown, to make the best use of the limited time now available and achieve as many of the original objectives as possible. Ongoing supply chain issues also meant that many protocols also had to be adapted, to make the best use of what limited resources were available. However, this also presented the opportunity to learn how to conduct research in a more economically and environmentally conscious way.

Another challenge was learning how to conduct research in a more isolated way. Due to the new safety measures that were put in place post-lockdown, including social distancing and building capacity limits, experiments often had to be conducted where there was no immediate help or advice available. This meant that these experiments had to be more thoughtfully planned out and executed.

The lack of in-person conferences and other similar events during this period also had an impact. These are often ideal opportunities to showcase ongoing research, to network, and identify opportunities for future collaborations. Many virtual conferences were held during this time, which provided some of the same opportunities, but were no replacement for the real thing. However, because these were often free to attend or heavily discounted, many more could be attended for the same cost. Additionally, learning how to effectively present research in a virtual format is perhaps going to be a valuable skill post-pandemic, with many virtual conferences and events still being made available.

Despite the frustrations these obstacles and challenges presented, they also presented opportunity to learn and grown as an independent researcher. The ability to conduct more economically and environmentally conscious research, to more thoughtfully plan out and conduct experiments, to be able to work independently, and to communicate research in a variety of formats are all useful skills to have acquired for a future career in science.

4.7.3 Concluding remarks

The work presented in this report hopes to provide another steppingstone towards the development of a fully synthetic, customisable *in vitro* model platform that can accurately recapitulate the complexities of *in vivo* tissues in a physiologically- and human-relevant way, without the need for animal-derived material. These types of models will hopefully provide future researchers a better way to model development and disease for the purpose of drug discovery and investigative research. It is also hoped that this research may also contribute towards the reduction, and eventual replacement, of animals used in research.

References

1.   Fang, Y. and R.M. Eglen, *Three-Dimensional Cell Cultures in Drug Discovery and Development.* SLAS Discov, 2017. **22**(5): p. 456-472.
2.   Hickman, J.A., et al., *Three-dimensional models of cancer for pharmacology and cancer cell biology: capturing tumor complexity in vitro/ex vivo.* Biotechnol J, 2014. **9**(9): p. 1115-28.
3.   DiMasi, J.A. and H.G. Grabowski, *Economics of new oncology drug development.* Journal of Clinical Oncology, 2007. **25**(2): p. 209-216.
4.   Ocana, A., et al., *Preclinical development of molecular-targeted agents for cancer.* Nature reviews Clinical oncology, 2011. **8**(4): p. 200.
5.   Madhusoodanan, J., *Matrix mimics shape cell studies.* Nature, 2019. **566**(7745): p. 563-566.
6.   Cruz-Acuña, R. and A.J. García, *Synthetic hydrogels mimicking basement membrane matrices to promote cell-matrix interactions.* Matrix Biology, 2017. **57**: p. 324-333.
7.   Kleinman, H.K. and G.R. Martin. *Matrigel: basement membrane matrix with biological activity*. in *Seminars in cancer biology*. 2005. Elsevier.
8.   Buxton, P., et al., *Dense collagen matrix accelerates osteogenic differentiation and rescues the apoptotic response to MMP inhibition.* Bone, 2008. **43**(2): p. 377-385.
9.   Levental, K.R., et al., *Matrix crosslinking forces tumor progression by enhancing integrin signaling.* Cell, 2009. **139**(5): p. 891-906.
10.   Miao, Z., et al., *Collagen, agarose, alginate, and Matrigel hydrogels as cell substrates for culture of chondrocytes in vitro: A comparative study.* Journal of cellular biochemistry, 2018. **119**(10): p. 7924-7933.
11.   Gillette, K.M., K. Forbes, and I. Sehgal, *Detection of matrix metalloproteinases (MMP), tissue inhibitor of metalloproteinase-2, urokinase and plasminogen activator inhibitor-1 within matrigel and growth factor-reduced matrigel basement membrane.* Tumori Journal, 2003. **89**(4): p. 421-425.
12.   Vukicevic, S., et al., *Identification of multiple active growth factors in basement membrane Matrigel suggests caution in interpretation of cellular activity related to extracellular matrix components.* Experimental cell research, 1992. **202**(1): p. 1-8.
13.   Peterson, N.C., *From bench to cageside: risk assessment for rodent pathogen contamination of cells and biologics.* ILAR journal, 2008. **49**(3): p. 310-315.
14.   Liu, H., et al., *Removal of lactate dehydrogenase-elevating virus from human-in-mouse breast tumor xenografts by cell-sorting.* Journal of virological methods, 2011. **173**(2): p. 266-270.
15.   Riley, V., et al., *The LDH virus: an interfering biological contaminant.* Science, 1978. **200**(4338): p. 124-126.
16.   Aisenbrey, E.A. and W.L. Murphy, *Synthetic alternatives to Matrigel.* Nature Reviews Materials, 2020. **5**(7): p. 539-551.
17.   Caliari, S.R. and J.A. Burdick, *A practical guide to hydrogels for cell culture.* Nature methods, 2016. **13**(5): p. 405-414.
18.   Zustiak, S.P. and J.B. Leach, *Hydrolytically degradable poly (ethylene glycol) hydrogel scaffolds with tunable degradation and mechanical properties.* Biomacromolecules, 2010. **11**(5): p. 1348-1357.
19.   Krsko, P. and M. Libera, *Biointeractive hydrogels.* Materials today, 2005. **8**(12): p. 36-44.
20.   Lutolf, M. and J. Hubbell, *Synthetic biomaterials as instructive extracellular microenvironments for morphogenesis in tissue engineering.* Nature biotechnology, 2005. **23**(1): p. 47-55.

21. Annabi, N., et al., *25th anniversary article: Rational design and applications of hydrogels in regenerative medicine.* Advanced materials, 2014. **26**(1): p. 85-124.

22. Thakuri, P.S., et al., *Biomaterials-Based Approaches to Tumor Spheroid and Organoid Modeling.* Advanced healthcare materials, 2018. **7**(6): p. 1700980.

23. Wolf, M.T., et al., *Naturally derived and synthetic scaffolds for skeletal muscle reconstruction.* Advanced drug delivery reviews, 2015. **84**: p. 208-221.

24. Zhu, J., *Bioactive modification of poly (ethylene glycol) hydrogels for tissue engineering.* Biomaterials, 2010. **31**(17): p. 4639-4656.

25. Lee, H.J., et al., *Collagen mimetic peptide-conjugated photopolymerizable PEG hydrogel.* Biomaterials, 2006. **27**(30): p. 5268-5276.

26. Gjorevski, N., et al., *Designer matrices for intestinal stem cell and organoid culture.* Nature, 2016. **539**(7630): p. 560-564.

27. Gjorevski, N. and M.P. Lutolf, *Synthesis and characterization of well-defined hydrogel matrices and their application to intestinal stem cell and organoid culture.* Nature protocols, 2017. **12**(11): p. 2263-2274.

28. Ehrbar, M., et al., *Biomolecular hydrogels formed and degraded via site-specific enzymatic reactions.* Biomacromolecules, 2007. **8**(10): p. 3000-3007.

29. Zisch, A.H., M.P. Lutolf, and J.A. Hubbell, *Biopolymeric delivery matrices for angiogenic growth factors.* Cardiovascular pathology, 2003. **12**(6): p. 295-310.

30. Licht, C., et al., *Synthetic 3D PEG-anisogel tailored with fibronectin fragments induce aligned nerve extension.* Biomacromolecules, 2019. **20**(11): p. 4075-4087.

31. Kozlowski, M.T., C.J. Crook, and H.T. Ku, *Towards organoid culture without Matrigel.* Communications biology, 2021. **4**(1): p. 1-15.

32. Sankar, S., et al., *Clinical use of the self-assembling peptide RADA16: a review of current and future trends in biomedicine.* Frontiers in Bioengineering and Biotechnology, 2021. **9**: p. 465.

33. Ashworth, J.C., et al., *Peptide gels of fully-defined composition and mechanics for probing cell-cell and cell-matrix interactions in vitro.* Matrix Biol, 2020. **85-86**: p. 15-33.

34. Ruoslahti, E., *RGD and other recognition sequences for integrins.* Annual review of cell and developmental biology, 1996. **12**(1): p. 697-715.

35. Ozbek, S., et al., *The evolution of extracellular matrix.* Mol Biol Cell, 2010. **21**(24): p. 4300-5.

36. Hynes, R.O., *The extracellular matrix: not just pretty fibrils.* Science, 2009. **326**(5957): p. 1216-1219.

37. Lu, P., V.M. Weaver, and Z. Werb, *The extracellular matrix: a dynamic niche in cancer progression.* J Cell Biol, 2012. **196**(4): p. 395-406.

38. Egeblad, M., M.G. Rasch, and V.M. Weaver, *Dynamic interplay between the collagen scaffold and tumor evolution.* Current opinion in cell biology, 2010. **22**(5): p. 697-706.

39. Harburger, D.S. and D.A. Calderwood, *Integrin signalling at a glance.* Journal of cell science, 2009. **122**(2): p. 159-163.

40. Humphries, J.D., A. Byron, and M.J. Humphries, *Integrin ligands at a glance.* Journal of cell science, 2006. **119**(19): p. 3901-3903.

41. Leitinger, B. and E. Hohenester, *Mammalian collagen receptors.* Matrix Biology, 2007. **26**(3): p. 146-155.

42. Xian, X., S. Gopal, and J.R. Couchman, *Syndecans as receptors and organizers of the extracellular matrix.* Cell and tissue research, 2010. **339**(1): p. 31-46.

43. Page-McCaw, A., A.J. Ewald, and Z. Werb, *Matrix metalloproteinases and the regulation of tissue remodelling.* Nat Rev Mol Cell Biol, 2007. **8**(3): p. 221-33.

44. Järveläinen, H., et al., *Extracellular matrix molecules: potential targets in pharmacotherapy.* Pharmacological reviews, 2009. **61**(2): p. 198-223.

45. Schaefer, L. and R.M. Schaefer, *Proteoglycans: from structural compounds to signaling molecules.* Cell and tissue research, 2010. **339**(1): p. 237-246.

46. Alberts, B., et al., *Molecular biology of the cell.* Scandinavian Journal of Rheumatology, 2003. **32**(2): p. 125-125.

47. Myllyharju, J. and K.I. Kivirikko, *Collagens, modifying enzymes and their mutations in humans, flies and worms.* TRENDS in Genetics, 2004. **20**(1): p. 33-43.

48. Gordon, M.K. and R.A. Hahn, *Collagens.* Cell and tissue research, 2010. **339**(1): p. 247-257.

49. De Wever, O., et al., *Stromal myofibroblasts are drivers of invasive cancer growth.* International journal of cancer, 2008. **123**(10): p. 2229-2238.

50. Robins, S., *Biochemistry and functional significance of collagen cross-linking.* Biochemical Society Transactions, 2007. **35**(5): p. 849-852.

51. Wise, S.G. and A.S. Weiss, *Tropoelastin.* The international journal of biochemistry & cell biology, 2009. **41**(3): p. 494-497.

52. Kielty, C.M., M.J. Sherratt, and C.A. Shuttleworth, *Elastic fibres.* Journal of cell science, 2002. **115**(14): p. 2817-2828.

53. Lucero, H. and H. Kagan, *Lysyl oxidase: an oxidative enzyme and effector of cell function.* Cellular and Molecular Life Sciences CMLS, 2006. **63**(19): p. 2304-2316.

54. Gheduzzi, D., et al., *Heparan sulphate interacts with tropoelastin, with some tropoelastin peptides and is present in human dermis elastic fibers.* Matrix Biology, 2005. **24**(1): p. 15-25.

55. Smith, M.L., et al., *Force-induced unfolding of fibronectin in the extracellular matrix of living cells.* PLoS biology, 2007. **5**(10): p. e268.

56. Pankov, R. and K.M. Yamada, *Fibronectin at a glance.* Journal of cell science, 2002. **115**(20): p. 3861-3863.

57. Iozzo, R.V. and A.D. Murdoch, *Proteoglycans of the extracellular environment: clues from the gene and protein side offer novel perspectives in molecular diversity and function.* The FASEB Journal, 1996. **10**(5): p. 598-614.

58. Kreuger, J., et al., *Interactions between heparan sulfate and proteins: the concept of specificity.* The Journal of cell biology, 2006. **174**(3): p. 323.

59. Kirkpatrick, C.A. and S.B. Selleck, *Heparan sulfate proteoglycans at a glance.* Journal of cell science, 2007. **120**(11): p. 1829-1832.

60. Nam, E.J. and P.W. Park, *Shedding of cell membrane-bound proteoglycans.* Proteoglycans, 2012: p. 291-305.

61. Esko, J.D. and S.B. Selleck, *Order out of chaos: assembly of ligand binding sites in heparan sulfate.* Annual review of biochemistry, 2002. **71**(1): p. 435-471.

62. Kramer, K.L. and H.J. Yost, *Heparan sulfate core proteins in cell-cell signaling.* Annual review of genetics, 2003. **37**(1): p. 461-484.

63. Bülow, H.E. and O. Hobert, *The molecular diversity of glycosaminoglycans shapes animal development.* Annu. Rev. Cell Dev. Biol., 2006. **22**: p. 375-407.

64. Bishop, J.R., M. Schuksz, and J.D. Esko, *Heparan sulphate proteoglycans fine-tune mammalian physiology.* Nature, 2007. **446**(7139): p. 1030-1037.

65. Kjellen, L., *Glucosaminyl N-deacetylase/N-sulphotransferases in heparan sulphate biosynthesis and biology.* Biochemical Society Transactions, 2003. **31**(2): p. 340-342.

66. Drickamer, K., et al. *New insights into heparan sulphate biosynthesis from the study of mutant mice.* in *Biochemical Society Symposia.* 2002. Portland Press.

67. Wilson, V.A., J.T. Gallagher, and C.L. Merry, *Heparan sulfate 2-O-sulfotransferase (Hs2st) and mouse development.* Glycoconjugate journal, 2002. **19**(4): p. 347-354.

68. Johnson, C.E., et al., *Essential alterations of heparan sulfate during the differentiation of embryonic stem cells to Sox1-enhanced green fluorescent protein-expressing neural progenitor cells.* Stem Cells, 2007. **25**(8): p. 1913-23.

69. Gallagher, J.T. and J.E. Turnbull, *Heparan sulphate in the binding and activation of basic fibroblast growth factor.* Glycobiology, 1992. **2**(6): p. 523-528.

70. Turnbull, J.E., et al., *Identification of the basic fibroblast growth factor binding sequence in fibroblast heparan sulfate.* Journal of Biological Chemistry, 1992. **267**(15): p. 10337-10341.

71. Pye, D.A., et al., *Heparan sulfate oligosaccharides require 6-O-sulfation for promotion of basic fibroblast growth factor mitogenic activity.* Journal of Biological Chemistry, 1998. **273**(36): p. 22936-22942.

72. Rapraeger, A.C., A. Krufka, and B.B. Olwin, *Requirement of heparan sulfate for bFGF-mediated fibroblast growth and myoblast differentiation.* Science, 1991. **252**(5013): p. 1705-1708.

73. Zehe, C., et al., *Cell-surface heparan sulfate proteoglycans are essential components of the unconventional export machinery of FGF-2.* Proceedings of the National Academy of Sciences, 2006. **103**(42): p. 15479-15484.

74. Ashikari-Hada, S., et al., *Specific inhibition of FGF-2 signaling with 2-O-sulfated octasaccharides of heparan sulfate.* Glycobiology, 2009. **19**(6): p. 644-654.

75. Yayon, A., et al., *Cell surface, heparin-like molecules are required for binding of basic fibroblast growth factor to its high affinity receptor.* Cell, 1991. **64**(4): p. 841-848.

76. Pickford, C.E., et al., *Specific glycosaminoglycans modulate neural specification of mouse embryonic stem cells.* Stem Cells, 2011. **29**(4): p. 629-40.

77. Bornemann, D.J., et al., *Abrogation of heparan sulfate synthesis in Drosophila disrupts the Wingless, Hedgehog and Decapentaplegic signaling pathways.* 2004.

78. Han, C., et al., *Distinct and collaborative roles of Drosophila EXT family proteins in morphogen signalling and gradient formation.* 2004.

79. Takei, Y., et al., *Three Drosophila EXT genes shape morphogen gradients through synthesis of heparan sulfate proteoglycans.* 2004.

80. Melrose, J., et al., *Chondroitin sulphate and heparan sulphate sulphation motifs and their proteoglycans are involved in articular cartilage formation during human foetal knee joint development.* Histochemistry and cell biology, 2012. **138**(3): p. 461-475.

81. DuFort, C.C., M.J. Paszek, and V.M. Weaver, *Balancing forces: architectural control of mechanotransduction.* Nat Rev Mol Cell Biol, 2011. **12**(5): p. 308-19.

82. Sawada, Y., et al., *Force sensing by mechanical extension of the Src family kinase substrate p130Cas.* Cell, 2006. **127**(5): p. 1015-26.

83. del Rio, A., et al., *Stretching single talin rod molecules activates vinculin binding.* Science, 2009. **323**(5914): p. 638-41.

84. Discher, D.E., D.J. Mooney, and P.W. Zandstra, *Growth factors, matrices, and forces combine and control stem cells.* Science, 2009. **324**(5935): p. 1673-1677.

85. Wang, N., J.D. Tytell, and D.E. Ingber, *Mechanotransduction at a distance: mechanically coupling the extracellular matrix with the nucleus.* Nature reviews Molecular cell biology, 2009. **10**(1): p. 75-82.

86. Clark, R.A., *Fibrin and wound healing.* Annals of the New York Academy of Sciences, 2001. **936**: p. 355-367.

87. Schultz, G.S. and A. Wysocki, *Interactions between extracellular matrix and growth factors in wound healing.* Wound repair and regeneration, 2009. **17**(2): p. 153-162.

88. Kisseleva, T. and D.A. Brenner, *Mechanisms of fibrogenesis.* Experimental biology and medicine, 2008. **233**(2): p. 109-122.

89.   Acerbi, I., et al., *Human breast cancer invasion and aggression correlates with ECM stiffening and immune cell infiltration.* Integrative Biology, 2015. **7**(10): p. 1120-1134.

90.   Naba, A., et al., *The matrisome: in silico definition and in vivo characterization by proteomics of normal and tumor extracellular matrices.* Mol Cell Proteomics, 2012. **11**(4): p. M111 014647.

91.   Lu, P., et al., *Extracellular matrix degradation and remodeling in development and disease.* Cold Spring Harbor perspectives in biology, 2011. **3**(12): p. a005058.

92.   Desmouliere, A., C. Guyot, and G. Gabbiani, *The stroma reaction myofibroblast: a key player in the control of tumor cell behavior.* International Journal of Developmental Biology, 2004. **48**(5-6): p. 509-517.

93.   Cook, D., et al., *Lessons learned from the fate of AstraZeneca's drug pipeline: a five-dimensional framework.* Nature reviews Drug discovery, 2014. **13**(6): p. 419-431.

94.   Hay, M., et al., *Clinical development success rates for investigational drugs.* Nature biotechnology, 2014. **32**(1): p. 40-51.

95.   Arrowsmith, J., *Phase II failures: 2008-2010.* Nature reviews Drug discovery, 2011. **10**(5).

96.   Baker, B.M. and C.S. Chen, *Deconstructing the third dimension–how 3D culture microenvironments alter cellular cues.* Journal of cell science, 2012. **125**(13): p. 3015-3024.

97.   Cukierman, E., et al., *Taking cell-matrix adhesions to the third dimension.* Science, 2001. **294**(5547): p. 1708-12.

98.   Kelm, J.M., et al., *Method for generation of homogeneous multicellular tumor spheroids applicable to a wide variety of cell types.* Biotechnology and bioengineering, 2003. **83**(2): p. 173-180.

99.   Friedrich, J., et al., *Spheroid-based drug screen: considerations and practical approach.* Nature protocols, 2009. **4**(3): p. 309-324.

100.   Myungjin Lee, J., et al., *A three-dimensional microenvironment alters protein expression and chemosensitivity of epithelial ovarian cancer cells in vitro.* Laboratory investigation, 2013. **93**(5): p. 528-542.

101.   Vinci, M., et al., *Advances in establishment and analysis of three-dimensional tumor spheroid-based functional assays for target validation and drug evaluation.* BMC biology, 2012. **10**(1): p. 1-21.

102.   Song, K.-D., et al., *Three-dimensional expansion: in suspension culture of SD rat's osteoblasts in a rotating wall vessel bioreactor.* Biomedical and Environmental Sciences, 2007. **20**(2): p. 91.

103.   Frankel, A., R. Buckman, and R.S. Kerbel, *Abrogation of taxol-induced G2-M arrest and apoptosis in human ovarian cancer cells grown as multicellular tumor spheroids.* Cancer research, 1997. **57**(12): p. 2388-2393.

104.   Kerr, D., et al., *The effect of adriamycin and 4'-deoxydoxorubicin on cell survival of human lung tumour cells grown in monolayer and as spheroids.* British journal of cancer, 1986. **54**(3): p. 423-429.

105.   Kobayashi, H., et al., *Acquired multicellular-mediated resistance to alkylating agents in cancer.* Proceedings of the National Academy of Sciences, 1993. **90**(8): p. 3294-3298.

106.   Longati, P., et al., *3D pancreatic carcinoma spheroids induce a matrix-rich, chemoresistant phenotype offering a better model for drug testing.* BMC cancer, 2013. **13**(1): p. 1-13.

107.   Tung, Y.-C., et al., *High-throughput 3D spheroid culture and drug testing using a 384 hanging drop array.* Analyst, 2011. **136**(3): p. 473-478.

108. Tunggal, J.K., et al., *Penetration of anticancer drugs through solid tissue: a factor that limits the effectiveness of chemotherapy for solid tumors.* Clinical cancer research, 1999. **5**(6): p. 1583-1586.

109. Wenzel, C., et al., *3D high-content screening for the identification of compounds that target cells in dormant tumor spheroid regions.* Experimental cell research, 2014. **323**(1): p. 131-143.

110. Green, S.K., et al., *Antiadhesive antibodies targeting E-cadherin sensitize multicellular tumor spheroids to chemotherapy in vitro.* Molecular cancer therapeutics, 2004. **3**(2): p. 149-159.

111. Song, C.W., R. Griffin, and H.J. Park, *Influence of tumor pH on therapeutic response*, in *Cancer drug resistance*. 2006, Springer. p. 21-42.

112. Khramtsov, V.V. and R.J. Gillies, *Janus-faced tumor microenvironment and redox.* Antioxidants & redox signaling, 2014. **21**(5): p. 723-729.

113. Zeng, W., et al., *Hypoxia and hypoxia inducible factors in tumor metabolism.* Cancer letters, 2015. **356**(2): p. 263-267.

114. Getzenberg, R.H. and D.S. Coffey, *Changing the energy habitat of the cancer cell in order to impact therapeutic resistance.* Molecular pharmaceutics, 2011. **8**(6): p. 2089-2093.

115. Russell, W.M.S. and R.L. Burch, *The principles of humane experimental technique*. 1959: Methuen.

116. Olson, H., et al., *Concordance of the toxicity of pharmaceuticals in humans and in animals.* Regulatory Toxicology and Pharmacology, 2000. **32**(1): p. 56-67.

117. Collins, F.S. and L.A. Tabak, *Policy: NIH plans to enhance reproducibility.* Nature, 2014. **505**(7485): p. 612-613.

118. Denayer, T., T. Stöhr, and M. Van Roy, *Animal models in translational medicine: Validation and prediction.* New Horizons in Translational Medicine, 2014. **2**(1): p. 5-11.

119. Meigs, L., et al., *Animal testing and its alternatives–The most important omics is economics.* ALTEX-Alternatives to animal experimentation, 2018. **35**(3): p. 275-305.

120. Doke, S.K. and S.C. Dhawale, *Alternatives to animal testing: A review.* Saudi Pharmaceutical Journal, 2015. **23**(3): p. 223-229.

121. Bédard, P., et al., *Innovative human three-dimensional tissue-engineered models as an alternative to animal testing.* Bioengineering, 2020. **7**(3): p. 115.

122. Takahashi, K., et al., *Human induced pluripotent stem cells on autologous feeders.* PloS one, 2009. **4**(12): p. e8067.

123. Yu, J., et al., *Induced pluripotent stem cell lines derived from human somatic cells.* science, 2007. **318**(5858): p. 1917-1920.

124. Benam, K.H., et al., *Engineered in vitro disease models.* Annual Review of Pathology: Mechanisms of Disease, 2015. **10**: p. 195-262.

125. Nishihara, S., *Glycans in stem cell regulation: from Drosophila tissue stem cells to mammalian pluripotent stem cells.* FEBS letters, 2018. **592**(23): p. 3773-3790.

126. Evans, M.J. and M.H. Kaufman, *Establishment in culture of pluripotential cells from mouse embryos.* nature, 1981. **292**(5819): p. 154-156.

127. Martin, G.R., *Isolation of a pluripotent cell line from early mouse embryos cultured in medium conditioned by teratocarcinoma stem cells.* Proceedings of the National Academy of Sciences, 1981. **78**(12): p. 7634-7638.

128. Thomson, J.A., et al., *Embryonic stem cell lines derived from human blastocysts.* science, 1998. **282**(5391): p. 1145-1147.

129. Beltrami, G., et al., *Hereditary multiple exostoses: a review of clinical appearance and metabolic pattern.* Clinical Cases in Mineral and Bone Metabolism, 2016. **13**(2): p. 110.

130. Lind, T., et al., *The putative tumor suppressors EXT1 and EXT2 are glycosyltransferases required for the biosynthesis of heparan sulfate.* Journal of Biological Chemistry, 1998. **273**(41): p. 26265-26268.

131. McCormick, C., et al., *The putative tumour suppressor EXT1 alters the expression of cell-surface heparan sulfate.* Nature genetics, 1998. **19**(2): p. 158-161.

132. Jones, K.B., M. Pacifici, and M.J. Hilton, *Multiple hereditary exostoses (MHE): elucidating the pathogenesis of a rare skeletal disorder through interdisciplinary research.* Connective tissue research, 2014. **55**(2): p. 80-88.

133. Scherer, W.F., J.T. Syverton, and G.O. Gey, *Studies on the propagation in vitro of poliomyelitis viruses: IV. Viral multiplication in a stable strain of human malignant epithelial cells (strain HeLa) derived from an epidermoid carcinoma of the cervix.* The Journal of experimental medicine, 1953. **97**(5): p. 695-710.

134. Gillet, J.-P., S. Varma, and M.M. Gottesman, *The clinical relevance of cancer cell lines.* Journal of the National Cancer Institute, 2013. **105**(7): p. 452-458.

135. Gottfried, E., et al., *Brave little world: spheroids as an in vitro model to study tumor-immune-cell interactions.* Cell Cycle, 2006. **5**(7): p. 691-695.

136. Hauptmann, S., et al., *Macrophages and multicellular tumor spheroids in co-culture: a three-dimensional model to study tumor-host interactions. Evidence for macrophage-mediated tumor cell proliferation and migration.* The American journal of pathology, 1993. **143**(5): p. 1406.

137. Kunz-Schughart, L.A., et al., *Potential of fibroblasts to regulate the formation of three-dimensional vessel-like structures from endothelial cells in vitro.* American Journal of Physiology-Cell Physiology, 2006. **290**(5): p. C1385-C1398.

138. Kunz-Schughart, L.A., et al., *A heterologous 3-D coculture model of breast tumor cells and fibroblasts to study tumor-associated fibroblast differentiation.* Experimental cell research, 2001. **266**(1): p. 74-86.

139. Seidl, P., et al., *Three-dimensional fibroblast–tumor cell interaction causes downregulation of RACK1 mRNA expression in breast cancer cells in vitro.* International journal of cancer, 2002. **102**(2): p. 129-136.

140. Brouty-Boyé, D. and V. Magnien, *Myofibroblast and concurrent ED-B fibronectin phenotype in human stromal cells cultured from non-malignant and malignant breast tissue.* European Journal of Cancer, 1994. **30**(1): p. 66-73.

141. Costa, E.C., et al., *Optimization of liquid overlay technique to formulate heterogenic 3D co-cultures models.* Biotechnology and bioengineering, 2014. **111**(8): p. 1672-1685.

142. Amann, A., et al., *Development of an innovative 3D cell culture system to study tumour-stroma interactions in non-small cell lung cancer cells.* PloS one, 2014. **9**(3): p. e92511.

143. Timmins, N.E. and L.K. Nielsen, *Generation of multicellular tumor spheroids by the hanging-drop method*, in *Tissue engineering*. 2007, Springer. p. 141-151.

144. Massai, D., et al., *A versatile bioreactor for dynamic suspension cell culture. Application to the culture of cancer cell spheroids.* PloS one, 2016. **11**(5): p. e0154610.

145. Yoshii, Y., et al., *The use of nanoimprinted scaffolds as 3D culture models to facilitate spontaneous tumor cell migration and well-regulated spheroid formation.* Biomaterials, 2011. **32**(26): p. 6052-6058.

146. Doublier, S., et al., *HIF-1 activation induces doxorubicin resistance in MCF7 3-D spheroids via P-glycoprotein expression: a potential model of the chemo-resistance of invasive micropapillary carcinoma of the breast.* BMC Cancer, 2012. **12**(1): p. 4.

147. Hamer, P.D.W., et al., *The genomic profile of human malignant glioma is altered early in primary cell culture and preserved in spheroids.* Oncogene, 2008. **27**(14): p. 2091-2096.

148. Huch, M. and B.-K. Koo, *Modeling mouse and human development using organoid cultures.* Development, 2015. **142**(18): p. 3113-3125.

149. Rossi, G., A. Manfrin, and M.P. Lutolf, *Progress and potential in organoid research.* Nature Reviews Genetics, 2018. **19**(11): p. 671-687.

150. Homan, K.A., et al., *Flow-enhanced vascularization and maturation of kidney organoids in vitro.* Nature methods, 2019. **16**(3): p. 255-262.

151. Veenvliet, J.V., et al., *Sculpting with stem cells: how models of embryo development take shape.* Development, 2021. **148**(24): p. dev192914.

152. van den Brink, S.C. and A. van Oudenaarden, *3D gastruloids: a novel frontier in stem cell-based in vitro modeling of mammalian gastrulation.* Trends in cell biology, 2021. **31**(9): p. 747-759.

153. Van den Brink, S.C., et al., *Symmetry breaking, germ layer specification and axial organisation in aggregates of mouse embryonic stem cells.* Development, 2014. **141**(22): p. 4231-4242.

154. Baillie-Johnson, P., et al., *Generation of aggregates of mouse embryonic stem cells that show symmetry breaking, polarization and emergent collective behaviour in vitro.* JoVE (Journal of Visualized Experiments), 2015(105): p. e53252.

155. Girgin, M.U., et al., *Gastruloids generated without exogenous Wnt activation develop anterior neural tissues.* Stem cell reports, 2021. **16**(5): p. 1143-1155.

156. van den Brink, S.C., et al., *Single-cell and spatial transcriptomics reveal somitogenesis in gastruloids.* Nature, 2020. **582**(7812): p. 405-409.

157. Veenvliet, J.V., et al., *Mouse embryonic stem cells self-organize into trunk-like structures with neural tube and somites.* Science, 2020. **370**(6522): p. eaba4937.

158. Vianello, S. and M.P. Lutolf, *In vitro endoderm emergence and self-organisation in the absence of extraembryonic tissues and embryonic architecture.* BioRxiv, 2021: p. 2020.06. 07.138883.

159. Rossi, G., et al., *Capturing cardiogenesis in gastruloids.* Cell stem cell, 2021. **28**(2): p. 230-240. e6.

160. Moris, N., et al., *An in vitro model of early anteroposterior organization during human development.* Nature, 2020. **582**(7812): p. 410-415.

161. Forsberg, E. and L. Kjellén, *Heparan sulfate: lessons from knockout mice.* The Journal of clinical investigation, 2001. **108**(2): p. 175-180.

162. Rossant, J. and P.P. Tam, *Blastocyst lineage formation, early embryonic asymmetries and axis patterning in the mouse.* 2009.

163. Khademhosseini, A., et al., *Microscale technologies for tissue engineering and biology.* Proceedings of the National Academy of Sciences, 2006. **103**(8): p. 2480-2487.

164. Whitesides, G.M., *The origins and the future of microfluidics.* nature, 2006. **442**(7101): p. 368-373.

165. Zhang, Y.S., et al., *From cardiac tissue engineering to heart-on-a-chip: beating challenges.* Biomedical Materials, 2015. **10**(3): p. 034006.

166. Huh, D., et al., *Reconstituting organ-level lung functions on a chip.* Science, 2010. **328**(5986): p. 1662-1668.

167. Li, L., M. Fukunaga-Kalabis, and M. Herlyn, *The three-dimensional human skin reconstruct model: a tool to study normal skin and melanoma progression.* JoVE (Journal of Visualized Experiments), 2011(54): p. e2937.

168. Gao, D., et al., *Characterization of drug permeability in Caco-2 monolayers by mass spectrometry on a membrane-based microfluidic device.* Lab on a chip, 2013. **13**(5): p. 978-985.

169. Birgersdotter, A., R. Sandberg, and I. Ernberg. *Gene expression perturbation in vitro—a growing case for three-dimensional (3D) culture systems*. in *Seminars in cancer biology*. 2005. Elsevier.

170. Benton, G., et al., *Multiple uses of basement membrane-like matrix (BME/Matrigel) in vitro and in vivo with cancer cells.* International journal of cancer, 2011. **128**(8): p. 1751-1757.

171. Hughes, C.S., L.M. Postovit, and G.A. Lajoie, *Matrigel: a complex protein mixture required for optimal growth of cell culture.* Proteomics, 2010. **10**(9): p. 1886-1890.

172. Talbot, N.C. and T.J. Caperna, *Proteome array identification of bioactive soluble proteins/peptides in Matrigel: relevance to stem cell responses.* Cytotechnology, 2015. **67**(5): p. 873-883.

173. Hansen, K.C., et al., *An in-solution ultrasonication-assisted digestion method for improved extracellular matrix proteome coverage.* Molecular & Cellular Proteomics, 2009. **8**(7): p. 1648-1657.

174. Zaman, M.H., et al., *Migration of tumor cells in 3D matrices is governed by matrix stiffness along with cell-matrix adhesion and proteolysis.* Proceedings of the National Academy of Sciences, 2006. **103**(29): p. 10889-10894.

175. Semler, E.J., C.S. Ranucci, and P.V. Moghe, *Mechanochemical manipulation of hepatocyte aggregation can selectively induce or repress liver-specific function.* Biotechnology and bioengineering, 2000. **69**(4): p. 359-369.

176. Kane, K.I., et al., *Determination of the rheological properties of Matrigel for optimum seeding conditions in microfluidic cell cultures.* AIP Advances, 2018. **8**(12): p. 125332.

177. Alcaraz, J., et al., *Laminin and biomimetic extracellular elasticity enhance functional differentiation in mammary epithelia.* The EMBO journal, 2008. **27**(21): p. 2829-2838.

178. Reed, J., et al., *In situ mechanical interferometry of matrigel films.* Langmuir, 2009. **25**(1): p. 36-39.

179. Waterston, R.H. and L. Pachter, *Initial sequencing and comparative analysis of the mouse genome.* Nature, 2002. **420**(6915): p. 520-562.

180. Guénet, J.L., *The mouse genome.* Genome research, 2005. **15**(12): p. 1729-1740.

181. Harada, A., et al., *Essential involvement of interleukin-8 (IL-8) in acute inflammation.* Journal of leukocyte biology, 1994. **56**(5): p. 559-564.

182. Friess, W., *Collagen–biomaterial for drug delivery.* European journal of pharmaceutics and biopharmaceutics, 1998. **45**(2): p. 113-136.

183. Gudjonsson, T., et al., *Normal and tumor-derived myoepithelial cells differ in their ability to interact with luminal breast epithelial cells for polarity and basement membrane deposition.* Journal of cell science, 2002. **115**(1): p. 39-50.

184. Fairbanks, B.D., et al., *A versatile synthetic extracellular matrix mimic via thiol-norbornene photopolymerization.* Advanced materials, 2009. **21**(48): p. 5005-5010.

185. Nair, D.P., et al., *The thiol-Michael addition click reaction: a powerful and widely used tool in materials chemistry.* Chemistry of Materials, 2014. **26**(1): p. 724-744.

186. Ranga, A., et al., *Hyaluronic acid hydrogels formed in situ by transglutaminase-catalyzed reaction.* Biomacromolecules, 2016. **17**(5): p. 1553-1560.

187. Li, S., *Hydrolytic degradation characteristics of aliphatic polyesters derived from lactic and glycolic acids.* Journal of Biomedical Materials Research: An Official Journal of The Society for Biomaterials, The Japanese Society for Biomaterials, and The Australian Society for Biomaterials, 1999. **48**(3): p. 342-353.

188.   Grizzi, I., et al., *Hydrolytic degradation of devices based on poly (DL-lactic acid) size-dependence.* Biomaterials, 1995. **16**(4): p. 305-311.
189.   Athanasiou, K.A., G.G. Niederauer, and C.M. Agrawal, *Sterilization, toxicity, biocompatibility and clinical applications of polylactic acid/polyglycolic acid copolymers.* Biomaterials, 1996. **17**(2): p. 93-102.
190.   Peters, M.C., P.J. Polverini, and D.J. Mooney, *Engineering vascular networks in porous polymer matrices.* Journal of Biomedical Materials Research: An Official Journal of The Society for Biomaterials, The Japanese Society for Biomaterials, and The Australian Society for Biomaterials and the Korean Society for Biomaterials, 2002. **60**(4): p. 668-678.
191.   Smith, M.K., et al., *Locally enhanced angiogenesis promotes transplanted cell survival.* Tissue engineering, 2004. **10**(1-2): p. 63-71.
192.   Lam, C.X., et al., *Dynamics of in vitro polymer degradation of polycaprolactone-based scaffolds: accelerated versus simulated physiological conditions.* Biomedical materials, 2008. **3**(3): p. 034108.
193.   Lam, C.X., et al., *Evaluation of polycaprolactone scaffold degradation for 6 months in vitro and in vivo.* Journal of Biomedical Materials Research Part A: An Official Journal of The Society for Biomaterials, The Japanese Society for Biomaterials, and The Australian Society for Biomaterials and the Korean Society for Biomaterials, 2009. **90**(3): p. 906-919.
194.   Guelcher, S.A., *Biodegradable polyurethanes: synthesis and applications in regenerative medicine.* Tissue Engineering Part B: Reviews, 2008. **14**(1): p. 3-17.
195.   Lin, D.-T., T.-H. Young, and Y. Fang, *Studies on the effect of surface properties on the biocompatibility of polyurethane membranes.* Biomaterials, 2001. **22**(12): p. 1521-1529.
196.   Edwards-Gayle, C.J. and I.W. Hamley, *Self-assembly of bioactive peptides, peptide conjugates, and peptide mimetic materials.* Organic & biomolecular chemistry, 2017. **15**(28): p. 5867-5876.
197.   Lee, S., et al., *Self-assembling peptides and their application in the treatment of diseases.* International journal of molecular sciences, 2019. **20**(23): p. 5850.
198.   Zhang, S., et al., *Spontaneous assembly of a self-complementary oligopeptide to form a stable macroscopic membrane.* Proceedings of the National Academy of Sciences, 1993. **90**(8): p. 3334-3338.
199.   Kisiday, J., et al., *Self-assembling peptide hydrogel fosters chondrocyte extracellular matrix production and cell division: implications for cartilage tissue repair.* Proceedings of the National Academy of Sciences, 2002. **99**(15): p. 9996-10001.
200.   Kretsinger, J.K., et al., *Cytocompatibility of self-assembled β-hairpin peptide hydrogel surfaces.* Biomaterials, 2005. **26**(25): p. 5177-5186.
201.   Holmes, T.C., et al., *Extensive neurite outgrowth and active synapse formation on self-assembling peptide scaffolds.* Proceedings of the National Academy of Sciences, 2000. **97**(12): p. 6728-6733.
202.   Mohammed, A., A.F. Miller, and A. Saiani. *3D Networks from Self-Assembling Ionic-Complementary Octa-Peptides*. in *Macromolecular Symposia*. 2007. Wiley Online Library.
203.   Song, H., et al., *Three-dimensional culture and clinical drug responses of a highly metastatic human ovarian cancer HO-8910PM cells in nanofibrous microenvironments of three hydrogel biomaterials.* Journal of Nanobiotechnology, 2020. **18**(1): p. 1-19.
204.   Caplan, M.R., et al., *Control of self-assembling oligopeptide matrix formation through systematic variation of amino acid sequence.* Biomaterials, 2002. **23**(1): p. 219-227.

205. Caplan, M.R., et al., *Effects of systematic variation of amino acid sequence on the mechanical properties of a self-assembling, oligopeptide biomaterial.* Journal of Biomaterials Science, Polymer Edition, 2002. **13**(3): p. 225-236.

206. Caplan, M.R., et al., *Self-assembly of a β-sheet protein governed by relief of electrostatic repulsion relative to van der Waals attraction.* Biomacromolecules, 2000. **1**(4): p. 627-631.

207. Paradís-Bas, M., et al., *RADA-16: A Tough Peptide–Strategies for Synthesis and Purification.* European Journal of Organic Chemistry, 2013. **2013**(26): p. 5871-5878.

208. Ding, X., et al., *Synthetic peptide hydrogels as 3D scaffolds for tissue engineering.* Advanced Drug Delivery Reviews, 2020. **160**: p. 78-104.

209. Mujeeb, A., et al., *Self-assembled octapeptide scaffolds for in vitro chondrocyte culture.* Acta biomaterialia, 2013. **9**(1): p. 4609-4617.

210. Castillo Diaz, L.A., et al., *Human osteoblasts within soft peptide hydrogels promote mineralisation in vitro.* Journal of tissue engineering, 2014. **5**: p. 2041731414539344.

211. Castillo Diaz, L.A., et al., *Osteogenic differentiation of human mesenchymal stem cells promotes mineralization within a biodegradable peptide hydrogel.* Journal of tissue engineering, 2016. **7**: p. 2041731416649789.

212. Burgess, K., et al., *Functionalised peptide hydrogel for the delivery of cardiac progenitor cells.* Materials Science and Engineering: C, 2021. **119**: p. 111539.

213. Adamiak, K. and A. Sionkowska, *Current methods of collagen cross-linking.* International Journal of Biological Macromolecules, 2020. **161**: p. 550-560.

214. Arkenberg, M.R., D.M. Moore, and C.C. Lin, *Dynamic control of hydrogel crosslinking via sortase-mediated reversible transpeptidation.* Acta Biomater, 2019. **83**: p. 83-95.

215. Loebel, C., R.L. Mauck, and J.A. Burdick, *Local nascent protein deposition and remodelling guide mesenchymal stromal cell mechanosensing and fate in three-dimensional hydrogels.* Nature materials, 2019. **18**(8): p. 883-891.

216. Muschler, J. and C.H. Streuli, *Cell–matrix interactions in mammary gland development and breast cancer.* Cold Spring Harbor perspectives in biology, 2010. **2**(10): p. a003202.

217. Stone, R.L., et al., *Focal adhesion kinase: an alternative focus for anti-angiogenesis therapy in ovarian cancer.* Cancer biology & therapy, 2014. **15**(7): p. 919-929.

218. Hersel, U., C. Dahmen, and H. Kessler, *RGD modified polymers: biomaterials for stimulated cell adhesion and beyond.* Biomaterials, 2003. **24**(24): p. 4385-4415.

219. Philip, D.L., et al., *RGD-functionalized nanofibers increase early GFAP expression during neural differentiation of mouse embryonic stem cells.* Biomacromolecules, 2019. **20**(3): p. 1443-1454.

220. Mazmanian, S.K., et al., *Staphylococcus aureus sortase, an enzyme that anchors surface proteins to the cell wall.* Science, 1999. **285**(5428): p. 760-763.

221. Clancy, K.W., J.A. Melvin, and D.G. McCafferty, *Sortase transpeptidases: insights into mechanism, substrate specificity, and inhibition.* Peptide Science, 2010. **94**(4): p. 385-396.

222. Bradshaw, W.J., et al., *Molecular features of the sortase enzyme family.* The FEBS journal, 2015. **282**(11): p. 2097-2114.

223. Cambria, E., et al., *Covalent Modification of Synthetic Hydrogels with Bioactive Proteins via Sortase-Mediated Ligation.* Biomacromolecules, 2015. **16**(8): p. 2316-26.

224. Piluso, S., et al., *Site-specific, covalent incorporation of Tus, a DNA-binding protein, on ionic-complementary self-assembling peptide hydrogels using transpeptidase Sortase A as a conjugation tool.* Soft Matter, 2013. **9**(29): p. 6752-6756.

225. Chan, L., et al., *Covalent attachment of proteins to solid supports and surfaces via Sortase-mediated ligation.* PLoS One, 2007. **2**(11): p. e1164.

226. Dai, X., A. Böker, and U. Glebe, *Broadening the scope of sortagging.* RSC advances, 2019. **9**(9): p. 4700-4721.

227. Yamamura, Y., et al., *Enhancement of sortase A-mediated protein ligation by inducing a β-hairpin structure around the ligation site.* Chemical Communications, 2011. **47**(16): p. 4742-4744.

228. Antos, J.M., M.C. Truttmann, and H.L. Ploegh, *Recent advances in sortase-catalyzed ligation methodology.* Current opinion in structural biology, 2016. **38**: p. 111-118.

229. Naik, M.T., et al., *Staphylococcus aureus sortase A transpeptidase: calcium promotes sorting signal binding by altering the mobility and structure of an active site loop.* Journal of Biological Chemistry, 2006. **281**(3): p. 1817-1826.

230. Bootman, M.D., et al. *Calcium signalling—an overview*. in *Seminars in cell & developmental biology*. 2001. Elsevier.

231. Jeong, H.-J., et al., *Generation of Ca2+-independent sortase A mutants with enhanced activity for protein and cell surface labeling.* PloS one, 2017. **12**(12): p. e0189068.

232. Samantaray, S., et al., *Peptide– Sugar Ligation Catalyzed by Transpeptidase Sortase: A Facile Approach to Neoglycoconjugate Synthesis.* Journal of the American Chemical Society, 2008. **130**(7): p. 2132-2133.

233. Kolb, H.C., M. Finn, and K.B. Sharpless, *Click chemistry: diverse chemical function from a few good reactions.* Angewandte Chemie International Edition, 2001. **40**(11): p. 2004-2021.

234. Himo, F., et al., *Copper (I)-catalyzed synthesis of azoles. DFT study predicts unprecedented reactivity and intermediates.* Journal of the American Chemical Society, 2005. **127**(1): p. 210-216.

235. Boren, B.C., et al., *Ruthenium-catalyzed azide– alkyne cycloaddition: Scope and mechanism.* Journal of the American Chemical Society, 2008. **130**(28): p. 8923-8930.

236. Brabec, V. and O. Nováková, *DNA binding mode of ruthenium complexes and relationship to tumor cell toxicity.* Drug Resistance Updates, 2006. **9**(3): p. 111-122.

237. Wang, J., et al., *The antitumor effect and toxicity of a ruthenium (II) complex in vivo.* Inorganic Chemistry Communications, 2018. **87**: p. 49-52.

238. Wittig, G. and A. Krebs, *Zur Existenz niedergliedriger cycloalkine, I.* Chemische Berichte, 1961. **94**(12): p. 3260-3275.

239. Meier, H., H. Petersen, and H. Kolshorn, *Die Ringspannung von Cycloalkinen und ihre spektroskopischen Auswirkungen.* Chemische Berichte, 1980. **113**(7): p. 2398-2409.

240. Turner, R.B., et al., *Heats of hydrogenation. IX. Cyclic acetylenes and some miscellaneous olefins.* Journal of the American Chemical Society, 1973. **95**(3): p. 790-792.

241. Shea, K.J. and J.S. Kim, *Influence of strain on chemical reactivity. Relative reactivity of torsionally distorted double bonds in MCPBA epoxidations.* Journal of the American Chemical Society, 1992. **114**(8): p. 3044-3051.

242. Xu, J., et al., *Cytocompatible Poly (ethylene glycol)-co-polycarbonate Hydrogels Cross-Linked by Copper-Free, Strain-Promoted Click Chemistry.* Chemistry–An Asian Journal, 2011. **6**(10): p. 2730-2737.

243. Fu, S., et al., *Injectable hyaluronic acid/poly (ethylene glycol) hydrogels crosslinked via strain-promoted azide-alkyne cycloaddition click reaction.* Carbohydrate polymers, 2017. **169**: p. 332-340.

244. Madl, C.M., L.M. Katz, and S.C. Heilshorn, *Bio-orthogonally crosslinked, engineered protein hydrogels with tunable mechanics and biochemistry for cell encapsulation.* Advanced functional materials, 2016. **26**(21): p. 3612-3620.

245. Swarup, S. and E.M. Verheyen, *Wnt/wingless signaling in Drosophila.* Cold Spring Harbor perspectives in biology, 2012. **4**(6): p. a007930.

246. Baeg, G.-H., et al., *Heparan sulfate proteoglycans are critical for the organization of the extracellular distribution of Wingless.* Development, 2001. **128**(1): p. 87-94.

247. Eggington, H.R., E.J. Mulholland, and S.J. Leedham, *Morphogen regulation of stem cell plasticity in intestinal regeneration and carcinogenesis.* Developmental Dynamics, 2022.

248. Merrifield, B., *Solid phase synthesis.* Science, 1986. **232**(4748): p. 341-347.

249. Fisher, J.P., S.A. Hope, and M.L. Hooper, *Factors influencing the differentiation of embryonal carcinoma and embryo-derived stem cells.* Experimental cell research, 1989. **182**(2): p. 403-414.

250. Ahn, J., et al., *Cloning of the putative tumour suppressor gene for hereditary multiple exostoses (EXT1).* Nature genetics, 1995. **11**(2): p. 137-143.

251. Lin, X., et al., *Disruption of gastrulation and heparan sulfate biosynthesis in EXT1-deficient mice.* Developmental biology, 2000. **224**(2): p. 299-311.

252. Ashworth, J.C., et al., *Preparation of a User-Defined Peptide Gel for Controlled 3D Culture Models of Cancer and Disease.* Journal of Visualized Experiments, 2020. **166**.

253. Kuzmin, A., et al., *Surface functionalization using catalyst-free azide– alkyne cycloaddition.* Bioconjugate chemistry, 2010. **21**(11): p. 2076-2085.

254. Mao, H., et al., *Sortase-mediated protein ligation: a new method for protein engineering.* J Am Chem Soc, 2004. **126**(9): p. 2670-1.

255. Anlas, K., et al., *Gastruloids: Embryonic organoids from mouse embryonic stem cells to study patterning and development in early mammalian embryos*, in *Programmed Morphogenesis*. 2021, Springer. p. 131-147.

256. Drury, J.L. and D.J. Mooney, *Hydrogels for tissue engineering: scaffold design variables and applications.* Biomaterials, 2003. **24**(24): p. 4337-4351.

257. Lorsch, J.R., F.S. Collins, and J. Lippincott-Schwartz, *Fixing problems with cell lines.* Science, 2014. **346**(6216): p. 1452-1453.

258. Weinstein, J.N., *Cell lines battle cancer.* Nature, 2012. **483**(7391): p. 544-545.

259. Czechanski, A., et al., *Derivation and characterization of mouse embryonic stem cells from permissive and nonpermissive strains.* Nature protocols, 2014. **9**(3): p. 559-574.

260. Tremml, G., M. Singer, and R. Malavarca, *Culture of mouse embryonic stem cells.* Current protocols in stem cell biology, 2008. **5**(1): p. 1C. 4.1-1C. 4.19.

261. Hansenová Maňásková, S., et al., *Staphylococcus aureus sortase A-mediated incorporation of peptides: effect of peptide modification on incorporation.* PloS one, 2016. **11**(1): p. e0147401.

262. Oh, K.-B., et al., *Inhibition of sortase-mediated Staphylococcus aureus adhesion to fibronectin via fibronectin-binding protein by sortase inhibitors.* Applied microbiology and biotechnology, 2006. **70**(1): p. 102-106.

263. Parthasarathy, R., S. Subramanian, and E.T. Boder, *Sortase A as a novel molecular "stapler" for sequence-specific protein conjugation.* Bioconjug Chem, 2007. **18**(2): p. 469-76.

264. Wu, X., et al., *Effects of DMEM and RPMI 1640 on the biological behavior of dog periosteum-derived cells.* Cytotechnology, 2009. **59**(2): p. 103-111.

265. Negrini, N.C., et al., *Scaffold-based developmental tissue engineering strategies for ectodermal organ regeneration.* Materials Today Bio, 2021: p. 100107.

266. DeForest, C.A., B.D. Polizzotti, and K.S. Anseth, *Sequential click reactions for synthesizing and patterning three-dimensional cell microenvironments.* Nature materials, 2009. **8**(8): p. 659-664.

267. Arkenberg, M.R., et al., *Dynamic Click Hydrogels for Xeno-Free Culture of Induced Pluripotent Stem Cells.* Advanced Biosystems, 2020. **4**(11): p. 2000129.

268. Nimmo, C.M., S.C. Owen, and M.S. Shoichet, *Diels– Alder click cross-linked hyaluronic acid hydrogels for tissue engineering.* Biomacromolecules, 2011. **12**(3): p. 824-830.

269. Ossipov, D.A. and J. Hilborn, *Poly (vinyl alcohol)-based hydrogels formed by "click chemistry".* Macromolecules, 2006. **39**(5): p. 1709-1718.

270. Harvey, D., et al., *Antibiotic Spider Silk: Site-Specific Functionalization of Recombinant Spider Silk Using "Click" Chemistry.* Adv Mater, 2017. **29**(10).

271. Harvey, D., et al., *Cyclo (RGDfK) Functionalized Spider Silk Cell Scaffolds: Significantly Improved Performance in Just One Click.* Macromolecular Bioscience, 2020. **20**(12): p. 2000255.

272. Pfaff, M., et al., *Selective recognition of cyclic RGD peptides of NMR defined conformation by alpha IIb beta 3, alpha V beta 3, and alpha 5 beta 1 integrins.* Journal of Biological Chemistry, 1994. **269**(32): p. 20233-20238.

273. Meade, K.A., et al., *Immobilization of Heparan Sulfate on Electrospun Meshes to Support Embryonic Stem Cell Culture and Differentiation*[S].* Journal of Biological Chemistry, 2013. **288**(8): p. 5530-5538.

274. Dráberová, E., et al., *Class III β-tubulin is constitutively coexpressed with glial fibrillary acidic protein and nestin in midgestational human fetal astrocytes: implications for phenotypic identity.* Journal of Neuropathology & Experimental Neurology, 2008. **67**(4): p. 341-354.

275. Turner, D.A., et al., *Anteroposterior polarity and elongation in the absence of extra-embryonic tissues and of spatially localised signalling in gastruloids: mammalian embryonic organoids.* Development, 2017. **144**(21): p. 3894-3906.

276. Gonzalez-Fernandez, T., A.J. Tenorio, and J.K. Leach, *Three-dimensional printed stamps for the fabrication of patterned microwells and high-throughput production of homogeneous cell spheroids.* 3D Printing and Additive Manufacturing, 2020. **7**(3): p. 139-147.

277. Chen, B., et al., *High-throughput acoustofluidic fabrication of tumor spheroids.* Lab on a Chip, 2019. **19**(10): p. 1755-1763.

278. Lee, Y.B., et al., *Engineering spheroids potentiating cell-cell and cell-ECM interactions by self-assembly of stem cell microlayer.* Biomaterials, 2018. **165**: p. 105-120.

279. Devarasetty, M., et al., *In vitro modeling of the tumor microenvironment in tumor organoids.* Tissue Engineering and Regenerative Medicine, 2020. **17**(6): p. 759-771.

280. Smith, R.A., et al., *Glycosaminoglycans as regulators of stem cell differentiation.* Biochem Soc Trans, 2011. **39**(1): p. 383-7.

281. Aston, R., et al., *Evaluation of the impact of freezing preparation techniques on the characterisation of alginate hydrogels by cryo-SEM.* European Polymer Journal, 2016. **82**: p. 1-15.

282. Chui, M.M., R.J. Phillips, and M.J. McCarthy, *Measurement of the porous microstructure of hydrogels by nuclear magnetic resonance.* Journal of colloid and interface science, 1995. **174**(2): p. 336-344.

283. Taraballi, F., et al., *Glycine-spacers influence functional motifs exposure and self-assembling propensity of functionalized substrates tailored for neural stem cell cultures.* Frontiers in neuroengineering, 2010. **3**: p. 1.

284. Taraballi, F., et al., *Effect of functionalization on the self-assembling propensity of β-sheet forming peptides.* Soft matter, 2009. **5**(3): p. 660-668.

285. Silva, D., et al., *Synthesis and characterization of designed BMHP1-derived self-assembling peptides for tissue engineering applications.* Nanoscale, 2013. **5**(2): p. 704-718.

286. Lundin, L., et al., *Selectively desulfated heparin inhibits fibroblast growth factor-induced mitogenicity and angiogenesis.* Journal of Biological Chemistry, 2000. **275**(32): p. 24653-24660.

287. Kang, Y., et al., *Fibronectin stimulates the osteogenic differentiation of murine embryonic stem cells.* Journal of Tissue Engineering and Regenerative Medicine, 2017. **11**(7): p. 1929-1940.

288. Hazenbiller, O., N.A. Duncan, and R.J. Krawetz, *Reduction of pluripotent gene expression in murine embryonic stem cells exposed to mechanical loading or Cyclo RGD peptide.* BMC Cell Biology, 2017. **18**(1): p. 1-15.

289. Humphries, D.E. and J.E. Silbert, *Chlorate: a reversible inhibitor of proteoglycan sulfation.* Biochemical and biophysical research communications, 1988. **154**(1): p. 365-371.

290. Baeuerle, P.A. and W.B. Huttner, *Chlorate—a potent inhibitor of protein sulfation in intact cells.* Biochemical and biophysical research communications, 1986. **141**(2): p. 870-877.

291. Kenny, P.A., et al., *The morphologies of breast cancer cell lines in three-dimensional assays correlate with their profiles of gene expression.* Molecular oncology, 2007. **1**(1): p. 84-96.

292. Fontoura, J.C., et al., *Comparison of 2D and 3D cell culture models for cell growth, gene expression and drug resistance.* Materials Science and Engineering: C, 2020. **107**: p. 110264.

293. Martyn, I., et al., *Self-organization of a human organizer by combined Wnt and Nodal signalling.* Nature, 2018. **558**(7708): p. 132-135.

294. Simunovic, M., et al., *A 3D model of a human epiblast reveals BMP4-driven symmetry breaking.* Nature Cell Biology, 2019. **21**(7): p. 900-910.

295. Kuhl, P.R. and L.G. Griffith-Cima, *Tethered epidermal growth factor as a paradigm for growth factor–induced stimulation from the solid phase.* Nature medicine, 1996. **2**(9): p. 1022-1027.

296. Mehta, G., et al., *Synergistic effects of tethered growth factors and adhesion ligands on DNA synthesis and function of primary hepatocytes cultured on soft synthetic hydrogels.* Biomaterials, 2010. **31**(17): p. 4657-4671.

297. Silva, G.A., et al., *Selective differentiation of neural progenitor cells by high-epitope density nanofibers.* Science, 2004. **303**(5662): p. 1352-1355.

298. Schrader, J., et al., *Matrix stiffness modulates proliferation, chemotherapeutic response, and dormancy in hepatocellular carcinoma cells.* Hepatology, 2011. **53**(4): p. 1192-205.

299. Özdemir, B.C., et al., *Depletion of carcinoma-associated fibroblasts and fibrosis induces immunosuppression and accelerates pancreas cancer with reduced survival.* Cancer cell, 2014. **25**(6): p. 719-734.

300. Choi, J.R., et al., *Recent advances in photo-crosslinkable hydrogels for biomedical applications.* BioTechniques, 2019. **66**(1): p. 40-53.

301. Zarzhitsky, S., et al., *The effect of pH and calcium ions on the stability of amphiphilic and anionic β-sheet peptide hydrogels.* Peptide Science, 2013. **100**(6): p. 760-772.

302. Stark, M., et al., *Macroscopic fibers self-assembled from recombinant miniature spider silk proteins.* Biomacromolecules, 2007. **8**(5): p. 1695-1701.

303. Hedhammar, M., et al., *Structural properties of recombinant nonrepetitive and repetitive parts of major ampullate spidroin 1 from Euprosthenops australis: implications for fiber formation.* Biochemistry, 2008. **47**(11): p. 3407-3417.

304. Rising, A. and J. Johansson, *Toward spinning artificial spider silk.* Nature chemical biology, 2015. **11**(5): p. 309-315.

305. Hedhammar, M., et al., *Sterilized recombinant spider silk fibers of low pyrogenicity.* Biomacromolecules, 2010. **11**(4): p. 953-959.

306. Widhe, M., et al., *Recombinant spider silk as matrices for cell culture.* Biomaterials, 2010. **31**(36): p. 9575-9585.

307. Salehi, S., K. Koeck, and T. Scheibel, *Spider silk for tissue engineering applications.* Molecules, 2020. **25**(3): p. 737.

308. Fredriksson, C., et al., *Tissue response to subcutaneously implanted recombinant spider silk: an in vivo study.* Materials, 2009. **2**(4): p. 1908-1922.

309. Jansson, R., et al., *Spider silk materials genetically engineered with enzyme activity.* Frontiers in Bioengineering and Biotechnology, 2016.

310. Nieberler, M., et al., *Exploring the role of RGD-recognizing integrins in cancer.* Cancers, 2017. **9**(9): p. 116.

311. Fraser, J.R.E., T.C. Laurent, and U. Laurent, *Hyaluronan: its nature, distribution, functions and turnover.* Journal of internal medicine, 1997. **242**(1): p. 27-33.

312. Aruffo, A., et al., *CD44 is the principal cell surface receptor for hyaluronate.* Cell, 1990. **61**(7): p. 1303-1313.

313. Sherman, L., et al., *Hyaluronate receptors: key players in growth, differentiation, migration and tumor progression.* Current opinion in cell biology, 1994. **6**(5): p. 726-733.

314. Baier Leach, J., et al., *Photocrosslinked hyaluronic acid hydrogels: natural, biodegradable tissue engineering scaffolds.* Biotechnology and bioengineering, 2003. **82**(5): p. 578-589.

315. Shu, X.Z., et al., *In situ crosslinkable hyaluronan hydrogels for tissue engineering.* Biomaterials, 2004. **25**(7-8): p. 1339-1348.

316. Ananthanarayanan, B., Y. Kim, and S. Kumar, *Elucidating the mechanobiology of malignant brain tumors using a brain matrix-mimetic hyaluronic acid hydrogel platform.* Biomaterials, 2011. **32**(31): p. 7913-23.

317. Roper, S.J., et al., *3D spheroid models of paediatric SHH medulloblastoma mimic tumour biology, drug response and metastatic dissemination.* Scientific reports, 2021. **11**(1): p. 1-17.

318. Jones, C.J., S. Beni, and C.K. Larive, *Understanding the effect of the counterion on the reverse-phase ion-pair high-performance liquid chromatography (RPIP-HPLC) resolution of heparin-related saccharide anomers.* Analytical chemistry, 2011. **83**(17): p. 6762-6769.

319. Marchini, A., C. Favoino, and F. Gelain, *Multi-functionalized self-assembling peptides as reproducible 3D cell culture systems enabling differentiation and survival of various human neural stem cell lines.* Frontiers in neuroscience, 2020. **14**: p. 413.

320. Pugliese, R., et al., *Branched peptides integrate into self-assembled nanostructures and enhance biomechanics of peptidic hydrogels.* Acta biomaterialia, 2018. **66**: p. 258-271.

321. Gelain, F., et al., *New bioactive motifs and their use in functionalized self-assembling peptides for NSC differentiation and neural tissue engineering.* Nanoscale, 2012. **4**(9): p. 2946-2957.

322.   Caprini, A., et al., *A novel bioactive peptide: assessing its activity over murine neural stem cells and its potential for neural tissue engineering.* New biotechnology, 2013. **30**(5): p. 552-562.

323.   Mazunin, D. and J.W. Bode, *Potassium Acyltrifluoroborate (KAT) Ligations are Orthogonal to Thiol-Michael and SPAAC Reactions: Covalent Dual Immobilization of Proteins onto Synthetic PEG Hydrogels.* Helvetica Chimica Acta, 2017. **100**(2): p. e1600311.

324.   Omenn, G.S., et al., *Progress on identifying and characterizing the human proteome: 2019 metrics from the HUPO Human Proteome Project.* Journal of proteome research, 2019. **18**(12): p. 4098-4107.

325.   Cree, I.A., *Chemosensitivity and chemoresistance testing in ovarian cancer.* Current Opinion in Obstetrics and Gynecology, 2009. **21**(1): p. 39-43.

326.   Roy, L. and K.D. Cowden Dahl, *Can stemness and chemoresistance be therapeutically targeted via signaling pathways in ovarian cancer?* Cancers, 2018. **10**(8): p. 241.

327.   Taron, M., et al., *BRCA1 mRNA expression levels as an indicator of chemoresistance in lung cancer.* Human molecular genetics, 2004. **13**(20): p. 2443-2449.

328.   Bazdyrev, E., et al., *Lung Fibrosis after COVID-19: treatment prospects.* Pharmaceuticals, 2021. **14**(8): p. 807.

329.   Udwadia, Z.F., P.A. Koul, and L. Richeldi, *Post-COVID lung fibrosis: The tsunami that will follow the earthquake.* Lung India: Official Organ of Indian Chest Society, 2021. **38**(Suppl 1): p. S41.

330.   Knoepfler, P. *What is Matrigel, why a shortage, & alternatives?* The Niche 2022 [cited 14th October 2022]; Available from: https://ipscell.com/2022/03/what-is-matrigel-why-a-shortage-alternatives/.